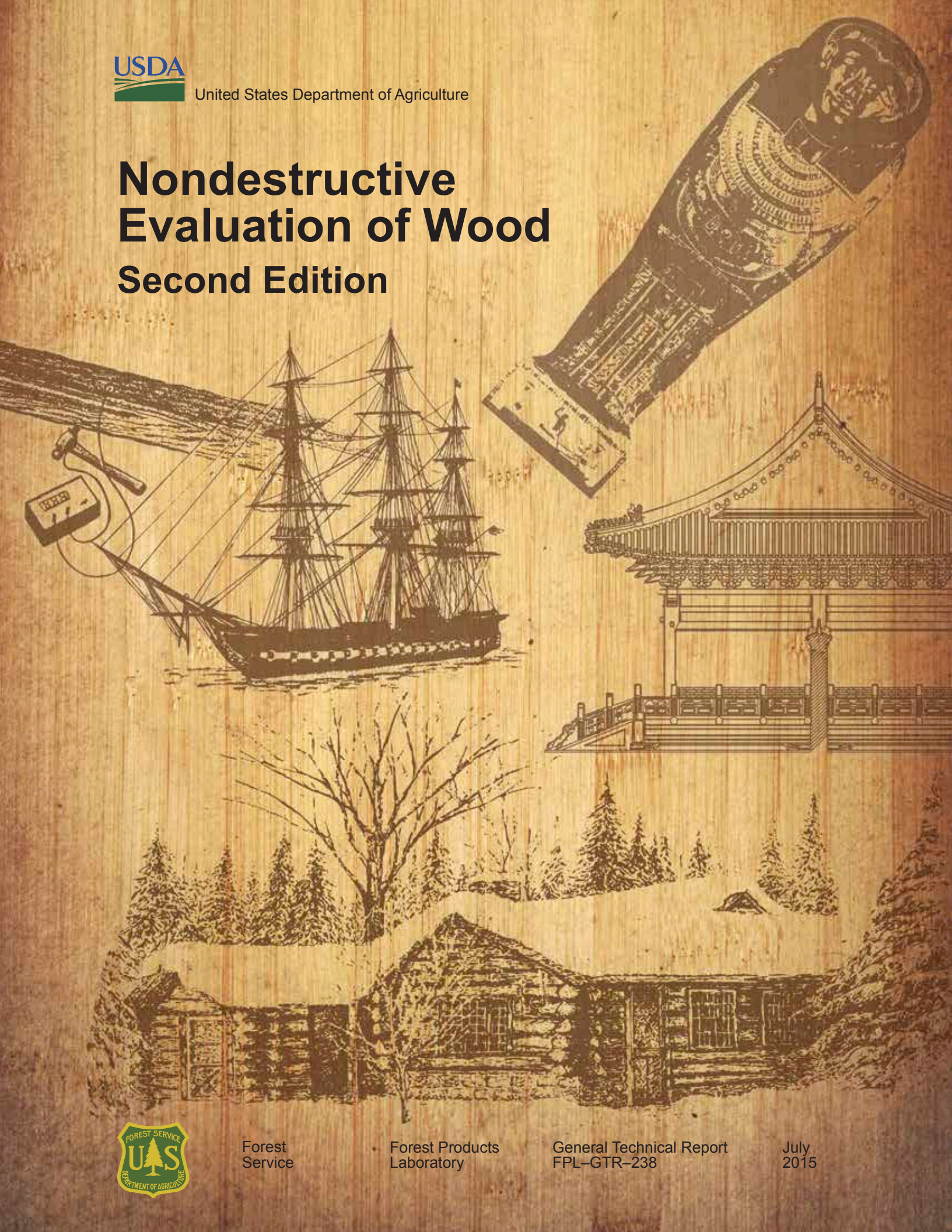

USDA
United States Department of Agriculture

Nondestructive Evaluation of Wood

Second Edition

Forest Service
Forest Products Laboratory
General Technical Report FPL–GTR–238
July 2015

Abstract

This report summarizes information on nondestructive testing and evaluation of wood. It includes information on a wide range of nondestructive assessment technologies and their uses for evaluating various wood products.

Keywords: Wood, timber, nondestructive testing, nondestructive evaluation

Conversion Table

English unit	Conversion factor	SI unit
inch (in.)	25.4	millimeter (mm)
foot (ft)	0.3048	meter (m)
board foot	0.0023597	cubic meter ($m^{3)}$) (nominal)
feet per minute (ft/min)	0.005080	meters per second (m/s)
pound (lb)	0.448	newton (N)
pounds per square inch (lb/in^2)	0.0069	pascal (Pa)
in^4	4.162×10^{-7}	m^4

July 2015

Ross, Robert J. (Ed.). 2015. Nondestructive evaluation of wood: second edition. General Technical Report FPL-GTR-238. Madison, WI: U.S. Department of Agriculture, Forest Service, Forest Products Laboratory. 169 p.

A limited number of free copies of this publication are available to the public from the Forest Products Laboratory, One Gifford Pinchot Drive, Madison, WI 53726–2398. This publication is also available online at www.fpl.fs.fed.us. Laboratory publications are sent to hundreds of libraries in the United States and elsewhere.

The Forest Products Laboratory is maintained in cooperation with the University of Wisconsin.

Nondestructive Evaluation of Wood

Second Edition

Edited by
Robert J. Ross

Forest Products Laboratory

Contents

Preface

This edition of *Nondestructive Evaluation of Wood* builds upon the first edition with important new content:

- Ultrasonic nondestructive testing methods (Chapter 3)
- Piezoelectric effect in wood (Chapter 6)
- Urban tree assessment (Chapter 7), reflecting significant research and technology transfer advances
- Laser scanning of logs and lumber (Chapter 9), reflecting the importance of scanning systems in the wood manufacturing industry
- Updates on mechanical grading methods for structural lumber (Chapter 11)
- Use of laser scanning technologies for evaluation of historic, covered timber bridges (Chapter 13)
- An appendix providing information to access digital copies of all proceedings from the International Nondestructive Testing and Evaluation of Wood Symposium Series

The objective of this book is the same as that of the first edition—to serve as a primary reference on nondestructive evaluation of wood. Sections of the book originally appeared in technical journals, research reports, and proceedings from various symposia. For example, the chapters on ultrasonic nondestructive testing methods, the piezoelectric effect in wood, and the use of laser scanning technologies for evaluation of bridges were originally published as USDA Forest Products Laboratory (FPL) reports.

I worked with several well-respected technical authorities in preparing this edition. I thank the technical contributors to this edition:

- R. Bruce Allison, PhD, Adjunct Professor, University of Wisconsin–Madison; and Allison Tree, LLC, Verona, Wisconsin, USA
- Brian K. Brashaw, PhD, Program Manager, Forest Products Marketing Unit, USDA Forest Service, Madison, Wisconsin, USA
- Peter Carter, CEO, Fibre-gen, New Zealand
- William Galligan, Consultant, USA
- Gregory Schueneman, PhD, Project Leader, USDA Forest Products Laboratory, USA
- C. Adam Senalik, PhD, P.E., Research General Engineer, USDA Forest Products Laboratory, USA
- Edward Thomas, Research Computer Scientist, USDA Forest Products Laboratory, USA
- Xiping Wang, PhD, Research Forest Products Technologist, USDA Forest Products Laboratory, USA

I also acknowledge Professor (retired) Roy F. Pellerin, Washington State University, for his valuable contributions to the first edition of *Nondestructive Evaluation of Wood*.

Financial support from the USDA Forest Service for this second edition of *Nondestructive Evaluation of Wood* is gratefully acknowledged.

This edition of *Nondestructive Evaluation of Wood* is dedicated to Roy F. Pellerin and John R. Erickson, my good friends and colleagues.

> Roy F. Pellerin is a pioneer in the field of nondestructive testing and evaluation, leading the successful nondestructive evaluation research program at Washington State University for nearly 40 years. His technical accomplishments are numerous, and his leadership of the International Nondestructive Testing and Evaluation of Wood Symposium Series has resulted in the worldwide development and use of nondestructive evaluation. He is an inspiration and source of knowledge to a generation of graduate students, scientists, and engineers working in the field.

John R. Erickson (1934–2014), P.E., Director and Research Engineer, FPL, was an internationally recognized leader in the wood science profession. He conducted research on wood harvesting and utilization issues with wood and guided the FPL through numerous changes. He initiated new research initiatives at FPL in recycling, green technologies, biotechnology, and ecosystem management. Under his leadership, FPL provided critical technical support to the Forest Service, wood products industry, and various government agencies, including the Department of Defense, Department of Energy, National Park Service, and Department of Housing and Urban Development. John was a strong supporter and advocate for the nondestructive evaluation field; after retiring from the Forest Service he joined the staff at Michigan Technological University, where he worked on the development of advanced tree and log nondestructive assessment and grading technologies that have been widely adapted for use. John was a well-respected scientist, worldwide, and he served the public in a professional manner for over 40 years. His reputation is impeccable.

Nondestructive Evaluation of Wood, Second Edition is available in digital format from the USDA Forest Service Forest Products Laboratory website.

Special thanks to Jim Anderson, Madelon Wise, Tivoli Gough, and Karen Nelson for their extraordinary efforts in the production of this book.

Robert J. Ross, Editor

Preface to the First Edition

This book on nondestructive evaluation (NDE) of wood was prepared at the request of our colleagues throughout the world who expressed the desire for a synthesized source of information on the subject. We have attempted to meet their needs through this book.

We contacted several widely respected technical authorities and asked them to prepare chapters dealing with their areas of expertise. Professor Frank Beall (University of California–Berkeley), Brian Brashaw (University of Minnesota–Duluth), Kevin Cheung (Western Wood Products Association), Bill Galligan (retired, Frank Lumber Company), John Kearns (Weyerhaeuser Company), and Xiping Wang (University of Minnesota–Duluth) responded positively to our request and prepared excellent chapters on acoustic emission/acousto–ultrasonics, ultrasonic veneer grading, visual grading of lumber, mechanical grading of lumber, and recent research on NDE of green materials, respectively.

Sections of the book originally appeared in technical journals, research reports, and various symposia proceedings. We have included, for example, a chapter on inspection of timber structures that originally appeared as a research paper, which was widely distributed and used by engineering consultants who inspect structures as a part of their business.

We prepared this book to serve as a primary reference on NDE of wood. More than 400 technical articles are cited in the chapters or listed in the Appendix. We also intended it to be used as a primer or handbook on several widely used NDE technologies. The chapters on machine grading of lumber, ultrasonic veneer grading, and inspection of wood in service were written to provide a concise source of information to manufacturers and users of wood products who are considering use of various commercially available NDE technologies in their manufacturing operation or consulting business.

This book was made possible through the efforts of dedicated scientists who spent countless hours in laboratories developing our technical knowledge base on NDE of wood.

Roy F. Pellerin

Robert J. Ross

Chapter 1

Nondestructive Testing and Evaluation of Wood

Robert J. Ross, Supervisory Research General Engineer
Forest Products Laboratory, Madison, Wisconsin

Wood is an extremely valuable material because it is renewable, widely distributed, and requires relatively small amounts of energy to be converted into useful products. As a consequence, wood has been used for centuries for both shelter and as an industrial raw material.

It is important to note that wood is a material of biological origin. Consequently, its molecular composition and basic physiological structure are fixed by nature. The fact that it is a biological material provides the basis for many of its unique properties and the challenges manufacturers and subsequent users of wood products are confronted with.

The following list of wood characteristics, originally prepared by Marra (1979), summarizes some characteristics of wood that are important to introducing the subject of nondestructive evaluation of wood.

1. Wood is a fibrous material. The fiber is a small tubular structure, incorporating nature's engineering to make it an efficient load-carrying member. The microstructure of the walls of a fiber present an interesting arrangement related to biological functions performed in the living tree and a contribution to the properties of wood as a material. Alignment of fibers primarily in longitudinal aspect in the tree is the main source of wood's anisotropic properties.
2. Wood is a complex chemical material. Made up largely of several chemical identities, such as cellulose and lignin, it can be infiltrated with numerous extraneous compounds. The type and amount of these extraneous compounds are often distinctive with certain species of trees, and in some cases, have a pronounced effect of properties.
3. Wood is anisotropic. Perhaps the most striking quality of wood from an engineering standpoint is its properties along the grain compared to properties across the grain. This ratio may reach as high as 50 for some properties.
4. Wood is viscoelastic. Although wood follows Hooke's law at low stresses, the proportional limit is difficult to precisely define. Under high stress, wood exhibits creep behavior, which is greatly influenced by the presence of moisture and is temperature dependent.
5. Wood is hygroscopic. Wood is characterized chemically by an abundance of hydroxyl groups. These groups have an affinity for water molecules and seek to maintain equilibrium with the partial vapor pressure of moisture in the surrounding environment. The immediate consequence of the gain or loss of moisture is a swelling or shrinkage of wood. Moisture also has a profound effect on properties.
6. Wood is variable. Wood varies in properties between species, between trees of the same species, and between pieces from the same tree.
7. Wood in its original solid form has adequate properties for many uses.
8. Wood is plentiful. Each major land mass in the world is blessed with extensive forest lands.
9. Wood is renewable. This factor is extremely important when considering the roles of various non-renewable materials in sustaining a technologically based society.
10. Wood is beautiful. The beauty of wood, aside from the warmth for which it is universally cherished, arises principally from variability in its fibrous structure.

Fundamental Concept

By definition, nondestructive evaluation is the science of identifying the physical and mechanical properties of a piece of material without altering its end-use capabilities and then using this information to make decisions regarding appropriate applications. Such evaluations rely upon nondestructive testing technologies to provide accurate information pertaining to the properties, performance, or condition of the material in question.

Many tests or techniques can be categorized as nondestructive (Fig. 1.1). A variety of tests can be performed on a material or product, with selection of the appropriate test dictated by the particular performance or quality characteristic of interest. Evaluation of visual characteristics of a piece of lumber is probably one of the most widely used nondestructive techniques in the forest products industry. Characteristics such as the size, number, and location of knots are common visual characteristics considered when grading both structural and nonstructural lumber.

Nondestructive evaluation of wood

Evaluation of visual characteristics

Color

Presence of defects

Physical tests

Electrical properties

Vibrational properties

Wave propagation

Acoustic emissions

Chemical tests

Composition

Presence of treatments
- Preservatives
- Fire retardants

Mechanical tests

Flexural stiffness

Proof loading
- Bending
- Tension
- Compression

Probes/coring

Figure 1.1—Nondestructive techniques.

Figure 1.2—A late 18th-century Hudson Bay Compay York boat.

One of the first uses of a nonvisual nondestructive testing method involved a procedure to evaluate timbers for boats used by the Hudson Bay Company, Canada (Fig. 1.2):

> A York boat, which took two skilled men only two weeks to build, would last three seasons with minimum maintenance. The trickiest part of the construction process was to find the proper piece of spruce or tamarack for a seaworthy keel. Samples were tested by being placed on stocks and a pocket watch held against the butt at one end. The builder listened for the tick at the other. Only if the ticking resonated loudly and clearly through the wood was it judged suitable to withstand the stresses of being carved into a keel. From *Caesars of the Wilderness: Company of Adventures, Volume II,* by Peter C. Newman.

The field of nondestructive testing (NDT) and nondestructive evaluation (NDE) of materials is constantly evolving. This is especially true in the area of wood and fiber-based materials. For example, early research on NDT/NDE technologies for wood products focused on methods for assessing the performance characteristics of structural lumber in North America. Nondestructive testing techniques, equipment, and evaluation procedures that resulted from those efforts are now in widespread use. Currently, worldwide research and development efforts are under way to examine potential use of a wide range of NDT technologies for evaluating wood and woodbased materials—from assessment of standing trees to in-place structures.

The original impetus for research in NDT/NDE of wood was the need to provide methodologies for assessing woodbased materials and products so that more accurate decisions could be made about proper use. This remains the major driving force for NDT/NDE wood research, with two significant additional challenges. First, there is an increased emphasis around the world to address forest and ecosystem health issues. Utilization of woody biomass from widely varying growing conditions will play a key role in providing economical options for managing the health of these forests and ecosystems. Second, the marketplace has become increasingly global in nature. Shipments of raw materials and products between countries on different continents is now commonplace. Both of these challenges will require accurate, cost-effective NDT/NDE technologies.

An international forest products research community is responding to these driving forces by conducting NDT/NDE research to provide the technologies needed to address these challenges.

International Nondestructive Testing and Evaluation of Wood Symposium Series

In an effort to provide a forum for researchers, the international NDT/NDE research community sponsors a series of technical symposia for exchange of technical information. These symposia are scheduled on a biannual basis at locations throughout the world.

The International Nondestructive Testing and Evaluation of Wood Symposium Series was initiated by Washington State University and the USDA Forest Products Laboratory (FPL). The first symposium was held at FPL in the fall of 1963, with proceedings produced and distributed in 1964. At the meeting, nearly 100 scientists, engineers, and industry leaders discussed possibilities of a wide range of scientific means for testing wood nondestructively.

This symposium series has two goals:

1. To provide a technical and scientific forum for researchers to present and exchange results from their latest research endeavors.

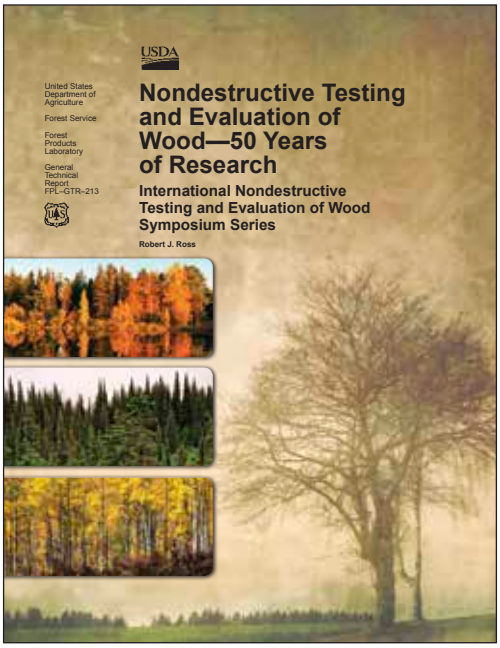

Figure 1.3—***Nondestructive Testing and Evaluation of Wood—50 Years of Research.***

2. To bring researchers and industry together in an attempt to bridge the gap between the results of research efforts and the use of those results by the wood industry.

In 2012, an FPL report was prepared that contained digital copies of earlier proceedings (Fig. 1.3), and proceedings of the 2013 symposium were distributed at the meeting (Ross and Wang 2012, 2013; see Appendix). Eighteen symposia have been held to date, and the nineteenth is scheduled for September 22–25, 2015, in Rio de Janeiro, Brazil (Table 1.1).

Although the early symposia focused on basic NDE principles and lumber assessment procedures, the symposium now attracts researchers and industry representatives from throughout the world and represents the full spectrum of technical interests, from basic and applied science to the use of various methods in industrial and field applications. Recently, papers have been presented on the latest NDT techniques including those that focus on tomography, near infrared scanning, and innovative combinations of stress wave, laser, and ultrasound techniques. A significant number of papers have been presented on assessment of trees and logs, with most of the work on lumber focusing on the use of established NDT techniques for evaluating species in Asia, Europe, and South America.

Objectives

The objectives of this book are (1) to serve as a primary reference on the subject of nondestructive testing and evaluation of wood and (2) to present a synthesized source of information on the subject.

In an attempt to meet these objectives, we have prepared chapters on various nondestructive testing techniques and basic concepts, including ultrasound, stress wave, transverse vibration, and proof-loading methods. Application of NDE,

Table 1.1—Dates and locations for the International Nondestructive Testing and Evaluation of Wood Symposia

Symposium	Dates held	Host institution and location
1	October 7–9, 1963	U.S. Forest Products Laboratory, Madison, WI, USA
2	April, 1964	Washington State University, Spokane, WA, USA
3	April–May, 1970	Washington State University, Vancouver, WA, USA
4	August 28–30, 1978	Washington State University, Vancouver, WA, USA
5	September 9–11, 1985	Washington State University, Pullman, WA, USA
6	September 14–16, 1987	Washington State University, Pullman, WA, USA
7	September 27–29, 1989	U.S. Forest Products Laboratory, Madison, WI, USA
8	September 23–25, 1991	Washington State University, Vancouver, WA, USA
9	September 22–24, 1993	U.S. Forest Products Laboratory, Madison, WI, USA
10	August 26–28, 1996	IBOIS-Chair of Timber Construction of the Swiss Federal Institute of Technology, Lausanne, Switzerland
11	September 9–11, 1998	U.S. Forest Products Laboratory, Madison, WI, USA
12	September 13–15, 2000	University of West Hungary, Sopron, Hungary
13	August 19–21, 2002	University of California, Berkeley Campus, CA, USA
14	May 2–4, 2005	University of Applied Sciences Eberswalde, Hanover, Germany
15	September 10–12, 2007	University of Minnesota Duluth, Duluth, MN, USA
16	May 11–13, 2009	Beijing Forestry University, Beijing, P.R. China
17	September 14-16, 2011	University of West Hungary, Sopron, Hungary
18	September 24-27, 2013	U.S. Forest Products Laboratory, Madison, WI, USA

including applications that highlight the use of various NDE methodologies to assess the entire spectrum of wood, from standing trees to historic structures, are included in subsequent chapters.

Literature Cited

Marra, G.G. 1979. Overview of wood as a material. In: F.F. Wangaard, Ed. Wood: its structure and properties. 42 p.

Ross, R.J.; Wang, Xiping. 2012. Nondestructive testing and evaluation of wood research. 50 years of research. International nondestructive testing and evaluation of wood symposium series. General Technical Report. FPL-GTR-213. Madison, WI: U.S. Department of Agriculture, Forest Service, Forest Products Laboratory. 6,702 p.

Ross, R.J.; Wang, Xiping. 2013. Proceedings, 18th international nondestructive testing and evaluation of wood symposium. General Technical Report. FPL-GTR-226. Madison, WI: U.S. Department of Agriculture, Forest Service, Forest Products Laboratory. 808 p.

Chapter 2

Static Bending, Transverse Vibration, and Longitudinal Stress Wave Nondestructive Evaluation Methods

Robert J. Ross, Supervisory Research General Engineer
Forest Products Laboratory, Madison, Wisconsin

Static Bending Nondestructive Evaluation Methods

Measuring the modulus of elasticity (MOE) of a member by static bending methods is a relatively simple procedure that involves using the load–deflection relationship of a simply supported beam. Modulus of elasticity can be computed directly by using equations derived from fundamental mechanics of materials.

Initial laboratory studies to verify the relationships between static bending methods and structural performance characteristics were conducted with lumber products. Considerable research in the early 1960s examined the relationships between static bending test methods and the strength of softwood dimension lumber. Summaries of various projects designed to examine this relationship are presented in Tables 2.1 to 2.3. A wide range of lumber products was evaluated, and the bending, compressive, and tensile strength of the materials was investigated. In all cases, useful correlative relationships were discovered.

Some commercially available equipment uses static bending techniques to evaluate the MOE of structural lumber. A detailed discussion of equipment is included in Chapter 11, Machine Grading of Lumber.

The following text outlines essential laboratory testing procedures and additional key information to be used in a laboratory or field environment.

Centerpoint Loading Test Setup

Figure 2.1 illustrates a typical centerpoint loading test setup. The specimen is simply supported at both ends, a load applied, and the midspan deflection that results from the load measured. MOE of the specimen is calculated as

Table 2.1—Research on the correlation between modulus of elasticity (tested flatwise) and flatwise bending strength of softwood dimension lumber

Reference	Species	Nominal moisture content (%)	Grade[a]	Nominal width (in.)[b]	Growth location	Correlation coefficient *r*
Hoyle (1961)	Douglas-fir	12	SS, C, U	4, 6, 10	Western Oregon, Washington, Idaho	0.79
					Washington	0.72
	Western hemlock	12	SS, C, U	4, 6, 10	Western Oregon, Washington	0.74
	Western larch	12	SS, C, U	4, 6, 8	Idaho, Washington	0.70
Hoyle (1962)	Grand fir	12	C, S, U	8	Idaho	0.75
Hofstrand and Howe (1963)	Grand fir	12	C, S	4, 6, 8	Idaho	0.75
Pellerin (1963b)	Douglas-fir	12	Combination of visual grades	4, 8	Idaho	0.76
Hoyle (1964)	Southern Pine	12	1D, 1, 2D, 2, 3	4, 6, 8	Southeastern United States	0.76
Kramer (1964)	Southern Pine	12	1D, 2, 3	4 , 6, 10	Southeastern United States	0.88
Johnson (1965)	Douglas-fir	10	SS, C, U	6	Western Oregon, Washington	0.85
	Western hemlock	10	SS, C, U	6	Western Oregon, Washington	0.86

[a]Grades are by regional rules in use at time of research. Western Products Association and West Coast Lumber Inspection Bureau Grades: SS, Select Structural; C, Construction; S, Standard; U, Utility. Western Wood Products Association Grades: 1, 2, 3. Southern Pine Inspection Bureau Grades: 1D, No. 1 Dense; 1, No. 1; 2D, No. 2 Dense; 2, No. 2; 3, No. 3.

[b]1 in. = 25.4 mm.

Table 2.2—Research on the correlation between modulus of elasticity (tested flatwise and on edge) and edgewise bending strength of softwood dimension lumber

Reference	Species	Nominal moisture content (%)	Grade[a]	Nominal width (in.)[b]	Growth location	Correlation coefficient
Hoerber (1962)	Douglas-fir	12	SS, C, U	4, 6, 8	Idaho, eastern Washington	0.651
Hoyle (1962)	Grand fir	12	C, S, U, SS	8	Idaho	0.59–0.701
Hoyle (1964)	Southern Pine	12	1D, 1, 2D, 2, 3	4, 6, 8	Southeastern United States	0.571
Sunley and Hudson (1964)	Norway spruce and Scots pine (pooled)	—	—	4, 7	Great Britain	0.681
Corder (1965)	Douglas-fir	12	SS, C, S	4, 6, 10	Inland northwestern United States	0.64
Johnson (1965)	Douglas-fir	10	SS, C, U	6	Western Oregon, Washington	0.80–0.87
Johnson (1965)	Western hemlock	10	SS, C, U	6	Western Oregon, Washington	0.86
Littleford (1965)	Douglas-fir	10	—	6	British Columbia, Canada	0.74
	Western hemlock	10	—	6		0.70–0.77
	Noble fir	12	—	6		0.66
	Western white spruce	12	—	6		0.79
	Lodgepole pine	12	—	6		0.80
		17		6		
Miller (1965)	White spruce	12	—	6	Eastern Canada	0.78–0.84
	Jack pine	12	—	6		0.69–0.73
Doyle and Markwardt (1966)	Southern Pine	12	1D, 1, 2D, 2, 3	4, 6, 8, 10	Southeastern United States	0.66
Hoyle (1968)	Southern Pine	12	1D, 1, 2D, 2, 3	4, 6, 8	Southeastern United States	0.671

[a]Grades are by regional rules in use at time of research. Western Products Association and West Coast Lumber Inspection Bureau Grades: SS, Select Structural; C, Construction; S, Standard; U, Utility. Western Wood Products Association Grades: 1, 2, 3. Southern Pine Inspection Bureau Grades: lD, No. 1 Dense; 1, No. 1; 2D, No. 2 Dense; 2, No. 2; 3, No. 3.

[b]1 in. = 25.4 mm.

Table 2.3—Research on the correlation between modulus of elasticity (tested flatwise) and the compressive and tensile strength of softwood dimension lumber

Strength property	Reference	Species	Nominal moisture content (%)	Grade[b]	Nominal width (in.)[b]	Growth location	Compression coefficient *r*
Compressive	Hofstrand and Howe (1963)	Grand fir	12	Ungraded	4, 8	Idaho	0.84
	Pellerin (1963a)	Douglas-fir	12	SS, S, E	4, 8	Idaho	0.78
	Hoyle (1968)	Southern Pine	12	1, 2, 3	4, 8	Southeastern United States	0.67
Tensile	Hoyle (1968)	Douglas-fir	15	1.0, 1.4, 1.8, 2.2	4, 8	Idaho	0.74
		White fir	14			Idaho	0.75
		Western hemlock	15			Western Oregon, Washington	0.81

[a]Grades are by regional rules in use at time of research. Western Products Association and West Coast Lumber Inspection Bureau Grades: SS, Select Structural; S, Standard; E, Economy. Western Wood Products Association Grades: 1, 2, 3. Machine Stress Grades: 1.0, 1.4, 1.8, 2.2.

[b]1 in. = 25.4 mm.

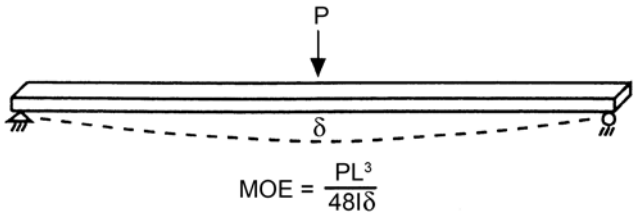

Figure 2.1—Centerpoint loading test setup.

$$\text{MOE} = \frac{PL^3}{48I\delta} \tag{2.1}$$

where P is applied load (lb), L is span (in.), I is moment of inertia (in^4), and δ is midspan deflection (in.).

Alternative Bending Test Setup

Figure 2.2 shows an alternative bending test setup. The only difference between this setup and a centerpoint setup is that equal loads are applied at a known distance from each end. MOE of a specimen is calculated using

$$\text{MOE} = \frac{Pa\left(3L^2 - 4a^2\right)}{48I\delta} \tag{2.2}$$

For both test setups, significant attention must be placed on design of the end supports. Ideally, the supports should be rigid so that no vertical displacement of the supports occurs. In addition, horizontal movement of the specimen on the end support should not be restricted, and the end supports need to be rotated and fixed to accommodate twist in the specimen.

Transverse Vibration Techniques

Background

Transverse vibration techniques have received considerable attention for nondestructive evaluation (NDE) applications. To illustrate these methods, an analogy can be drawn between the vibration of a mass that is attached to a weightless spring and internal damping force and the behavior of a vibrating beam (Fig. 2.3). In Figure 2.3, mass M is supported from a rigid body by a weightless spring whose stiffness is denoted by K. Internal friction or damping is represented by the dashpot D. A forcing function equaling $P_0 \sin \omega t$ or zero is applied for forced and free vibration, respectively. When M is set into vibration, its equation of motion can be expressed by the following:

$$M\left(\frac{d^2x}{dt^2}\right) + D\left(\frac{dx}{dt}\right) + Kx = P_0 \sin \omega t \tag{2.3}$$

Equation (2.3) can be solved for either K or D. A solution for K will lead to an expression for modulus of elasticity

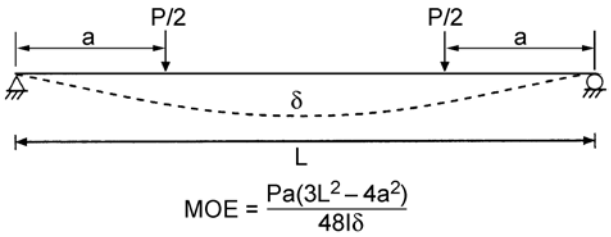

Figure 2.2—Alternative bending test setup.

(MOE) where for a beam freely supported at two nodal points

$$\text{MOE} = \frac{f_r^2 WL^3}{12.65Ig} \tag{2.4}$$

and for a beam simply supported at its ends

$$\text{MOE} = \frac{f_r^2 WL^3}{2.46Ig} \tag{2.5}$$

In Equations (2.4) and (2.5),

MOE is	dynamic modulus of elasticity (lb/in^2, Pa),
f_r	resonant frequency (Hz),
W	beam weight (lb, kg·g),
L	beam span (in., m),
I	beam moment of inertia (in^4, m^4), and
g	acceleration due to gravity (386 in/s^2, 9.8 m/s^2).

Solving Equation (2.3) for D leads to an expression of the internal friction or damping component. The logarithmic decrement of vibrational decay δ is a measure of internal friction and can be expressed in the form (for free vibrations)

$$\delta = \frac{1}{n-1} \ln \frac{A_1}{A_n} \tag{2.6}$$

where A_1 and A_n are the amplitudes of two oscillations $n - 1$ cycles apart (Fig. 2.4).

For forced vibrations,

$$\delta = \frac{\pi \Delta f}{f_r} \frac{1}{\sqrt{\left(A_r / A\right)^2 - 1}} \tag{2.7}$$

where Δf is difference in frequency of two points of amplitude A on each side of a resonance curve, f_r is frequency at resonance, and A_r is amplitude at resonance (Fig. 2.4b).

Sharpness of resonance Q is frequently used to measure damping capacity; Q is defined as the ratio $f_r/\Delta f$. Note that if the value $0.707A_r$ (half-power point method) is substituted for A in Equation (2.7), the equation reduces to

$$\delta = \frac{\pi \Delta f}{f_r} \tag{2.8}$$

and

$$Q = \frac{\pi}{\delta} \tag{2.9}$$

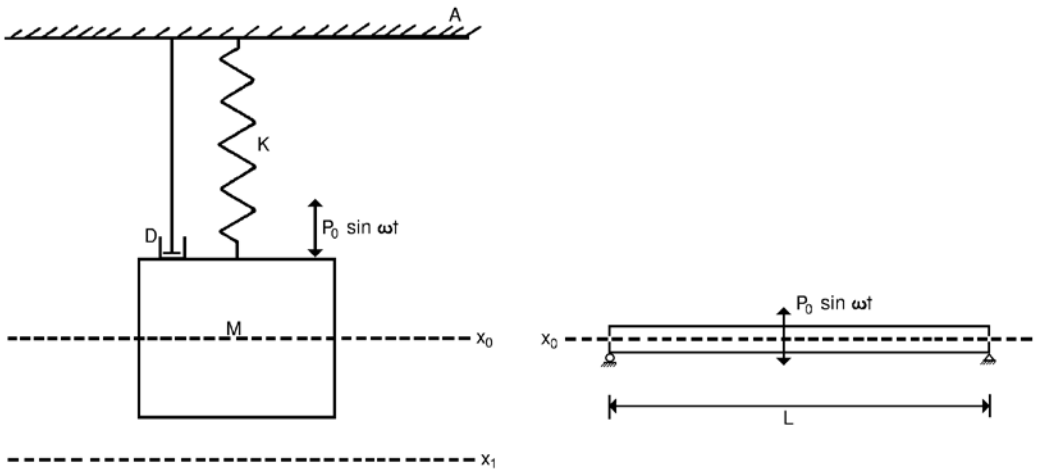

Figure 2.3—Mass-spring dashpot vibration model (left) and transversely vibrating beam (right).

Research and Development

Table 2.4 summarizes research on the use of transverse vibration NDE techniques. Jayne (1959) designed and conducted one of the first studies that used these techniques for evaluating the strength of wood. He was successful in demonstrating a relationship between energy storage and dissipation properties measured by forced transverse vibration techniques and the static bending properties of small clear wood specimens. Using a laboratory experimental setup, Jayne (1959) was able to determine the resonant frequency of a specimen from a frequency response curve. In addition, sharpness of resonance (energy loss) was obtained using the half-power point method.

Pellerin (1965a,b) used a similar experimental setup to examine the free transverse vibration characteristics of dimension lumber and glulam timbers. After obtaining a damped sine waveform for a specimen, he analyzed it using equations for MOE and logarithmic decrement. Measured values of MOE and logarithmic decrement were then compared to static MOE and strength values. O'Halloran (1969) used a similar apparatus and obtained comparable results with softwood dimension lumber. Wang et al. (1993) used transverse vibration techniques to evaluate the static bending MOE of structural lumber. Ross et al. (1991) obtained comparable results through coupling relatively inexpensive personal computer technologies and transverse vibration NDE techniques. Research on the use of transverse vibration techniques to assess the potential of hardwood lumber for structural applications is summarized in Table 2.5.

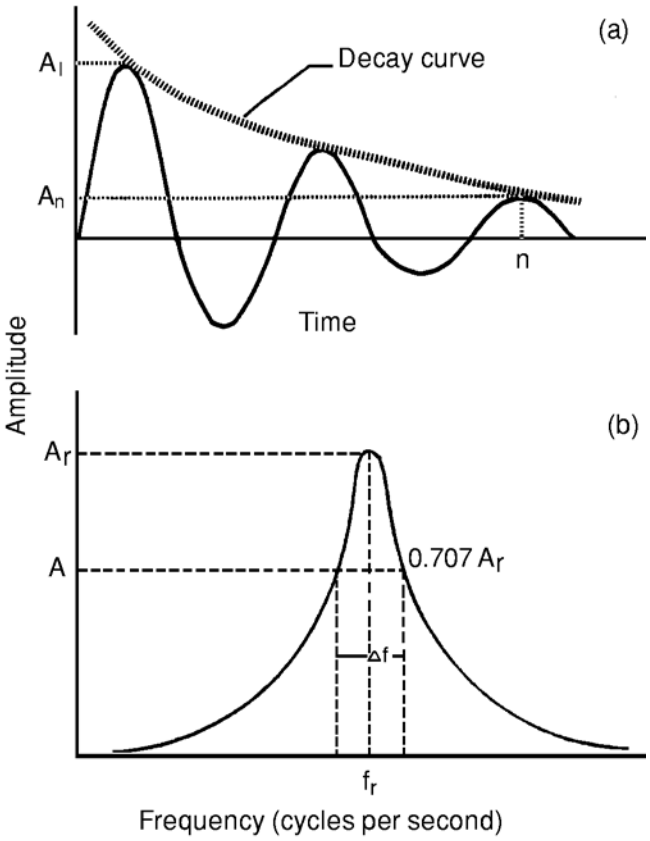

Figure 2.4—Transverse vibration of a beam: (a) damped sine wave for a free vibration, (b) frequency response curve for a forced vibration.

The use of transverse vibration techniques has evolved considerably, especially in the 1990s. Excellent equipment that uses free transverse vibration techniques is described in Table 2.6. The equipment uses relatively low-cost personal computer technologies as part of their data acquisition and computing package. This equipment is used by lumber grading agencies and research organizations worldwide to assist in assessing the potential yield of structural lumber that can be obtained from a given wood species or species group.

Table 2.4—Summary of research using transverse vibration nondestructive evaluation techniques[a]

Reference	NDE technique	Material	NDE parameter measured	Static test	Reported properties	Comparison of NDE parameters and properties (correlation coefficient *r*, unless noted)
Jayne (1959)[b]	Forced tranverse vibration	Small clear Sitka spruce specimens	Resonant frequency, E_d, Q	Bending	E_{SB}, MOR	E_{SB} and E_d, 1,00,000 lb/in^2 MOR and E_d, 1,000 lb/in^2 MOR and E_d, 1,000 lb/in^2 MOR and density/Q, ± 1,000 lb/in^2 MOR and E_d/δ, ± 900 lb/in^2
Pellerin (1965a)	Free transverse vibration	Douglas-fir glulam	Natural frequency, E_d, δ	Bending	E_{SB}, MOR	Predicted relative strength of three glued-laminated members
Pellerin (1965b)	Free transverse vibration	Inland Douglas-fir dimension lumber	Natural frequency, E_d,δ	Bending	E_{SB}, MOR	E_{SB} and E_d, 0.98 MOR and E_d, 0.67–0.93 MOR and 1/δ, 0.46–0.88 MOR and 1/δ, 0.68–0.92
O'Halloran (1969)	Free transverse vibration	Lodgepole pine dimension lumber	Natural frequency, E_d, δ	Bending	E_{SB}, MOR	E_{SB} and E_d, 0.98 MOR and E_d, 0.89 MOR and 1/δ, 0.82 MOR and E_d/δ, 0.91
Wang et al. (1993)	Free transverse vibration	Spruce–Pine–Fir dimension lumber	E_d	Bending	E_{SB}	E_{SB} and E_d, 0.96–0.99
Ross et al. (1991)	Free transverse vibration	Spruce–Pine–Fir dimension lumber	E_d	Bending	E_{SB}	E_d and E_{SB}, 0.99

[a]δ, logarithmic decrement; E_d, dynamic modulus of elasticity (MOE); E_{SB}, MOE obtained from static bending test; MOR, modulus of rupture; Q, sharpness of resonance. 1 lb/in^2 = 6.9 kPa.
[b]Correlation coefficients were not reported by Jayne. However, he did report 95% confidence intervals.

Table 2.5—Summary of research on the correlation between modulus of elasticity and other mechanical properties of hardwood lumber[a]

Reference	Species group	Nominal moisture content (%)	Grade[b]	Nominal width (in.)	Growth location	NDE technique	Static property	Correlation coefficient
Green and McDonald (1993a)	Northern red oak (*Quercus velutina, Q. rubra*)	12	1, 2, 3	4	Central Wisconsin	Transverse vibration (flatwise)	E_{SB}, UCS, UTS, MOR	E_{SB} and E_d, 0.92 MOR and E_d, 0.58 UTS and E_d, 0 54 UCS and Ed, 0.70 E_{SB} and E_d, 0.85
Green and McDonald (1993b)	Maple (*Acer rubra*)	12	SS, 2, 3	4	Central Vermont	Transverse vibration (flatwise)	E_{SB}, UCS UTS, MOR	E_{SB} and E_d, 0.85 E_{SB} and E_d, 0.42 UTS and E_d, 0.46 UTS and E_d, 0.60

[a]E_d, dynamic modulus of elasticity (MOE) obtained from transverse vibration measurements; E_{SB}, MOE obtained from static bending test; MOR, modulus of rupture; UTS, ultimate tensile stress; UCS, ultimate compressive stress. 1 lb/in^2 = 6.9 kPa.
[b]Grades by procedures given in the National Grading Rule performed by a quality supervisor of Southern Pine Inspection Bureau.
SS, Select Structural.

Table 2.6—Equipment for free transverse vibration techniques

Manufacturer	Description of equipment
Metriguard, Inc. 2465 NE Hopkins Court Pullman, WA 99163 www.metriguard.com	Model 340 Transverse Vibration E Computer—Measures modulus of elasticity, weight, specific gravity, and damping ratio from transverse vibration of simply supported specimens.

Essential Laboratory Testing Procedures and Key Information

Figure 2.5 illustrates a typical free transverse vibration test setup. The specimen is simply supported at both ends. A slight deflection is introduced at the midspan of the specimen. The specimen is then allowed to freely oscillate in the vertical (transverse) direction. Frequency of oscillation is determined and, along with the specimen weight and dimensions, used to compute MOE. The MOE is calculated from the following formula:

$$\text{MOE} = \frac{f^2 W S^3}{2.46 I g} \qquad (2.10)$$

where

f is resonant frequency (Hz),

W weight of specimen (lb),

S span (in.),

I moment of inertia (in^4), and

g acceleration due to gravity (386 in/s^2).

Three elements are essential to the test setup: a support apparatus, an excitation system, and a measurement system.

Support Apparatus

- The apparatus should provide vertical support to the ends of the specimen yet permit rotation.
- The specimen should be supported so as to prevent damage at the point of contact between the specimen and the reaction support. The reactions should be such that shortening and rotation of the specimen about the reaction resulting from deflection are not restricted.
- Provisions should be made at the reactions to allow for initial twist in the length of the specimen. If the bearing surfaces of the specimen at its reaction are not parallel, the specimen should be shimmed or the bearing surfaces rotated about an axis parallel to the span to provide adequate bearing across the width of the specimen.
- No lateral support should be applied. Specimens unstable in this mode should not be tested.
- The specimen should be positioned such that an equal portion of the length overhangs each support. Excessive overhang may alter results. If Equation (2.10) is used,

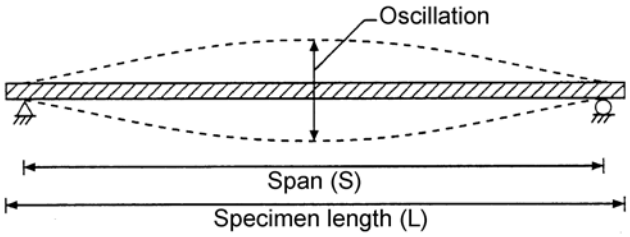

Figure 2.5—Schematic of typical free transverse vibration test setup.

the span to length (S/L) ratio of the specimen should exceed 0.98. Other S/L ratios may be used, but a more exacting analysis and equation are needed (Murphy 1997). An overhang of approximately 1 in. (25.4 mm) on each end is often used in tests of dimension lumber. The amount of overhang may be influenced by the convenience of handling and positioning, but it should be kept uniform from specimen to specimen.

Excitation System

- The member should be excited so as to produce a vertical oscillation in a reproducible manner in the fundamental mode.
- Manual deflection of the specimen will provide sufficient impetus for oscillation for many products. The deflection should be vertical with an effort to exclude lateral components; neither excessive impact nor prolonged contact with the specimen is recommended. For example, a manual tap on a 16-ft. (4.8-m) nominal 2- by 12-in. (standard 38- by 286-mm) piece of lumber with MOE of 2.0 × 10^6 lb/in^2 (13.8 GPa) and supported flatwise will result in a vertical oscillation of 3 to 4 Hz.
- Specimens with very high stiffness require mechanical excitation by a high force or carefully regulated impact/release.

Measurement System

- Measurement of the frequency of oscillation should be obtained by either a force or displacement measuring device.
- Changes in force in response to the vibration at one or both supports are used to obtain frequency of oscillation.
- Frequency of oscillation can also be determined by measuring midspan displacement in response to initial displacement.

- It is critical that only the frequency associated with the fundamental vertical oscillation mode be used. Immediately after the specimen is excited, many vibration modes appear. The modes associated with higher frequencies than the fundamental bending frequency usually dissipate rapidly. Therefore, a short delay is necessary before acquiring the data to ensure that the data are related only to the fundamental vertical mode. This is an effective way to filter undesired modes from the data.
- The span-to-depth ratio should be greater than 60 unless special precautions are taken to permit higher frequency measurements. With small span-to-depth ratios, it is difficult to verify that the specimen is oscillating in a bending mode. Best results are obtained when the frequency of oscillation is less than 30 Hz.

Longitudinal Stress Wave Techniques

Background

Several techniques that employ stress wave propagation have been researched for use as NDE tools. Speed-of-sound transmission and attenuation of induced stress waves in a material are frequently used as NDE parameters.

To illustrate longitudinal stress wave techniques, consider application of one-dimensional wave theory to a homogeneous viscoelastic bar (Fig. 2.6). After an impact hits the end of the bar, a compression wave is generated. This wave immediately begins moving down the bar as particles at the leading edge of the wave become excited, while particles at the trailing edge come to rest. The wave depth or the distance between the leading and trailing edges of the wave is controlled by the length of the impactor and the velocity of propagation of the material that makes up the impactor. The wave moves along the bar at a constant speed, but its individual particles have only small longitudinal movements as a result of the wave passing over them. After traveling the length of the bar, this forward-moving wave impinges on the free end of the bar and is reflected as a tensile wave traveling back down the bar (Fig. 2.7). The velocity of the wave is independent of the intensity of the impact.

Energy is dissipated as the wave travels through the bar; therefore, although the speed of the wave remains constant, movement of particles diminish with each successive passing of the wave. Eventually all particles of the bar come to rest. Monitoring the movement of a cross section near the end of such a bar in response to a propagating stress wave results in waveforms that consist of a series of equally spaced pulses whose magnitude decreases exponentially with time (Fig. 2.8).

The propagation speed C of such a stress wave can be determined by coupling measurements of the time between pulses, Δt, and the length of the bar L by

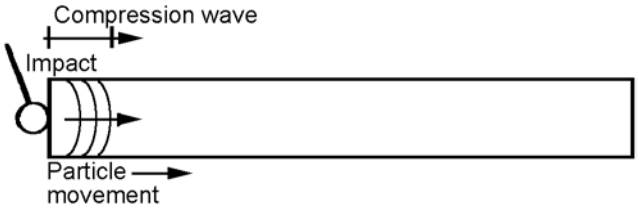

Figure 2.6—Viscoelastic bar of length L subjected to an impact.

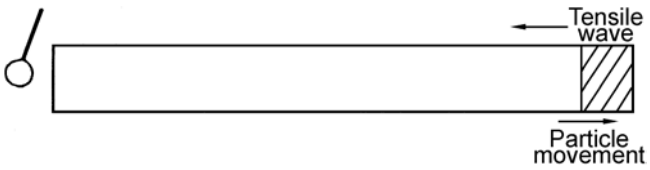

Figure 2.7—Travel of compression wave along bar. The forward-moving wave impinges on the free end of the bar, is reflected as a tensile wave, and begins to travel back down the bar.

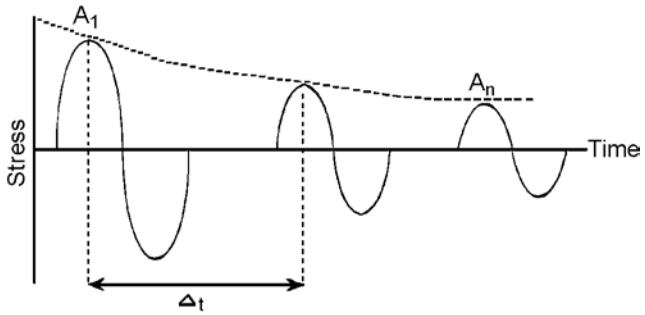

Figure 2.8—Waveforms consist of a series of equally spaced pulses whose magnitude decreases exponentially with time.

$$C = \frac{2L}{\Delta t} \tag{2.11}$$

The MOE can be computed using C and the mass density of the bar ρ:

$$\text{MOE} = C^2 \rho \tag{2.12}$$

Wave attenuation can be determined from the rate of decay of the amplitude of pulses using Equation (2.6) for logarithmic decrement.

Note that wave attenuation calculated by this formula is highly dependent upon characteristics of the excitation system used. Thus, results reported by various researchers cannot be directly compared because several excitation systems were employed. Nonetheless, these results show that energy loss characteristics as measured by stress wave techniques provide useful information on the performance of wood-based materials.

A more rigorous treatise on the measurement of energy loss by stress wave techniques is presented by Kolsky (1963). In

general, a more appropriate method for evaluating energy loss would be to determine the quantity of energy imparted into a member and the corresponding rate of energy loss. Loss of energy would be calculated using an integral of a waveform, as is done for determining the energy emitted during acoustic emission testing of materials (Harris et al. 1972). This is defined as the root mean square (RMS) value.

Wood is neither homogeneous nor isotropic; therefore, the usefulness of one-dimensional wave theory for describing stress wave behavior in wood could be considered dubious. However, several researchers have explored application of the theory by examining actual waveforms resulting from propagating waves in wood and wood products and have found that one-dimensional wave theory is adequate for describing wave behavior. For example, Bertholf (1965) found that the theory could be used to accurately predict dynamic strain patterns in small wood specimens. He verified predicted stress wave behavior with actual strain wave measurements as well as dependence of propagation velocity on the MOE of clear wood. Ross (1985) examined wave behavior in both clear wood and wood-based composites and observed excellent agreement with one-dimensional theory. Similar results were obtained with clear lumber in tests conducted by Kaiserlik and Pellerin (1977).

An interesting series of experiments designed to explore wave behavior in lumber was conducted by Gerhards (1981, 1982). He observed changes in the shape of a wave front in lumber containing knots and cross grain by measuring the change in wave speed in the vicinity of such defects. He concluded that a stress wave traveling in lumber containing knots and cross grain does not maintain a planar wave front.

One common technique that employs stress wave NDE technology uses simple time-of-flight type measurement systems to determine stress wave propagation speed (Figs. 2.9 and 2.10). In these measurement systems, a mechanical or ultrasonic impact is used to impart a longitudinal wave into a member. Piezoelectric sensors are placed at two points on the member and used to sense passing of the wave. The time required for the wave to travel between sensors is measured and used to compute wave propagation speed.

Stress wave transmission times on a per length basis for various wood species are summarized in Table 2.7. Note that stress wave transmission times are shortest along the grain (parallel to fiber) and longest across the grain (perpendicular to fiber). Note that for Douglas-fir and Southern Pine, stress wave transmission times parallel to the grain are approximately 200 μs/m (60 μs/ft). Stress wave transmission times perpendicular to the grain range from 850 to 1,000 μs/m (259 to 305 μs/ft).

Several research projects have been conducted on the use of one-dimensional wave theory for assessing the MOE of clear wood, lumber, and veneer. These studies have examined relationships between MOE values obtained from stress

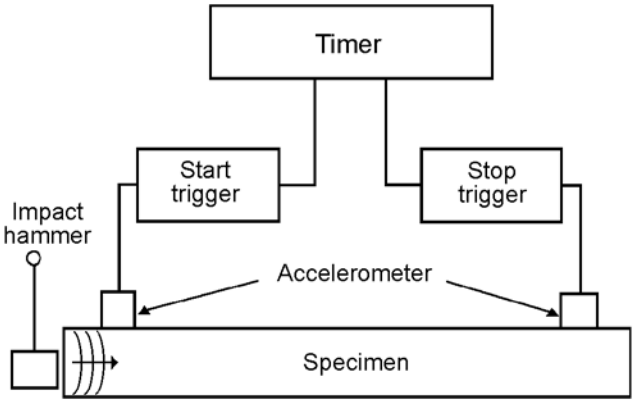

Figure 2.9—System used to measure impact-induced stress wave propagation speed in various wood products.

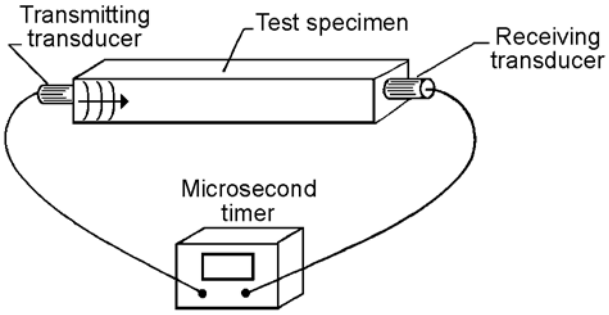

Figure 2.10—Ultrasonic measurement system used to measure speed-of-sound transmission in various wood products.

wave measurements and those obtained by static testing techniques. The strong correlative relationships found in these studies are shown in Table 2.8.

Table 2.9 summarizes research on the use of longitudinal stress wave techniques for assessing the strength properties of lumber and composite products. Kaiserlik and Pellerin (1977), for example, used stress wave techniques to evaluate the tensile strength of a small sample of clear lumber containing varying degrees of slope of grain. They used the one-dimensional wave equation, Equation (2.11), to compute MOE and the equation presented by Pellerin (1965b) for logarithmic decrement.

Extensive research has been conducted on the use of stress wave techniques for assessing the mechanical properties of wood composites (Fagan and Bodig 1985; Pellerin and Morschauser 1974; Ross 1984; Ross and Pellerin 1988; Vogt 1985). Pellerin and Morschauser (1974) used the setup in Figure 2.11 to show that stress wave speed could be used to predict the flexural behavior of underlayment-grade particleboard. Ross (1984) and Ross and Pellerin (1988) showed that wave attenuation is sensitive to bonding characteristics and is a valuable NDE parameter that contributes significantly to the prediction of tensile and flexural mechanical

Table 2.7—Summary of research on stress wave transmission times for various wood species

Reference	Species	Moisture content (% ovendry)	Stress wave transmission time (μs/m (μs/ft)) Parallel to grain	Perpendicular to grain
Smulski (1991)	Sugar maple	12	256–194 (78–59)	—
	Yellow birch	11	230–180 (70–55)	—
	White ash	12	252–197 (77–60)	—
	Red oak	11	262–200 (80–61)	
Armstrong et al. (1991)	Birch	4–6	213–174 (65–53)	715–676 (218–206)
	Yellow-poplar	4–6	194–174 (59–53)	715–676 (218–206)
	Black cherry	4–6	207–184 (63–56)	689–620 (210–189)
	Red oak	4–6	226–177 (69–54)	646–571 (197–174)
Elvery and Nwokoye (1970)	Several	11	203–167 (62–51)	—
Jung (1979)	Red oak	12	302–226 (92–69)	—
Ihlseng (1878, 1879)	Several	—	272–190 (83–58)	—
Gerhards (1978)	Sitka spruce	10	170 (52)	—
	Southern Pine	9	197 (60)	
Gerhards (1980)	Douglas-fir	10	203 (62)	—
Gerhards (1982)	Southern Pine	10	197–194 (60–59)	—
Rutherford (1987)	Douglas-fir	12	—	1,092–623 (333–190)
Ross (1982)	Douglas-fir	—	—	850–597 (259–182)
Hoyle and Pellerin (1978)	Douglas-fir	9	—	1,073 (327)
Pellerin et al. (1985)	Southern Pine	9	200–170 (61–52)	613–1,594 (187–486)
Soltis et al. (1992)	Live oak	12	—	613–1,594 (187–486)
Ross et al. (1994)	Northern red and white oak	Green	—	795 (242)

Table 2.8—Summary of research on correlation between stress wave and static modulus of elasticity of clear wood, lumber, and veneer

Reference	Material	Static loading	Correlation coefficient *r*
Bell et al. (1954)	Clear wood	Compression	0.98
	Clear wood	Bending	0.98
Galligan and Courteau (1965)	Clear wood	Bending	0.96
	Lumber		
Koch and Woodson (1968)	Veneer	Tension	0.96–0.94
Porter et al. (1972)	Lumber	Bending	0.90–0.92
Pellerin and Galligan (1973)	Lumber	Bending	0.96
	Veneer	Tension	0.96
McAlister (1976)	Veneer	Tension	0.99
Gerhards (1982)	Knotty lumber	Bending	0.87
	Clear lumber	Bending	0.95

behavior of wood-based particle composites. Vogt (1985) examined the use of stress wave techniques with wood-based fiber composites. In an additional study, Vogt (1986) found a strong relationship between internal bond and stress wave parameters of particle and fiber composites.

The use of stress wave techniques with wood subjected to different levels of biodeterioration, which adversely affects mechanical properties, has been limited to studies that have employed only energy storage parameters (Table 2.10). For example, Pellerin et al. (1985) showed that stress wave speed could used to monitor the degradation of small, clear wood specimens exposed to brown-rot fungi. They showed a strong correlative relationship between stress wave speed and parallel-to-grain compressive strength of exposed wood. Rutherford et al. (1987) showed similar results. These authors also revealed that MOE perpendicular to the grain, measured using stress wave NDE techniques, was significantly affected by degradation from brown-rot decay and could be used to detect incipient decay. Chudnoff et al. (1984) reported similar results from experiments that utilized an ultrasonic measurement system and several hard-wood and softwood species. Patton-Mallory and De Groot

Table 2.9—Summary of results from studies using nondestructive stress wave testing techniques on lumber and wood composite products[a]

Reference	NDE technique	Material	NDE parameter measured	Static test	Reported properties	Comparison of NDE parameters and static properties (correlation coefficient *r*, unless noted)
Kaiserlik and Pellerin (1977)	Longitudinal stress wave	Douglas-fir boards	C E_d, δ	Tension	UTS	UTS and E_d, 0.84; UTS and combination of E_d, δ, 0.90
Pellerin and Morschauser (1974)	Longitudinal stress wave	Underlayment particleboard	C	Bending	E_{SB}, MOR	E_{SB}, and C^2, 0.93–0.95 MOR and C^2, 0.87–0.93
Ross (1984), Ross and Pellerin (1988)	Longitudinal stress wave	Underlayment and industrial particleboard, structural panel products	C, E_d, δ	Tension	E_{ST}, UTS	E_{ST} and C^2, 0.98 E_{ST} and E_d, 0.98 UTS and C^2, 0.91 UTS and E_d, 0.93 UTS and 1/δ, 0.63 UTS and combination of E_d, 1/δ, 0.95
Fagan and Bodig (1985)	Longitudinal stress wave	Wide range of wood composites	C	Bending	MOR	Simulated and actual MOR distributions were similar.
Vogt (1985)	Longitudinal stress wave	Medium-density fiberboard	C, E_d, δ	Tension	E_{ST}, UTS	E_{ST} and C^2, 0.90 E_{ST} and E_d, 0.88 UTS and C^2, 0.81 E_{SB}, and E_d, Combination, 0.88
		Underlayment and industrial particleboard		Bending	ESB, MOR	E_{SB}, and C^2, 0.76 E_{SB}, and E_d, 0.72 MOR and C^2, 0.96 MOR and C^2, 10.92 Combination, 0.97
Vogt (1986)	Stress wave (through transmission)	Underlayment and industrial particleboard, structural panel products	C_t, E_{dt}	Internal bond	IB	IB and C_t^2, 0.70–0.72 IB and E_{dt}, 0.80–0.99

[a] C, speed of sound; C_t, speed-of-sound transmission through thickness; δ, logarithmic decrement; E_d, dynamic modulus of elasticity (MOE) from transverse vibration or stress wave measurements; E_{dt}, dynamic MOE through thickness orientation; E_{SB}, MOE from static bending test; IB, internal bond; MOR, modulus of rupture; UTS, ultimate tensile stress.

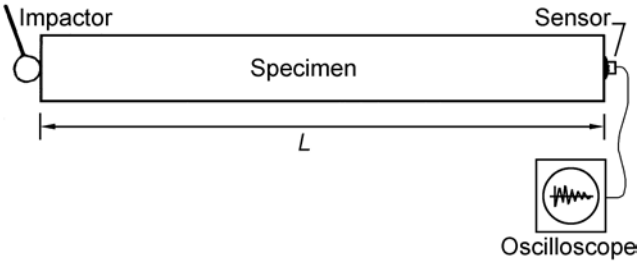

Figure 2.11—Typical pulse echo test setup.

(1989) reported encouraging results from a fundamental study dealing with the application of acousto-ultrasonic techniques. Their results showed that energy loss parameters may provide useful additional information on early strength loss from incipient decay caused by brown-rot fungi.

Verkasalo et al. (1993) and Ross et al. (1992) obtained encouraging results when using stress wave techniques to identify bacterially infected red oak. They found that speed of sound transmission perpendicular to the grain was significantly slower in sections of wood containing bacterial infection.

Stress wave techniques, especially those relying on measurement of transmission times, are used worldwide. Current manufacturers of stress wave timing equipment are listed in Table 2.11.

Essential Laboratory Testing Procedures and Key Information

The following text describes essential laboratory testing procedures and additional key information for using stress wave measurements in a laboratory environment.

Pulse Echo Test Setup

Figure 2.11 illustrates a typical pulse echo test setup. An impact or "pulse" on one end of the specimen induces a

Table 2.10—Research summary of correlation between nondestructive testing parameters and properties of degraded wood

Reference	NDE technique	Material	Degradation agent	NDE parameter measured	Static test	Reported properties	Comparison of NDE parameters and static properties (correlation coefficient *r*, unless noted)
Chudnoff et al. (1985)	Longitudinal stress wave (parallel to the grain)	Decayed and sound mine props; 26 species or species groupings	—	E_d	Compression parallel to grain	E_c, UCS	E_c and E_d, 0.84–0.97 (all species combined, hardwoods, maple, and oaks) E_c and E_d, 0.73–0.81 (all species, combined, southern pines, lodgepole pine) UCS and E_d, 0.85–0.95 (all species combined, hardwoods, maple, and oaks)
Pellerin et al. (1985)	Longitudinal stress wave (parallel to the grain)	Small clear southern yellow pine specimens	Brown rot fungi (*Gloeophyllum trabeum*)	C, E_d	Compression parallel to grain	UCS	UCS and *C*: 0.47 (control) 0.73 (exposed) 0.80 (control and exposed) UCS and E_d, 0.86 (control) 0.86–0.89 (exposed) 0.94 (control and exposed)
			Termites (subterranean)	C, E_d			UCS and C: 0.65 (control) 0.21 (exposed) 0.28 (control and exposed) UCS and E_d: 0.90 (control) 0.79 (exposed) 0.80 (control and exposed)
Rutherford (1987), Rutherford et al. (1987)	Longitudinal stress wave (parallel to the grain)	Small, clear Douglas-fir specimens	Brown-rot fungi (*Gloeophyllum trabeum*)	C, E_d	Compression parallel to the grain	E_c, UCS	E_c and *C*, 0.91 E_c and E_d, 0 94 UCS and *C*, 0.67–0.70 UCS and E_d, 0 79 UCS and MOE, 0.80
Patton-Mallory and De Groot (1989)	Longitudinal stress wave	Small, clear southern yellow pine specimens	Brown rot fungi (*Gloeophyllum trabeum*)	*C*, root mean square voltage frequency content of received signal	Bending	Maximum moment, alkali solubility	Linear decrease in *C* and decrease in strength with increased wood degradation. High-frequency components of signal attenuated in very early stages of decay.
Ross et al. (1992)	Longitudinal stress wave (parallel to the grain)	Red and white oak lumber	Bacteria (*Clostridium* and *Erwinia* sp.)	*C*	None	Presence of infection	Decrease in *C* with presence of infection
Verkasalo et al. (1993)	Longitudinal stress wave (perpedicular to the grain)	Red oak lumber	Bacteria (*Clostridium* and *Erwinia* sp.)	*C*	Tension perpendicular to grain	UTS, presence of infection	Decrease in *C* and UTS with presence of infection

[a]AE, acoustic emission; *C*, speed of sound; E_c, modulus of elasticity (MOE) from static compression test; E_d, dynamic M or stress wave measurements; MOR, modulus of rupture; UCS, ultimate compressive stress; UTS, ultimate tensile stress.

wave to flow along the length of a specimen. The pulse is "echoed" from the opposite end of the specimen, hence the term pulse echo. Characteristics of waveforms observed when using the pulse echo technique are highly dependent upon the type of sensor used. Various types of sensors, including those that measure particle displacement, particle velocity, and particle acceleration or strain, can be used with this type of test setup. Figure 2.12 illustrates example waveforms obtained by transducers that measure particle velocity and acceleration. Note that the time required for a pulse to

Table 2.11—Commercially available stress wave timing equipment

Manufacturer	Product	Website	Location
Agricef	USLab	www.agricef.com.br	
CBS-CBT	Sylvatest-Duo	www.cbs-cbt.com	Saint-Sulpice, Switzerland
Fakopp Enterprise	Various models	www.fakopp.com	Agfalva, Hungary
IML GmbH	IML Micro Hammer	www.imlusa.com	Moultonborough, New Hampshire, USA
Metriguard, Inc.	Models 239A Stress Wave Timer	www.metriguard.com	Pullman, Washington, USA
James Instruments, Inc.	V-Meter MK IV	www.ndtjames.com	Chicago, Illinois, USA
Olson Instruments, Inc.	Various models	www.olsoninstruments.com	Wheat Ridge, Colorado, USA

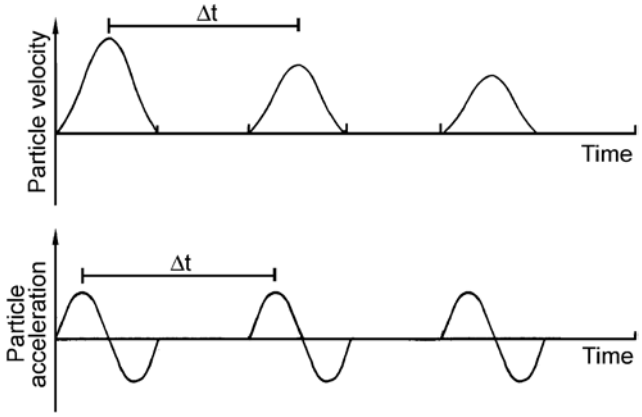

Figure 2.12—Example waveforms obtained by transducers that measure particle velocity and acceleration.

travel a round trip through the specimen can be obtained by using any of these transducers. The formula for transmission time is

$$\text{Transmission time} = \frac{\Delta t}{2L}$$

where Δt is time between pulses and L is specimen length. Note that this technique, as described, requires that both ends of the specimen are freely supported. A fixed end support condition will yield waveforms with different characteristics.

Pitch and Catch Test Setup

Figure 2.13 illustrates a typical pitch and catch test setup. A pulse is introduced in the specimen, sensed by a transducer, and then allowed to flow through the specimen. The leading edge of the pulse is then sensed by a second transducer located further down the specimen. A pitch and catch test setup yields an electronic signal similar to that illustrated in Figure 2.14. The time required for the wave or pulse to travel between the sensors can be calculated by the following equation:

$$\text{Transmission time} = \frac{\Delta t}{L}$$

where Δt is time between pulses and L is distance between transducers.

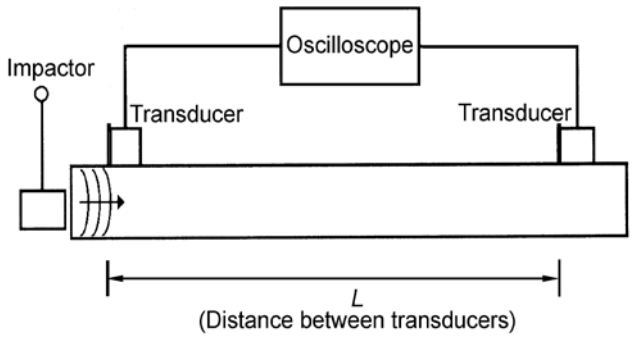

Figure 2.13—Typical pitch and catch test setup. Pulse is introduced in specimen, sensed by transducer, and allowed to flow through specimen.

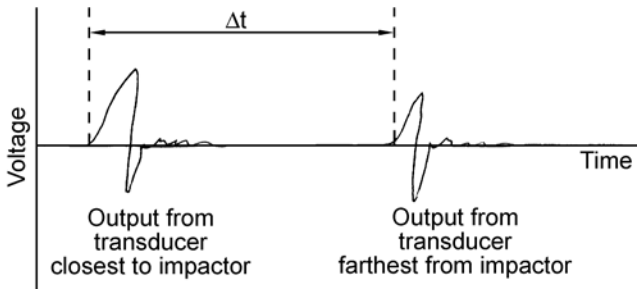

Figure 2.14—Electronic signal yielded by pitch and catch test setup.

There are two key points to consider when using the pitch and catch test setup:

1. The transducers must be in line with each other.
2. Many transducers are sensitive to the manner in which they are installed. For example, commonly used accelerometers yield wave forms that are strongly dependent upon which direction they sense the pulse. Note that in Figure 2.15, the base of the accelerometer directly faces an approaching compressive wave. Simply turning the accelerometer so that its base faces away from the approaching compressive wave changes the characteristics of the waveform.

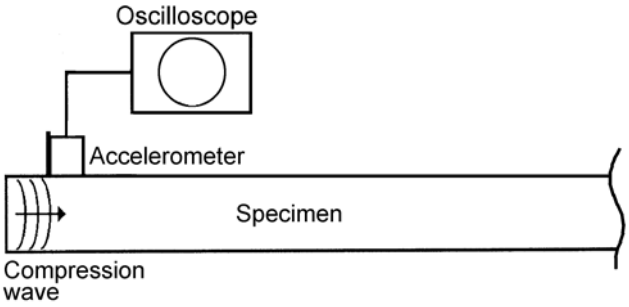

Figure 2.15—Accelerometer positioned so that its base faces approaching compressive wave. Orientation of accelerometer influences characteristics of waveform.

Literature Cited

Armstrong, J.P.; Patterson, D.W.; Sneckenberger, J.E. 1991. Comparison of three equations for predicting stress wave velocity as a function of grain angle. Wood and Fiber Science. 23(1): 32–43.

Bell, E.R.; Peck, E.C.; Krueger, N.T. 1950. Young's modulus of wood determined by a dynamic method. Rep. 1775. Madison, WI: U.S. Department of Agriculture, Forest Service, Forest Products Laboratory.

Bell, E.R.; Peck, E.C.; Krueger, N.T. 1954. Modulus of elasticity of wood determined by dynamic methods. Rep. 1977. Madison, WI: U.S. Department of Agriculture, Forest Service, Forest Products Laboratory.

Bertholf, L.D. 1965. Use of elementary stress wave theory for prediction of dynamic strain in wood. Bull. 291. Pullman, WA: Washington State University, College of Engineering.

Corder, S.E. 1965. Localized deflection related to bending strength of lumber. In: Proceedings, 2nd nondestructive testing of wood symposium; 1965 April; Spokane, WA. Pullman, WA: Washington State University: 461–472.

Chudnoff, M.; Eslyn, W.E.; McKeever, D.B. 1984. Decay in mine timbers: Part III, Species-independent stress grading. Forest Products Journal. 34(3): 43–50.

Doyle, D.V.; Markwardt, L.J. 1966. Properties of Southern Pine in relation to strength grading of dimension lumber. Res. Pap. FPL–RP–64. Madison, WI: U.S. Department of Agriculture, Forest Service, Forest Products Laboratory.

Elvery, R.H.; Nwokoye, D.N. 1970. Strength assessment of timber for glued laminated beams. In: Proceedings, Paper II, Nondestructive testing of concrete and timber, organized by the Institution of Civil Engineering and the British Commission for Nondestructive Testing; 1969 June 11–12. London, BC: Institute of Civil Engineering: 105–110.

Fagan, G.B.; Bodig, J. 1985. Computer simulation as a nondestructive evaluation tool. In: Proceedings, 5th nondestructive testing of wood symposium; 1985 September 9–11; Pullman, WA. Pullman, WA: Washington State University: 3–37.

Galligan, W.L.; Courteau, R.W. 1965. Measurement of elasticity of lumber with longitudinal stress waves and the piezo-electric effect of wood. In: Proceedings, 2nd nondestructive testing of wood symposium; 1965 April; Spokane, WA. Pullman, WA: Washington State University: 223–244.

Gerhards, C.C. 1978. Effect of earlywood and latewood on stress-wave measurements parallel to the grain. Wood Science. 11(2): 69–72.

Gerhards, C.C. 1980. Effect of cross grain on stress waves in lumber. Res. Pap. FPL–RP–368. Madison, WI: U.S. Department of Agriculture, Forest Service, Forest Products Laboratory.

Gerhards, C.C. 1981. Effect of cross grain on stress waves in lumber. Res. Pap. FPL–RP–368. Madison, WI: U.S. Department of Agriculture, Forest Service, Forest Products Laboratory.

Gerhards, C.C. 1982. Effect of knots on stress waves in lumber. Res. Paper FPL–RP–384. Madison, WI: U.S. Department of Agriculture, Forest Service, Forest Products Laboratory.

Green, D.W.; McDonald, K.A. 1993a. Investigation of the mechanical properties of red oak 2 by 4's. Wood and Fiber Science. 25(1): 35–45.

Green, D.W.; McDonald, K.A. 1993b. Mechanical properties of red maple structural lumber. Wood and Fiber Science. 25(4): 365–374.

Harris, D.O.; Tetleman, A.S.; Darwish, F.A.I. 1972. Detection of fiber cracking by acoustic emission. Acoustic emission. ASTM 505. Philadelphia, PA: American Society for Testing and Materials. 11 p.

Hoerber, G.F. 1962. A study of modulus of elasticity and modulus of rupture in Douglas-fir dimension lumber. Lewiston, ID: Potlatch Forests, Inc.

Hofstrand, A.D.; Howe, J.P. 1963. Relationship between modulus of elasticity and compression strength of white fir. Lewiston, ID: Potlatch Forests, Inc.

Hoyle, R.J. 1961. A nondestructive test for stiffness of structural lumber. Forest Products Journal. 11(6): 251–254.

Hoyle, R.J. 1962. Analysis of relationship between stiffness and strength of 2" x 8" white fir (Abies grandis) used as joist and plank. Lewiston, ID: Potlatch Forests, Inc.

Hoyle, R.J. 1964. Research results on machine stress rated Southern Pine lumber. Lewiston, ID: Potlatch Forests, Inc.

Hoyle, R.J. 1968. Background to machine stress rating. Forest Products Journal. 18(4): 87–97.

Hoyle, R.J.; Pellerin, R.F. 1978. Stress wave inspection of

a wood structure. In: Proceedings, 4th symposium on nondestructive testing of wood. 1978 August 28-30; Vancouver, WA. Pullman, WA: Washington State University. 33–45.

Ihlseng, M.C. 1878. The modulus of elasticity in some American woods, as determined by vibration. Van Nostrand's Engineering Magazine. Vol. XIX: 8–9.

Ihlseng, M.C. 1879. On a mode of measuring the velocity of sound in wood. American Journal of Science. 3d Series. 17(98): 125–133.

Jayne, B.A. 1955. A nondestructive test of glue bond quality. Forest Products Journal. 5(5): 294–301.

Jayne, B.A. 1959. Vibrational properties of wood as indices of quality. Forest Products Journal. 9(11): 413–416.

Johnson, J.W. 1965. Relationships among moduli of elasticity and rupture. In: Proceedings, 2nd nondestructive testing of wood symposium; 1965 April; Spokane, WA. Pullman, WA: Washington State University: 419–457.

Jung, J. 1979. Stress wave grading techniques on veneer sheets. Gen. Tech. Rep. FPL–GTR–27. Madison, WI: U.S. Department of Agriculture, Forest Service, Forest Products Laboratory.

Kramer, P.R. 1964. Correlation of bending strength and stiffness of Southern Pine. Forest Products Journal. 14(10): 495–496.

Kaiserlik, J.H.; Pellerin, R.F. 1977. Stress wave attenuation as an indicator of lumber strength. Forest Products Journal. 27(6): 39–43.

Koch, P.; Woodson, G.E. 1968. Laminating butt-jointed, log-run southern pine veneers into long beams of uniform high strength. Forest Products Journal. 18(10): 45–51.

Kolsky, H. 1963. Stress waves in solids. New York: Dover Publications, Inc.

Littleford, T.W. 1965. Mechanical stress rating of western Canadian species. In: Proceedings, 2nd nondestructive testing of wood symposium; 1965 April; Spokane, WA. Pullman, WA: Washington State University: 475–485.

McAlister, R.H. 1976. Modulus of elasticity distribution of loblolly pine veneer as related to location within the stem and specific gravity. Forest Products Journal. 26(10): 37–40.

Miller, D.G. 1965. In: Proceedings, 2nd Nondestructive testing of wood symposium. 1965 April, Spokane, Washington. Pullman: Washington: Washington State University. 485–491.

Murphy, J.F. 1997. Transverse vibration of a simply supported beam with symmetric overhang of arbitrary length. Journal of Testing and Evaluation. 25(5): 522–524.

O'Halloran, M.R. 1969. Nondestructive parameters for lodgepole pine dimension lumber. Fort Collins, CO: Colorado State University. M.S. thesis.

Patton-Mallory, M.; De Groot, R.C. 1989. Acousto-ultrasonics for evaluating decayed-wood products. In: Proceedings, 2nd Pacific timber engineering conference; 1989 August 28–29; Auckland, New Zealand.

Pellerin, R.F. 1963a. Compression parallel to grain versus modulus of elasticity for Douglas-fir dimension lumber. Washington State University, Division of Industrial Research. Lewiston, ID: Potlatch Forest, Inc.

Pellerin, R.F. 1963b. Correlation of Strength properties of 1-inch lumber. Washington State University, Division of Industrial Research. Lewiston, ID: Potlatch Forests, Inc.

Pellerin, R.F. 1965a. The contributions of transverse vibration grading to design and evaluation of 55-foot laminated beams. In: Proceedings, 2nd nondestructive testing of wood symposium; 1965 April; Spokane, WA. Pullman, WA: Washington State University: 337–347.

Pellerin, RF. 1965b. A vibrational approach to nondestructive testing of structural lumber. Forest Products Journal. 15(3): 93–101.

Pellerin, R.F.; Galligan, W.L. 1973. Nondestructive method of grading wood materials. Canadian Patent 918286.

Pellerin, R.F.; Morschauser, C.R. 1974. Nondestructive testing of particleboard. In: Proceedings, 7th international particleboard symposium; 1973 March; Pullman, WA. Pullman, WA: Washington State University.

Pellerin, R.F.; De Groot, R.C.; Esenther, G.R. 1985. Nondestructive stress wave measurements of decay and termite attack in experimental wood units. In: Proceedings, 5th nondestructive testing of wood symposium; 1985 September 9–11; Pullman, WA. Pullman, WA: Washington State University: 319–353.

Porter, A.W.; Kusec, D.J.; Olson, S.L. 1972. Digital computer for determining modulus of elasticity of structural lumber. WFPL Info. Rep. VP–X–99. Vancouver, BC: Department of Environment, Canadian Forest Service.

Ross, R.J. 1982. Quality assessment of the wooden beams and columns of Bay C of the east end of Washington State University's football stadium. Unpublished research. Pullman, WA: Washington State University.

Ross, R.J. 1984. Stress wave speed and attenuation as predictors of the tensile and flexural properties of wood-based particle composites. Pullman, WA: Washington State University. Ph.D. dissertation.

Ross, R.J. 1985. Stress wave propagation in wood products. In: Proceedings, 5th nondestructive testing of wood symposium; 1985 September 9–11; Pullman, WA. Pullman, WA: Washington State University: 291–318.

Ross, R.J.; Pellerin, R.F. 1988. NDE of wood-based composites with longitudinal stress waves. Forest Products Journal. 38(5): 39–45.

Ross, R.J.; Geske, E.A.; Larson, G.L.; Murphy, J.F. 1991. Transverse vibration nondestructive testing using a personal computer. Res. Pap. FPL–RP–502. Madison, WI: U.S. Department of Agriculture, Forest Service, Forest Products Laboratory.

Ross, R.J.; Ward, J.C.; TenWolde, A. 1992. Identifying bacterially infected oak by stress wave nondestructive evaluation. Res. Pap. FPL–RP–512. Madison, WI: U.S. Department of Agriculture, Forest Service, Forest Products Laboratory.

Ross, R.J.; Ward, J.C.; TenWolde, A. 1994. Stress wave nondestructive evaluation of wetwood. Forest Products Journal. 48(7/8): 79–83.

Rutherford, P.S. 1987. Nondestructive stress wave measurement of incipient decay in Douglas Fir. Pullman, WA: Washington State University. M.S. thesis.

Rutherford, P.S.; Hoyle, R.J.; De Groot, R.C.; Pellerin, R.F. 1987. Dynamic vs. static MOE in the transverse direction in wood. In: Proceedings, 6th nondestructive testing of wood symposium; 1987 September 14–16; Pullman, WA. Pullman, WA: Washington State University: 67–80.

Smulski, S.J. 1991. Relationship of stress wave and static bending determined properties of four northeastern hardwoods. Wood and Fiber Science. 23(1): 44–57.

Soltis, L; Baker. A.; Ferge, L. [et al.]. 1992. USS Constitution—inspection and evaluation procedures for live and white oak members. Report submitted to U.S. Navy, Maintenance and Repair, USS Constitution, Boston Naval Shipyard, Charlestown, MA.

Sunley, J.G.; W.M. Hudson. 1964. Machine-grading lumber in Britain. Forest Products Journal. 14(4): 155–158.

Verkasalo, E.; Ross, R.J.; TenWole, A.; Youngs, R.L. 1993. Properties related to drying defects in red oak wetwood. Res. Pap. FPL–RP–516. Madison, WI: U.S. Department of Agriculture, Forest Service, Forest Products Laboratory.

Vogt, J.J. 1985. Evaluation of the tensile and flexural properties and internal bond of medium density fiberboard using stress wave speed and attenuation. Pullman, WA: Washington State University. M.S. thesis.

Vogt, J.J. 1986. Longitudinal stress waves as predictors of internal bond strength. In: Proceedings, 12th international particleboard/composite materials symposium; 1986 March; Pullman, WA. Pullman, WA: Washington State University.

Wang, Z.; Ross, R.J.; Murphy, J.F. 1993. A comparison of several NDE techniques for determining the modulus of elasticity of lumber. Wood Forestry Research. 6(4): 86–88. (In Chinese).

Additional Sources of Information

Galiginaitis, S.V.; Bell, E.R.; Fine, A.M. [et al.]. 1954. Nondestructive testing of wood laminates. Final report. Louisville, KY: Office of Naval Research, Institute of Industrial Research, University of Louisville.

James, W.L. 1959. A method for rapid measurement of the rate of decay of free vibrations. Bull. 2154. Madison, WI: U.S. Department of Agriculture, Forest Service, Forest Products Laboratory.

McKean, H.B.; Hoyle, R.J. 1962. Stress grading method for dimension lumber. Special Tech. Pub. 353. Philadelphia, PA: American Society for Testing Materials.

Chapter 3

Ultrasonic-Based Nondestructive Evaluation Methods for Wood

C. Adam Senalik, Research General Engineer
Greg Schueneman, Supervisory Research Materials Engineer
Robert J. Ross, Supervisory Research General Engineer

Forest Products Laboratory, Madison, Wisconsin

The purpose of this chapter is twofold: to provide a basic primer to nondestructive testing using ultrasonic inspection and to provide a literature review of the use of ultrasonic techniques in the inspection, characterization, classification, and evaluation of wood and wood products. This chapter does not present a detailed explanation of wave theory, a robust description of wave propagation through heterogeneous anisotropic mediums, such as wood, or derivations of fundamental equations. For a more rigorous explanation of ultrasonic wave motion through wood and foundational equations upon which the motion is based, the reader is directed to Bucur (2003, 2006, 2011a).

This chapter was originally published in 2014 as a Forest Products Laboratory General Technical Report:

> Senalik, C. Adam; Schueneman, Greg; Ross, Robert J. 2014. Ultrasonic-based nondestructive evaluation methods for wood: a primer and historical review. General Technical Report FPL–GTR–235. Madison, WI: U.S. Department of Agriculture, Forest Service, Forest Products Laboratory. 31 p.

Background

When preparing an ultrasonic test of a specimen, several factors must be considered. Among these are source, power, frequency, receiver, and coupling. These factors must be determined holistically for any inspection as the choice of any one affects the others. For example, a particularly large specimen might require high power for the signal to be observable. Generally the size at which internal defects are discernable is related to the frequency used to inspect the specimen; higher frequencies can detect smaller defects. The source selected must be capable of generating the necessary signal power at the desired frequency. The source may also act as the receiver, such as in a pulse-echo test setup. If the receiver is non-contact, such as a microphone or non-contact transducer, then no coupling is needed. If contact is necessary, then a coupling agent must be chosen that is adequate for the test and will not corrupt the condition of the specimen.

Sources generate stress waves that are used to inspect the specimen. A source may be anything capable of generating detectable stress waves. In a nondestructive test, the chosen source must be able to generate the desired signal without altering the condition of the specimen post-test. Two common external sources are mechanical impacts and piezoelectric transducers. The source may originate from within the specimen itself. Some internal phenomena are capable of generating a detectable emission. Microfractures, check formation, water movement, and pit aspiration are just a few internal phenomena in wood that may be detectable by external receivers. This type of inspection is known as acoustic emission.

Ultrasonic waves have frequencies of 20 kHz and higher. The resolution of any ultrasonic scan is dependent upon the frequency. As frequency increases, wavelength decreases. The smallest discernable feature during an ultrasonic scan is about one half the wavelength. Signal attenuation in wood increases as frequency increases; the phenomenon becomes more evident at higher frequencies. As attenuation increases, the energy loss of the wave as it transverses the wood cross section becomes large. Balance must be struck between obtaining the best resolution possible while maintaining an observable level of signal energy. Today, ultrasonic inspection equipment exists with sufficient power for inspection of standing trees and poles, but this has not always been the case. Historically, because of power limitations of the inspection equipment, ultrasonic waves have more commonly been used for inspection of members with smaller cross sections such as rectangular members and engineered wood products. Standing trees and poles were more often inspected with higher power acoustic techniques using mechanical impacts as the signal source. Ultrasonic waves for testing are commonly produced by piezoelectric transducers that convert voltage to mechanical motion. Inspectors can purchase ultrasonic transducers with center frequencies between 20 kHz and up to the megahertz range.

Transducers may or may not require contact with the wood specimen. If contact is necessary, a coupling agent, known

as couplant, is normally required. The couplant aids the transmission of the transducer pulses into the test specimen. The couplant used is chosen based upon inspection or test application. Common couplants include water, grease, glycerin gels, petroleum jelly, starch glucose, cellophane sheets, and silicone rubber, just to name a few. Care must be used when selecting a couplant, as they may be capable of corrupting the condition of the specimen (Bucur 2006). Pressure between transducers and the specimen must also be considered. In general, as the pressure between the source and specimen increases, the power transmission increases; however, there is a point of diminishing returns above which additional applied pressure yields little additional transmitted energy. Non-contact transducers use the medium surrounding the test specimen as the coupling agent. Air-coupled transducers, as the name implies, use surrounding air as the coupling agent. Immersion tests submerge transducers and specimen in a liquid that acts as the coupling agent.

Stress Waves in Wood

Wood in its natural form is often assumed to be a cylindrically orthotropic material with three principle directions: longitudinal along the tree length, radial from the exterior to the tree center, and tangential around the tree center circumferentially. Orthotropic materials have nine independent elastic constants: three Young's moduli, three shear moduli, and three Poisson's ratios (Hearmon 1961). For wood, an assumption of six independent Poisson's ratios rather than three has been found to more accurately represent wood structure (Bucur 2006).

Within an infinite solid medium are two types of waves, longitudinal and shear. Longitudinal waves have particle motion normal to the wave front and parallel to the direction of wave propagation. Shear waves have particle motion parallel to the wave front and normal to the direction of wave propagation. In an orthotropic material, each principle direction will have an associated longitudinal wave velocity and two shear wave velocities. The relationship between stress-wave velocity and material stiffness has been established through the equations of motion, Hooke's law, and Christoffel stiffness tensors (Hearmon 1961; Graff 1975; Bucur 2006). Derivation of the relationship can be found in many texts, including the two references provided and will not be repeated here. For a longitudinal stress waves traveling along a principle axes, the relationship can be expressed as

$$C_D = \rho V_L^2 \quad (1)$$

where

C_D is dynamic stiffness,
ρ density, and
V_L velocity of the longitudinal wave.

Similar relationships can be developed for shear waves (Bucur 2006). Stress-wave velocity, therefore, yields information about elastic constants of the material. In many analyses, velocity or the squared value of velocity is correlated to modulus of elasticity. Whereas modulus of elasticity and stiffness are related, it is important to remember that values are not interchangeable and that stiffness is influenced by the Poisson's ratio of the material. The description above characterizes bulk wave behavior. Wave velocity is affected by dimensions of the specimen. Wave motion through plates and rods require special consideration beyond the simple analysis given here and can be found in Hearmon (1961), Graff (1975), and Bucur (2006).

Energy storage and dissipation properties of wood and engineered wood products are controlled by the same mechanisms that dictate many of their physical and mechanical properties. For example, consider how the microscopic structure of clear wood affects its energy storage, loss properties, and mechanical behavior. Clear wood is a composite material composed of long microfibrils of cellulose and hemicellulose cemented together with lignin. At the microscopic level, energy storage properties are controlled by orientation of the microfibrils and their structural composition, factors that contribute to stiffness and strength. Energy storage properties are observable as frequency of oscillation in vibration or speed of sound transmission. Conversely, energy dissipation properties are controlled by internal friction characteristics, to which bonding behavior within and between microfibrils contribute significantly. Rate of decay of free vibration or wave attenuation are frequently used to observe energy dissipation properties of wood-based materials (Pellerin and Ross 2002).

Wave velocity and attenuation are directly related to material properties. As a result, they are often used for defect detection. Fungal decay, cracks, and voids are defects that can degrade the structure of wood, lessening its strength and toughness. Fungal-infected wood decreases wave velocity and increases signal attenuation. Waves traveling from a source to a receiver will have to travel around cracks and void lengthening their travel distances. Greater travel distances increase both travel time and signal attenuation. Sensitivity to internal defects makes wave velocity and attenuation useful and commonplace parameters when assessing wood. However, there are a myriad of parameters that researchers have used for condition assessment. The list of parameters includes but is not limited to spectral content, rise time, pulse count above a threshold, signal length, root mean square of signal energy, time centroid, frequency centroid, decay rate, peak amplitude, and peak frequency. Inspectors and researchers may use one or dozens within a single assessment and often create new parameters to correlate to particular phenomenon.

Table 3.1 contains several common analysis techniques that are applied to ultrasonic measurements and recorded signals obtained during testing. Descriptions of techniques and

Table 3.1—Data analysis techniques

Ultrasonic parameter	Description	Mathematical expression
Time of flight (TOF)	Measure of the time required for an ultrasonic packet of energy to travel through the material. Usually expressed as per unit length.	$\mathrm{TOF} = \frac{t_2 - t_1}{l}$ where t_2 is arrival time, t_1 initiation time, and l travel distance between source and receiver.
Pulse length (PL)	Measure of spreading of received waveform with respect to a standard waveform. Influenced by differences in path length and sound speed that tend to spread waveform.	$\mathrm{PL} = K\Delta t \int v(t)^2 \mathrm{d}t$ where K is a constant, Δt time required for received wave energy integral from 10% to 90% of its final value, v signal voltage as a function of time, and t time.
Insertion loss (IL)	Ratio of energy received, after transmission through material, to energy input.	$\mathrm{IL} = 10 \log\left(G\frac{E_\mathrm{r}}{E_\mathrm{t}}\right)$ where E_r is received energy, E_t transmitted energy, and G receiver gain.
Elastic constants determination	Relate longitudinal and shear wave velocities to Poisson's ratio and dynamic modulus of elasticity.	$C_\mathrm{D} = \rho V_\mathrm{L}^2\ G_\mathrm{D} = \rho V_\tau^2$ where μ is Poisson's ratio, V_L longitudinal wave velocity, V_τ shear wave velocity, ρ density, C_D dynamic stiffness, and G_D dynamic shear elastic modulus.

the mathematical expression for each are also given. The literature review that follows this section contains several examples where these and other analysis techniques are applied. The study ends with Table 3.2, which is a list of the tree species examined by studies in the literature review and associated bibliographic references.

Ultrasonic Inspection Methods

Several types of ultrasonic inspection can be used. Presented here are summaries of basic one or two sensor methods. Many other methods use multiple sensors; for instance, in linear arrays (Bray and Stanley 1997) or oriented around the specimen at multiple locations (Divos and Divos 2005). Single sensor methods are often referred to as pulse-echo methods. Two sensor methods are often referred to as through transmission methods. The stress waves from the source may be either longitudinal or shear waves depending upon the source selected. The source may be oriented such that the pulse incident to the specimen surface is either normal or angled. Below are brief descriptions of pulse-echo, through-transmission, and angled beam techniques. For greater detail regarding ultrasonic inspection techniques, the reader is directed to Bray and Stanley (1997), Bucur (2002, 2006), and Divos and Divos (2005).

Pulse Echo Test Method

Figure 3.1 illustrates a typical normal oriented pulse echo test configuration. A pulse on one side of the specimen induces stress waves that travel through the cross section, as shown in Figure 3.1a. As previously mentioned, stress waves may be either longitudinal or shear waves depending upon the source selected. A common pulse source is a piezoelectric transducer with a center frequency and power selected by the user. The pulse is initiated from the same transducer used to sense returning waves. As shown in Figure 3.1c, waves created by the pulse strike the opposite side of the specimen and are reflected, or "echoed," back toward the transmitting sensor; hence the term pulse echo. Characteristics of waveforms observed are highly dependent upon the type of sensor used. Various types of sensors, including those that measure particle displacement, particle velocity, and particle acceleration can be used with this type of setup.

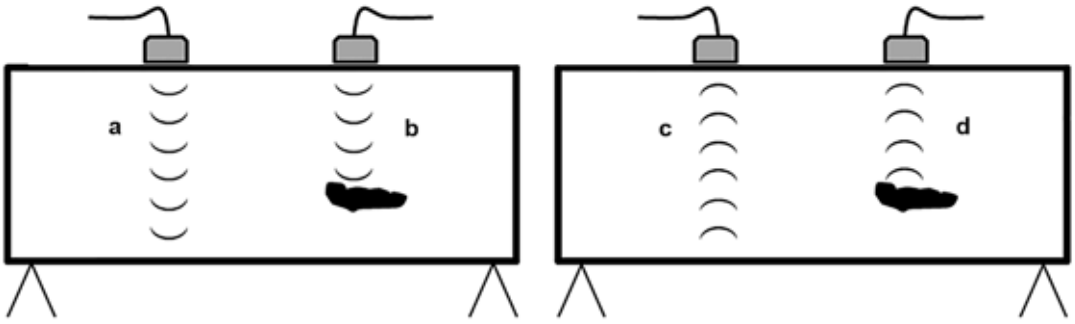

Figure 3.1—Typical pulse-echo test configuration using (a) clear path from transducer to opposite specimen edge, (b) defect is in the wave path, (c) wave reflects off opposite specimen edge and returns to the sensor, (d) wave reflects off the defect and returns to sensor.

Defects such as splits and voids can also be detected in this manner. Incident waves are reflected from these defects as shown in Figure 3.1b. If reflected waves are reflected back to the transmitting/receiving sensor as shown in 3.1d, then the depth of the defect can be calculated using the known speed of the traveling wave. Orientation of the defect with respect to the direction of wave travel can greatly affect how well it is discerned. A wood split oriented perpendicular to the wave travel path will reflect more wave energy than a split oriented parallel to the wave path. In a worst case inspection scenario, it is possible for a narrow split parallel to the wave path to be completely unobserved because of low defect reflectivity. A wave could travel on either side of a narrow split, reflect from the far edge of the specimen, and return to the transmitting/receiving sensor. In this case, the inspector may believe the specimen is completely free of defects. A more common case is a defect that is oriented at an angle to the wave path other than perpendicular (90°) or parallel (0°). In this case, some portion of the wave energy may be reflected away from the transmitting/receiving sensor. The inspector may be able to determine presence of the defect by a drop in magnitude in the received signal or a lack of an echo from the far edge of the specimen (Bray and Stanley 1997), or both.

Pulse echo method is convenient as only one side of the specimen needs be accessible for inspection. Also, if the wave speed through the specimen is known, depth of defects and thickness of specimen can be estimated from the travel time of the wave. Pulse echo does have some drawbacks. The pulse source must impart sufficient energy into the specimen such that an observable reflected signal is measureable. Wood is highly attenuating, and the traveling wave will need to be of sufficient magnitude to lose energy during two trips across the cross section and still be measureable at the end. If the transmitting and receiving transducer is one in the same, then ring down time must be considered. After the transducer pulses, the mechanical element requires a finite period of time to come to rest. This time is known as the ring down time. If the specimen is thin, the traveling wave can reflect from the far side of the specimen and return to the sensor before the mechanical element in the sensor has come to rest. In this case, the reflected signal will be contaminated by element motion still present from the initial pulse.

Through Transmission Test Method

Figure 3.2 illustrates a typical normal oriented through transmission test configuration. Like the pulse echo method, the signal source initiates a pulse that travels through the cross section of the specimen. As previously mentioned, stress waves may be either longitudinal or shear waves depending upon the source selected. Unlike the pulse echo method, a second separate sensor receives the signal and the source and receiving sensor are not co-located. For simplicity in this description, the source is a transducer of the same type as the receiving transducer; however, many different types of signal sources may be used. In Figure 3.2a, the source is on one side of the specimen and the receiver is directly across the specimen on the opposite side. This configuration is commonly known as through transmission. Because the waves need only travel across the specimen once, the power for the source signal can be lower than in pulse echo. This method reduces the probability of ring-down contamination as the receiving sensor was not in a state of motion prior to arrival of the wave. In Figure 3.2b, presence of a defect blocks the wave from the receiver. The defect may also redirect the wave energy around the defect that increases travel time between the source and receiver. Defects are detected by a loss of signal or an increase in time of flight; however, the depth of the defect is not known. One practical consideration of through transmission methods is that operating two sensors increases testing complexity and can increase complexity of analysis of results.

Angled Beam Methods

Figure 3.3 shows an alternative through transmission configuration. The transmitting source is tilted off normal to the specimen edge to direct the wave path at an angle to the cross section. Pulse-echo test configurations may also have an off-normal pulse direction. The incident wave reflects

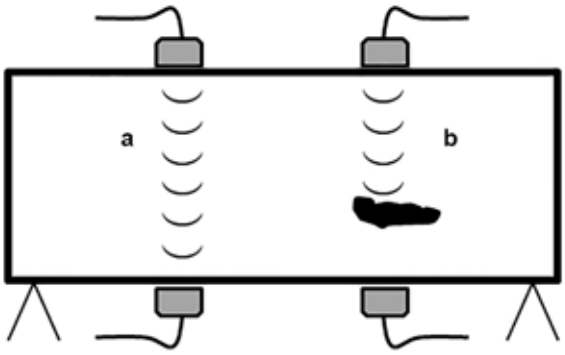

Figure 3.2—Typical through transmission test configuration: (a) clear specimen, (b) defect blocking the wave from the receiver.

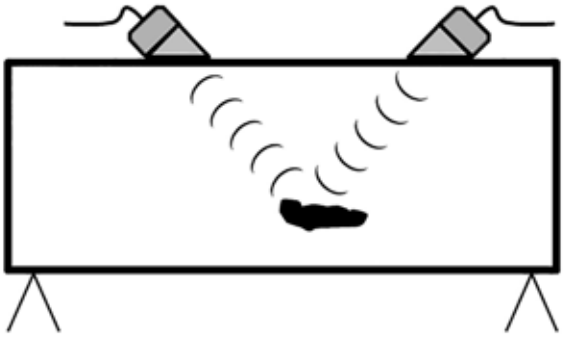

Figure 3.3—Angled through transmission test configuration.

off of observable boundaries such as the opposite edge of the specimen or defects, and travels back towards the edge from which the wave originated. The reflecting wave arrives at a location away from the source and is observed with a second sensor. This method is capable of detecting defects that are oriented normal to the edges of the specimen. This method can require more power than the through transmission method, as the wave travel distances are often greater.

A surface inspection can be performed by angling the source sensor to initiate a surface wave. This type of inspection is used to assess surface quality. The wave travels along the specimen surface and reflects off of near surface defects or sharp corners. Presence of surface waves in subsurface inspections has potential to cause spurious signals to be observed.

Literature Review

This literature review is divided into two subject areas: testing and analysis and inspection and assessment. Testing and analysis describes studies in which the process of testing using ultrasonic stress waves was the focus. Inspection and assessment describes studies that focus upon inspection of wood members or structures, determining their strength, and defect detection.

Testing and Analysis

There are several considerations when testing using ultrasonics. Beyond source, power, frequency, receiver, and coupling, other concerns include testing methodology, moisture content (MC), specimen geometry, and post-test analysis. The purpose of testing is also relevant; evaluating elastic properties of wood can involve testing protocols that are very different than those needed for inspection and assessment. This section describes how researchers have dealt with many of these issues.

The subsections address testing considerations, acoustic emission/acousto-ultasonics, MC, and determination of elastic constants of wood. The first subsection addresses testing considerations and focuses upon testing methodologies and post-test analyses. Moisture content of wood has great potential to change wood properties and affect ultrasonic results. Ultrasonic techniques are powerful tools when determining elastic constants of any material, including anisotropic materials such as wood. Acoustic emission is a testing method that uses stress waves emitted from the examined specimen. Acousto-ultrasonics assumes a source other than the specimen itself, but uses many of the same post-test analysis techniques.

Testing Considerations

Reliable and repeatable test results are only achieved when testing parameters are well suited for the testing conditions and specimen. Sensor placement, sensor coupling, resolution, specimen shape, and wood anisotropy are a few of the issues that must at be considered. Several researchers have examined the effect these conditions have upon the test results.

Anthony and Phillips (1991) refined the use of acousto-ultrasonic technique to evaluate fingerjoint strength through an examination of the test configuration. Advantages and disadvantages of various sensor locations were assessed. Broadband and narrowband excitation signals were compared. High frequencies of the broadband excitation were greatly attenuated. Narrowband excitation focused the signal energy in a narrow range, maximized the potential of high frequency signals to propagate through the wood. Several transducer types were studied with a variety of coupling agents. At the time of the study in 1991, Anthony and Phillips concluded that the ideal dry couplant for a manufacturing environment was compliant with respect to wood, had low creep properties, did not attenuate stress waves, and bonded easily to transducers. No such material was available at that time.

Hamstad and others (1993) explored farfield wideband acoustic wave behavior in wood rods and plates. Orientation of the waveform source and use of narrow band measurement systems were found to significantly affect the measured waveform. Potential to measure frequency

dependence of material attenuation with a single waveband experiment was examined.

Relationship between wavelength and resolution and difficulties in visualizing data from acoustic microscopy were discussed in Bucur (1996).

Feeny and others (1996) examined how the frequency domain was affected by changes in wave speed through different types of wood within a tree. Speed through juvenile earlywood, juvenile latewood, adult earlywood, and adult latewood were measured. The goal of the research was to determine whether periodicity of wood caused stop bands within the frequency spectrum. Evidence of stop bands was found in Scots pine (*P. sylvestris* L.) but not spruce; however, wood variability and mode conversion made measurements difficult.

Berndt and others (2000) explored movement of wave energy through wood and noted that anisotropy had significant interaction with wave pulses. The experimental setup was constructed to primarily examine bulk waves. Phase shift was investigated as a tool to determine arrival time when high frequencies with attenuation are used. Mode conversion led to inaccuracies in energy measurements. The results strongly suggest that single path measurements were not advisable.

Bucur (2002) described three algorithms used for ultrasonic tomographic imaging: transform, iterative, and direct inversion.

Andrews (2002) examined the differences in measured wave velocity depending upon the method used and sensor location. Wave velocity of radiata pine (*Pinus radiata*) logs was measured end to end and incrementally along the length along the edge of the log. Wave speed measurements taken incrementally along the length of the log were highest, followed by time of flight end to end of the log, then followed by resonance methods. Time of flight was found to differ by as much as 6% depending upon source and receiver location. Resonance methods were not affected by sensor location on opposite sides of the log. Differences between wave velocity measured using resonance methods and end to end time of flight were expected to decrease with increasing length to diameter ratio.

Berdnt (2002) noted a stiffness gradient across tree trunks in specimens of white fir. Mature wood had a greater stiffness than juvenile wood.

He and others (2005) applied a series of filters to acoustic emission to increase the signal to noise ratio. Five different filters were applied to measurements collected from through transmission ultrasonic tests. Filters used included averaging, symmetrical moving average, two infinite impulse responses, and a filter created through fuzzy logic, which was the subject of the study.

In a 2005 study, Berndt and others developed phase slope methods to increase accuracy of time of flight measurements. The threshold method of measuring time of flight was affected by low amplitude or high attenuation. The phase slope method was effective at measuring thin wood samples. The phase slope method was also effective at separating multiple pulses within a single pulse.

Tjondro and Soryoatmono (2007) explored how specimen geometry affected elastic constant measurements. The assumption that MOE was the same as stiffness yielded an error of 6% in the longitudinal direction and up to 24% in the radial and tangential directions. Higher length to diameter ratios yielded higher estimates for longitudinal velocity. A square cross section for the specimen was found to yield the best results.

The effect of coupling media upon wave attenuation for longitudinal and transverse transducers was explored by Trinca and others (2009). A 100-kHz transducer was coupled to nine different species of Brazilian woods using six different coupling agents. Attenuation for each coupling was measured. To obtain consistent measurements, it was necessary to apply pressure to transducers.

Agrawal and Choudhari (2011) estimated the strength of wood using 22 measured NDE parameters. Signals collected using a through transmission test setup were subjected to FFT and the power spectral density was obtained. The model, known as IDSAM, was reported to yield strength estimates, which correlated to actual strength at a level higher than most other contemporary and previous studies.

Acoustic Emission/Acousto-Ultrasonics

In acoustic emission (AE), stress waves caused by a source within a structure are monitored. Internal sources of stress waves include, but are not limited to, microfractures, check formation, water movement, and pit aspiration. Several parameters are extracted from recorded waves, and the extracted parameters are then correlated to different phenomenon or properties inherent to the structure. Any number of parameters can be examined, including but not limited to, time of flight, peak voltage, time to peak voltage, stress-wave factor, root mean square voltage, number of threshold crosses, signal length, time centroid, frequency centroid, attenuation, etc. Acousto-ultrasonics (AU) uses many of the same post-test analysis techniques; however, the source is user-dictated such as a transducer.

The fundamentals of AE and AU were described in Beall (1987a). AE was not repeatable; AU was repeatable. AU relied on averaging several signals to minimize variability, and narrow band filters were used to improve signal-to-noise ratio. Attenuation of signals traveling through wood increased as frequency increased. Issues of coupling to wood-based material such as porosity and surface roughness were discussed. Pressure and couplant together minimized

signal loss. A limited glossary of terms was included (Beall 1987a). In a follow-up paper, the future uses of AE/AU were discussed. Potential areas of use were laboratory testing, field testing, proof testing, online sensing, sensing adhesive integrity, sensing creep, fracture analysis, and drying defects (Beall 1987b).

Sandoz and others (2000) used AU variables in conjunction with stress-wave information to increase the reliability of strength grading. Parameters examinded included stress-wave factor, maximum peak, energy, and attenuation after first peak. MOE of glued-laminated beams was highly correlated to ultrasonic wave speed, whereas local defects had a significant effect upon MOR.

Kánnár (2000) examined the influence of moisture and temperature upon the Kaiser effect in Scots pine. The Kaiser effect is a phenomenon in which acoustic emissions are absent in a material for a load at or beneath previous loading levels. The Kaiser effect was observed in short-term experiments; however, the effect diminished as time elapsed. The Kaiser effect was observed 95% of the time if a second load was applied immediately, 60% if applied within 15 days, and 25% after two months.

Ballarin and others (2002) explored parameters that could be correlated to the physio-mechanical properties of clear wood. Douglas-fir, redwood, and spruce–pine–fir specimens were used. Time domain parameters exhibited more differences than frequency domain parameters.

In a follow-up study, Seeling (2002) examined additional parameters. The parameters included time of flight, maximum and minimum voltage, time to voltage maximum and minimum, root mean square voltage, total power, time and frequency centroid, stress-wave factor, and maximum frequency for the first quarter of the wave. Most of the AU parameters examined showed weak correlation to wood characteristics.

Moisture Content and Drying

Wood physical and mechanical properties are affected by MC of wood. Modulus of elasticity, wave speed, attenuation, and creep characteristic are just a few of the properties of wood affected by MC. Wave behavior through medium is dictated by properties of material. As properties change, wave propagation alters. Several researchers have explored how wave propagation changes as a function of MC with the goal of assessing and monitoring wood MC level.

Quarles and Zhou (1987) monitored the development of defects during drying using AE. The rate of acoustic emission events was correlated to drying conditions of California black oak (*Quercus kelloggii*) In addition, defects created during drying were related to the AE signals.

Groom (1991) examined the integrity of the truss-plate joint during moisture cycling using acousto-ultrasonics (AU). Signal energy was strongly correlated to the number of teeth of the plate and quality of the coupling between the teeth and the wood but was poorly correlated to the total coupling surface area. Presence of high frequencies in signals passing across the truss plate to the wood was indicative of sound joints. Weakened joints exhibited stronger low-frequency components.

Kawamoto (1993) used several AE parameters to predict the location of check formation during drying of Japanese red pine (*Pinus densiflora*). Low frequencies were associated with check growth. The number of checks in the location of the transducer was correlated to the AE count rate. Radial attenuation was an indicator of large check formation during drying. In a follow-up study, Kawamoto (1996) concluded that using only AE parameters for the detection of checking was imprecise.

Booker and others (1996) examined radiata pine (*P. radiata*) for variation in both sound velocity and dynamic MOE in three principle directions with changing MC. Velocity increased linearly as the MC decreased from fiber saturation point (FSP) to oven dry. The dynamic MOE had the lowest value at FSP, increasing both above and below. Below FSP, approximately 60% of the variation in MOE was attributed to wood shrinkage.

Schafer and others (1998) identified wetwood and honeycombing defects using TOF measurements. They concluded that wetwood increased viscoelastic damping in the wood and that honeycombing caused scattering of waves. Despite having different mechanisms, both types of defects decreased signal amplitude across the wood.

Booker and others (2000a) examined the timeframe of internal check development of radiata pine using AE. Internal checking occurred within the first 6 hours of drying. The maximum rate of checking occurred between 1.6 and 2 hours after drying began. This timeframe corresponded to within a half hour of the kiln reaching operating temperature. The number of AE events did not correlate to the number of internal checks.

Soma and others (2000) examined the effects of frozen moisture upon wave velocity in frozen cubes of Japanese cedar (*Cryptomeria japonica*). Wave velocity through the cubes was recorded in all three principle directions: longitudinal, radial, and tangential. Wave velocity through the frozen cube increased. The increase was most noticeable in the longitudinal, radial, and tangential directions for MC above 200%, 150%, and 150%, respectively.

Kang and Booker (2002) examined moisture gradient within radiata pine during kiln drying. The boards were weighed and the wave velocity was measured during the kiln-drying process. The velocity appeared to be both a function of MC and moisture gradient.

Miettinen and others (2005) made electrical and ultrasonic measurements of pine specimens. Measurements were correlated to MC, density, growth ring angle, hardness, and strength. A multivariable model accounted for a greater amount of the variability of parametric estimators such as density and MC.

A 2005 study by Rosner and Wimmer used acoustic emissions to monitor spruce trees during drying. The trees were debarked and dried. Mature trees were more susceptible to dehydration than juvenile wood. Juvenile wood had more AE events because of a higher number of tracheids per volume. High energy AE events were measured at the start of the drying process and were caused by the shrinking process.

Gonçalves and Costa (2005) performed a combined examination of ultrasonic wave velocity and stiffness on several Brazilian tree species. Stiffness terms decreased with increasing MC up to the FSP. Above the FSP, stiffness would sometimes increase with increasing MC. Stiffness values were partially corrected by accounting for mobility of free water in the wood. The MC had a greater effect upon wave velocity in the longitudinal direction than in the radial or tangential directions. Correlations were positive, but key supporting figures were absent.

In a later study (Rosner 2011), explored reversible and irreversible effects of drying upon spruce were explored using acoustic emission. Specimens were dried and then rewetted in successive cycles. During the first drying, the highest peak amplitudes were associated with moderate moisture loss. After rewetting, the highest peak amplitudes occurred near the end of the drying cycle. Wood that had never been dried had a higher rate of AE events below 175 kHz. Earlywood appeared more sensitive to irreversible changes during drying than latewood.

In a 2011 study, van der Beek and Tiitta (2011) monitored the drying process of spruce using AE. One goal of the research was to discriminate between AE events caused by crack formation and propagation and those caused by water movement. The cool down and moisture conditioning phases of drying were most critical in crack formation.

Gao and others (2011) examined the combined effects of temperature and MC on specimens of red pine. Specimens were conditioned to four different MC levels: green, 24%, 12%, and 0%. Wave velocity and energy loss through the specimens was measured over a range of temperatures from –45 °C to 35 °C. The MC had a significant effect upon the relationship between velocity and temperature. When green wood was well above freezing, temperature had little effect upon wave velocity. When green wood was near freezing, energy loss and wave velocity changed abruptly because of the phase change of water held in the cell lumens. As MC decreased, change near freezing became less pronounced.

In subsequent research from many of the same authors, the combined effects of temperature and MC upon modulus of elasticity was examined. Dynamic and static bending tests were performed upon specimens of red pine. Similar to velocity and energy loss, green wood had abrupt changes in MOE near freezing. As MC decreased, the change near freezing became less pronounced (Gao and others 2013).

In a similar study conducted by Llana and others (2013), the combined effects of temperature and MC upon MOE and ultrasonic velocity were examined on Scots pine. Between 10% and 18% MC, the effects of MC were close to linear. Trends above and below 0 °C were different from each other.

Dunbar and others (2013) used ultrasound to predict dimensional stability of sweet chestnut (*Castanea sativa*) and sessile oak (*Quercus petraea*). Wood samples were below the FSP. Wave velocity in the woods decreased as MC increased. Specific gravity alone was a poor predictor of wood shrinkage; ultrasonic velocity alone was a good predictor. The combination of both parameters produced the best predictor, explaining 72% and 77% of shrinkage in oak and chestnut, respectively.

Determination of Wood Elastic Constants and Properties

Ultrasound has been used in a variety of ways to quantify elastic constants of wood. The relationship between stress-wave velocity, density, and stiffness make it a powerful experimental tool.

An early property assessment study used vibrations and high frequency waves to explore the theoretical relationship between wave velocity, density, and stiffness (Hearmon 1965).

Bucur (1978) correlated changes in velocity to stress levels in wood. Stress was normalized by the rupture stress. Normalized values were between zero and one. Four stress levels were identified and correlated to physical phenomenon: 0.2, 0.2 to 0.7, 0.7 to 0.9, and 0.9 and above. In the first zone, velocity values increased. In the second zone, velocity was close to constant. The third and fourth were both characterized by a decreasing slope, but the slopes are different from each other.

Ross and Pellerin (1988) reported on use of acoustic techniques for assessing mechanical properties of a wide range of wood composite materials. They obtained excellent correlative relationships between acoustic parameters and mechanical properties.

Bucur (1996) discussed methods by which three different wave techniques were used to obtain material constants. Vibratory, acoustic, and ultrasound techniques were described, and an explanation of the theoretical foundation of the relating wave velocity and elastic constants was given.

The complex modulus of anisotropic materials, such as wood, was derived by Navi (1996). Navi noted that the inhomogeneity and viscosity of wood causes both dispersion and attenuation in waves traveling through the material. A dispersion relationship was developed by measuring the phase velocity by frequency. Attenuation was measured by frequency as well. Together, these properties were used to develop the complex modulus for anisotropic materials.

de Oliveira and others (2002) measured static and dynamic MOE of loblolly pine. Like many similar tests, dynamic MOE was approximately 20% higher than the static, and good correlation existed between the two MOE values.

Bucur and Berndt (2002) calculated nine elastic constants of an orthotropic material, which wood is often considered to be, using wave velocity and energy flux deviation. Six of the nine constants were calculated using longitudinal and shear wave velocity measurements. The six terms were along the diagonal of the stiffness matrix; the three remaining terms were off of the diagonal. Accuracy of the calculated value of three off-diagonal terms was greatly increased if considerations were made for energy flux.

Karlinasari and others (2009) calculated the MOE of two tropical species, mangium (*Acacia mangium*) and jackfruit (*Artocarpus heterophyllus*) using three different methods: dynamic method using ultrasonic velocity, static bending, and a mechanical grader. Each MOE was correlated to MOR. The best correlation existed between static MOE and MOR, with dynamic MOE second best; however, overall, the correlation between dynamic MOE and MOR was low.

Baradit and Niemz (2011) investigated mechanical properties of four Chilean species of wood using ultrasonic measurements. Longitudinal and transverse waves were used to determine MOE in three primary directions as well as the three shear moduli. Four hardwoods species: tepa, olivillo, laurel, and lenga, and two softwood species, alerce and manio, were tested. Hardwoods tested were found to have higher anisotropy than softwoods.

Grimberg and others (2011) determined the elastic tensors of wood plates using the phase velocity of lamb waves. Both symmetric and antisymmetric modes were employed in the calculation process. Good agreement was found between calculated values and the destructive tests. Wood plates were made of sycamore, alder, cherry, beech, and pine. Air-coupled transducers were employed to determine several elastic constants.

Wood specimens of three distinct shapes were tested ultrasonically by Gonçalves and others (2011) to obtain elastic constant data. The shapes were a 26-sided polyhedron, a multifaceted disk, and cubic prisms. Three species were tested: eucalipto, garapeira, and cupiúba. Cubic prisms were cut at specific angles to the wood grain. The prisms produced the best correlation to elastic constant values obtained from static test; however, prism specimens themselves were used for static tests after ultrasonic testing was concluded. The multifaceted disc and the polyhedron exhibited the second and third highest correlation to the static tests, respectively. Poisson's ratios proved harder to correlate with static results with some matching across all shapes and some diverging for all shapes.

In two related studies, Inés and others (2011) and Palacios and others (2011) used 30 wood species to develop correlations between MOE static bending, MOE from resonant frequency, MOE from ultrasound velocity, MOR, and specimen density. The high number of species represented made this study unique. Specimens were grouped according to density. Strong agreement existed between the MOE from ultrasonic velocity and MOR.

In a follow-up study to Gonçalves and others (2011), Vázquez and others (2013) extracted samples from 13 specimens of *Castanea sativa* and shaped them into 26-faced polyhedrons. Ultrasonic time of flight measurements for longitudinal and shear waves were used to estimate elastic constants of the polyhedron. Prisms were extracted from the specimens and used in compression tests to obtain the same elastic constants. No significant difference was found between the elastic constant values obtained using the two methods.

The acoustoelasticity of three wood species, *Eucalyptus citriodora*, *E. grandis*, and *E. pellita*, was explored by Bertoldo and others (2013). Specimens were subjected to bending tests and strain was measured using extensometers. Wave speeds longitudinal and transverse to the wood grain were measured. Longitudinal wave velocity tended to decrease as strain increased regardless of whether the strain was compressive or tensile in nature. Longitudinal wave speed was more affected by presence of strain than transverse traveling waves. Waves traveling in the radial or tangential direction during the bending test exhibited differing behaviors depending upon whether the specimen was a hardwood or softwood. Velocity increased with increasing strain for hardwoods and decreased for increasing strain for softwoods.

Inspection and Assessment

The purpose of ultrasonic inspections is to assess the condition of a member or structure. The condition assessment allows the inspector to decide whether or not the current condition is sufficient for the member or structure to perform its function safely and reliably. Internal defects can have a significant and deleterious effect on member strength. Therefore, a reliable assessment can be made if the inspection process can detect defects. The studies in this section focus upon defect detection and strength assessment using ultrasonic inspection. The literature review begins with studies involving inspection of wood in its least refined state, standing trees. Subsequent sections will focus upon inspection methods on increasingly processed wood products:

round members, sawn lumber, and engineered wood products. Inspection of structures and artifacts follows.

Standing Trees

Modern ultrasonic equipment is capable of generating sufficient signal energy to perform inspection and assessment of standing trees and poles, and its use in that area has noticeably increased in the last decade. Historically, ultrasonic inspection of standing trees was not as common as acoustic stress-wave inspection. Acoustic stress waves were more commonly used to inspect standing trees and round members such as logs, poles, and piles. Acoustic stress waves have frequencies below 20 kHz and are often caused by an external impact. Impacts from hammers, pendulums, and BBs have greater signal energy than that produced using piezoelectric transducers. Also, low frequencies attenuate more slowly than high frequencies and can therefore travel farther in wood. As a result, signals from impacts had a greater probability of being sensed across the diameter of full-sized trees. Acoustic stress-wave inspection is not covered in this paper. With technological improvements, use of ultrasonic inspection of standing trees is becoming more widespread.

Huang (2000) used ultrasonic wave propagation through the outer wood of standing trees to predict lumber stiffness of loblolly pine. Wave velocity measurements were taken radially at 50 and 150 cm above the ground on standing trees. Speeds were correlated to modulus of elasticity (MOE) in an effort to determine the quality of stands of trees prior to harvesting. Huang (2000) found that trees with large percentages of corewood had higher radial wave velocity.

In a 2009 study, Najafi and others inspected a group of 112 Iranian birch trees for internal decay. Wave velocity was measured parallel and perpendicular to the slope of the grain. Trees were felled and cross sections were compared to inspection results. The study found that of the trees containing defect, 95% were detectable. When defects did occur in birch trees, they were usually around the pith. Because of the mountainous nature of the region in which the study took place, many trees contained reaction wood, causing eccentricities in the cross sections. Eccentricities could cause velocity measurements taken perpendicular to the grain to miss the decayed pith regions.

Pedroso and others (2011) measured the longitudinal ultrasonic velocity of a group of 210 Brazilian trees including the species *Eucalyptus grandis*, *Pinus elliottii*, and *Toona ciliata*. The measurements were taken vertically along the trunk above and below breast height. The trees were felled, cut into logs, and ultrasonic velocity through the logs was measured. Whereas it was possible to correlate velocity values between logs and trees, a nonlinear relationship existed because of differences in the manner in which waves traveled through each.

In a 2011 study, Brancheriau and others (2011) constructed an automatic ultrasonic inspection system mounted on a track around a standing tree. Initially, a 300-kHz transducer was used as a source, but attenuation through the tree was too great. An 80-kHz transducer was then used. Resolution provided by the lower frequency transducer was 17.7 mm longitudinally and 36.4 mm lateral to the tree. Radial wave velocity measurements were used to construct a tomographic view of an eastern cottonwood (*Populus deltoides*).

The effect of pruning upon a variety of loblolly pine was examined in eastern Argentina. Fassola and others (2011) found that trees without pruning had higher wave speeds. The trend continued when trees were cut into logs.

Several tree species in Bogor City, Indonesia, were examined (Karlinasari and others 2011). The focus of the study was evaluating trees in an urban environment. Tree species included *Swietenia* sp., *Pterocarpus indicus*, *Bauhinia purpurea*, *Mimusops elengi*, and *Agathis alba*. Trees were selected for radial ultrasonic testing based upon visual inspection. Sound, decayed, and questionable trees were selected. The velocity values were compared with results of the visual inspections, and a tree soundness criterion was developed based upon ultrasonic velocity. Trees with velocities above 1600 m/s were assumed to be good; decayed trees had velocities less than 500 m/s.

Song and others (2011) correlated radial ultrasonic and acoustic stress-wave velocities for the tree species *Populus simonii*, *Ulmus pumila*, *Salix matsudana* Koidz, and *Fraxinus mandshurica*. Good agreement was found between the two measurement methods in standing trees, although ultrasonic velocities were higher than acoustic velocities.

In a 2011 study by Yoza and Mallque, tangential and radial measurements were taken on *Cedrelinga cateniformis* Ducke. Elastic constants were determined using two ultrasonic frequencies, 23 kHz and 45 kHz.

Karlinasari and others (2013) used ultrasound inspection to determine if a commercially important fungus, known as agarwood, was present in standing *Aquilaria microcarpa* trees. Karlinasari and others (2013) found that radial ultrasound velocities less than 1000 m/s were indicative of agarwood.

Ultrasonic cross-sectional tomographs formed from radial and tangential wave velocity measurements were found in a 2013 study by Lino and others to be sensitive to the degree of irregularity (non-round) trees. Wave paths in irregularly shaped trees were complex and difficult to determine. Exterior digital tomographic profiles of the trees were obtained using triangulated laser measurements. The digital profiles were used to supplement ultrasonic measurements to make a more accurate ultrasonic tomograph.

Round Members

Round members include logs, poles, and piles. In round members, the orthotropic structure of the original tree remains largely intact. Historically, acoustic stress-wave inspection was generally favored over ultrasonic inspection for round members. The size of round members was such that the greater power and lower attenuation of acoustic stress-wave inspection yielded more easily observed signals. An example of the differences between acoustic stress-wave and ultrasonic inspection can be found in Booker and others (2000b). In that study, radiata pine logs were examined with several ultrasonic and acoustic measuring devices. This study found that ultrasonic devices were unsuitable because of the low power of their signals. The final evaluations were made with the acoustic devices only. Modern ultrasonic equipment produces greater signal power than those of past devices. Advancements in technology have overcome previous limitations, and use of ultrasonic techniques in inspection and assessment of round members, like standing trees, has increased in the last decade.

Strength and Grading

Log grading and strength characterization are important to the commercial value of logs. The ability to grade wood while it is still a standing tree or a log aids in obtaining the highest quality yields from each piece of wood and minimizes waste. Several papers have been written about log grading and characterization. Sandoz (1996) developed a transducer that was driven through the bark to the wood, eliminating the need for a couplant. Longitudinal wave speeds of logs were used for log grading and estimating performance of lumber made from the logs.

In a 1996 study, Curtu and others evaluated Romanian beech trees at three different levels: bottom, middle, and top. This study found variations in the wave speeds depending upon stress in the wood. Wave speeds decreased from base to canopy. In addition, the wave speed of logs cut from the trees was different than the wave speed of lumber cut from the logs.

Hauffe and Mahler (2000) compared the capability of two inspection methods for estimating log strength. They used x-ray inspection and ultrasound to evaluate 225 spruce logs. Ultrasound was found to be superior to x-rays in log strength estimation.

In a 2005 study, Yin and others estimated MOE of Chinese fir logs using ultrasound, stress wave, and vibration methods. Correlations were drawn between static MOE and modulus of rupture (MOR). The MOE based upon vibration methods had the best correlation. Between the top and bottom of the trees, the variation of MOE was significant, whereas the variation of MOR was insignificant.

In a related study, Gonçalves and others (2009) evaluated *Eucalyptus citriodora* poles using both ultrasonic and static tests. The static tests were carried out in accordance with ASTM D1036/1999 and NBR 6231/1980 specifications. The research goal was to evaluate the variability between new poles and suppliers and establish a nondestructive method of grading. The researchers found that ultrasound assessment allowed poles to be sorted by strength and suppliers to be sorted by quality.

Turpening (2011) constructed high frequency ultrasonic tomographs using densely spaced transducers positioned around a log. The images produced showed a high correlation with sandalwood oil, an important commercial derivative of sandalwood trees.

In 2013, Freitas and others evaluated deteriorated Brazilian utility poles for reuse in other capacities after they were removed from use. *Eucalyptus citriodora* and *E. saligna* poles were inspected using ultrasound. The research showed ultrasonic inspection can be used to determine which poles can be reused and which ones must be discarded.

Defect Detection

Abbott and Elcock (1987) inspected poles in Europe using a 40-kHz transducer. Signal attenuation was examined as an indicator of internal rot. The proposed procedure required multiple tests around the circumference of the pole.

A more recent study by Han and Birkeland (1991) used three ultrasonic techniques to evaluate logs: pulse echo, through-transmission, and grain sounding trace. Correlations were drawn between test results, and an attempt was made to use artificial intelligence to improve automated defect detection.

Lemaster and others (1993) examined the sensitivity of acousto-ultrasonic parameters in detecting holes in Douglas-fir utility poles. Three pole conditions were studied: lightly checked, heavily checked, and creosote treated. Several parameters were pulled from the signal data to evaluate sensitivity. Parameters that showed sensitivity to the presence of holes included transit time, centroid time, centroid frequency, and velocity. The technique detected holes 50 mm or larger in a 300-mm-diameter pole.

A group of six sensors was employed by Dill-Langer and others (2002) along with acoustic emission techniques to identify and locate defects within a European spruce (*Picea abies*) wooden pole. Approximately 90% of the source locations were identified to an accuracy of ±7% of the transverse dimension and ±4.4% of the longitudinal dimension.

Divos and Divos (2005) explored the resolution of acoustic tomography to determine the dimension of the smallest detectable defect. Artificial defects were created within discs of larch. Defect sizes ranged from 10 mm to 100 mm. The number of sensors used to construct a tomograph of the cross section was varied from 6 to 30. The 10-mm defect was not detected using 30 sensors; a 25-mm defect

was detected. In another study of detecting voids in cross sections, holes of different shapes, circular versus slots, were manually created in large wood discs. Wave velocity decreased linearly with the size of the hole, but slots had a greater adverse effect.

In the Najafi and others (2007) study on beech trees, the location of the hole had no influence on the wave velocity. The potential to detect the presence of tension wood using ultrasonic inspection was confirmed.

Yang and others (2007) measured the radial and longitudinal wave velocities in *Eucalyptus globulus* discs. Longitudinal velocity was found to be higher in areas of tension wood, but radial velocity was lower.

A portable ultrasonic CT device was developed by Kim and others (2007) to detect decay in wood poles. The devices created tomographs that were capable of detecting decay regions with less than 10% mass loss and less than 30% loss in strength.

Gonçalves and others (2011) examined the presence of artificial holes in wood cross sections composed of Pequía (*Aspidosperma desmanthum*). Tomographic images were created, but the image shapes of the holes were distorted.

In another void analysis, Wang and others (2013) constructed wave time of flight isolines along the surface of a Korean birch (*Betula costata*) log. Cavities of varying diameters were created within the log. The study examined how waves traveled through the cross section. The accuracy of the simulated reconstructions was able to identify the smallest defect, 40 mm, with an 83% accuracy. The accuracy improved as the hole size increased.

Oh and others (2013) used signal attenuation to detect small holes in round red pine members. The holes were used to simulate insect damage to the poles. A through transmission setup was used to collect data with varying levels of contact pressure on the transducers. A spectral analysis was carried out on the data. The results indicate that spectral analysis had great potential in locating insect damage.

Sawn Lumber

Sawn lumber has been cut from trees into rectangular cross sections. The dimensions of the cross section are typically smaller than those of round members and standing trees. The sawn lumber review is broken into two subsections, strength and grading and defect detection.

Strength and Grading

Like log grading, grading sawn lumber is important for its commercial value. Ultrasonic inspection has been used in a variety of applications to grade sawn lumber. Joint assessment has been included in this section as it directly relates to strength of the final member. In an effort to improve grading beyond what could be assessed visually, Sandoz (1991) measured ultrasonic wave velocity in spruce and fir beams. The ultrasonic longitudinal wave speed was correlated to the values of MOR and MOE. Moisture content and temperature were taken into account in the calculations.

Anthony and Phillips (1993) conducted a study in which the original finger joint paper was expanded with an examination of the sensors and the sensor coupling to the board. The signal from air-coupled transducers was found to lack the power necessary for use in tests. The signal from wheel sensors varied as the wheel turned, causing unacceptable inconsistencies. Coupling materials were limited to those that could be used in a manufacturing environment. Silicone rubber sheets and moldable urethane were examined and their relative advantages and disadvantages were discussed. Sensor placement was moved from the narrow edge of the boards to the wide face.

In a 2000 study of timbers, Duju and others applied six methods of measuring MOE to five different timber species of Malaysian wood: *Parashorea macrophlla*, *Gonystylus bancanus*, *Shorea albida*, *Dipterocarpus rigidus*, and *Cotylelobium burcki*. One MOE measurement method relied upon ultrasonic wave velocity. Good correlation was found between the calculated MOE and the values of MOR.

Another study (Diebold and others 2000) examined several methods of grading for hardwood and softwood. Softwoods examined included spruce, pine, larch, and Douglas-fir. Hardwoods included oak and beech. Testing methods included bending tests, x-ray, transverse vibration, and ultrasonic inspection. Of the methods used, ultrasonic inspection had the lowest correlation to bending strength.

In a similar study, visual grading and MOE estimated from the ultrasonic wave velocity were correlated to the bending strength. Kuklik and Kuklikova (2000) found that in the majority of cases, knottiness of the board was the decisive visual grading criteria.

Sasaki and Hasegawa (2000) examined changes in shear velocity with applied stress in Japanese magnolia (*Magnolia obovata* Thunb.). Compressive loading caused a reduction in shear velocity; tensile loads caused increases. The changes in shear velocity were less than 1%.

Gonçalves and Bartholomeu (2002) examined MOR and MOE for boards harvested at different heights within a Cupiúba (*Goupia glabra*) tree. MOR and MOE were highest in boards harvested near the base of the tree. The MOR and MOE were found to be weakly correlated; however, the MOE was found to be capable of reliably evaluating rigidity properties.

In 2002, Machado created a profile of bending strength using boards of maritime pine. Ultrasonic signals were applied to the boards perpendicular to the grain. Acousto-ultrasonic parameters were extracted from the signals and used to estimate modulus of elasticity through correlated relationships established by the author in a previous work. Bending

tests were then performed along the length of the same boards. The results of the bending tests were correlated to modulus of elasticity values estimated using the acousto-ultrasonic parameters. The results showed that a lengthwise bending strength profile could be created using acousto-ultrasonic parameters.

While using timber grading, Sandoz and Benoit (2002) developed a relationship between the pair of parameters wave speed and transmitted energy and the properties of MOE and MOR. Empirical equations expressing the relationships were given. Energy damping of the wave was found to be directly dependent upon local singularities such as knots, decay, and grain angle.

Plinke (2005) proposed a finger joint inspection method in which high powered ultrasonic waves would generate friction at the joint and could be observed using infrared cameras. The method would be effective at defect detection, but not strength estimation.

Terezo and others (2005) tested two different species of Brazilian woods, Peroba (*Aspidosperma pirycollum*) and Angelim (*Hymenolobium petraeum*), using two commercially available ultrasonic tools to obtain estimates of the wave velocity. The correlation between MOE and wave velocity was lower than for most similar studies. Conversely, the correlation between wave velocity and MOR was higher than most similar studies.

Bartholomeu and Gonçalves (2007) examined the correlation between ultrasonic wave speed and MOE obtained from static bending. The six species were *Eucalyptus citriodora*, *E. grandis*, *E. saligna*, Cupiuba (*Goupia glabra*), Angelim araroba (*Votaireopsis araroba*), and *Pinus elliottii*. High correlation was found.

Iñiguez and others (2007) related changes in ultrasonic wave velocity to specimen length. The studies were conducted on Scots pine. For each meter of wood traveled, the wave velocity decreased approximately 83 m/s. The test was conducted to propose velocity adjustments during timber assessment.

Karlinasari and others (2007) examined the correlation between the dynamic modulus determined from ultrasound and the static modulus for Jeunjing (*Paraserianthes falcataria*).

Mechanical properties of three European species, radiata pine (*P. radiata* D. Don.), Scots pine (*P. sylvestris* L.), and Laricio pine (*P. nigra* Am. Ssp. salzmannii), were evaluated by Iñiguez and others (2009) using ultrasonic wave velocity perpendicular and parallel to the grain of the wood. Empirical relationships were constructed relating the wave speed to MOE and MOR; however, correlation values were low for ultrasonic values.

Yin and others (2009) investigated the feasibility of using ultrasonic wave velocities to estimate compressive and tensile strength of structural lumber composed of Larch (*Larix gmelini*). The author determines that lumber strength can be estimated from ultrasonic wave velocity, but correlation between the values is low.

Massak and others (2009) examined the influence of tree age on wave velocity and MOE. Beams were cut from *P. elliottii* trees of various ages ranging from 8 to 23 years. Both longitudinal velocity and MOE increased with age up to approximately 20 years. There were two groups of variation based upon age, 13 years and below, and 15 years and above. Rigidity properties would increase with age, but eventually become constant.

In a 2011 study, Pires and others estimated the MOE of eight Brazilian species using stress wave, transverse vibration, and ultrasound and then correlated to MOE determined from static bending tests. The species were *Pouteria guianensis*, *P. pachycharpa*, *Holopyxidium jarana*, *Vatairea sericea*, *Chrysophyllum venezuelanense*, *Astronium lecontei*, *Endopleura uchi,* and *Lecythis pisonis*. Ultrasound and stress-wave inspection were similarly correlated with respect to MOE. None of the testing methods correlated to density.

Rohanová and others (2011) studied Slovakian spruce (*Picea abies*) and found that ultrasonic-based strength estimates for this species were higher than those estimated using the European standard EN 408.

Iñiguez-Gonzalez and others (2013) presented preliminary work for use of nondestructive techniques to evaluate properties of sawn lumber. The goal was to establish common procedures to be used. The species examined included several Spanish species: Scots pine, laricio pine, radiata pine, maritime pine (*Pinus pinaster* Ait.) and sweet chestnut (*Castanea sativa* Mill.).

A 2013 study by Ferreira and others investigated the adequacy of Brazilian standards for grading wood using ultrasonic inspection by testing the predicted compressive and tensile stiffness and loading on *Eucalyptus grandis* boards. The results largely supported the standards on compressive loading and stiffness. The study raised concerns about tensile loading and stiffness as outlined by the standard.

Hermoso and others (2013) examined a combined visual grading and ultrasonic grading technique using 116 Scots pine boards. Boards were accepted or rejected using three methods, visual grading, ultrasonic grading, and a combined method. Boards accepted using ultrasonic inspection had a higher modulus of elasticity and higher modulus of rupture than the rejected boards. The boards accepted using visual grading had higher MOE than the rejected boards, but the rejected boards had a higher modulus of rupture. Also, the mean MOE of the visually graded boards was higher than that of the ultrasonically graded boards. The combined visual–ultrasonic grading increased the MOE of the

accepted boards over the ultrasonic method alone by 0.5%. and decreased the modulus of rupture by 1.3%.

Another study (van Dijk and others 2013) examined the degree of mode conversion of ultrasonic waves traveling through wood. A 7-m beam composed of Cabreúva (*Myrocarpus frondosus*) was used as the medium to observe traveling waves. Three frequencies were used for the tests: 25 kHz, 45 kHz, and 80 kHz. The receiving transducer was placed every 100 mm along the length of beam with its face parallel to the longitudinal axis. Two source transducer orientations were explored, direct, with the transducer directing wave energy along the longitudinal axis, and indirect, with the transducer directing wave energy perpendicular to the longitudinal axis. When the measurements were taken at a distance greater than five wavelengths, the velocities from both types of measurements were equivalent for all transducers. The degree of dispersion increased as the transducer frequency increased.

Defect Detection

In one early paper (Lee 1965), the possibility of using ultrasonic inspection as a safety measure was explored. Differences in wave speeds as a function of the wave angle to the grain orientation were examined. The possibility of detecting delamination as a function of amplitude and wave velocity was discussed. Energy reflection based upon the size of the reflecting defect was calculated.

An early paper in ultrasonic inspection (McDonald 1978) put a board in a fluid tank. McDonald sent signals through the specimen and recorded the time of flight (TOF). A good correlation between the TOF and defect location was observed. Also, a strong relationship between grain direction and the velocity of sound was noted.

Pellerin and others (1985) were the first to report on a systematic examination of the effect of biological attack on the acoustic properties of clear wood. They used small, clear Southern Pine specimens in a laboratory study designed to examine the effect of brown-rot decay fungi and termite attack on acoustic velocity and static strength. Time-of-flight measurements, parallel to the fiber axis, were made using a through transmission system on specimens after various exposure times. The researchers observed a considerable change in acoustic time of flight with exposure time. More importantly, they were able to make several conclusions. Changes in time of flight occurred well before measureable loss of either weight loss (density) or strength was observed. A significant correlation was observed between residual strength and acoustic time of flight. Time of flight measurements parallel to the fiber axis were not useful for monitoring changes in corresponding strength for termite attack because of their preferential consumption of the early wood sections of the specimens.

Hamm and Lam (1987) used transit times of waves traveling longitudinally as a metric for locating compression wood in western hemlock. Moisture content, grain angle, thickness, knots, and wane complicated the transit time measurement. Transit time uniformity along the board was used to eliminate the effects of knots and wanes. Moisture content and thickness did not completely mask the presence of compression wood. Grain angle was a factor that still affected compression wood identification.

In a 1987 study, Patton-Mallory and others used acousto-ultrasonics to determine the presence of brown rot in Southern Pine. Coupling the sensors to the wood proved difficult. Hot melt adhesives produced the most repeatable results. Time centroid and peak time were the most repeatable waveform parameters.

Hamm and Lum (1991) explored the feasibility of using ultrasound as an online tool to identify compression wood. A slope of grain indicator was also investigated using western hemlock, but its accuracy was insufficient for compression wood identification.

DeGroot and others (1994, 1995, 1998) reported both energy storage and loss parameters for monitoring the deterioration of clear wood when exposed to natural populations of decay fungi and subterranean termites.

Ross and others (1994) used a pulse echo test setup to measure speed of sound transmission and wave attenuation, parallel to the fiber axis, in small clear Southern Pine specimens in field exposure conditions.

In studies in 1996 and 1997, Ross and others also developed empirical models that used both parameters capable of predicting residual compressive strength with a high level of accuracy.

Ross and DeGroot (1998) reported on a test setup they developed to monitor deterioration in full-size lumber specimens that were exposed, above ground, to naturally occurring decay fungi. The setup was based on a through transmission concept, with rolling ultrasonic transducers used to transmit and receive the pulse, perpendicular to the fiber axis. Time of flight was measured with a commercially available timing unit. The specimens used in this study were completely free of natural defects. Consequently, changes in acoustic parameters after exposure were solely attributed to deterioration resulting from decay fungi.

Niemz and Kucera (1998) examined the ability of ultrasound to detect defects using small holes drilled into Norway spruce specimens. Holes were varied in both size and orientation. Small defects were difficult to discern because of wood variability. The influence frequency upon of wave speed was also studied. This study modeled velocity of waves traveling at angles across the wood grain using the Hankison equation.

Dolwin and others (2000) used both stress-wave and ultrasonic inspection to detect decay in cross sections of English oak (*Quercus robur* L.) and European beech (*Fagus*

sylvatica L.). Cubes of wood were inoculated with white-rot, brown-rot, or soft-rot. The wave speeds were measured using ultrasonic and acoustic stress waves. The slowing effect that rot had upon waves was more noticeable in acoustic waves than in ultrasonic waves.

Brashaw and others (2000) used ultrasound conjunction with gas chromatography mass spectroscopy to identify wetwood in red oak lumber. The study also identified a relationship between the level of wetwood and energy-based ultrasound parameters.

Ross and others (2001) examined the relationship between time of flight (TOF) measurements made perpendicular to the fiber axis of large timbers that had been in service and their residual strength in compression (both parallel and perpendicular to fiber axis). Noting that the sample size they used was very small, they observed a strong relationship between TOF and compression strength.

Kabir and Araman (2002) examined several parameters derived from ultrasonic signals recorded during inspection of wooden pallets. Signal amplitude was decreased in the presence of defects. The severity and types of the defects correlated to the degree of dispersion of the power spectrum. Energy loss parameters were more sensitive to defects than time of flight measurements.

Schubert and others (2005) used resonant ultrasonic spectroscopy to determine the shear modulus of decayed and sound specimens of Norway spruce. The specimens were excited using ultrasonic transducers and displacement at the faces were measured using laser interferometers. The natural frequencies of the specimens were determined from the displacement response measurements. The reduction in shear modulus was six to ten times larger than the density loss from fungal decay. The shear velocity and damping were calculated at different stages of fungal rot.

Hasenstab and others (2005) used echo technique to detect local defects. Measurements were taken transverse and parallel to the grain. The echo technique only required access to one side of the inspected specimen.

The sensitivity of different MOE calculation methods to the presence of holes in a beam was explored in 2005 by Castellanos and others. Several 50-mm holes were drilled in beams of *Cryptomeria japonica* (Japanese Sugi). The MOE of the boards were then determined using four different methods. The four MOE calculation methods, ordered by increased sensitivity, were static bending, ultrasonic, acoustic stress wave, and longitudinal vibration.

Schubert and others (2006) used modal analysis and ultrasonic inspection to determine the change in shear modulus of Norway spruce upon exposure to white-rot fungus (*Heterobasidion annosium* and *Ganoderma lipsiense*). During the 12 weeks of exposure, *H. annosium* induced a 10% and *G. lipsiense* a 50% reduction in shear modulus.

Lin and others (2007) examined the degradation of railroad ties that had been taken out of service after 20 years. The goal of this research was to evaluate the possibility of reusing ties in the same or other applications. Hence, the ties were tested as is and after being cut down to lumber of two smaller sizes. The sound velocity was found to have the best correlation to the residual strength of the ties with it decreasing as the samples tested ranged from small lumber piece to larger lumber to tie. The dynamic modulus of elasticity was found to have a weaker correlation with residual strength and the values generally higher.

Hyvärinen (2007) used air-coupled transducers to detect defects in Scots pine. Knots, cracks, and heartwood were identified. The signal attenuation was capable of detecting heartwood while the board was moving between 1 and 3 m/s, opening the possibility of online grading. Air transducer sorting comported with visual sorting for 90% of the boards.

Tomographic views of timber members were constructed by Riggio and Piazza (2011) using ultrasonic transducers. Heterogeneities that affect wood strength were mapped using ultrasound and were then related to external features using digital photogrammetry. Drilling resistance tests were also used to corroborate results.

Examining the effect of fungal decay on Norway spruce, Reinprecht and Hibky (2011) demonstrated that sound velocity and dynamic modulus were suitable for revealing which fungal agent was responsible for the decay with known decreases in wood density. Yet, the study could not tell the difference between various strains of brown-rot fungus.

Ritschel and others (2013) studied damage mechanisms within failing spruce specimens in virtually real time using a combination of acoustic emission and synchrotron radiation x-ray tomographic microscopy (SRXTM). Acoustic emission enabled sub-millisecond resolution when determining damage initiation. The SRXTM produced high-resolution visualizations of the inner wood cellular structure in three dimensions. The visualizations allowed observation of changes in the microscopic wood structure in both time and space that led to ultimate failure.

White and others (2013) reviewed the ability of several nondestructive techniques to assess wood damaged by heat and fire. The study found that changes in time delay and wave velocity for charred yellow poplar specimens was minor, but the area under the power spectral density plot changed significantly. Several other non-ultrasonic NDE techniques were also discussed but were not included in this review.

Engineered Wood Products

Engineered wood products cover a variety of material including oriented strandboard (OSB), fiberboard, particleboard, plywood, glued-laminated (glulam) beams, and veneers.

Strength and Grading

An early review of ultrasonic evaluation of wood composites was given in Szabo (1978). This reference covered many aspects of ultrasonic inspection including anisotropy, coupling issues, wave types, attenuation, basic ultrasonic testing setups, transducer descriptions, and the advantages and disadvantages of higher frequency usage. The concepts presented were fundamental when ultrasound was used in inspection applications.

In a 1978 study, Kunesh found visual grading of parallel laminated veneer (PLV) made from Douglas-fir to be unsatisfactory with grading for strength. Ultrasonic inspection was capable of grading the material at a rate such that it could be used on a production line. A similar study was conducted using laminated veneer lumber with similar results and conclusions (Sharp 1985).

Petit and others (1991) examined the changes in ultrasonic behavior through laboratory aged structural flakeboard. The boards were tested before an aging process was applied. Ultrasonic wave velocity decreased as the angle diverged from parallel with the length of the boards. The aging processes were hygrothermal treatments and were performed in accordance with French standards NF 51-262 and NF 51-263. Ultrasonic wave velocity, modulus of elasticity, and modulus of rupture decreased after the aging process was applied. High correlation between wave velocity and MOE both prior to and after the aging process supported the hypothesis that the relationship could be used to develop nondestructive evaluation techniques. The correlation between wave velocity and modulus of rupture was not as high as wave velocity and MOE, but the potential to use the relationship in an evaluation technique still existed.

Lemaster and Beall (1993) examined surface roughness of medium density fiberboard (MDF) using acoustic emission. Wave guides of various shapes were moved across surfaces of MDF that were previously sanded using various sized grit sandpaper. The motion and the waveguides caused measurable acoustic emission events. The technique was capable of detecting groves and snaking.

A 1996 study by Kruse and others used contact and non-contact methods to measure wave speed through MDF and particleboard. Surface sanding affected the ultrasonic waves, so the two groups were tested separately. Unsanded boards had lower velocities. Non-contact methods were better correlated than contact methods for both internal bond of sanded boards and also swelling of unsanded boards. Wave velocity was measured through both MDF and particleboards with thicknesses of 34 mm or less without problems caused by signal attenuation.

Beall and Chen (1998) used ultrasonic waves and acousto-ultrasonic techniques to monitor particleboard curing. Wave guides allowed signals to be taken from the boards during pressing, but without interfering with the process. Strength development, board thickness, resin content, and press temperature correlated to the root mean square (RMS) of the collected signals.

In 1998, Tucker and others evaluated several ultrasonic frequencies for monitoring wood plastic composites. The study determined wave speed and attenuation from ultrasonic signals. Strong correlation existed between wave speed and MOE. Good correlation existed between MOE and MOR. High frequencies were significantly attenuated over short distances.

The relationship between wave velocity through wood-based composite materials and several different parameters was explored by Bekhta and others (2000). Particleboard, OSB, and MDF were studied. Parameters examined included relative humidity, temperature, direction of measurements, and frequency. Empirical equations relating modulus of rupture, resonance frequency, wave velocity, MOE calculated from resonance frequency, MOE calculated from wave velocity, and MOE measured from static bending tests as well as the associated correlation values for each relationship were given.

Vun and others (2000) used contact and non-contact sensors to inspect OSB. Wave velocities were higher when contact sensors, rather than non-contact, were used. Internal voids were found to reduce MOE and dimensional stability. Wave velocity and attenuation were fitted to a third order polynomial to density. The percentage of board resin affected the velocity trends.

Kruse (2000) explored use of various NDT technologies for process control of panel production. A good reference on several NDT technologies and their individual uses in panel production was provided. Ultrasonic velocity was useful in determining panel thickness, MOE, and internal bond for particleboard and MDF. The use of ultrasound to evaluate internal bond was thought to potentially reduce production cost between 2% and 8%.

Vun and others (2002) characterized the horizontal density of OSB using several parameters including ultrasonic velocity. Other parameters examined were attenuation and RMS. A polynomial and a power model were constructed. The power model provided a higher correlation with the measured density values.

A 2002 study by Moore and Bier found that veneer grading using both ultrasonic velocity and density produced lower variable grades than using ultrasonic velocity alone. Much of the discussion focused upon methods of adjusting calculations for veneers with higher MC so grading could be ultimately performed on green wood veneer.

Tucker and others (2002) evaluated the elastic properties of natural fiber composite panels using antisymmetric plate waves excited by an ultrasonic tone burst. Flexural and

transverse shear rigidity values were obtained from dispersion curves using fundamental plate wave propagation theory. Good agreement existed between the shear modulus calculated from transverse through-thickness tests and the plate wave tests. The effects of panel othrotropy on the shear modulus and rigidity calculations were discussed. The method was determined to be feasible and accurate for panels less than 6.4 mm thick.

Najafi and Ebrahimi (2005) tested three different methods for predicting the longitudinal velocity in particleboard and fiberboard. Longitudinal wave velocity was found to change within particle and fiber boards because of constituent material aligning with manufacturing machinery during production. Hankinson and Jacoby equations were used to model the change in longitudinal velocity. Cubic and quadratic equations, using angle as the independent variable, were also examined. All three methods were effective at modeling the velocity changes to manufacturing angle.

Defect Detection

The success of ultrasonic inspection to detect voids led to a discussion of the feasibility of online production inspection of plywood and composite boards. Baker and Carlson (1978) found use of non-contact sensors as part of quality control had great potential to benefit both manufacturers and customers.

Beall and Biernacki (1991) evaluated Douglas-fir glulam beams using acousto-ultrasonic techniques. To minimize variation in reference tests conducted on control zones, the time to peak amplitude was used as a parameter. The acousto-ultrasonic techniques were not directly sensitive to bond strength, but were sensitive to the presence of certain defects.

Illman and others (2002) were the first to examine use of acoustic parameters for monitoring the deterioration of a commonly used wood structural composite, oriented strandboard (OSB). In a closely controlled laboratory experiment, they obtained similar results to those observed for clear wood. In a follow-up analysis of the data, Ross and others (2003) were successful at developing strong correlative models between acoustic parameters and the residual strength of deteriorated OSB.

Dill-Langer and others (2005) evaluated defects in adhesive boding between laminates of glulam beams using several ultrasonic parameters. Defects included lack of adhesive, adhesive curing prior to bonding, and epoxy block gluing. The parameters examined were time of flight (TOF), peak to peak amplitude, and amplitude of initial peak. The amplitude of the initial peak was found to be useful when detecting glue line defects. Both TOF and peak to peak amplitude showed large fluctuations and limited contrast. Three coupling conditions were also explored: dry, paste, and elastomer. Dry coupling produced the worst test results with low signal to noise ratio; paste coupling provided the best. Elastomer coupling had a higher signal to noise ratio than dry but did not alter the condition of the beam as did paste.

In 2009, Bobadilla and others artificially aged particle- and fiberboards and then tested using several inspection methods including ultrasound. Strong correlation was found between ultrasonic wave velocity and changes in mechanical properties of the boards subjected to aging. The independent variables were used to estimate the natural logarithm of density rather than density itself, which might have contributed to the strength of the correlation.

Sanabria and others (2009) identified delamination defects between two solid spruce boards bonded together with polyurethane adhesive by using ultrasonic inspection. The boards were 5-mm thick. The boards were bonded with adhesive, but portions of the bonding surfaces were left free of adhesive. Air-coupled transducers were used to perform through transmission measurements. The signal loss due to lack of glue bonding far exceeded the loss from normal wood heterogeneity spruce.

Divos and others (2009) measured the depth of cracks within glulam beams using ultrasonic techniques. Transducers were places on either side of the crack within 20 to 50 mm. The crack depth was estimated based upon TOF measurements and was accurate to within 10% of the true crack depth. Initial tests were carried out to estimate shear strength between lamina. Estimations of residual stresses within glulam beams were caused by the manufacturing process and changes to the climate condition.

In a follow-up to the study conducted by Bobadilla and others (2009), the researchers artificially aged OSB panels and then tested the panels using several inspection methods including ultrasound. Strong correlation was found between ultrasonic wave velocity and changes in mechanical properties of the OSB panels. During the inspection, the transducers were inclined 45° to the plane of the panel surface. The feasibility of using the technique in the field was demonstrated.

In 2011b, Bucur performed a dual high and low frequency inspection on wood based composites. A dual high and low frequency inspection was carried out on wood based composites. Local defects were detected using high frequency ultrasonic techniques. Global damage detection was based upon low frequency vibrations. A finite element model of the analyzed structure was used to estimate modal shapes, frequencies, and damping.

Sanabria and others (2011) examined the structural integrity of multilayered glued-laminated beams using air coupled transducers. Bonding defect between lamina were identified for specimens 520 mm (20.5 in.), demonstrating for the first time the feasibility of using air coupled transducers on lamina of such thickness.

Acoustic Emission

Acoustic emission is not strictly an ultrasonic method. The frequencies excited during an acoustic emission event can be within the acoustic or ultrasonic ranges, or both. The studies presented here involve researchers that have applied acoustic emission techniques within the ultrasonic range of frequencies to engineered wood products. Beall (1989) presented a literature review covering work in the area of acoustic emissions prior to 1989.

Sato and Fushitani (1991) used acoustic emission to detect poor bonding in plywood. A three-point bending test allowed both MOE and acoustic emissions to be monitored in a single test. The number of AE events was found to be a better indicator of MOR than the number of knots. Regions of poor bonding were characterized by an increased number of acoustic emission events.

Lemaster (1993) conducted a study in which the individual particles and flakes used to make engineered wood panels were characterized using acoustic emissions. Particles and flakes were dropped onto a plate and the waveform was recorded. Waveforms were analyzed in both the time and frequency domain. Size classes were best defined by the number of threshold crossings. Frequency centroid was used to describe the category of particles and flakes.

A two part study was conducted by Adams and Morris in 1996. In the first part, Adams and Morris (1996) used acoustic emission in conjunction with fracture pullout to observe how changes in MC affected the fracture of OSB and MDF. Adams and Morris (1996) used acoustic emission in conjunction with fracture pullout to observe how changes in MC affected the fracture of OSB and MDF. A beam specimen was notched and then loaded in three-point bending. The notch on the beam was in line with the center load and opened towards the opposite side. As the test continued, the specimen fractured and the acoustic emission events were counted. The speed of the tests strongly influenced the results. In the second portion of the study, Morris and Adams (1996) correlated acoustic emissions to crack propagation. OSB and MDF were again the materials examined. Acoustic emissions were used to identify different stages of fracture during a three point bending test. The specimens were notched boards as described above. Crack formation initiated with high numbers of acoustic emission events; crack propagation had fewer events than formation. High MC lowered the number of events making it difficult to identify phases for crack formation and propagation.

Beall (1996) explored duration of load behavior of OSB by loading specimens to 40%, 65%, and 80% of ultimate load and monitoring acoustic emission events. The number of events increased at a rate similar to the rate of specimen deformation until a constant load point was reached; at which point, the number of events decreased exponentially. The difficulty of typical ultrasonic techniques to detect tensile damage in wood led to an investigation into identification through acoustic emissions. Pierre (2000) found that acoustic emissions showed promise as a tool to monitor tensile damage.

Vun and Beall (2002) demonstrated that acoustic emission was an effective tool in monitoring creep of OSB. The cumulative number of acoustic emission events correlated strongly to specimen deflection. The test also showed a potential future use of acoustic emission to evaluate fracture mechanisms and locating the source location.

Locations of fractures within specimens of OSB, plywood, and MDF were later located by Niemz and others (2007) using acoustic emissions. Four sensors were placed around the specimen. The difference in arrival time of the events allowed the fracture location to be estimated parallel to the panel. Perpendicular location was not possible as perpendicular wave speed was only a third of the wave speed parallel to the panel.

Ritschel and others (2011) performed tensile tests on LVL and monitored plywood samples using acoustic emission and digital image correlation. The rate and intensity of acoustic emission events changed with different strain behavior of the specimen, indicating that acoustic emissions were suitable for analyzing micro-mechanisms of damage growth.

El-Hajjar and Qamhia (2013) used acoustic waveforms produced by acoustic emissions during tensile testing of triaxially braided regenerated cellulose composites to identify failure modes. The study confirmed that acoustic emissions could be monitored to identify onset of internal damage.

Buildings and Structures

Many different ultrasonic inspection tools are commercially available. Ultrasonic inspection technology is well established, relatively low cost, and can be ruggedized for use outside ideal laboratory conditions. These features make ultrasound an attractive tool for use in situ. Palaia-Perez (1993) examined the time and frequency domain of ultrasonic signals through beams. Identifying conclusive patterns from the time domain signal was difficult; frequency domain signals provided useful information. Amplitude of the highest frequency decreases with the size of interior voids.

Baldassino (1996) used several nondestructive techniques in conjunction with each other including hardness testing, steel pin penetration, drilling resistance, and ultrasonic inspection. Beams were removed from the structure and tested. Baldassino determined that multiple techniques were necessary to assess the material behavior.

Anthony and others (1998) inspected timber piles from the Queens Boulevard Bridge in Queens, New York, using

radial ultrasonic inspection and micro-drilling techniques. Ultrasound was used to determine areas that needed to be inspected using a resistograph. The study was part of a comprehensive inspection using innovative techniques.

Transducer coupling was a focus when Emerson and others (1998) inspected creosote-coated timbers. TOF and frequency were collected in a grid along each timber. Advanced decay was easily identified using TOF. Spectral analysis and peak frequency showed potential in identifying incipient decay. A dry flexible membrane was used as a couplant. Greater consistency of coupling force was needed.

During shear wall testing, Beall and others (2005) found that few acoustic emission events occurred up to 40% of the maximum load. The absence of AE events indicates the deformation was reversible. AE events were more likely to be observed in the frame than the panel.

A description of an ultrasonic through transmission setup for clear wood timbers was provided in Agrawal and Choudhari (2009).

Karlinasari and Bahtiar (2011) examined the differences between boards end-jointed using finger joints and those using scarf joints. The process of end-jointing did not significantly change ultrasonic wave velocity and dynamic MOE from those of the constituent boards. The correlations between dynamic MOE from ultrasound and static MOE or MOR were higher in finger-jointed boards than scarf-jointed.

Teder and others (2011) examined the effect of sensor spacing on structural timber assessment. The study determined that decreasing the sensor spacing caused the inspection results to yield more localized value. A sensor distance of 600 mm was found to be the best arrangement for determining physical and mechanical properties using either longitudinal or indirect measurements. This finding matched the literature reviewed upon the subject. A brief description of ultrasonic inspection was also provided.

Teder and Wang (2013) used several nondestructive techniques to examine 75-year old glulam arches extracted from a building during deconstruction. The arches were tested using stress-wave timing, ultrasonic wave propagation, resistance microdrilling, and visual inspection along cutting planes. This study found that wave propagation was a good indicator of moderate to large delaminations and internal decay.

Historical Structures and Artifacts

There are many historical structures and artifacts of cultural significance. The alteration of these structures and objects would be considered at best, undesirable and, at worst, a loss for a society or the world. Nondestructive testing is especially well suited for inspecting these places and things as the ending condition is unchanged, insuring their preservation for future generations.

Ceccotti and Togni (1996) used several nondestructive techniques to evaluate beams from a fifteenth century Florentine building under restoration. Techniques used included visual inspection, stress wave, free vibration, hardness testing, and ultrasound. Wave inspection was poor at detecting ring shakes, localized decay, and variations in MC. A multiparameter inspection had the best correlation with strength.

The copper pins and the wood surrounding the pins from the USS Constitution were tested by Ross and others (1998) for signs of deterioration using ultrasound.

Kandemir-Yucel and others (2005) examined timbers from the Aslanhane Mosque in Ankara, Turkey, using thermographic and ultrasonic inspection. Ultrasound measurements were taken perpendicular to grain of pillars to evaluate their soundness. Infrared was used in conjunction with ultrasound to determine the effects of MC.

Lee and others (2009) evaluated an ancient Korean wood building, Daeseongjeon in Yeosan, Hyanggyo, using wave TOF measurements. Ultrasonic tomographic cross sections of supporting pillars were created. Coupling the sensors to the pillars was major difficulty during the inspection process due to poor surface conditions.

In 2009, Arriaga and others proposed a methodology of testing ancient Spanish timbers composed of Scots pine and Laricio pine. Twenty-five timber pieces were extracted from an eighteenth century building and tested in the proposed method and mechanical testing. The correlation between the proposed method and mechanical testing was low for MOE and poor for MOR.

Ross and Dundar (2012) inspected a 2,500-year-old Egyptian wooden inner coffin of Meretites using ultrasound. The bottom portion of the coffin was found to have deterioration.

In 2011, Lee and others presented a portable device capable of inspecting rafters from an ancient Korean wooden building. Conventional TOF was ineffective for rafter inspection. Several ultrasonic parameters were examined including TOF, amplitude, energy, pulse length, and RMS voltage. A poor correlation relationship was developed to estimate deterioration depth using the TOF and pulse length parameters.

Beikircher and others (2013) tested timber strength in buildings constructed over a wide range of dates 1250 AD to 2011 AD using both nondestructive and destructive methods. The nondestructive methods included visual inspection, electrical resistance, and ultrasound; the destructive methods were drill resistance and fractometer. The goal was to compare aged wood with virgin wood. Temperature, MC, and natural variability of wood caused results to lack precision. Indirect ultrasound measurements were not reliable when estimating strength of the wood.

Table 3.2—List of tree species studies and associated bibliographic reference

Tree species	Reference
Agathis alba	Karlinasari and others 2011
Alan batu (*Shorea albida*)	Duju and others 2000
Alder	Grimberg and others 2011
Alerce (*Fitzroya cupressoides*)	Baradit and Niemz 2011
Angelim (*Hymenolobium petraeum*)	Terezo and others 2005
Angelim araroba (*Votaireopsis araroba*)	Bartholomeu and Gonçalves 2007
Annona duckei	Inés and others 2011
Apeiba membranaceae	Inés and others 2011
Apuleia leiocarpa	Trinca and others 2009
	Inés and others 2011
Aquilaria microcarpa	Karlinasari 2013
Aspidosperma polyneuro	Trinca and others 2009
Aspidosperma rigidum	Inés and others 2011
Aspidosperma schultesii	Inés and others 2011
Astronium lecontei	Pires and others 2011
Balfourodendron riedelianum	Trinca and others 2009
Bauhinia purpurea	Karlinasari and others 2011
Beech	Diebold and others 2000
	Grimberg and others 2011
Betula costata	Wang and others 2013
Bilat (*Parashorea macrophlla*)	Duju and others 2000
Black oak (*Quercus kelloggii*)	Quarles and Zhou 1987
Brosimum potabile	Inés and others 2011
Cabreúva (*Myrocarpus frondosus*)	van Dijk and others 2013
Caesalpinia echinata	Trinca and others 2009
Caryocar glabrum	Inés and others 2011
Cavanillesia umbellate	Inés and others 2011
Cedrelinga cateniformis	Inés and others 2011
Cedrelinga Cateniformis Ducke	Yoza and Mallque 2011
Cherry	Grimberg and others 2011
Cherry (*Prunus sar gentii* Rehd. subsp. *jamasakura* Ohwi)	Kawamoto 1996
Chinese fir (*Cunninghamia lanceolata* (lamb.) Hook)	Yin and others 2005
Chrysophyllum prieurii	Inés and others 2011
Chrysophyllum venezuelanense	Pires and others 2011
Clarisia racemosa	Inés and others 2011
Croton matourensis	Inés and others 2011
Cupiúba (*Goupia glabra*)	Gonçalves and Bartholomeu 2002
	Gonçalves and Costa 2005
	Bartholomeu and Gonçalves 2007
Cupiúba (*Goupia glabra*)	Gonçalves and others 2011
Dacroides nitens	Inés and others 2011
Diplotropis purpurea	Inés and others 2011
Dipteryx micrantha	Inés and others 2011
Dipteryx odorata	Trinca and others 2009
Douglas-fir (*Pseudotsuga menziesiii*)	Kunesh 1978
	Lemaster and others 1993
	Anthony and Phillips 1991
	Beall and Biernacki 1991
	Anthony and Phillips 1993
	Diebold and others 2000
	Ballarin and others 2002
	Seeling 2002
Eastern cottonwood (*Populus deltoids*)	Brancheriau and others 2011
Endopleura uchi	Pires and others 2011
English oak (*Quercus robur* L.*)*	Dolwin and others 2000
Eucalipto (*Eucalyptus saligna*)	Gonçalves and others 2011
Eucalyptus citriodora	Bartholomeu and Gonçalves 2007
	Gonçalves and others 2009
	Bertoldo and others 2013
	Freitas and others 2013
Eucalyptus globulus	Yang and others 2007

Table 3.2—List of tree species studies and associated bibliographic reference (cont.)

Tree species	Reference
Eucalyptus grandis	Bartholomeu and Gonçalves 2007
	Pedroso and others 2011, 2013
	Ferreira and others 2013
Eucalyptus pellita	Bertoldo and others 2013
Eucalyptus saligna	Bartholomeu and Gonçalves 2007
	Freitas and others 2013
European beech (*Fagus sylvatica*)	Dolwin and others 2000
Ficus Americana	Inés and others 2011
Fraxinus mandshurica	Song and others 2011
Gallesia integrifólia	Trinca and others 2009
Garapeira (*Apulleia leiocarpa*)	Gonçalves and others 2011
Guarea kuntiana	Inés and others 2011
Holopyxidium jarana	Pires and others 2011
Imbuia (*Ocotea porosa*)	Gonçalves and Costa 2005
Jacaranda copaia	Inés and others 2011
Jackfruit (*Artocarpus heterophyllus* Lamk.)	Karlinasari and others 2009
Japanese cedar (*Cryptomeria japonica* D. Don)	Soma and others 2000
Japanese magnolia (*Magnolia obovata* Thunb.)	Sasaki and Hasegawa 2000
Japanese Sugi (*Cryptomeria japonica*)	Castellanos and others 2005
Jeunjing (*Paraserianthes falcataria*)	Karlinasari and others 2007
Keruing utap (*Dipterocarpus rigidus*)	Duju and others 2000
Kruing (*Dipterocarpus* spp.)	Tjondro and Soryoatmono 2007
Larch	Diebold and others 2000
Larch (*Larix gmelini*)	Yin and others 2009
Laricio pine (*Pinus nigra* Arn. ssp. *salzmannii*)	Arriaga and others 2009
	Iñiguez and others 2009
	Iñiguez-Gonzalez and others 2013
Laurel (*Laurelia sempervirens*)	Baradit and Niemz 2011
Lecythis pisonis	Pires and others 2011
Lenga (*Nothofagus pumilio*)	Baradit and Niemz 2011
Licania elata	Inés and others 2011
Loblolly pine	Huang 2000
Loblolly pine (*Pinus taeda*)	Oliveira and others 2002
	Fassola and others 2011
Madrone (*Arbutus menziesii*).	Hamstad and others 1993
Mangium (*Acacia mangium* Willd.)	Karlinasari and others 2009
Manio (*Podocarpus nubigena*)	Baradit and Niemz 2011
Maple (*Acer* spp.)	Hamstad and others 1993
Maritime pine (*Pinus pinaster* Ait.)	Machado 2002
	Iñiguez-Gonzalez and others 2013
Matisia bracteolosa	Inés and others 2011
Meranti (*Shorea* spp.)	Karlinasari and Bahtiar 2011
Mezilaurus	Trinca and others 2009
Mimusops elengi	Karlinasari and others 2011
Myroxylon Balsamum	Trinca and others 2009
Naucleopsis glabra	Inés and others 2011
Nectandra	Trinca and others 2009
Oak	Ross and others 1998
	Diebold and others 2000
Ocotea fragantisima	Inés and others 2011
Olivillo (*Aextoxicon punctatum*)	Baradit and Niemz 2011
Oriental beech (*Fagus orientalis*)	Najafi and others 2007, 2009
P. pachycharpa	Pires and others 2011
Pequía (*Aspidosperma desmanthum*)	Gonçalves and others 2011
Peroba (*Aspidosperma pirycollum*)	Terezo and others 2005
Pine	Diebold and others 2000
	Miettienen and others 2005
	Grimberg and others 2011
Pinho do Parana (*Araucaria angustifolia*)	Gonçalves and Costa 2005
Populus simonii	Song and others 2011

Table 3.2—List of tree species studies and associated bibliographic reference (cont.)

Tree species	Reference
Pouteria guianensis	Pires and others 2011
Pterocarpus indicus	Karlinasari and others 2011
Radiata pine (*Pinus radiata* D. Don)	Booker and others 1996, 2000
	Andrews 2002
	Moore and Bier 2002
	Kang and Booker 2002
	Iñiguez and others 2009
	Iñiguez-Gonzalez and others 2013
Ramin (*Gonystylus bancanus*)	Duju and others 2000
Red oak	Schafer and others 1998; Brashaw and others 2000
Red pine (*Pinus densiflora*)	Kawamoto 1993,1996
	Kim and others 2007; Oh and others 2013
Red pine (*Pinus resinosa*)	Gao and others 2011, 2013
Redwood (*Sequoia sempervirens*)	Hamstad and others 1993
	Ballarin and others 2002
	Seeling and others 2002
Resak durian (*Cotylelobium burcki*)	Duju and others 2000
Romanian beech	Curtu and others 1996
Salix matsudana Koidz	Song and others 2011
Sandalwood (*Santalum album*)	Turpening 2011
Schefflera morototoni (*Sacha cetico*)	Inés and others 2011
Scots pine (*Pinus sylvestris* L.)	Abbott and Elcock 1987
	Feeney and others 1996
	Kánnár 2000
	Iñiguez and others 2007
	Hyvärinen 2007
	Arriaga and others 2009
	Iñiguez and others 2009
	Hermoso and others 2013
	Iñiguez-Gonzalez and others 2013
	Llana and others 2013
	Noya 2013
Sessile oak (*Quercus petrea*)	Dundar and others 2013
Silver fir (*Abies alba* Mill.)	Ceccotti and Tongi 1996
Simarouba amara	Inés and others 2011
Slash pine (*Pinus elliottii*)	Bartholomeu and Gonçalves 2007
	Massak and others 2009
	Pedroso and others 2011
Southern pine	Patton-Mallory and others 1987
Spruce	Sandoz 1991
	Feeney and others 1996
	Diebold and others 2000
	Hauffe and Mahler 2000
	Kuklík and Kuklíkova 2000
	Pierre 2000
Spruce (*Picea abies*)	Niemz and Kucera 1998
	Dill-Langer et al 2002
	Seeling and others 2002
	Rosner and Wimmer 2005
	Schubert and others 2005
	Sanabria and others 2009
	Rohanová and others 2011
	Rosner 2011
	Sanabria and others 2011
	van der Beek and Tiitta 2011
Sterculia frondosa	Inés and others 2011
Sweet chestnut (*Castanea sativa* Mill.)	Dundar and others 2013
	Iñiguez-Gonzalez and others 2013
	Vásquez and others 2013
Swietenia sp.	Karlinasari and others 2011
Sycamore	Grimberg and others 2011

Table 3.2—List of tree species studies and associated bibliographic reference (cont.)

Tree species	Reference
Sycamore fig (*Ficus sycomorus*)	Dundar and Ross 2011
Tabebuia serratifolia	Inés and others 2011
Tepa (*Laureliopsis philipiana*)	Baradit and Niemz 2011
Tetragastris panamensis	Inés and others 2011
Toona ciliata	Pedroso and others 2011
Ulmus pumila	Song and others 2011
Unonopsis floribunda	Inés and others 2011
Vatairea sericea	Pires and others 2011
Vochysia lomatifolia	Inés and others 2011
Western hemlock	Hamm and Lam 1987, 1991
White fir (*Abies concolor*)	Berdnt 2002
Xylopia nitida	Inés and others 2011
Yellow pine	Groom 1991

Noya (2013) examined two Scots pine structural members of the seventeenth century roof of the library of the College of San Pablo in Granada, Spain, using ultrasound, MC measurements, and fungal cultures. Ultrasound measurements were taken perpendicular to the grain of the timbers. Data from the inspection led to the conclusion that high decay was present.

Concluding Remarks

Ultrasonic inspection of wood has evolved over a half a century of research and development. In this chapter, a comprehensive literature review of the use of ultrasound in wood inspection was presented and information regarding basic ultrasonic inspection techniques and analyses were described. Table 3.2 at the end of this chapter contains a list of over one hundred species of wood that have been inspected using ultrasound.

Strength grading, determination of elastic constants, and evaluation of MC effects are a few of the fields to which ultrasonic inspection have been successfully applied. The most widespread application of ultrasonic inspection with wood is arguably defect detection. There is an ongoing need to detect and assess defects within standing trees, poles, lumber, structures, and engineered wood products. Increased sensitivity and more accurate approximations of remaining wood strength aid inspectors in the evaluating the utility and safety of wood structures. Wood is already the most common building material in the world, but with the increased reliability that comes with advanced ultrasonic inspection techniques, its use can only grow.

Literature Cited

Abbott, A.R.; Elcock, G. 1987. Pole testing in the European context. In: Proceedings, 6th Symposium, Nondestructive Testing of Wood. Pullman, WA. 277–302.

Adams, J.; Morris, V. 1996. Acoustic emission and fracture pullout of wood-based panel products. In: Proceedings, 10th Symposium, Nondestructive Testing of Wood. Lausanne, Switzerland. 3–11.

Agrawal, G.H.; Choudhari, N.K. 2009. Ultrasonic NDT for evaluation of wood quality in engineering structures. 2009. In: Proceedings, 16th Symposium, Nondestructive Testing of Wood. Beijing, China. 158–161.

Agrawal, G.H.; Choudhari, N.K. 2011. Ultrasonic NDT of wood using IDSAM 443. In: Proceedings, 17th Symposium, Nondestructive Testing of Wood, Vol. 2. Sopron, Hungary. 443–451.

Andrews, M.K. 2002. Which acoustic speed? In: Proceedings 13th Symposium Nondestructive Testing of Wood. Berkeley, CA. 159–165.

Anthony, R.W.; Phillips, G.E. 1991. Process control of finger joint strength using acousto-ultrasonics. In: Proceedings, 8th Symposium Nondestructive Testing of Wood. Vancouver, WA. 45–56.

Anthony, R.W.; Phillips, G.E. 1993. An update on acousto-ultrasonics applied to fingerjoints. In: Proceedings, 9th Symposium Nondestructive Testing of Wood. Madison, WI. 55–60.

Anthony, R.W.; Pandey, A.K.; Arnette, C.G. 1998. Integrating nondestructive evaluation tools for the inspection of timber structures. In: Proceedings, 11th Symposium Nondestructive Testing of Wood. Madison, WI. 169–174.

Arriaga, F.; Íñiguez, G.; Esteban, M.; Bobadilla, I. 2009. Proposal of a methodology for the assessment of existing timber structures in Spain. In: Proceedings, 16th Symposium Nondestructive Testing of Wood. Beijing, China. 145–151.

Baker, D.E.; Carlson, D.C. 1978. Online product inspection by non-contact ultrasonics. In: Proceedings, 4th Symposium Nondestructive Testing of Wood. Vancouver, WA. 233–237.

Baldassino, N.; Piazza, M.; Zanon, P. 1996. In situ evaluation of the mechanical properties of timber structural elements. In: Proceedings, 10th Symposium Nondestructive Testing of Wood. Lausanne, Switzerland. 369–377.

Ballarin, A.W.; Seeling, U.; Beall, F.C. 2002. Process and analysis of signals through clear wood using acousto-ultrasonics. In: Proceedings, 13th Symposium Nondestructive Testing of Wood. Berkeley, CA. 167–171.

Baradit, E.; Niemz, P. 2011. Selected physical and mechanical properties of Chilean wood species Tepa, Olivillo, Laurel, Lenga, Alerce and Manio. In: Proceedings, 17th Symposium Nondestructive Testing of Wood, Vol. 2. Sopron, Hungary. 395–401.

Bartholomeu, A.; Gonçalves, R. 2007. Ultrasound and transverse vibration to determine modulus of elasticity of wood. In: Proceedings, 15th Symposium Nondestructive Testing of Wood. Duluth, MN. 85–88.

Beall, F.C. 1987a. Fundamentals of acoustic emission and acousto-ultrasonics. In: Proceedings, 6th Symposium Nondestructive Testing of Wood. Pullman, WA. 3–28.

Beall, F.C. 1987b. Future applications of acoustic emission and acousto-ultrasonics. In: Proceedings, 6th Symposium Nondestructive Testing of Wood. Pullman, WA. 369–375.

Beall, F.C. 1989. Use of AE/AU for evaluation of adhesively bonded wood base materials. In: Proceedings, 7th Symposium Nondestructive Testing of Wood. Madison, WI. 45–53.

Beall, F.C. 1996. The use of acoustic emission to assess duration of load behavior in oriented strand board. In: Proceedings, 10th Symposium Nondestructive Testing of Wood. Lausanne, Switzerland. 33–41.

Beall, F.C.; Biernacki, J.M. 1991. An approach to the evaluation of glulam beams through acousto-ultrasonics. In: Proceedings, 8th Symposium Nondestructive Testing of Wood. Vancouver, WA. 73–88.

Beall, F.C.; Chen, L. 1998. Monitoring of resin curing in a laboratory press using acousto-ultrasonics. In: Proceedings, 10th Symposium Nondestructive Testing of Wood. Lausanne, Switzerland. 9–18.

Beall, F.C.; Li, J.; Breiner, T.A. 2005. Monitoring cumulative damage in shear wall testing with acoustic emission. In: Proceedings, 14th Symposium Nondestructive Testing of Wood. Eberswalde, Germany. 93–100.

Beikircher, W.; Zingerle, P.P., Kraler, A., Flach, M. 2013. Evaluation of wood strength with nondestructive and semi-destructive test methods on historical buildings in northern Italy. In: Proceedings, 18th Symposium Nondestructive Testing of Wood. Madison, WI. 207–215.

Bekhta, P.; Niemz, P.; Kucera, L. 2000. The study of sound propagation in the wood-based composite materials. In: Proceedings, 12th Symposium Nondestructive Testing of Wood. Sopron, Hungary. 33–41.

Berndt, H. 2002. Improving comparability of ultrasonic measurements on wood. In: Proceedings, 13th Symposium Nondestructive Testing of Wood. Berkeley, CA. 173–177.

Berndt, H.; Schntewind, A.P.; Johnson, G.C. 2000. Ultrasonic energy propagation through wood: where, when, how much. In: Proceedings, 12th Symposium Nondestructive Testing of Wood. Sopron, Hungary. 57–65.

Berndt, H.; Johnson, G.C.; Schniewind, A.P. 2005. Using phase slope for arrival time determination. 2005. In: Proceedings, 14th Symposium Nondestructive Testing of Wood. Eberswalde, Germany. 317–322.

Bertoldo, C.; Gonçalves, R.; Lorensani, R. 2013. Acoustoelasticity of wood determined by static bending experiments. In: Proceedings, 18th Symposium Nondestructive Testing of Wood. Madison, WI. 469–476.

Bobadilla, I.; de Hijas, M.M.; Esteban, M.; Íñiguez, G.; Arriaga, F. 2009. Nondestructive methods to estimate physical and biological aging of particle and fibre boards. In: Proceedings, 16th Symposium, Nondestructive Testing of Wood. Beijing, China. 222–228.

Bobadilla, I.; Robles, M.; Martínez, R.; Íñiguez-Gonzalez, G.; Arriaga, F. 2011. In situ acoustic methods to estimate the physical and mechanical aging of oriented strand board. In: Proceedings, 17th Symposium Nondestructive Testing of Wood, Vol. 1. Sopron, Hungary. 375–380.

Booker, R.E.; Froneberg, J.; Collins, F. 1996. Variation of sound velocity and dynamic Young's modulus with moisture content in the three principal directions. In: Proceedings, 10th Symposium Nondestructive Testing of Wood. Lausanne, Switzerland. 279–295.

Booker, R.E.; Haslett, T.N.; Sole, J.A. 2000a. Acoustic emission study of within-ring internal checking in radiata pine. In: Proceedings, 12th Symposium Nondestructive Testing of Wood. Sopron, Hungary. 43–48.

Booker, R.E.; Ridoutt, B.G.; Wealleans, K.R.; McConchie, D.L.; Ball, R.D. 2000b. Evaluation of tools to measure the sound velocity and stiffness of green radiata pine logs. In: Proceedings, 12th Symposium Nondestructive Testing of Wood. Sopron, Hungary. 223–231.

Brancheriau, L.; Gallet, P.; Lasaygues, P. 2011. Ultrasonic imaging of defects in standing trees - development of an automatic device for plantations. In: Proceedings, 17th Symposium Nondestructive Testing of Wood, Vol. 1. Sopron, Hungary. 93–100.

Brashaw, B.K.; Adams, R.D.; Schafer, M.S.; Ross, R.J.; Pettersen, R.C. 2000. Detection of wetwood in green red oak lumber by ultrasound and gas chromatography mass

spectrometry analysis. In: Proceedings, 12th Symposium Nondestructive Testing of Wood. Sopron, Hungary. 49–56.

Brashaw, B.K.; Vatalaro, R.J.; Wang, X.; Ross, R.J.; Wacker, J.P. 2005. Condition assessment of timber bridges. 2. Evaluation of several stress wave tools. General Technical Report FPL–GTR–160, USDA Forest Products Laboratory, Madison, WI. 11 pp.

Bray, D.E.; Stanley, R.K. 1997. Nondestructive evaluation: a tool in design, manufacturing, and service, revised edition. Boca Raton, FL: CRC Press, Inc.

Bucur, V. 1978. Wood failure testing in ultrasonic methods. In: Proceedings, 4th Symposium Nondestructive Testing of Wood. Vancouver, WA. 223–226.

Bucur, V. 1996. Acoustics of wood as a tool for nondestructive testing. In: Proceedings, 10th Symposium Nondestructive Testing of Wood. Lausanne, Switzerland. 53–59.

Bucur, V. 2002. High resolution imaging of wood. In: Proceedings, 13th Symposium Nondestructive Testing of Wood. Berkeley, CA. 231–236.

Bucur, V. 2003. Nondestructive characterization and imaging of wood. Berlin Heidelberg, Germany: Springer-Verlag.

Bucur, V. 2006. Acoustics of wood. Berlin, Heidelberg, Germany: Springer-Verlag.

Bucur, V. (ed.). 2011a. Delamination in wood, wood products and wood based composites. Berlin Heidelberg, Germany: Springer-Verlag.

Bucur, V. 2011b. Delamination in wood products and wood based composites—the state of the art. In: Proceedings, 17th Symposium Nondestructive Testing of Wood, Vol. 2. Sopron, Hungary. 617–624.

Bucur, V.; Berndt, H. 2002. Ultrasonic energy flux deviation and off-diagonal elastic constants of wood. In: Proceedings, 13th Symposium Nondestructive Testing of Wood. Berkeley, CA. 273–276.

Castellanos, J.R.S.; Nagao, H.; Ido, H.; Kato, H.; Onishi, Y. 2005. NDE methods applied to the study of a wood beam's discontinuity. In: Proceedings, 14th Symposium Nondestructive Testing of Wood. Eberswalde, Germany. 361–372.

Ceccotti, A.; Togni, M. 1996. NDT on ancient timber beams: assessment of strength/stiffness properties combining visual and instrumental methods. In: Proceedings, 10th Symposium Nondestructive Testing of Wood. Lausanne, Switzerland. 379–388.

Curtu, I.; Rosca, C.; Barbu, M.C.; Curtu; L.A.; Crisan, R.L. 1996. Research regarding the growth stress measurement in beech using ultrasound technique. In: Proceedings, 10th Symposium Nondestructive Testing of Wood. Lausanne, Switzerland. 155–164.

De Groot, R.; Ross, R.; Nelson, W. 1994. Nondestructive assessment of biodegradation in southern pine sapwood exposed to attack by natural populations of decay fungi and subterranean termites. Proceedings, Twenty-Fifth Annual Meeting, The International Research Group on Wood Preservation, Bali, Indonesia, May 29–June 3, 1994. 13 p.

De Groot, R.C.; Ross, R.J.; Nelson, W.J. 1995. Natural progression of decay in unrestrained, southern pine sapwood lumber exposed above ground. Proceedings, Twenty Sixth Annual Meeting, IRG, Helsinger, Denmark. June 11–16, 1995.

De Groot, R.C.; Ross, R.J.; Nelson, W.J. 1998. Nondestructive assessment of wood decay and termite attack in southern pine sapwood. Wood Protection 3(2):25–34.

de Oliveira, F.G.R.; de Campos, J.A.O.; Pletz, E.; Sales, A. 2002. Assessment of mechanical properties of wood using an ultrasonic technique. In: Proceedings, 13th Symposium Nondestructive Testing of Wood. Berkeley, CA. 75–78.

Diebold, R.; Schleifer, A.; Glos, P. 2000. Machine grading of structural sawn timber from various softwood and hardwood species. In: Proceedings, 12th Symposium Nondestructive Testing of Wood. Sopron, Hungary. 139–146.

Dill-Langer, G.; Ringger, T.; Höfflin, F.; Aicher, S. 2002. Location of acoustic emission sources in timber loaded parallel to grain. In: Proceedings, 13th Symposium Nondestructive Testing of Wood. Berkeley, CA. 179–186.

Dill-Langer, G.; Bernauer, W.; Aicher, S. 2005. Inspection of glue-lines of glued-laminated timber by means of ultrasonic testing. In: Proceedings, 14th Symposium Nondestructive Testing of Wood. Eberswalde, Germany. 49–60.

Divos, F.; Divos, P. 2005. Resolution of the stress wave based acoustic tomography. In: Proceedings, 14th Symposium Nondestructive Testing of Wood. Eberswalde, Germany. 309–314.

Divos, F.; Szalai, J.; Garab, J.; Toth, A. 2009. Glued-laminated timber evaluation. In: Proceedings, 16th Symposium Nondestructive Testing of Wood. Beijing, China. 287–293.

Dolwin, J.A.; Lawday, G.; Lonsdale, D.; Barnett, J.R.; Hodges, P. 2000. Development and use of stress wave meter, to detect the presence of decay in wood blocks. In: Proceedings, 12th Symposium Nondestructive Testing of Wood. Sopron, Hungary. 187–196.

Duju, A.; Nakai, T.; Nagao, H.; Tanaka, T. 2000. Nondestructive evaluation of mechanical strength of sarawak timbers. In: Proceedings, 12th Symposium Nondestructive Testing of Wood. Sopron, Hungary. 131–137.

Dundar, T.; Ross, R.J. 2011. Condition assessment of a 2500 year old mummy coffin. In: Proceedings, 17th Symposium Nondestructive Testing of Wood. Vol. 2. Sopron, Hungary. 561–565.

Dundar, T., Wang, X., As, N., Avcı, E., 2013. Assessing the dimensional stability of two hardwood species grown in Turkey with acoustic measurements. In: Proceedings, 18th Symposium Nondestructive Testing of Wood. Madison, WI. 459–468.

El-Hajjar, R.; Qamhia, I. 2013. Kinematic and acoustic emission methodology for investigation of progressive damage behavior of triaxially braided regenerated cellulose composites. In: Proceedings, 18th Symposium Nondestructive Testing of Wood. Madison, WI. 301–308.

Emerson, R.N.; Pollock, D.G.; McLean, D.I.; Fridley, K.J.; Ross, R.J.; Pellerin, R.F. 1998. Nondestructive testing of large bridge timbers. In: Proceedings, 11th Symposium Nondestructive Testing of Wood. Madison, WI. 175–184.

Fassola, H.E.; Videla, D.; Winck, R.A.; Pezzutti, R. 2011. Effect of pruning of *Pinus taeda* on longitudinal ultrasound speed of standing trees and logs in plantations of north eastern Argentina. In: Proceedings, 17th Symposium Nondestructive Testing of Wood, Vol. 1. Sopron, Hungary. 113–120.

Feeney, F.E.; Chivers, R.C.; Evertsen, J.A.; Keating, J. 1996. The influence of inhomogeneity on the propagation of ultrasound in wood. In: Proceedings, 10th Symposium Nondestructive Testing of Wood. Lausanne, Switzerland. 73–81.

Ferreira, G.C.; Gonçalves, R.; Favalli, R.S.; Bertoldo, C. 2013. Adequacy of standards of wood grading using ultrasound to the standard of structural design. In: Proceedings, 18th Symposium Nondestructive Testing of Wood. Madison, WI. 410–417.

Freitas, F.F.F.; Gonçalves, R.; Coelho, E., Jr. 2013. Ultrasound as a tool in defining the reuse potential of wood poles. In: Proceedings, 18th Symposium Nondestructive Testing of Wood. Madison, WI. 404–409.

Gao, S.; Wang, X.; Wang, L. 2013. Effect of temperature and moisture state changes on modulus of elasticity of red pine small clear wood. In: Proceedings, 18th Symposium Nondestructive Testing of Wood. Madison, WI. 442–450.

Gao, S.; Wang, X.; Wan, L.; Allison, R.B. 2011. Modeling temperature and moisture state effects on acoustic velocity in wood. In: Proceedings, 17th Symposium Nondestructive Testing of Wood, Vol. 2. Sopron, Hungary. 411–418.

Gonçalves, R.; Bartholomeu, A. 2002. Evaluation of longitudinal variability of rigidity in a cupiúba trunk using an ultrasonic device. In: Proceedings, 13th Symposium Nondestructive Testing of Wood. Berkeley, CA. 79–81.

Gonçalves, R.; Costa, O.A.L. 2005. Variation in ultrasonic wave velocity and stiffness terms of the diagonal matrix with moisture content for tree species of Brazilian wood. In: Proceedings, 14th Symposium Nondestructive Testing of Wood. Eberswalde, Germany. 325–328.

Gonçalves, R.; Herrera, S.; Gray, G.; Cerri, D.G. 2009. Grading wooden new poles by ultrasound-Brazilian experience. In: Proceedings, 16th Symposium Nondestructive Testing of Wood. Beijing, China. 86–90.

Gonçalves, R.; Secco, C.B.; Cerri, D.; Batista, F. 2011. Behavior of ultrasonic wave propagation in presence of holes on pequia (*Aspidosperma desmanthum*) wood. In: Proceedings, 17th Symposium Nondestructive Testing of Wood, Vol. 1. Sopron, Hungary. 159–165.

Gonçalves, R.; Trinca, A.J.; Cerri, D.G.P.; Pellis, B.P. 2011. Elastic constants of wood determined by ultrasound wave propagation. In: Proceedings, 17th Symposium Nondestructive Testing of Wood, Vol. 2. Sopron, Hungary. 435–441.

Graff, K.F. 1975. Wave motion in elastic solids. New York: Dover Publications, Inc.

Grimberg, R.; Savin, A.; Curtu, I.; Stanciu, M.D.; Lica, D.; Cosereanu, C. 2011. Assessment of wood using air-coupled US transducer. In: Proceedings, 17th Symposium Nondestructive Testing of Wood, Vol. 2. Sopron, Hungary. 427–434.

Groom, L.H. 1991. Determination of truss-plate joint integrity using acousto-ultrasonics. In: Proceedings, 8th Symposium Nondestructive Testing of Wood. Vancouver, WA. 143–161.

Hamm, E.A.; Lam, F. 1987. Compression wood detection using ultrasonics. In: Proceedings, 6th Symposium Nondestructive Testing of Wood. Pullman, WA. 137–165.

Hamm, E.A.; Lum, C. 1991. Application of ultrasonics and a slope of grain indicator to detection of compression wood in lumber. In: Proceedings, 8th Symposium Nondestructive Testing of Wood. Vancouver, WA. 105–130.

Hamstad, M.A.; Quarles, S.L; Lemaster, R.L. 1993. Experimental far-field wideband acoustic waves in wood rods and plates. In: Proceedings, 9th Symposium Nondestructive Testing of Wood. Madison, WI. 30–44.

Han, W.; Birkland, R. 1991. Log scanning through combination of ultrasonics and artificial intelligence. In: Proceedings, 8th Symposium Nondestructive Testing of Wood. Vancouver, WA. 163–187.

Hasenstab, A.; Krause, M.; Hillemeier, B. 2005. Defect localization in wood with low frequency ultrasound echo technique. In: Proceedings, 14th Symposium Nondestructive Testing of Wood. Eberswalde, Germany. 331–336.

Hauffe, P.; Mahler, G. 2000. Evaluation of internal log quality using x-ray and ultrasound. In: Proceedings, 12th Symposium Nondestructive Testing of Wood. Sopron, Hungary. 259–263.

He, Y.; Manful, D.; Bardossy, A.; Dill-Langer, G.; Aicher, S. 2005. Application of fuzzy logic methods to signal

processing of ultrasound measurements. In: Proceedings, 14th Symposium Nondestructive Testing of Wood. Eberswalde, Germany. 277–286.

Huang, C. 2000. Predicting lumber stiffness of standing trees. In: Proceedings, 12th Symposium Nondestructive Testing of Wood. Sopron, Hungary. 173–179.

Hearmon, R.F.S. 1961. Applied anisotropic elasticity. Oxford, Great Britain: Oxford University Press.

Hearmon, R.F.S. 1965. The assessment of wood properties by vibrations and high frequency acoustic waves. In: Proceedings, 2nd Symposium Nondestructive Testing of Wood. Pullman, WA. 49–65.

Hermoso, E.; Montero, M.J.; Esteban, M.; Mateo, R.; Llana, D.F. 2013. The classification of large cross section sawn timber in the structural use of *Pinus silvestris* L. using NDT together with visual grading. In: Proceedings, 18th Symposium Nondestructive Testing of Wood. Madison, WI. 418–424.

Hyvärinen, V. 2007. Non-contact ultrasonic inspection of boards. In: Proceedings, 15th Symposium Nondestructive Testing of Wood. Duluth, MN. 149–153.

Illman, B.L.; Yang, V.W.; Ross, R.J.; Nelson, W.J. 2002. Nondestructive evaluation of oriented strand board exposed to decay fungi. In: Proceedings, 33rd Annual Meeting of The International Research Group on Wood Preservation, Cardiff, United Kingdom. May 12–17, 2002. Stockholm, Sweden: IRG Secretariat, 2002. IRG/WP; 02-20243: 6 p.

Inés, P.; Palacios, C.; Yoza, L.; Mallque, M.; Kian, J. 2011. Elasticity modulus in Peruvian tropical woods using nondestructive techniques - preliminary study. In: Proceedings, 17th Symposium Nondestructive Testing of Wood, Vol. 1. Sopron, Hungary. 469–475.

Íñiguez, G.; Esteban, M.; Arriaga, F.; Bobadilla, I., Gil, M.C. 2007. Influence of specimen length on ultrasound wave velocity. In: Proceedings, 15th Symposium Nondestructive Testing of Wood. Duluth, MN. 155–159.

Íñiguez, G.; Martinez, R.; Babadilla, I.; Arriaga, F.; Esteban, M. 2009. Mechanical properties assessment of structural coniferous timber by means of parallel and perpendicular to the grain wave velocity. In: Proceedings, 16th Symposium Nondestructive Testing of Wood. Beijing, China. 79–84.

Iñiguez-Gonzalez, G.; Llana, D.F.; Montero, M.J.; Hermoso, E.; Esteban, M.; Ceca, J.L.G.; Bobadilla, I.; Mateo, R.; Arriaga, F. 2013. Preliminary results of a structural timber grading procedure in spain based on nondestructive techniques, Guillermo. In: Proceedings, 18th Symposium Nondestructive Testing of Wood. Madison, WI. 386–395.

Kabir, M.F.; Araman, P.A. 2002. Nondestructive evaluation of defects in wood pallet parts by ultrasonic scanning. In: Proceedings, 13th Symposium Nondestructive Testing of Wood. Berkeley, CA. 203–208.

Kandemir-Yucel, A.; Tavukcuoglu, A.; Caner-Saltik, E.N. 2005. Nondestructive analyses of historic timber elements to assess their state of preservation. In: Proceedings, 14th Symposium Nondestructive Testing of Wood. Eberswalde, Germany. 137–144.

Kang, H-Y.; Booker, R.E. 2002. The characteristics of ultrasonic stress wave transmitted through wood during drying. In: Proceedings, 13th Symposium Nondestructive Testing of Wood. Berkeley, CA. 209–212.

Kánnár, A. 2000. Kaiser effect experiments in wood by acoustic emission testing. In: Proceedings, 12th Symposium Nondestructive Testing of Wood. Sopron, Hungary. 393–401.

Karlinasari, L.; Bahtiar, E.T. 2011. Nondestructive evaluation of end-jointed in meranti wood (*Shorea* spp.) using ultrasonic wave techniques. In: Proceedings 17th Symposium Nondestructive Testing of Wood, Vol. 1. Sopron, Hungary. 337–341.

Karlinasari, L.; Surjokusumo, S.; Nugroho, N.; Hadi, Y. 2007. Evaluation of wood beam quality of *Paraserianthes falcataria*. In: Proceedings, 15th Symposium Nondestructive Testing of Wood. Duluth, MN. 187–190.

Karlinasari, L.; Oktarina, R.; Pebriansjah, E.W.; Mardikanto, T.R. 2009. Nondestructive testing of tropical wood for structural uses. In: Proceedings, 16th Symposium Nondestructive Testing of Wood. Beijing, China. 125–129.

Karlinasari, L.; Mariyanti, I.L.; Nandika, D. 2011. Ultrasonic wave propagation characteristic of standing tree in urban area. In: Proceedings, 17th Symposium Nondestructive Testing of Wood, Vol. 1. Sopron, Hungary. 151–157.

Karlinasari, L.; Uar, N.I.; Kusumo, H.T.; Santoso, E.; Nandika, D. 2013. Evaluation of Agarwood (*Aquilaria microcarpa*) trees using ultrasonic wave propagation. In: Proceedings, 18th Symposium Nondestructive Testing of Wood. Madison, WI. 107–111.

Kawamoto, S. 1993. Attenuation of acoustic emission waves during the drying of wood. In: Proceedings, 9th Symposium Nondestructive Testing of Wood. Madison, WI. 23–29.

Kawamoto, S. 1996. Detection of acoustic emissions associated with the drying of wood. In: Proceedings, 10th Symposium Nondestructive Testing of Wood. Lausanne, Switzerland. 23–31.

Kim, K-M.; Park, J-S.; Lee, S-J.; Yeo, H.; Lee, J-J. 2007. Development of a portable ultrasonic computed tomography system for detecting decay in wood. In: Proceedings, 15th Symposium Nondestructive Testing of Wood. Duluth, MN. 191–195.

Kruse, K.O. 2000. Process control with NDT methods in panel production. In: Proceedings, 12th Symposium Nondestructive Testing of Wood. Sopron, Hungary. 289–296.

Kruse, K.; Broker, F.W.; Frühwald, A. 1996. Non-contact method to determine ultrasonic velocity of wood-based panels. In: Proceedings, 10th Symposium Nondestructive Testing of Wood. Lausanne, Switzerland. 83–91.

Kuklík, P.; Kuklíkova, A. 2000. Evaluation of structural timber by dynamic methods. In: Proceedings, 12th Symposium Nondestructive Testing of Wood. Sopron, Hungary. 337–342.

Kunesh, R.H. 1978. Using ultrasonic energy to grade veneer. In: Proceedings, 4th Symposium Nondestructive Testing of Wood. Vancouver, WA. 275–278.

Lee, I.D.G. 1965. Ultrasonic pulse velocity testing considered as a safety measure for timber structures. In: Proceedings, 2nd Symposium Nondestructive Testing of Wood. Pullman, WA. 185–203.

Lee, S-I.; Oh, J-K.; Yeo, H.; Lee, J-J.; Kim, K-B.; Kim, K-M. 2009. Field application of nondestructive testing for detecting deterioration in korean historic wood buildings. In: Proceedings, 15th Symposium Nondestructive Testing of Wood. Duluth, MN. 227–232.

Lee, S-J.; Kim, C-K.; Kim, K-M.; Kim, K-B.; Lee, J-J. 2011. Condition assessment of ancient wooden building for determining reuse of the wooden members. In: Proceedings, 17th Symposium Nondestructive Testing of Wood, Vol. 2. Sopron, Hungary. 603–604.

Lemaster, R.L. 1993. Particle and flake classification using acoustic emission. In: Proceedings, 9th Symposium Nondestructive Testing of Wood. Madison, WI. 13–22.

Lemaster, R.L.; Beall, F.C. 1993. The use of dual sensors to measure surface roughness in wood-based composites. 1993 In: Proceedings, 9th Symposium Nondestructive Testing of Wood. Madison, WI. 123–130.

Lemaster, R.L.; Biernacki, J.M.; Beall, F.C. 1993. The feasibility of using acousto-ultrasonics to detect decay in utility poles. In: Proceedings, 9th Symposium Nondestructive Testing of Wood. Madison, WI. 84–91.

Lin, C.J.; Yang, T.H.; Zhang, D.Z.; Wang, S.Y.; Lin, F.C. 2007. Changes in the dynamic modulus of elasticity and bending properties of railroad ties after 20 years of service in Taiwan. Building and Environment 42(3): 1250–1256.

Lino, A.C.L.; Trinca, A.J.; Silva, M.V.G.; Gonçalves, R. 2013. Use of laser to determine profile of trees. In: Proceedings, 18th Symposium Nondestructive Testing of Wood. Madison, WI. 119–124.

Llana, D.F.; Iñiguez-Gonzalez, G.; Arriaga, F.; Niemz, P. 2013. Influence of temperature and moisture content in nondestructive values of Scots pine (*Pinus sylvestris* L.). In: Proceedings, 18th Symposium Nondestructive Testing of Wood. Madison, WI. 451–458.

Machado, J.S. 2002. Evaluation of the variation of bending stiffness of maritime pine timber by an acousto-ultrasonic approach. In: Proceedings, 13th Symposium Nondestructive Testing of Wood. Berkeley, CA. 125–130.

Massak, M.V.; Gonçalves, R.: Bertoldo, C.; Secco, C.B. 2009. Influence of tree age on longitudinal ultrasonic wave velocity and modulus of elasticity. In: Proceedings, 16th Symposium Nondestructive Testing of Wood. Beijing, China. 184–188.

McDonald, K.A. 1978. Lumber quality evaluation using ultrasonics. In: Proceedings, 4th Symposium Nondestructive Testing of Wood. Vancouver, WA. 5–13.

Miettinen, P.; Tiitta, M.; Lappalainen, R. 2005. Electrical and ultrasonic analysis of heat-treated wood. In: Proceedings, 14th Symposium Nondestructive Testing of Wood. Eberswalde, Germany. 267–273.

Moore, H.E.; Bier, H. 2002. Predicting laminated veneer lumber properties from the sonic propagation time and density of dried veneer in the production environment. In: Proceedings, 13th Symposium Nondestructive Testing of Wood. Berkeley, CA. 89–96.

Morris, V.; Adams, J. 1996. Using acoustic emission as a tool to study crack propagations in wood-based panel products. In: Proceedings, 10th Symposium Nondestructive Testing of Wood. Lausanne, Switzerland. 13–21.

Najafi, K.; Ebrahimi, G. 2005. Three methods for the prediction of longitudinal ultrasonic wave velocity in particleboard and fiberboard. In: Proceedings, 14th Symposium Nondestructive Testing of Wood. Eberswalde, Germany. 23–28

Najafi, S.K.; Bolandbakht, F.; Najafi, A. 2009. Detection of internal decay in standing beech trees using ultrasonic technique. In: Proceedings, 16th Symposium Nondestructive Testing of Wood. Beijing, China. 16–19.

Najafi, S.K.; Ebrahimi, G.; Shalbafan, A. 2007. Nondestructive evaluation of beech trees using the ultrasonic technique. In: Proceedings, 15th Symposium Nondestructive Testing of Wood. Duluth, MN. 55–58.

Navi, P. 1996. Determination of effective complex moduli of inhomogeneous anisotropic materials. In: Proceedings, 10th Symposium Nondestructive Testing of Wood. Lausanne, Switzerland. 61–72.

Niemz, P.; Kucera, L.J. 1998. Possibility of defect detection in wood with ultrasound. In: Proceedings, 11th Symposium Nondestructive Testing of Wood. Lausanne, Switzerland. 27–32.

Niemz, P.; Brunner, A.J.; Walter, O. 2007. Investigation of the mechanism of failure behavior of wood-based materials

using acoustic emission analysis and image processing. In: Proceedings, 15th Symposium Nondestructive Testing of Wood. Duluth, MN. 135–141.

Noya, J.R. 2013. Combined methodology for ultrasound testing in a timber structure of the 17th Century. In: Proceedings, 18th Symposium Nondestructive Testing of Wood. Madison, WI. 216–223.

Oh, J.; Eu, S.; Lee, J. 2013. Use of ultrasonic attenuation to detect internal small defects for maintenance of historic buildings. In: Proceedings, 18th Symposium Nondestructive Testing of Wood. Madison, WI. 261-268.

Palacios, P.I.C.; Yoza, L.Y.; Mallque, M.A. 2011. Elasticity modulus in Peruvian tropical woods using nondestructive techniques—preliminary study. In: Proceedings, 17th Symposium Nondestructive Testing of Wood, Vol. 2. Sopron, Hungary. 469–475.

Palaia-Perez, L.; Galvan-Llopis V.; Cervera-Moreno F.; Monzo-Hurtado, V. 1993. Using ultrasonic waves for the detection of timber decay in old buildings. In: Proceedings, 9th Symposium Nondestructive Testing of Wood. Madison, WI. 71–77.

Patton-Mallory, M.; Anderson, K.D.; De Groot, R.C. 1987. An acousto-ultrasonic method for evaluating decayed wood. In: Proceedings 6th Symposium Nondestructive Testing of Wood. Pullman, WA. 167–189.

Pedroso, C.B.; Gonçalves, R.; Batista, F.; Secco, C.B. 2011. Velocity of ultrasonic waves in live trees and in freshly-felled logs of exotic trees grown in Brazil. In: Proceedings, 17th Symposium Nondestructive Testing of Wood, Vol. 1. Sopron, Hungary. 69–75.

Pellerin, R.F.; Ross, R.J. 2002. Nondestructive evaluation of wood. Forest Products Society, Madison, WI. 210 p.

Pellerin, R.F.; DeGroot, R.C.; Esenther, G.R. 1985. Nondestructive stress wave measurements of decay and termite attack in experimental wood units. In: Proceedings, 5th Nondestructive Testing of Wood Symposium, Pullman, WA: Washington State University. 319–353.

Petit, M.H.; Bucur, V.; Viriot, C. 1991. Ageing monitoring of structural flakeboards by ultrasound. In: Proceedings, 8th Symposium Nondestructive Testing of Wood. Vancouver, WA. 191–201.

Pierre, M. 2000. The contribution of NDT tools to assessment of mechanical damage in wood. In: Proceedings, 12th Symposium Nondestructive Testing of Wood. Sopron, Hungary. 165–172.

Pires, F.A.C.; Menezzi, C.H.S.; Souza, M.R. 2011. Grading structural tropical lumber using stress wave, transverse vibration and ultrasonic method. In: Proceedings, 17th Symposium Nondestructive Testing of Wood, Vol. 1. Sopron, Hungary. 223–230.

Plinke, B. 2005. Nondestructive testing of finger-jointed structural timber: overview of possible methods, results of preliminary evaluations, and possibilities for industrial implementation. In: Proceedings, 14th Symposium Nondestructive Testing of Wood. Eberswalde, Germany. 75–85.

Quarles, S.L.; Zhou L. 1987. Use of acoustic emissions to detect drying defects: a preliminary report. In: Proceedings, 6th Symposium Nondestructive Testing of Wood. Pullman, WA. 95–111.

Reinprecht, L.; M. Hibky. 2011. The type and degree of decay in spruce wood analyzed by the ultrasonic method in three anatomical directions. Bioresources 6(4): 4953–4968.

Riggio, M.; Piazza, M. 2011. Stress waves tomography for the analysis of structural timber: limits, applications, possible combinations with other analysis techniques. In: Proceedings, 17th Symposium Nondestructive Testing of Wood, Vol. 2. Sopron, Hungary. 611–615.

Ritschel, F.; Niemz, P.; Brunner, A.J. 2011. Combining image correlation from optical methods and acoustic analysis for investigating damage evolution in plywood. In: Proceedings, 17th Symposium Nondestructive Testing of Wood, Vol. 1. Sopron, Hungary. 343–350.

Ritschel, F.; Zauner, M.; Sanabria, S.J.; Brunner, A.J.; Niemz, P. 2013. Acoustic emission and synchrotron radiation x-ray tomographic in situ microscopy of submacroscopic damage phenomena in wood. In: Proceedings, 18th Symposium Nondestructive Testing of Wood. Madison, WI. 434–441.

Rohanová, A.; Lagaňa, R.; Babiak, M. 2011. Comparison of nondestructive method of quality estimation of the construction spruce wood grown in Slovakia. In: Proceedings, 17th Symposium Nondestructive Testing of Wood, Vol. 1. Sopron, Hungary. 239–246.

Rosner, S. 2011. Waveform feature analysis of acoustic emission provides information about dehydration stress in spruce sapwood. In: Proceedings, 17th Symposium Nondestructive Testing of Wood, Vol. 1. Sopron, Hungary. 183–90.

Rosner, S.; Wimmer, R. 2005. acoustic detection of cavitation events in norway spruce sapwood. In: Proceedings, 14th Symposium Nondestructive Testing of Wood. Eberswalde, Germany. 125–134.

Ross, R.J.; De Groot, R.C. 1998. Scanning technique for identifying biologically degraded areas in wood members. Experimental Techniques 22(3): 32–33.

Ross, R.J.; Dundar, T. 2012. Condition assessment of 2,500-year-old mummy coffin. Res. Note. FPL–RN–0327. Madison, WI: U.S. Department of Agriculture, Forest Service, Forest Products Laboratory: 3 p.

Ross, R.J.; Pellerin, R.F. 1988. NDE of wood-based composites with longitudinal stress waves. Forest Products Journal 38(5): 39–45.

Ross, R.J.; De Groot, R.C.; Nelson, W.J. 1994. Technique for nondestructive evaluation of biologically degraded wood. Experimental Techniques 18(5): 29–32.

Ross, R.J.; De Groot, R.C.; Nelson, W.J.; Lebow, P.K. 1996. Assessment of the strength of biologically degraded wood by stress wave NDE. In: C. Sjostrom, ed., Proceedings, Seventh International Symposium on Durability of Building Materials and Components, Volume 1. E&FN Spon: London. p. 637–644.

Ross, R.J.; De Groot, R.C.; Nelson, W.J.; Lebow, P.K. 1997. Relationship between stress wave transmission characteristics and the compressive strength of biologically degraded wood. Forest Products Journal 47(5): 89–93.

Ross, R.J.; Soltis, L.A.; Otton, P. 1998. Role of nondestructive evaluation in the inspection and repair of the USS Constitution. In: Proceedings, 11th Symposium Nondestructive Testing of Wood. Madison, WI. 145–152.

Ross, Robert J.; Pellerin, Roy F.; Forsman, John W.; Erickson, John R.; Lavinder, Jeff A. 2001. Relationship between stress wave transmission time and compressive properties of timbers removed from service. Res. Note FPL–RN–0280. Madison, WI: U.S. Department of Agriculture, Forest Service, Forest Products Laboratory: 4 p.

Ross, Robert J.; Yang, Vina W.; Illman, Barbara L.; Nelson, William J. 2003. Relationship between stress wave transmission time and bending strength of deteriorated oriented strandboard. Forest Products Journal 53(3): 33–35.

Ross, R.J.; Brashaw, B.K.; Wang, X.; White, R.H.; Pellerin. R.F. 2004. Wood and timber condition assessment manual. Forest Products Society, Madison, WI. 73 p.

Sanabria, S.J.; Mueller, C.; Neuenschwander, J.; Niemz, P.; Sennhauser, U. 2009. Air-coupled ultrasound inspection of glued solid wood boards. In: Proceedings, 16th Symposium Nondestructive Testing of Wood. Beijing, China. 281–286.

Sanabria, S.J.; Furrer, R.; Neuenschwander, J.; Niemz, P.; Sennhauser, U. 2011. Monitored assessment of structural integrity of multilayered glued laminated timber beams with air-coupled ultrasound and contact ultrasound imaging. In: Proceedings, 17th Symposium Nondestructive Testing of Wood, Vol. 1. Sopron, Hungary. 359–366.

Sandoz, J.L. 1991. Nondestructive evaluation of building timber by ultrasound. In: Proceedings, 8th Symposium Nondestructive Testing of Wood. Vancouver, WA. 131–142.

Sandoz, J.L. 1996. Ultrasonic solid wood evaluation in industrial applications. In: Proceedings, 10th Symposium Nondestructive Testing of Wood. Lausanne, Switzerland. 147–153.

Sandoz, J.L.; Benoit, Y. 2002. AUS timber grading: industrial applications. In: Proceedings, 13th Symposium Nondestructive Testing of Wood. Berkeley, CA. 137–142.

Sandoz, J.L.; Benoit, Y.; Demay, L. 2000. Wood testing using acousto-ultrasonic technique. In: Proceedings, 12th Symposium Nondestructive Testing of Wood. Sopron, Hungary. 97–104.

Sasaki, Y.; Hasegawa, M. 2000. Ultrasonic measurement of applied stresses in wood by acoustoelastic birefringent method. In: Proceedings, 12th Symposium Nondestructive Testing of Wood. Sopron, Hungary. 67–75.

Sato, K.; Fushitani, M. 1991. Development of nondestructive testing system for wood-based materials utilizing acoustic emission technique. In: Proceedings, 8th Symposium Nondestructive Testing of Wood. Vancouver, WA. 33–43.

Schafer, M.E.; Ross, R.J.; Branshaw, B.K.; Adam, R.D. 1998. Ultrasonic inspection and analysis techniques in green and dried lumber. In: Proceedings, 10th Symposium Nondestructive Testing of Wood. Lausanne, Switzerland. 95–102.

Schubert, S.; Gsell, D.; Dual, J.; Motavalli, M.; Niemz, P. 2005. Resonant ultrasound spectroscopy applied to wood: comparison of the shear modulus g_{rt} of sound and decayed wood. In: Proceedings, 14th Symposium Nondestructive Testing of Wood. Eberswalde, Germany. 245–250.

Schubert, S.I.; Gsell, D.; Dual, J.; Motavalli, M.; Niemz, P. 2006. Rolling shear modulus and damping factor of spruce and decayed spruce estimated by modal analysis. Holzforschung 60 (1):78–84.

Seeling, U.; Ballarin, A.W.; Beall, F.C. 2002. Process and analysis of signals through dimension wood using acousto-ultrasonics. In: Proceedings, 13th Symposium Nondestructive Testing of Wood. Berkeley, CA. 213–219.

Sharp, D.J. 1985. Nondestructive testing techniques for manufacturing LVL and predicting performance. In: Proceedings, 5th Symposium Nondestructive Testing of Wood. Pullman, WA. 99–108.

Soma, T.; Shida, S.; Arima, T. 2000. Effect of freezing-treatment on estimating free water distribution in wood by ultrasonic wave. In: Proceedings, 12th Symposium Nondestructive Testing of Wood. Sopron, Hungary. 87–96.

Song, S.; Wang, L.; Xu, H.; You, X. 2011. Research on propagation velocity of stress wave and ultrasonic wave on indefectible cross section of standing tree. In: Proceedings, 17th Symposium Nondestructive Testing of Wood, Vol. 1. Sopron, Hungary. 167–174.

Szabo, T. 1978. Use of ultrasonics to evaluate or characterize wood composites. In: Proceedings, 4th Symposium Nondestructive Testing of Wood. Vancouver, WA. 239–260.

Teder, M.; Wang, X. 2013. Nondestructive evaluation of a 75-year old glulam arch. In: Proceedings, 18th Symposium Nondestructive Testing of Wood. Madison, WI. 624–632.

Teder, M.; Pilt, K.; Milijan, M.; Lainurm, M.; Kruuda, R. 2011. Overview of some nondestructive methods for in situ

assessment of structural timber. In: Proceedings, 17th Symposium Nondestructive Testing of Wood, Vol. 2. Sopron, Hungary. 583–591.

Terezo, R.F.; Valle, Â.; Padaratz, I.J. 2005. Comparative study in the estimate of timber elastic constants by destructive and non destructive testing in different wooden species. In: Proceedings, 14th Symposium Nondestructive Testing of Wood. Eberswalde, Germany. 387–398.

Tjondro, A.; Suryoatmono, B. 2007. Effects of specimen dimensions on the accuracy of the determination of moduli of elasticity using the ultrasonic longitudinal wave propagation method. In: Proceedings, 15th Symposium Nondestructive Testing of Wood. Duluth, MN. 181–186.

Trinca, A.J.; Gonçalves, R.; Ferreira, G.C. S. 2009. Effect of coupling media on ultrasound wave attenuation for longitudinal and transversal transducers. In: Proceedings, 16th Symposium Nondestructive Testing of Wood. Beijing, China. 189–194.

Tucker, B.J.; Bender, D.A.; Pollock, D.G. 1998. Nondestructive evaluation of wood-plastic composites. In: Proceedings, 10th Symposium Nondestructive Testing of Wood. Lausanne, Switzerland. 33–41.

Tucker, B.J.; Bender, D.A.; Pollock, D.G.; Wolcott, M.P. 2002. Ultrasonic plate wave evaluation of natural fiber composite panels. In: Proceedings, 13th Symposium Nondestructive Testing of Wood. Berkeley, CA. 221–227.

Turpening, R. 2011. Acoustic imaging of sandalwood (*Santalurn album*) logs. In: Proceedings, 17th Symposium Nondestructive Testing of Wood, Vol. 1. Sopron, Hungary. 101–103.

van der Beek, J., Tiitta, M. 2011. Monitoring drying and thermal modification of wood by means of acoustic emission technology. In: Proceedings, 17th Symposium Nondestructive Testing of Wood, Vol. 1. Sopron, Hungary. 351–357.

van Dijk, R.; Gonçalves, R.; Soriano, J.; Bertoldo, C. 2013. Conversion mode of the ultrasound wave. In: Proceedings, 18th Symposium Nondestructive Testing of Wood. Madison, WI. 477–484.

Vázquez, C.; Gonçalves, R.; Guaita, M.; Bertoldo, C. 2013. Determination of mechanical properties of *Castanea Sativa* Mill. by ultrasonic wave propagation and comparison with the compression method. In: Proceedings, 18th Symposium Nondestructive Testing of Wood. Madison, WI. 426–433.

Vun, R.Y.; Beall, F.C. 2002. Monitoring creep rupture in oriented strandboard using acoustic emission: influence of moisture content. In: Proceedings, 13th Symposium Nondestructive Testing of Wood. Berkeley, CA. 321–329.

Vun, R.Y.; Wu, Q.; Bhardwaj, M.; Stead, G. 2000. Through-thickness ultrasonic transmission properties of oriented strandboard. In: Proceedings, 12th Symposium Nondestructive Testing of Wood. Sopron, Hungary. 77–86.

Vun, R.Y.; Wu, Q.; Monlezun, C.J. 2002. Ultrasonic characterization of horizontal density variations in oriented strandboard. In: Proceedings, 13th Symposium Nondestructive Testing of Wood. Berkeley, CA. 53–63.

Wang, L.; Gao, S.; Wang, N.; Han, J. 2013. Quantitative detection of void defects in log section based on ultrasonic wave spread field. In: Proceedings, 18th Symposium Nondestructive Testing of Wood. Madison, WI. 171–179.

White, R.H.; Kukay, B.; Wacker, J.P. 2013. Options for NDE assessment of heat and fire damaged wood. In: Proceedings, 18th Symposium Nondestructive Testing of Wood. Madison, WI. 528–535.

Yang, J.L.; Bucur, V.; Ngo, D.; Ebdon, N. 2007. Detection of tension wood in eucalypt discs using ultrasonic and stress wave techniques. In: Proceedings, 15th Symposium Nondestructive Testing of Wood. Duluth, MN. 143–148.

Yin, Y.; Jiang, X.; Zhang, X.; Luo, B.; An, Y.; Song, K. 2009. Evaluation of bending, tensile and compressive strength of larch structural lumber using two acoustic nondestructive methods. In: Proceedings, 16th Symposium Nondestructive Testing of Wood. Beijing, China. 118–124.

Yin, Y.; Nagao, H.; Liu, X.; Nakai, T. 2005. Evaluating bending properties of Chinese fir plantation wood with three nondestructive methods. In: Proceedings, 14th Symposium Nondestructive Testing of Wood. Eberswalde, Germany. 375–380.

Yoza, L.Y.; Mallque, M.A. 2011. Measurement technique development in ultrasound applied to tropical woods. In: Proceedings, 17th Symposium Nondestructive Testing of Wood, Vol. 2. Sopron, Hungary. 453–460.

Chapter 4

Proof Loading

Roy F. Pellerin, Professor Emeritus
Washington State University, Pullman, Washington

Robert J. Ross, Supervisory Research General Engineer
Forest Products Laboratory, Madison, Wisconsin

This chapter provides a brief discussion of the topic of proof loading, including some of the earliest research published on the topic. The concept of proof loading is presented, and some original equipment development efforts. Much of the early work was conducted at Washington State University (Pellerin and Strickler 1971, 1972, 1977; Strickler et al. 1970; Strickler and Pellerin 1971, 1973, 1976). Subsequent to the foundation work, several excellent studies have been conducted on the topic. A listing of the publications that present these findings is included under the heading "Additional Sources of Information."

Concept

Structural end jointing of lumber has become a widespread practice, and high-strength end joints now permit the design of structures with long wood members that would not otherwise be considered feasible. Nevertheless, engineers and architects are often hampered in designing with wood because of the lack of complete quality assurance.

If the structural integrity of an efficiently designed building were to rely upon any one member, the engineer would need to know without question that the member would withstand a minimum known level of stress indefinitely.

Although present lumber stress grades assigned nondestructively by machine stress rating (MSR) have proven to be significantly more reliable than visually graded lumber grades, MSR systems now in commercial use are insensitive to the quality of end joints—except in the case of extremely weak joints. Other methods of nondestructive evaluation (NDE) of lumber have also proven to be unresponsive to end-joint properties. These methods include transverse vibration, longitudinal stress wave, and microwave systems. Consequently, the remaining method that appears to offer potential for complete quality assurance for end joints is a proof load.

The principle of a proof-load system is that each end joint or complete member is stressed to the maximum of its design limitation, times a factor, before the member is accepted for a critical-stress application. Pieces having characteristics, natural or otherwise, that preclude them from actually sustaining the intended working stress are fractured by the proof load and as a result are rejected. Proof loading, in a sense, serves to identify pieces of wood with superior strength properties that may then be used for higher design purposes. Consequently, in terms of structural integrity, much greater confidence can be placed in members that successfully withstand a proof load than in members that have not been subjected to proof loading.

As a practical example, the proof-load principle proved beneficial during fabrication of long critical-stress members for experimental houses. Finger joints in members intended as bottom chords in plywood-web I-beams were proof loaded before the beams were fabricated. Two finger joints broke under proof loading. They were shown later to have been poorly bonded, probably because of malfunction of the finger-joint machine. From the standpoint of all concerned, including the builder and homeowner, it was better to have proof loaded all members and broken some than to install poorly joined members in critical stress locations in the house.

As a result of experiences such as this, proof loading of end joints was embraced as an area for research, despite aversion to the principle in some quarters. This aversion is understandable—it stems from fear among some wood engineers that a proof load might cause incipient damage that would lead to early failure of members in service. Therefore, one purpose of research was to determine whether or not a weakening of end-jointed members would occur as a result of proof loading. A second purpose was to initiate an evaluation of practical methods of proof loading structural end-jointed lumber.

Proof-Loading Considerations

Two stress modes for proof loading of end-jointed dimension lumber are considered in this chapter: tension parallel to grain and flatwise bending.

In any practical proof-load system, the possibility of breaking or otherwise damaging or downgrading an excessive amount of material must be avoided. This possibility could be minimized by using only MSR lumber. The small amount of material that would normally break under proof loading could be salvaged by end-joining undamaged portions.

Furthermore, only critical-design members would require proof loading in practice. Familiar examples of critical members are bottom chords in trusses and box beams and outer tensile plies of laminated beams.

Tension Proof Loading

In the first attempt to research tension proof loading, researchers reasoned that the proof-load factor must be 2.1 (because the primary stress in the critical outside lamination of a beam was in tension) and that the minimum ultimate strength of the beam had to be 2.1 times the design stress.

The resultant strengths of beams fabricated from laminations that were proof loaded to a tensile stress of 2.1 times design stress are shown in Figure 4.1. These results made it apparent that the proof-load factor could be lowered to near 1 and still result in adequate beam strengths. Table 4.1 shows how a single proof-load value could be used to evaluate many proof-load factors. For example, proof loading to approximately 3,000 lb/in^2 would result in a proof load factor of 1.4 for a design value of 2,200 lb/in^2. After arriving at a proof-load factor of 1.4, another series of beams was fabricated. The resultant stress values (Fig. 4.2) show that the beams maintained the minimum allowable level.

The first commercial use of this tension proof-loading concept was in 1974 by Hood Industries in Laural, Mississippi. The company realized the need for such a concept because of customer complaints about joint failures. Since adopting the tension proof-loading concept, they claim to have had no complaints and in fact have used the concept to great marketing advantage. The second commercial installation (of a machine developed by Metriguard, Inc., Pullman, Washington) was by St. Regis in Libby, Montana.

The Hood Industries installation was out of line so that joints may adequately cure prior to proof loading, whereas the St. Regis in-line installation stresses the joints to the desired proof-load level after approximately 10 s out of the radiofrequency (RF) tunnel.

A portable model of a tension proof-loading machine was developed for the American Institute of Timber Construction (AITC). This machine was air transportable in three packages. AITC used this machine to qualify their member plants for minimum tension strength end joints.

Subsequently, Suddarth (1985) of Purdue University reported that strength performance of I-beams could be improved by a factor of 1.4 if built with tension proof loaded lumber.

Bending Proof Loading

Although results of research on tension proof loading demonstrated that significant improvements in allowable design properties of laminated beams can be obtained from proof loading and that commercial machines have performed adequately, the laminating industry, through AITC, requested research on a bending proof-load concept.

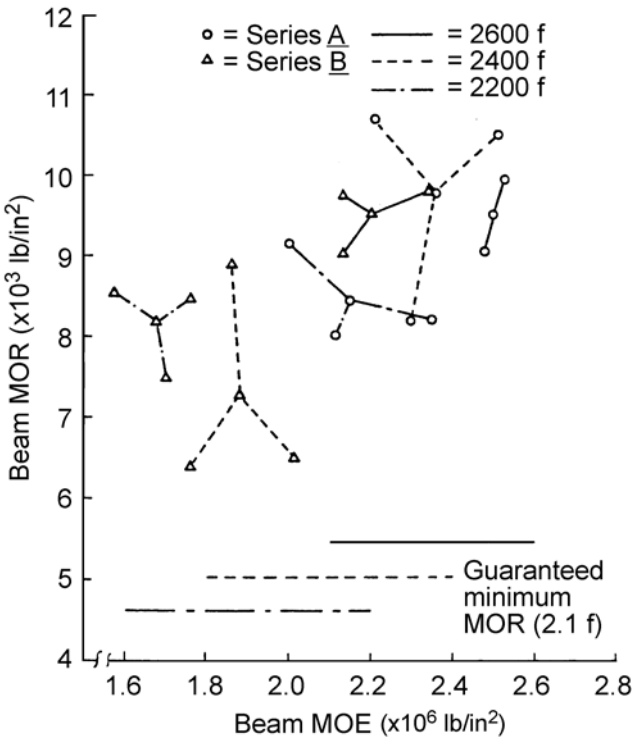

Figure 4.1—Properties of laminated beams fabricated from laminations proof loaded to 2.1 times design stress.

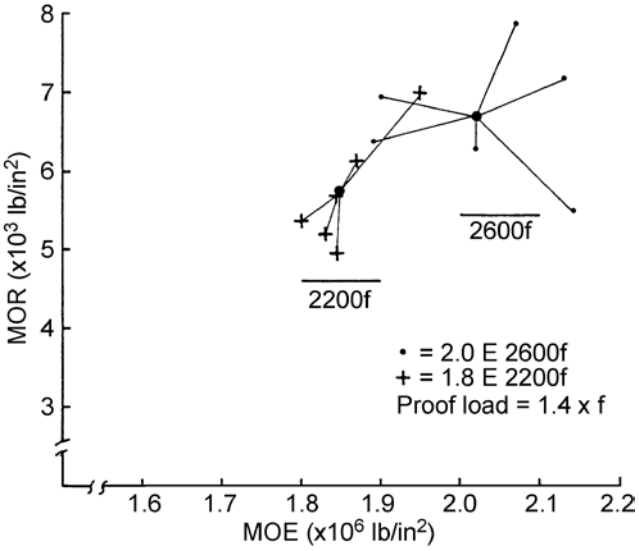

Figure 4.2—Properties of laminated beams fabricated from laminations proof loaded to 1.4 times design stress.

The goals of a bending proof-load concept were to

- improve the reliability of glued-laminated timbers by eliminating the occasional low-strength end joint,
- eliminate the need for spacing end joints within the beam when approved proof-loading procedures are followed, and

Table 4.1—Single proof-load value (lb/in^2) used to evaluate many proof-load factors

	Proof-load factor				
f	1.0	1.1	1.2	1.3	1.4
2,000	2,000	2,200	2,400	2,600	2,800
2,200	2,200	2,420	2,640	2,860	3,080
2,400	2,400	2,640	2,880	3,120	3,360
2,600	2,600	2,860	3,120	3,380	3,640
2,800	2,800	3,080	3,360	3,640	3,920
3,000	3,000	3,300	3,600	3,900	4,200
3,300	3,300	3,630	3,960	4,280	4,620

Table 4.2—Average ultimate values for lumber stressed in bending, tension, and tension after being proof loaded in bending

Mode of test	Average ultimate stress (lb/in^2)
Bending	9,066
Tension	5,413
Tension after 6,000-lb/in^2 bending proof load	5,403

Table 4.3—Average ultimate values for finger-jointed lumber stress in bending, tension, and tension after being proof loaded in bending

Mode of test	Average ultimate stress (lb/in^2)
Bending	9,556
Tension	5,724
Tension after 6,000-lb/in^2 bending proof load	5,927

- make it easier for glued-laminated timber to comply with reliability based procedures when the need arises. (In Canada, this is known as the limit states design procedure.)

The immediate objective of this research was to develop data and criteria, so that proof loading by bending could be incorporated into a laminating plant's production and quality control systems.

To achieve these goals and objectives, it was necessary to have information on the effects of proof loading on lumber, fully cured finger joints, hot finger joints, bending strength of fully cured joints that had been proof loaded while hot, tensile strength of fully cured joints that had been proof loaded while hot, and various configurations of finger joints (including horizontal and vertical).

Table 4.2 shows average ultimate values for lumber stressed in bending, tension, and tension after being proof loaded in bending. The resulting proportion of ultimate tensile stress to ultimate bending stress for lumber is 60%. Typical data for finger-jointed lumber are summarized in Table 4.3. The resulting proportion of ultimate tensile stress to ultimate bending stress for lumber containing finger joints is also 60%.

The objective of the second phase of the bending study was to determine the strength ratio of partially cured end joints to fully cured end joints. The procedure for this phase included the selection of a random sample of visually graded lumber for use in laminated beams designated as 301–24 Douglas-fir lumber from sources in southwest Oregon to northwest Washington. This lumber was used to make test specimens containing either a horizontal or a vertical finger joint. Sixty matched pairs of specimens of each finger-joint orientation were subjected to two different procedures. In the first, the specimens were assembled, cured by RF energy, and allowed to fully cure. In the second, specimens were assembled, cured by RF, and tested to failure in bending within 10 s after the RF generator had shut off. The fully cured specimens were then tested to failure in bending at the same rate of loading used for the partially cured joints.

Table 4.4—Hot and cold ultimate bending stresses of both vertical and horizontal finger joints and time to fail hot joints after removal from RF energy source

Type of joint	Joint condition	Average bending stress (lb/in^2)	Time to failure (s)
Vertical	Hot	5,145	7.27
	Cold	9,672	—
Horizontal	Hot	4,408	6.65
	Cold	8,484	—

Table 4.5—Proportions of hot to cold ultimate bending stresses for both horizontal and vertical joints

Type of joint	Proportion (%)
Vertical	53
Horizontal	52

Table 4.6—Properties of beams fabricated from proof-loaded laminations and with stacked joints in the three outermost tension laminations

	Proof load		
Beam series	No. of laminations	Stress level (lb/in^2)	Average ultimate stress (lb/in^2)
1.8–1	2	2,640	5,625
1.8–2	3	2,640	6,580
2.2–1	2	3,640	6,540
2.2–2	2	3,920	7,010

Results are summarized in Table 4.4. Ratios of hot to cold strengths for both horizontal and vertical joints are reported in Table 4.5.

The objective of the third phase was to determine if bending proof loading of the hot joint affects final cold strength of the joints. Three more groups, 60 specimens each, of the vertical finger joints were made. Two groups were proof loaded immediately out of the RF energy and then allowed to fully cure. The third group was assembled and allowed to fully cure without proof loading. Tensile strengths were determined for the group allowed to fully cure without proof loading and for one of the groups that had been proof loaded while hot.

Finally, a series of test beams were fabricated with the remaining group of laminations that had been proof loaded in bending for finger-joint quality assurance. The beams were layed-up so that finger joints in the three outermost tension laminations were stacked. The resulting beam properties are reported in Table 4.6.

Based on the results of this study and the commitment of AITC to proof loading, Mann-Russell Electronics (Tacoma, Washington) developed a bending proof loading machine for commercial application.

Literature Cited

Pellerin, R.F.; Strickler, M.D. 1971. Tension proof loading of lam stock for laminated beams. Forest Products Journal. 21(5): 50–55.

Pellerin, R.F.; Strickler, M.D. 1972. Proof loading of tension laminations for large glued-laminated beams. Forest Products Journal. 22(10): 24–30.

Pellerin, R.F.; Strickler, M.D. 1977. S. pine beams from E-rated and proof loaded lumber. Proceedings Paper 12656. Journal of the Structural Division, American Society of Chemical Engineers. 103(ST1): 270–274.

Strickler, M.D.; Pellerin, R.F. 1971. Tension proof loading of finger joints for laminated beams. Forest Products Journal. 21(6): 19–24.

Strickler, M.D.; Pellerin, R.F. 1973. Rate of loading effect on the tensile strength of wood parallel to grain. Forest Products Journal. 23(10): 34–36.

Strickler, M.D.; Pellerin, R.F. 1976. Tension proof loading for Southern pine beams. Proceedings Paper 11978. Journal of the Structural Division, American Society of Chemical Engineers. 102(ST3): 645–657.

Strickler, M.D.; Pellerin, R.F.; Talbott, J.W. 1970. Experiments in proof loading structural end-jointed lumber. Forest Products Journal. 20(2): 29–35.

Suddarth, S.K. 1985. Improved strength performance of I-beams built with proof tested lumber. In: Proceedings, 5th Symposium on Nondestructive Testing of Wood; 1985 September 9–11; Pullman, WA. Pullman, WA: Washington State University: 549–559.

Additional Sources of Information

Chen, Y.; Barrett, J.D.; Lam, F. 2009. Mechanical properties of Canadian coastal Douglas-fir and hem-fir. Forest Products Journal. 59(6):44–54.

Chen, Y.; Lam, F; Barrett, J.D. 2006. Bending strength and modulus of elasticity of BC coastal timbers. Proceedings, 9th World Conference on Timber Engineering, 9th World Conference on Timber Engineering, August 6–10, 2006. Volume 1: 544–548.

Enjily, V.; Fewell, A.R. 1992. The extent of damage in British grown Sitka spruce timber caused by proof loading. Journal of the Institute of Wood Science. 12(5): 279–284.

Evans, J.W.; Johnson, R.A.; Green, D.W. 1984. Estimating the correlation between variables under destructive testing, or how to break the same board twice. Technometrics. 26(3): 285–290.

Galligan, W.L.; Johnson, R.A.; Taylor, J.R. 1979. Examination of the concomitant properties of lumber. Proceedings, Metal Plate Wood Truss Conference, FPRS Proceedings. 79–28. Forest Products Society, Madison, WI. 65–70.

Gerhards, C.C. 1977. Time-related effects of loads on strength of wood. Proceedings, Environmental Degradation of Engineering Materials. 613–623.

Henery, R.J.; Ahmed, E. 1992. Using the moment generating function to estimate the correlation coefficient by the method of proof loading. American Journal of Mathematical and Management Sciences. 12(4): 301–319.

Lackner, R. 1990. Strength and grading of construction timber in small cross-sections. Hozforschung und Holzverwertung. 42(3): 43–48.

Lam, F.; Abayakoon, S.; Svensson, S.; Gyamfi, C. Influence of proof loading on the reliability of members. Holz als Roh-und Werkstoff. 61(6): 432–438.

McLain, T.E.; Woeste, F.E. 1988. Proof test damage evaluation with southern pine lumber. Forest Products Journal. 38(5): 31–32.

Marin, L.A.; Woeste, F.E. 1981. Reverse proof loading as a means of quality control in lumber manufacturing. American Society of Agricultural Engineers, Transactions. 24(5): 1273–1277, 1281.

Takeda, T.; Hashizume, T. 2000. Effective sampling method for estimating bending strength distribution of Japanese larch square-sawn timber. Journal of Wood Science. 46(5): 350–356.

Umble, E.J.; Seaman, J.W.; Martz, H.F. 1999. A distribution-free Bayesian approach for determining the joint probability of failure of materials subject to multiple proof loads. Technometrics. 41(3): 183–191.

Woeste, F.E.; DeBonis, A.L.; McLain, T.E.; Perumpral, J.V. 1984. Bending proof load as a quality control for compression parallel-to-grain in lumber. Transactions of the American Society of Agricultural Engineers. 27(6): 1859–1861.

Woeste, F.E.; Green, D.W.; Tarbell, K.A. 1984. Proof loading of lumber for quality control. American Society of Agricultural Engineers, Microfiche collection, Winter 1984, Paper no. 84-4509.

Woeste, F.E.; Green, D.W.; Tarbell, K.A.; Marin, L.A. 1987. Proof loading to assure lumber strength. Wood and Fiber Science. 19(3): 283–297.

Ziethen, R. 2006. The reliability of proof-loading as a strength grading technique. Proceedings, 9th World Conference on Timber Engineering, Volume 1, 152–159.

Ziethen, R. 2008. Reliability of proof-loaded Norway spruce. Holz als Roh-und Werkstoff. 66(6): 401–408.

Ziethen, R.; Lycken, A.; Bengtssen, C. 2010. Machine strength grading—“output control” as a method for production control. Proceedings, 11th World Conference on Timber Engineering, Volume 1: 763–769.

Chapter 5

Sounding, Probing, Moisture Content, and Resistance Drilling Techniques

Brian K. Brashaw, Program Manager
Forest Products Marketing Unit, USDA Forest Service, Madison, Wisconsin

Simple mechanical tests are frequently used for in-service inspection of wood elements in timber structures. For example, hammer sounding and probing are used in combination with visual inspection to conduct an initial assessment of the condition of a member. The underlying premise for such tests is that degraded wood is relatively soft and might sound hollow, with low resistance to penetration.

This chapter was originally published in 2014 as chapter 2 of the *Wood and Timber Condition Assessment Manual, Second Edition,* a Forest Products Laboratory General Technical Report:

White, Robert H.; Ross, Robert J. (Eds.). 2014. Wood and timber condition assessment manual: second edition. General Technical Report FPL–GTR–234. Madison, WI: U.S. Department of Agriculture, Forest Service, Forest Products Laboratory. 93 p.

Sounding and Probing

One of the most commonly used techniques for detecting deterioration is to hit the surface of a member with a hammer or other object. Based on the sound quality or surface condition, an inspector can identify areas of concern for further investigation using advanced tools like a stress wave timer or resistance microdrill. Deteriorated areas typically have a hollow or dull sound that may indicate internal decay. A pick hammer commonly used by geologists is recommended for use in timber structures because it allows inspectors to combine the use of sound and the pick end to probe the element (Fig. 5.1).

Probing with a moderately pointed tool, such as an awl or knife, locates decay near the wood surface as indicated by excessive softness or a lack of resistance to probe penetration and the breakage pattern of the splinters. A brash, or brittle break indicates decayed wood, whereas a splintered break indicates sound wood. Although probing is a simple inspection method, experience is required to interpret results. Care must be taken to differentiate between decay and water-softened wood, which may be sound but somewhat softer than dry wood. Assessing damage in soft-textured woods, such as western redcedar, is sometimes difficult. Figure 5.2 shows an awl probe inserted into a split to assess decay that is visible on the railing end.

Figure 5.1—A hammer pick is an effective tool for initial assessments of timber bridge elements.

Figure 5.2—An awl is used to assess depth and presence of decay in a horizontal split.

Probes can also be used to assess the depth of splits and checks in timber members. Flat bladed probes, such as pocket knives or feeler gauges, are recommended for use in this process. This is also important to understanding the effect of checks and cracks in other advanced techniques such as stress wave inspection. Figure 5.3 shows the use of probes to assess the depth of checks and cracks in timber bridge elements.

Figure 5.3—Probes are used to assess depth of cracks, checks, and through splits in timber bridge elements.

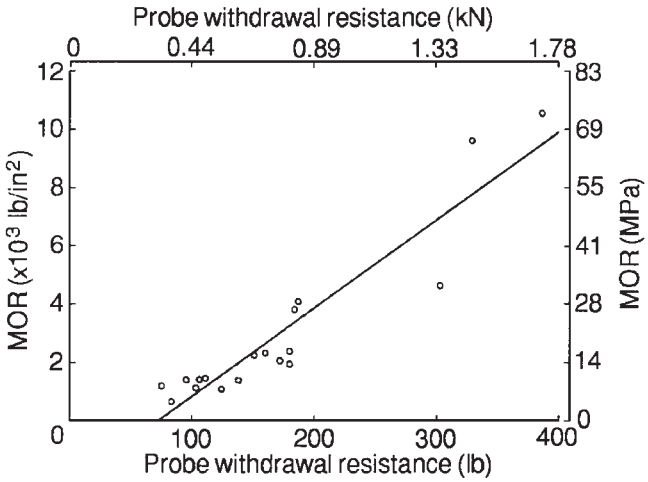

Figure 5.4—Relationship between withdrawal resistance and residual strength. MOR, modulus of rupture.

Screw withdrawal testing has been used as an indicator of biological deterioration in timber members. Additional research has correlated screw withdrawal resistance to physical and mechanical properties such as density, modulus of elasticity, modulus of rupture, and shear modulus. These tests are typically conducted by extracting a screw inserted at an angle perpendicular to the surface of the timber specimen. Although these tests are dependent on local material condition, information from both deteriorated and good material locations can be helpful during wood structure evaluations.

A quantitative test based on the premise that underlies mechanical probing tests (relative softness of degraded wood and consequent low resistance to probe penetration) was developed by Talbot (1982). His test differed from the probing-type test in that instead of evaluating penetration resistance of a probe, it examined withdrawal resistance of a threaded probe, similar to a wood screw, inserted into a member. Talbot believed that a correlative relationship between withdrawal resistance and residual strength should exist and would be relatively easy to determine. He conducted an experiment using several small Douglas-fir beams in various stages of degradation as a result of exposure to decay fungi. Prior to testing the wood to failure in bending, probe withdrawal resistance was measured at the neutral axis of the beams. Bending strength and corresponding probe resistance values were then compared. The results revealed a relationship between withdrawal resistance and residual strength (Fig. 5.4). Talbot used this test in conjunction with stress wave techniques to assess the extent of damage to solid-sawn timbers in the football stadium at Washington State University.

A modification to Talbot's technique was developed for use in evaluating in-service strength of fire-retardant-treated (FRT) plywood in the early 1990s. A portable screw withdrawal system was utilized to inspect FRT plywood and identify substantial degrade. An extensive research effort was devoted to the use of Talbot's test for assessing residual strength of in-service panel products treated with fire retardant. Winandy et al. (1998) designed and conducted tests on a large sample of plywood specimens that were treated with fire-retardant chemicals and subsequently exposed to elevated temperatures. Screw withdrawal loads were determined for each specimen prior to static bending tests. Correlative relationships were then established between screw withdrawal strength and static bending properties (Fig. 5.5).

Recent evaluations have been completed by other researchers and commercial companies (Cai et al. 2002, Fakopp 2014). Figure 5.6 shows one commercial screw withdrawal resistance unit.

Moisture Content Inspection

Moisture meters can be used effectively in inspecting timber elements. The presence of moisture is required for decay to occur in timber. Typically, moisture conditions in timber of less than 20% will not allow decay to occur; as moisture increases above 20%, the potential for decay to occur increases.

Serious decay occurs only when the moisture content of the wood is above 30%. This occurs when dry wood is exposed to direct wetting through rain, moisture infiltration, or contact with ground water or bodies of water. Wood decay fungi will not affect wood that is fully saturated with water and without oxygen. Timber members (such as bridge piling) should be carefully inspected near the water line because rivers and streams have varying water levels throughout the year and from year to year. Figure 5.7 shows the use of

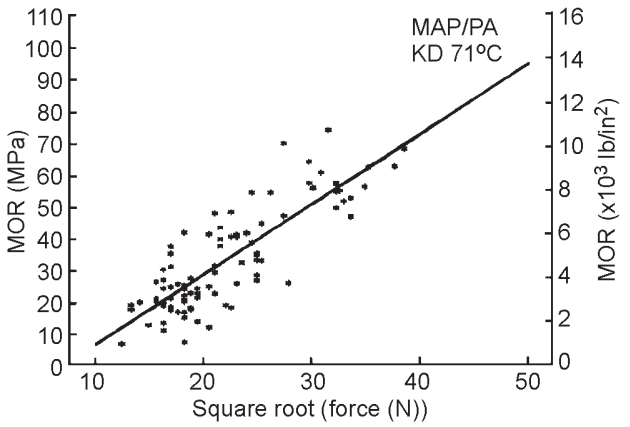

Figure 5.5—Relationship of screw-withdrawal force to bending strength for 12-mm- (1/2-in.-) thick plywood. MAP, mono-ammonium phosphate; PA, phosphoric acid; KD, dry-kiln drying temperature; and MOR, modulus of rupture.

Figure 5.6—Screw withdrawal resistance meter that can be used to assess local wood quality.

moisture meters with long insulated pins (up to 3 in. (75 mm) long) to assess moisture content of timber abutment caps. Pin-style moisture meters measure electrical resistance between two metal pins that are driven into the member and use this measurement to determine moisture content.

Figure 5.7—A pin-style moisture meter is used to determine moisture content of timber elements.

Drilling

Drilling and coring are the most common methods used to detect internal deterioration in wood members. Both techniques are used to detect the presence of voids and to determine the thickness of the residual shell when voids are present. Drilling utilizes an electric power drill or hand-crank drill equipped with a 9.5- to 19-mm- (3/8- to 3/4-in.-) diameter bit. Power drilling is faster, but hand drilling allows the inspector to monitor drilling resistance and may be more beneficial in detecting pockets of deterioration. In general, the inspector drills into the member in question, noting zones where drilling becomes easier and observing drill shavings for evidence of decay. The presence of common wood defects, such as knots, resin pockets, and abnormal grain, should be anticipated while drilling and should not be confused with decay. If decay is detected, remedial treatments, such as copper naphthenate, can be added to the wood through the inspection hole to help retard further decay. The inspection hole is probed with a bent wire or a thickness gauge to measure shell thickness. Because these holes are typically 3/8 to 3/4 in. diameter, they should be filled with a wood dowel section that has been soaked in a preservative.

Coring

Coring with an increment borer (often used for determining the age of a tree) also provides information on the presence of decay pockets and other voids. The resultant solid wood core can be carefully examined for evidence of decay. In addition, the core can be used to obtain an accurate measure of the depth of preservative penetration and retention. Figure 5.8 shows an increment core tool and the extracted core. The core can also be used to determine the wood species.

Figure 5.8—An increment core can be used to conduct inspections of timber bridge elements. This image shows an extracted core from an in-service timber pile ready for examination.

To prevent moisture and insect entry, a bored-out core hole should be filled with a wood plug treated with copper naphthenate.

Resistance Drilling

Another commercially developed drilling technique is the resistance drill system. Developed in the late 1980s, this system was originally developed for use by arborists and tree care professionals to assess tree rings, evaluate the condition of urban trees, and locate voids and decay. This technology is now being utilized to identify and quantify decay, voids, and termite galleries in wood beams, columns, poles, and piles. This technique is now the preferred drilling and coring technique for timber elements. Figure 5.9 shows a resistance microdrill being used to assess the level of decay in a timber.

Several machine types are available from different manufacturers. They operate under the same general principle of measuring electrical power consumption of a needle rotation motor. This value is proportional to mechanical torque at the needle and primarily depends on wood density (Rinn 2013). The purpose of the equipment is to identify areas in timber elements that have low density, indicating decay or deterioration.

Resistance drill equipment measures the resistance of wood members to a 0.6-in.- (1.5-mm-) diameter drill bit with a 0.18-in. (3.0-mm) head. This flat tipped drill bit travels through the member at a defined movement rate and generates information that allows an inspector to determine the exact location and extent of any damaged area. Figure 5.10 shows several drill bit ends that are used in resistance drills. Although the unit is usually drilled into a member in a direction perpendicular to the surface, it is also possible to drill into members at an angle (Fig. 5.11).

Figure 5.9—A resistance microdrill used for inspection of a historic Civilian Conservation Corps log cabin.

Figure 5.10—Flat-tipped resistance drill bits used to inspect timber materials.

Figure 5.11—Drilling can take place at an angle to assess the area below ground line.

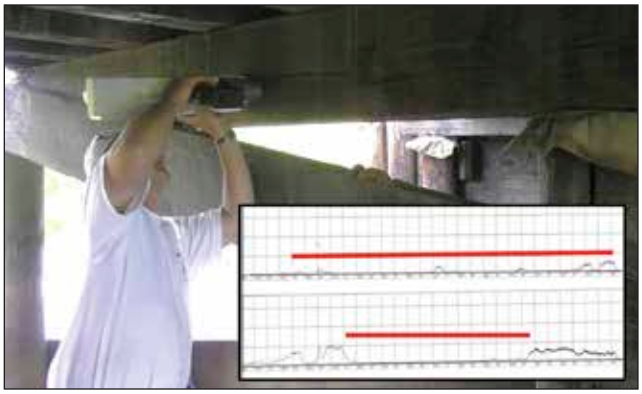

Figure 5.12—Resistance microdrilling showing significant decay in the bridge pile cap. The inlay shows the paper chart readout from a commercial drilling unit.

Figure 5.13—Electronic display on a resistance drill.

Figure 5.14—Silicone is used to fill the small drilling hole.

Resistance drills collect data electronically and can also product a chart or printout showing relative resistance over the drilling path. Modern tools are also promoting the ability to view the data on a tablet computer or hand-held mobile phone. Areas of sound wood have various levels of resistance, depending on the density of the species; voids show no resistance. The inspector can determine areas of low, mild, and high levels of decay with this tool, and quantify the level of decay in the cross section. Figure 5.12 shows a timber abutment cap being assessed with a resistance microdrill and the resulting chart image, which shows minimal drilling resistance and indicates that the majority of the cap is decayed. Figure 5.13 shows a commercial model with an electronic display that allows allow data to be reviewed in the field and then further processed using a computer in the office. All holes should be filled after drilling, especially if no decay is present. For the microdrill, this can be accomplished by injecting a small amount of silicone sealant or marine adhesive into the small opening (Fig. 5.14).

Interpreting Drilling Data Charts

Charts or printouts should be reviewed in the field and notes taken to ensure understanding of the testing location. Notes should be taken on a graphical data chart. Care should be exercised to ensure that low density profiles from intact but soft wood (such as conifers) not be misinterpreted as decay. The very center of softwood species near the pith will have low resistance and lack the defined growth rings visible in the outer sections. It is important to understand the type of wood that is being drilled. Sound wood from many hardwood species may have high levels of resistance (over 50%), whereas sound wood from softwood conifers may have low levels of resistance (in the range of 15% to 50+%, depending on its inherent density). It is important to evaluate the levels of decay across the full dimension, as some species have low resistance values but are not decayed. Further, each piece of commercial equipment provides different scales and may indicate different resistance levels. Table 5.1 shows a general assessment rating index that can provide support for the bridge inspector in evaluating resistance data collected during testing. Example electronic drilling charts for a southern yellow pine pile and a Douglas-fir pile cap are shown in Figures 5.15 and 5.16, respectively. Note that while the fundamental concept utilized by these pieces of equipment is essentially the same, data analysis and subsequent display of the data can vary significantly, depending on equipment manufacturer.

Table 5.1—General assessment of resistance drilling data for Douglas-fir and southern yellow pine bridge members

Drilling resistance (%)	Decay level	Comments
0	Severe	Decay resulting in an internal void
5–15	Moderate	Often adjacent to the internal void areas
20+	Low to none	Sound material often has resistance that is consistent across the full width

Note: These data must be carefully interpreted because of differences between commercial equipment.

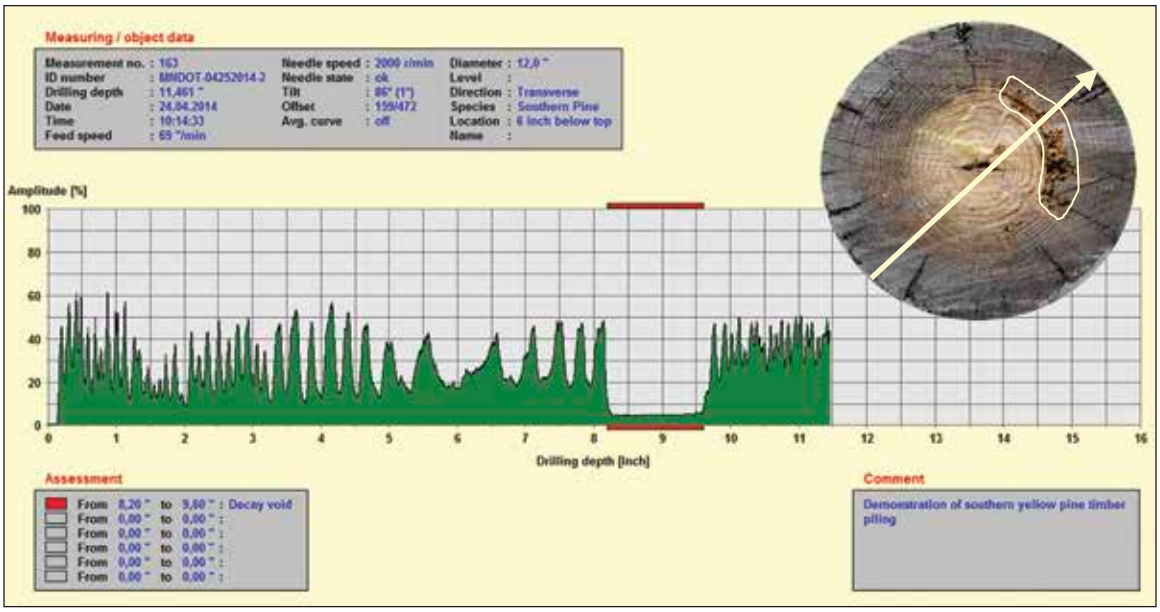

Figure 5.15—Electronic view of a southern yellow pine timber piling showing a decay pocket between 8 and 10 in. of the drilling profile.

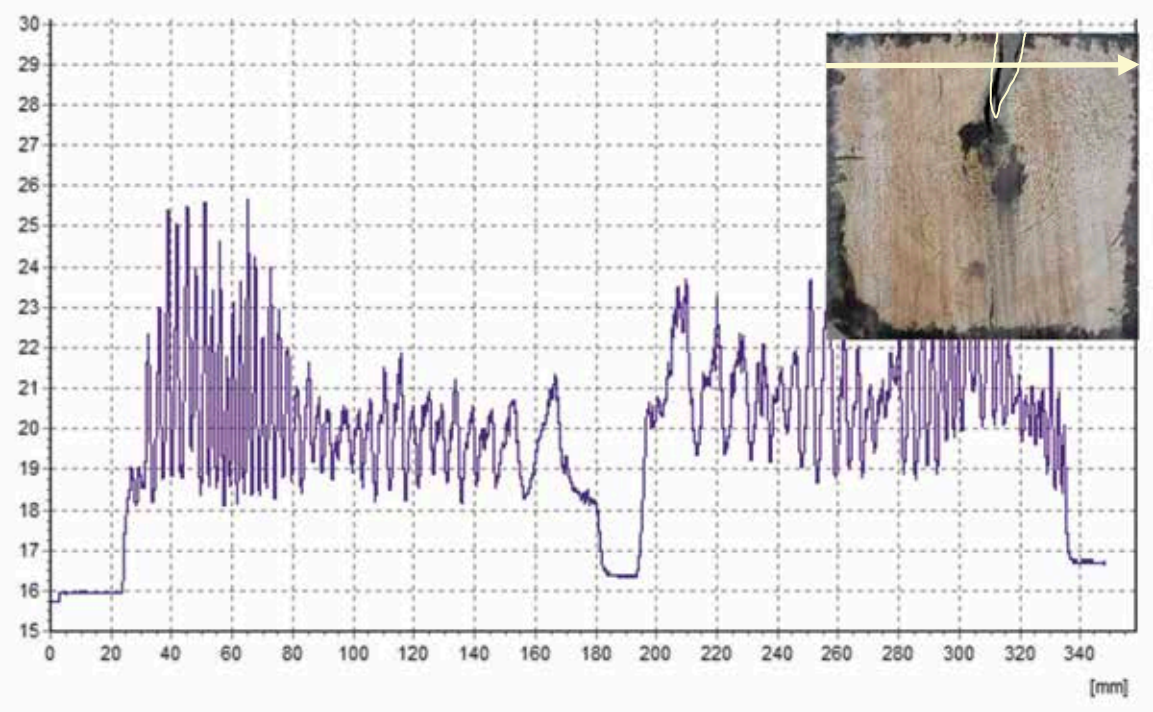

Figure 5.16—Electronic resistance chart of a Douglas-fir pile cap showing a large crack between 180 and 200 mm along the drilling path.

Commercial Equipment

Several companies produce equipment that is suitable for inspecting timber structures based on these concepts. Additional details for these companies and their equipment follow.

Increment Borers

Forestry Suppliers Inc.
Jackson, MS 39284-8397 USA
Telephone: (800) 647-5368
Website: www.forestry-suppliers.com

Ben Meadows Company
Janesville, WI USA 53547–5277
Telephone: (608) 743–8001
Fax: (608) 743–8007
Website: www.benmeadows.com

Resistance Microdrills

IML-RESI PD- and F-Series
IML North America, LLC
Moultonborough, NH 03254 USA
Telephone: (603) 253–4600
Website: www.iml-na.com

Resistograph 4- and 5-Series
RINNTECH, Inc.
St. Charles, IL 60174, USA
Telephone: (630) 377–2477
Website: www.rinntech.de

Digital microProbe
Sibtec Scientific
Sibert Technology Limited
2a Merrow Business Centre, Guildford
Surrey GU4 7WA England
Telephone: +44 1483 440 724
Fax: +44 1483 440 727
Website: www.sibtec.com

Screw Withdrawal Resistance Meter

FAKOPP Enterprise
Agfalva, Hungary
Telephone: +36 99 33 00 99
Website: www.fakopp.com

Literature Cited

Cai, Z.; Hunt, M.; Ross, R.J.; Soltis, L.A. 2002. Screw withdrawal—a means to evaluate densities of in-situ wood members. In: Proceedings, 13th International Symposium on Nondestructive Testing of Wood. Madison, WI: Forest Products Society: 277–281.

Fakopp. 2014. User's guide: screw withdrawal resistance meter. Agfalva, Hungary: Fakopp Enterprise. http://www.fakopp.com/site/downloads/Screw_Withdrawal.pdf. (Accessed April 24, 2014)

Rinn, F. 2013. From damage maps to condition inventories: a proven concept for documentation of results of inspection of timber bridges and other timber structures. International Conference on Timber Bridges. Las Vegas, NV. http://www.woodcenter.org/docs/ICTB2013/technical/papers/ID_139_Rinn.pdf

Talbot, J. 1982. Unpublished research. Pullman, WA: Wood Materials and Engineering Laboratory, Washington State University.

Winandy, J.E.; Lebow, P.K.; Nelson, W. 1998. Predicting bending strength of fire-retardant-treated plywood from screw withdrawal tests. Res. Pap. FPL–RP–568. Madison, WI: U.S. Department of Agriculture, Forest Service, Forest Products Laboratory.

Chapter 6

A Review of the Piezoelectric Effect in Wood

Robert J. Ross, Supervisory Research General Engineer
Forest Products Laboratory, Madison, Wisconsin

Jiangming Kan, Associate Professor
Beijing Forestry University, School of Technology, Beijing, China

Xiping Wang, Research Forest Products Technologist
Forest Products Laboratory, Madison, Wisconsin

Julie Blankenburg, Supervisory Librarian
National Forest Service Library, Forest Products Laboratory, Madison, Wisconsin

Janet I. Stockhausen, Patent Advisor
Forest Products Laboratory, Madison, Wisconsin

Roy F. Pellerin, Professor Emeritus
Washington State University, Pullman, Washington

Piezoelectricity is the charge that accumulates in certain solid materials (notably crystals, certain ceramics, and biological matter such as bone and various proteins) in response to applied mechanical stress. Piezoelectricity means electricity resulting from pressure and is the direct result of the piezoelectric effect.

Although wood is a complex biological material, it has been shown experimentally that wood exhibits a distinguishable piezoelectric effect. We conducted a worldwide literature review to examine the piezoelectric effect in wood. The goals of our review were to (1) examine the worldwide literature on the piezoelectric effect in wood and (2) summarize results of the main findings reported in the literature. The objective of this chapter is to present the results of our review.

This chapter was originally published in 2012 as a Forest Products Laboratory General Technical Report:

> Ross, Robert J.; Kan, Jiangming; Wang, Xiping; Blankenburg, Julie; Stockhausen, Janet I.; Pellerin, Roy F. 2012. Wood and wood-based materials as sensors—a review of the piezoelectric effect in wood. General Technical Report FPL–GTR–212. Madison, WI: U.S. Department of Agriculture, Forest Service, Forest Products Laboratory. 9 p.

To review the state-of-the-art in the piezoelectric effect in wood, an extensive literature search on the piezoelectric effect in wood was conducted using CAB Abstracts. CAB Abstracts is an applied life sciences bibliographic database emphasizing agricultural literature that is international in scope. The database covers international issues in agricultural, forestry, and allied disciplines in the life sciences from 150 countries in 50 languages. It includes English abstracts for most articles. Our review of abstracts covered the years from 1939 to 2010 and consisted of three searches of abstracts using three different sets of word descriptors. The first search required that the word "wood" was used and the word "piezo" could be anywhere in the records; this search yielded 12 records. Our second search of the abstracts used "wood" in the descriptor field and phrase "electrical properties" anywhere in the records; 334 records were discovered, of which 196 were selected for applicability. The third search we conducted used "wood" in the descriptor field and the truncation "piezo" anywhere in the records. Based on these results and several additional sources, 31 technical documents and 4 patents were selected for intensive review.

Technical Documents Reviewed in a Chronological Order

1. Shubnikov 1946
2. Bazhenov 1950
3. Fukada 1955
4. Fukada and others 1957
5. Bazhenov 1961
6. Galligan and Bertholf 1963
7. Fukada, E. 1965
8. Galligan and Courteau 1965
9. Kytmanov 1967
10. Lin, R.T. 1967
11. Fukada 1968
12. Hirai and others 1968a
13. Hirai and others 1968b
14. Hirai and others 1970

15. Hirai and others 1972
16. Maeda and others 1977
17. Hirai and Yamaguchi 1979
18. Kellog 1981
19. Pizzi and Eaton 1984
20. Knuffel and Pizzi 1986
21. Fei and Zeng 1987
22. Knuffel 1988
23. Hirai and others 1992
24. Suzuki and others 1992
25. Hirai and others 1993
26. Nakai and Takemura 1993
27. Suzuki and Hirai 1995
28. Nakai and others 1998
29. Smittakorn and Heyliger 2001
30. Suzuki and others 2003
31. Nakai and others 2005

Patents Selected for Review

1. Best 1935
2. Sanders 2001
3. Lammer 2006
4. Churchill and Arms 2010

Research Summary

Table 6.1 presents a summary of several of the significant findings in chronological order from the technical papers we reviewed. Note that a piezoelectric effect in wood was first hypothesized, and later discovered, by Russian scientists in the 1940s–1950s. Their work was initiated in an effort to find an appropriate trigger mechanism for military equipment, specifically missiles. Since then, research has been conducted to explore the relationships between fundamental wood characteristics and the piezoelectric effect observed.

Table 6.1—Significant findings in a chronological order

Year	Author	Reported findings
1946	Shubnikov	Discovery of piezo-effect in wood
1950	Bazhenov and Konstantinova	First reported experiments on piezoelectricity in wood
1955	Fukada	Inverse piezoelectric effect in wood
1963	Galligan and Bertholf	Use of piezoelectric textures to observe stress wave behavior in wood
1970	Hirai and others	Effects of tree growth, wood quality, degree of crystallinity, and micellar orientation
1984	Pizzi and Eaton	Correlation between molecular forces in cellulose I crystal and piezoelectric effect
1993	Nakai and Takemura	Species, grain orientation effects
1998	Nakai and others	Relationship to static and vibration properties
2005	Nakai and others	Relationship to crystal lattice strain and tension stress of individual wood fibers

Discussion

Fundamental Concepts

Piezoelectricity is the charge that accumulates in certain solid materials (notably crystals, certain ceramics, and biological matter such as bone and various proteins) in response to applied mechanical stress. Piezoelectricity means electricity resulting from pressure and is the direct result of the piezoelectric effect.

The piezoelectric effect is understood as the linear electromechanical interaction between mechanical and electrical state in crystalline materials. Piezoelectric effect is a reversible process in that materials exhibiting direct piezoelectric effect (the internal generation of electrical charge resulting from an applied mechanical force) also exhibit the reverse piezoelectric effect (internal generation of a mechanical strain resulting from an applied electrical field). For example, lead zirconate titanate crystals will generate measurable piezoelectricity when their static structure is deformed by about 0.1% of the original dimension. Conversely, those same crystals will change about 0.1% of their static dimension when an external electric field is applied to the material.

Piezoelectricity is found in useful applications such as the production and detection of sound, generation of high voltages, electronic frequency generation, microbalances, and ultrafine focusing of optical assemblies.

The electrical character of a piezoelectric material must be that of a dielectric wherein charge displacement far outweighs conduction. Thus, the material behaves according to the relationship: $C = Q/V$, where C is the capacitance (farads); Q the charge (coulombs); and V, the potential difference (volts).

At the molecular level, a further requirement is placed on the piezoelectric material; there must be planes of molecular symmetry and within these planes the molecular constituents must be oriented in such a manner that the electrical charge centers are not symmetrically located. Monocrystals are representative of materials that meet these requirements.

When a piezoelectric crystal is strained, the charge centers are displaced relative to one another, causing a net charge to occur on the crystal surface. The dielectric nature of the crystal, obeying the capacitance relationship, permits the charge to appear as a voltage. This voltage is the electrical evidence of the piezoelectric effect.

The fundamental equations that describe the relationship between mechanical stress and electrical charge are the following:

$$P = dS + \eta E$$
$$\gamma = JS + dE$$

where a stress S is given to a substance, a polarization P is produced.

At the same time, an electric field E is also caused by the polarization of the substance. The coefficient d is called the piezoelectric modulus and η the electric susceptibility. The converse effect is shown by the second equation. A mechanical strain γ is produced by an applied electric field E and is accompanied by a stress S. The coefficient d for the converse effect is the same as that for the direct effect. If the condition is made that $E = 0$, then, by an experimental procedure, the modulus d can be determined as a ratio of polarization P to stress S. Thus relations between electrical polarization and mechanical stress are generally given the following equations:

$$P_x = d_{11}S_x + d_{12}S_y + d_{13}S_z + d_{14}S_{xy} + d_{15}S_{yz} + d_{16}S_{zx}$$
$$P_y = d_{21}S_x + d_{22}S_y + d_{23}S_z + d_{24}S_{xy} + d_{25}S_{yz} + d_{26}S_{zx}$$
$$P_z = d_{31}S_x + d_{32}S_y + d_{33}S_z + d_{34}S_{xy} + d_{35}S_{yz} + d_{36}S_{zx}$$

Where P_x, P_y, P_z represent the polarizations in xx, yy, and zz-directions, S_{yz}, S_{zx}, and S_{xy} represent the shear stress in yz, zx, and xy planes, respectively. The piezoelectric modulus d_{ij} relates each component of the polarization to each component of stress. In general, there are 18 components of d_{ij} and they are represented by a piezoelectric tensor as follows:

$$\begin{matrix} d_{11} & d_{12} & d_{13} & d_{14} & d_{15} & d_{16} \\ d_{21} & d_{22} & d_{23} & d_{24} & d_{25} & d_{26} \\ d_{31} & d_{32} & d_{33} & d_{34} & d_{35} & d_{36} \end{matrix}$$

By examination of the geometrical relationship between applied stress and the resulting polarization in wood, the piezoelectric tensor for wood has been determined as follows:

$$\begin{matrix} 0 & 0 & 0 & d_{14} & 0 & 0 \\ 0 & 0 & 0 & 0 & d_{25} & 0 \\ 0 & 0 & 0 & 0 & 0 & 0 \end{matrix}$$

The modulus d_{14} means that shear stress in the yz plane produces polarization in the x-direction, and the modulus d_{25} means that shear stress in the zx plane produces polarization in the y-direction. Experimentally, their magnitudes are nearly the same and their sign is opposite. This fact makes evident that the piezoelectric effect is symmetrical about the z-axis.

Characteristics of piezoelectricity considered above apply directly to monocrystalline materials. Piezoelectricity of wood cannot be discussed easily in this context; while the same fundamental relations are believed applicable, it is necessary to consider the extremely heterogeneous nature of wood. Shubnikov (1946) noted this fact in some of the first reported work on piezoelectricity of wood; he proposed the concept of "piezoelectric texture" to represent a system consisting of many crystalline particles oriented unidirectionally.

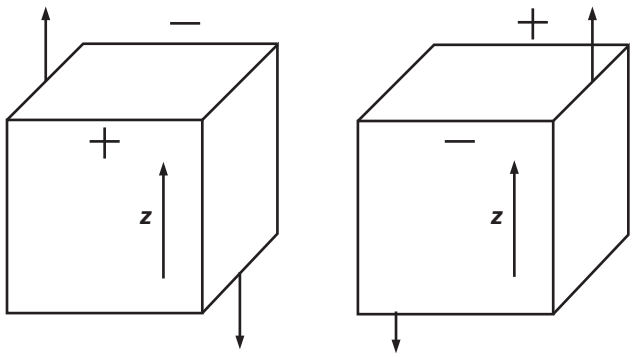

Figure 6.1—General scheme to produce piezoelectric polarization in wood (Fukada 1968). (Graphic used by permission of Washington State University, Pullman.)

The piezoelectric effect in wood may be observed as illustrated in Figure 6.1. The z-axis represents the fiber direction in wood. If a shearing stress is applied as indicated by arrows, an electrical polarization takes place in the direction perpendicular to the plane of the stress. The sign of the value of polarization is reversed when the direction of shear is reversed.

Rectangular coordinates are assigned to the wood structure with the z, x, and y axes representing the longitudinal, radial, and tangential directions in a tree trunk, respectively (Fig. 6.2).

It is known that cellulose is crystallized to a fairly large extent and that the unit cell of cellulose crystal belongs to monoclinic symmetry C_2. The piezoelectric tensor for a crystal is determined by the symmetry of a crystal lattice (Fukada 1968).

The tensor for a crystal with the symmetry C_2 is

$$\begin{matrix} 0 & 0 & 0 & d_{14} & d_{15} & 0 \\ 0 & 0 & 0 & d_{24} & d_{25} & 0 \\ d_{31} & d_{32} & d_{33} & 0 & 0 & d_{36} \end{matrix}$$

where the zz-axis is taken in the direction of the longitudinal axis of the molecules in the crystal. Eight components of the piezoelectric modulus should be finite.

The structure of wood composed of cellulose fiber is very complicated. Assume that the fiber is composed of many numbers of cellulose crystallites, orientated in the same direction, is the fiber axis, and that such fibers are regularly orientated parallel to the trunk axis. Figure 6.3 illustrates the

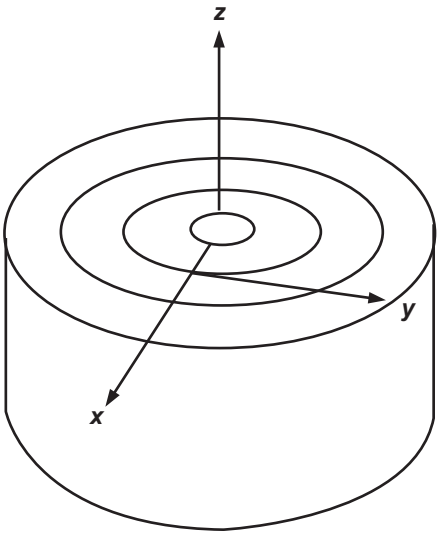

Figure 6.2—Rectangular coordinates assigned to wood (Fukada 1968). (Graphic used by permission of Washington State University, Pullman.)

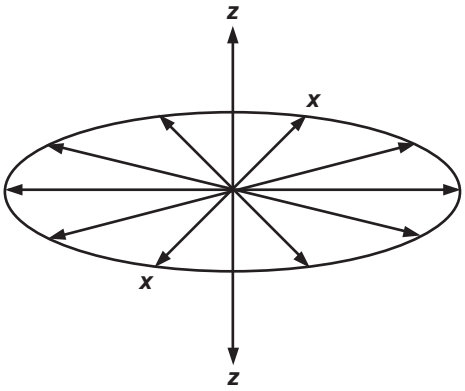

Figure 6.3—Uniaxial and non-polar orientation of crystallites (Fukada 1968). (Graphic used by permission of the *Journal of Wood Science and Technology*.)

uniaxial orientation of cellulose crystallites. The positive end of the *zz*-axis of each crystallite is distributed at random in the axis of symmetry, that is, with the same probability for two opposite directions. The *xx*-axis of each crystallite is distributed at random and uniformly in the plane perpendicular to the axis of symmetry. The piezoelectric modulus for such an assembled system of crystallites can be calculated by taking an average of the moduli of the crystallites. Then it turns out that only d_{14} and d_{25} are finite for the system and that the other moduli become zero due to cancellation of the effect. The values of d_{14} and d_{25} of the system are proportional to the mean value of d_{14} and d_{25} in the single crystal of cellulose. The coefficient of proportion is dependent on density, crystallinity, and degree of orientation.

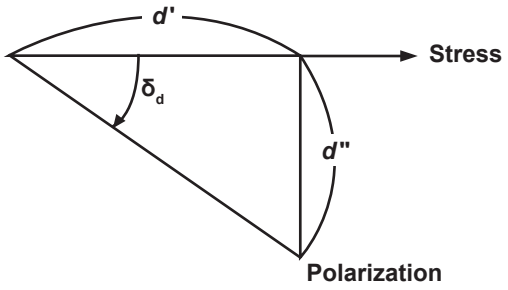

Figure 6.4—Vector representation of stress S and polarization P (Fukada 1968). (Graphic used by permission of the *Journal of Wood Science and Technology*.)

The piezoelectric tensor for such an assembly of unidirectionally orientated crystallites is

$$\begin{matrix} 0 & 0 & 0 & d_{14} & 0 & 0 \\ 0 & 0 & 0 & 0 & -d_{14} & 0 \\ 0 & 0 & 0 & 0 & 0 & 0 \end{matrix}$$

This tensor form is identical to that experimentally determined for wood.

Cellulose fibrils twist spirally with a certain angle to the longitudinal axis of the cell. However, if the average is taken for the layers in which fibrils describe a spiral form in alternative directions, the form of the resultant tensor of piezoelectric modulus is the same as derived above.

Since polymeric substances possess a viscoelastic property, it is anticipated that when stress is applied, electrical polarization does not appear instantly but arises gradually with time. Therefore, the piezoelectric modulus is treated as a complex quantity and determines the phase lag between stress and polarization as well as the absolute value of the modulus.

Figure 6.4 represents stress and polarization in a vector diagram. The polarization is delayed behind the stress by an angle δ_d. The component of polarization in phase with the stress represents the real part of modulus *d'* and the component of polarization 90º out of phase with the stress of the imaginary part of modulus *d"*. The ratio of *d"* to *d'* may be expressed as the tangent of δ_d. These relationships are very similar to those encountered with the complex mechanical compliance and the complex dielectric constant.

Baseline Studies

Table 6.2 provides a summary of the species used in several reported studies. Note that a wide range of species has been used in these studies, and all have exhibited a piezoelectric effect. Reported moisture content values of the specimens used in the studies varied considerably; from a relatively dry state (below 10%) to over 70%. The specimens used were relatively small, with any dimension not exceeding 60 mm. Galligan and Courteau (1965), Knuffel (1988), and Knuffel

Table 6.2—A list of wood species investigated for piezoelectric effect in previous studies

Reference	Species
Fei and Zeng 1987	*Magnolia grandiflora* Linn *Tilia amurensis* Rupr *Taxodium* ascendens Brongn *Pinus massoniana* Lamb *Cunninghamia lanceolata* Hook
Fukada and others 1957	(10 old timbers from 8 years to 1,300 years)
Galligan and Courteau 1965	Douglas-fir
Hirai and others 1968	Tsuga (*Tsuga sieboldii* Carr.) Shioji (*Fraxinus mandshurica* Rupr.) Shirakaba (*Betula platyphylla* SUKATCHEV. var.; *japonica* HARA.) Hônoki (*Magnolia obovata* THUNB) Taiwanhinoki (*Chamaecyparis taiwanensis* MASAM. et SUZUKI) Kiri (*Paulownia tomentosa* STEUD.) Hinoki (*Chamaecyparis obtuse* ENDL.) Sugi (*Cryptomeria japonica* D. DON) Konara (*Quercus serrata* MURRAY.) Akamatsu I (*Pinus densiflora* SIEB. et ZUCC.) Akamatsu II Douglas-fir (*Pseudotsuga taxifolia* BRITT.) Makanba
Hirai and others 1970	Sugi (summerwood and springwood)
Hirai and others 1972	Hinoki tree (*Chamaecyparis obtuse* SIEB. et ZUCC)
Hirai and Yamaguchi 1979	Hinoki
Knuffel and Pizzi 1986	*Pinus patula*
Knuffel 1988	*Pinus patula* *P. taeda* *P. elliottii*
Maeda and others 1977	Japanese cedar
Nakai and Takemura 1993	Beisugi (*Thuja plicata* Donn) Hinoki (*Chamaecyparis obtuse* ((S. and Z.)) Endl.) Beitsuga (*Tsuga heterophylla* ((Raf.)) Sarg.) Beimatsu (*Pseudotsuga menziesii* ((Mirb.)) Franco) Buna (*Fagus crenata* Bl.)
Nakai and others 1998	Sitka spruce (*Picea sitchensis* Carr.)
Nakai and others 2005	Japanese cypress (*Chamaecyparis obtuse* Endl.)
Suzuki and others 1992	Hinoki (*Chamaecyparis obtuse* ((S. and Z.)) Endl.) Beimatsu (*Pseudotsuga menziesii* ((Mirb.)) Franco) Beihiba (*Chamaecyparis nootkatensis* ((D. Don)) Spach) Agathis (*Agathis* sp.) Igem (*Podocarpus imbricatus* Bl.) Momi (*Abies firm* S. and Z.) White fir (*Abies alba* Mill.) Spruce (*Picea pungens* Engelm) Shinanoki (*Tilia japonica* Simk) Katsura (*Cercidiphyllum japonicum* S. and Z.) Buna (*Fagus crenata* Bl.) Lauan (*Pentacme contorta* Merr. and Rolfe) Nato (*Palaquium* sp.) Matoa (*Pometia pinnata* Forst.) Sugar maple (*Acer saccharum* Marsh.)
Suzuki and Hirai 1995	*Chamaecyparis botusa* Endlicher *Larix leptolepis* Gordon *Magnolia ovobata* Thunberg

and Pizzi (1986) were exceptions—they used lumber size specimens in their experiments.

Most reported work used test setups that resulted in a uniform compressive stress being applied to the specimen, orienting each specimen so that the angle between growth rings and the application of load was approximately 45º. The electric charge generated was detected by electrodes that consisted of conductive paint, glued-on metal foil, pins, or small metal buttons placed against a specimen's surface.

Based on early experimentation by Bazhenov (1961), Fukuda (1955, 1965), and Hirai and others (1970), the magnitude of the piezoelectric modulus of wood is approximately 1/20 of that of a quartz crystal. Bazhenov (1961) and Hirai and others (1970) found that the values of the piezoelectric modulus, d_{14}, increased gradually from the pith to the bark of a tree. They also reported that the values of the piezoelectric modulus for springwood and summerwood, for the same year's growth, were nearly equal.

Fukada and others (1957) found that the piezoelectric moduli increased with increasing density. Bazhenov (1961) found that the piezoelectric modulus d_{25} increased and that of d_{14} decreased with increasing density in pines. Hirai and others (1968a) confirmed that the d_{25} piezoelectric modulus increased with increasing density, but they show no data for d_{14}.

Bazhenov (1961) found that the piezoelectric modulus is related to temperature, and it increases as temperature increases. Maeda and others (1977) found that d' of the piezoelectric constant of the Japanese cedar at 74% of moisture content increased with the increasing temperature for the piezoelectric constant determined at 10 Hz.

Smittakorn and Heyliger (2001) developed a theoretical model for the steady-state and transient behavior of adaptive wood composite plates composed of layers of wood and other piezoelectric materials to simultaneously study the effects of mechanical, electrical, temperature, and moisture fields. They considered the theoretical model as a means of studying any laminated wood plate where the elastic, temperature, moisture, and electric fields influence the overall structural response. Their results of studying a representative example provided an indication of the level of response of adaptive wood composites, although no experimental verification had been conducted in their investigation.

Origin of the Piezoelectric Effect in Wood

Fukada (1955) and Bazhenov (1961) both hypothesized that the piezoelectric effect observed in wood originates in crystalline cellulose regions of the wood cell wall and that its intensity is dependent upon the degree of crystallinity. Hirai and others (1970) furthered that hypothesis, postulating that the magnitude of the piezoelectric modulus of wood depend upon degree of crystallinity and orientation of cellulose crystals in the cell wall.

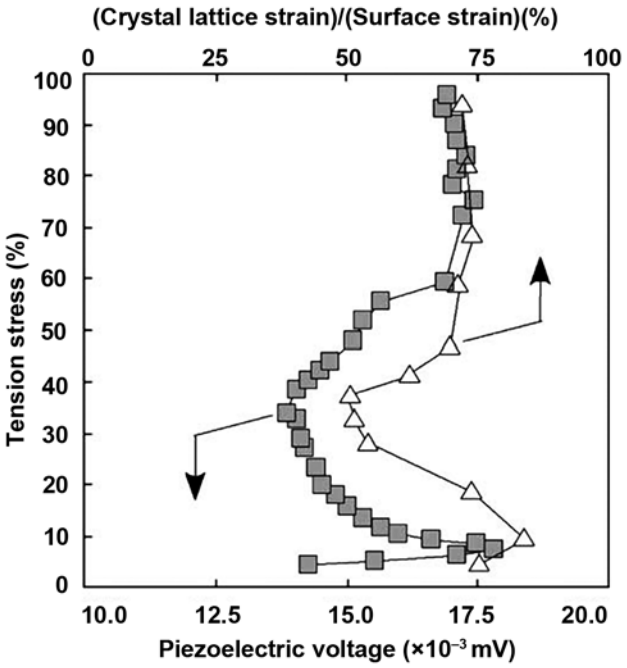

Figure 6.5—Relationships between the ratios of crystal lattice strain to surface strain (triangles), piezoelectric voltage (squares), and tension stress. Note: values of tension stress are shown as a percentage of ultimate tensile stress (Nakai and others 2005). (Graphic used by permission of the *Journal of Wood Science and Technology*.)

Using conformational analysis, Pizzi and Eaton (1984) concluded that van der Waal forces were responsible for the piezoelectric effect in wood. They concluded that the electrical charge most likely develops in response to an imposed shear force that results in laminar lateral–longitudinal deformations in the five-strand unit of the crystalline cellulose I molecule found in the microfibrils of wood. They also concluded that electrostatic and hydrogen bond interactions do not contribute to the piezoelectric effect.

Hirai and others (1968b, 1972) have shown that the piezoelectric modulus can be increased by increasing the crystallinity of the cellulose by treatment with gamma rays, exposure to high temperature for extended periods, liquid ammonia, ethlyenediamine, or sodium hydroxide. Fukada and others (1957) found that aging wood increased its crystallinity and its piezoelectric modulus. Based on his experimental results, he also postulated that fungal decomposition decreased both crystallinity and piezoelectric modulus.

Nakai and others (2005) found that the first and second peaks in the piezoelectric voltage appeared almost simultaneously with the peak of the ratio of crystal lattice strain to surface strain (Fig. 6.5). They also noted that the piezoelectric response decreased because of the effect of microscopic cracks in their specimens.

Piezoelectric Effect and the Properties of Wood and Wood Structural Members

Nakai and others (1998) measured the piezoelectricity of kiln-dried Sitka spruce specimens and simultaneously recorded scanning electron microscope images in real time to observe the deformation process of wood. Results of their experiments showed that there were two types of microscopic destruction in the specimens. With the first type, although a small uprush around the boundary of the annual ring was observed, the specimens were broken only by shearing fracture in the 45º direction. With the second type, the specimens were finally broken by shearing fracture after repeated buckling. They found that the piezoelectric voltage increased almost linearly in the elastic region, preceded to the maximal point, and then decreased gradually, and a clear peak appeared in the bucking and shearing fracture.

Nakai and Takemura (1993) measured the piezoelectricity of air-dried specimens (from five species) under time-varying load to investigate the possible relationship between piezoelectricity and the fracture of wood. A time-varying load was applied at a constant rate, accompanying a preliminary load and a sinusoidal load with a frequency of 20 Hz. They found that the greatest voltage of the piezoelectric signals as reported in a previous paper was in the case of a grain angle of 45º, and the voltages of the piezoelectric signals depended on the magnitude of the load, species, and grain angle. The results of their experiments showed that the piezoelectricity–time curves can be classified into three types (Type A, B, and C). Each curve consists of an initial rising part, a gradually increasing part, a subsequent decreasing part, and finally, a rapid rising and falling (Type A and B) or merely falling part (Type C), where the second part of the Type B is much flatter compared with that of the Type A. They also found that decreasing piezoelectricity against an increasing load was another characteristic behavior in the plastic region before a sudden fracture of a specimen.

Fukada and others (1957) found that the relation between the dynamic Young's modulus and the piezoelectric constant of the old timbers was linear (Fig. 6.6). Nakai and others (1998) reported a similar linear relation in the kiln-dried Sitka spruce with the exact relationship between the dynamic Young's modulus and the piezoelectric constant as

$$E_c\ (\times 10^3\ \text{kgf/cm}^2) = 1.18 \left(\frac{P_\text{p}}{\rho \times L_\text{p}} \right) + 3.15$$

Hirai and others (1968a) found that the piezoelectric effect varied with the angle between the direction of the stress and the direction of the fiber axis and that maximum piezoelectric polarization was obtained when the direction of the stresses were at angles of 45º and 135º with the direction of the fiber axis (Fig. 6.7).

Knuffel and Pizzi (1986) measured the piezoelectric effect in *Pinus patula* structural timber beams. They found that the

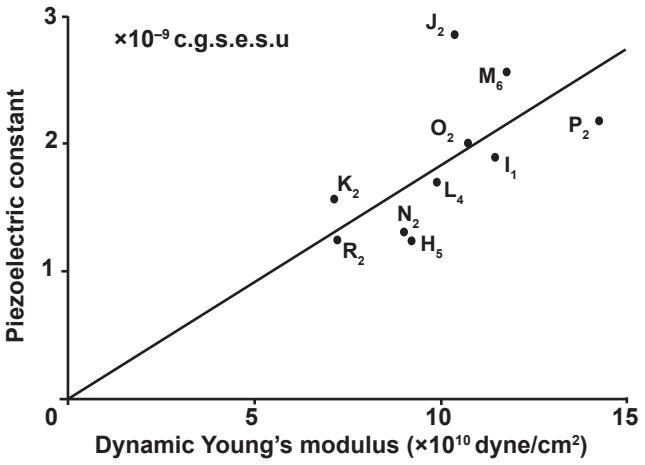

Figure 6.6—The relation between dynamic Young's modulus and the piezoelectric constants of old timbers (Fukada and others 1957). (Graphic used by permission of *Oyo Buturi*.)

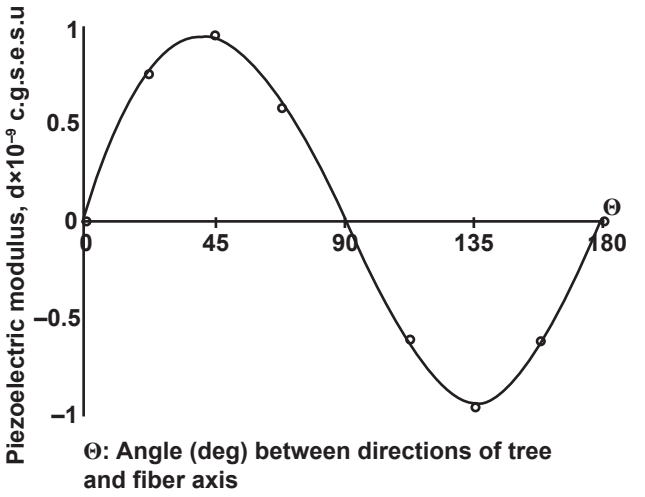

Figure 6.7—Anisotropy of piezoelectric modulus (Hirai and others 1968). (Graphic used by permission of Washington State University, Pullman.)

piezoelectric signal usually began smaller, increased to maximum after about five cycles, and then began to attenuate to zero. Also, the piezoelectric response started to develop almost simultaneously with the arrival of the stress wave and reached its first peak within 0.0001 s. They observed that the first peak of the piezoelectric signals might be either positive or negative, which are uncontaminated by resonance. They also found that the piezoelectric effect in the wet boards was still found to be very strong. But because of the conductive conditions, the electrical signal originating at the beginning of the board propagated faster than the stress wave, and at 20% moisture content, the piezoelectric effect began to coincide with the arrival of the stress wave.

Knuffel (1988) investigated the effect of the natural defects on the piezoelectric effect in structural timber. There were

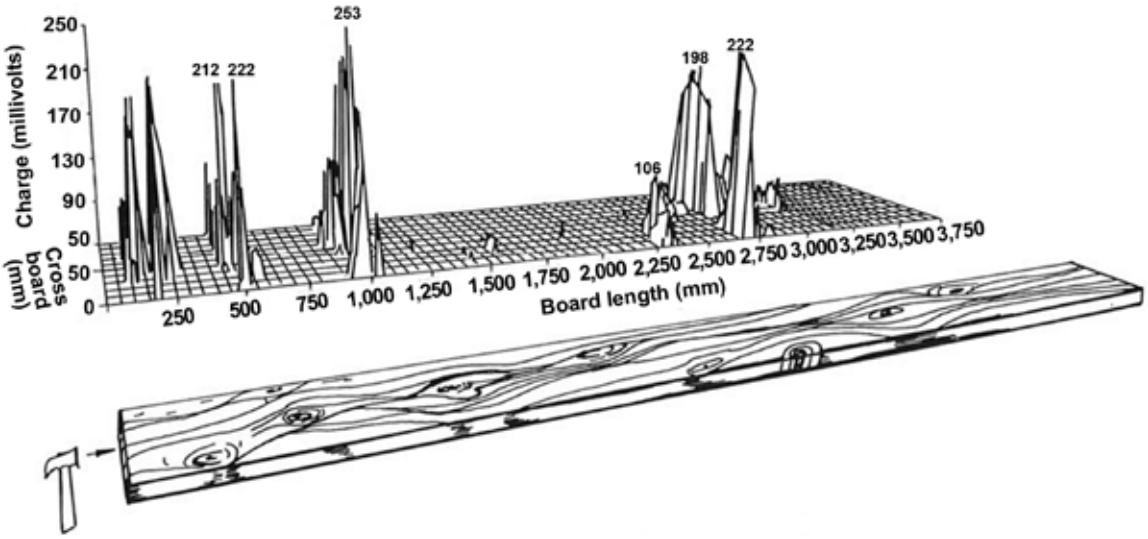

Figure 6.8—Piezoelectric response in structural timber (Knuffel 1988). (Graphic used by permission of *Holzforschung*.)

three findings from their investigation. Firstly, the piezoelectric first wavepeak values showed a definite and very sensitive increase in amplitude in the vicinity of knots and cross-grain (Fig. 6.8). Second, the piezoelectric response was far more sensitive to the defects than to MOE. At last, the piezoelectric effect was directly related to strain concentrations in the anatomical structure.

Summary

1. Research has been conducted on the piezoelectric effect in wood and wood materials, starting as early as the 1940s.
2. A number of wood species have been shown to exhibit a piezoelectric effect.
3. The magnitude of the piezoelectric modulus of wood is approximately 1/20 of that of a quartz crystal.
4. Several studies have been conducted to identify the origin of the piezoelectric effect in wood.
5. Studies have been conducted to explore its potential for evaluating the structural properties of wood structural members.

Literature Cited

Bazhenov, V.A. 1961. Piezoelectric properties of wood. New York: Consultants Bureau. 176 p.

Bazhenov, V.A.; Konstantinova, V.P. 1950. Piezoelectric properties of wood. Doklady Akod. Nauk SSSR 71(2). Chemical Abstracts. 45, 2747.

Best, F.M., inventor. 1935 (August 13). Method of and apparatus for utilizing energy of a vibratory nature. U.S. Patent 2,010,806.

Churchill, D.L.; Arms, S.W., inventors. 2010 (April 6). Slotted beam piezoelectric composite. U.S. Patent 7,692,365 B2.

Fei, Y.Y.; Zeng, S.X. 1987. Piezoelectric effect in wood. Journal of Nanjing Forestry University. 3: 100–104.

Fukada, E. 1955. Piezoelectricity of wood. Journal of the Physical Society of Japan. 10(2): 149–154.

Fukada, E. 1965. Piezoelectric effect in wood and other crystalline polymers. In: Galligan, W.L., ed. Proceedings, second symposium on nondestructive testing of wood. April, 1965. Spokane, WA: Washington State University. 143–170.

Fukada, E. 1968. Piezoelectricity as a fundamental property of wood. Wood Science and Technology. 2: 299–307.

Fukada, E.; Yasuda, S.; Kohara, J.; Okamoto, H. 1957. The dynamic Young's modulus and the piezoelectric constant of old timbers. Oyo Butsuri [Journal of Applied Physics, Japan]. 26: 25–28.

Galligan, W.L.; Bertholf, L.D. 1963. Piezoelectric effect in wood. Forest Products Journal. 12(12): 517–524.

Galligan, W.L.; Courteau, R.W. 1965. Measurement of elasticity of lumber with longitudinal stress waves and the piezoelectric effect in wood. In: Galligan, W.L., ed. Proceedings, second symposium on nondestructive testing of wood. April, 1965. Spokane, WA: Washington State University. 223–224.

Hirai, N.; Asano, I. Sobue, N., Naito, H. 1970. Studies on piezoelectric effect of wood. III. Tree growth and variations of piezoelectric modulus. Mokuzai Gakkaishi. 16(7): 310–318.

Hirai, N.; Date, M.; Fukada, E. 1968a. Studies on piezoelectric effect in wood. I. Mokuzai Gakkaishi. 14(5): 247–251.

Hirai, N.; Date, M.; Fukada, E. 1968b. Studies on piezoelectric effect in wood. II. Modification of crystal structures. Mokuzai Gakkaishi. 14(5): 252–256.

Hirai, N.; Hayamura, S.; Suzuki, Y.; Miyajima, K.; Matsuyama, S. 1992. Piezoelectric relaxation of wood in high temperature region. Mokuzai Gakkaishi—Journal of the Japan Wood Research Society. 38(9): 820–824.

Hirai, N.; Morita, M.; Suzuki, Y. 1993. Electrical properties of cyanoethylated wood meal and cyanoethylated cellulose. Mokuzai Gakkaishi. 35(5): 603–609.

Hirai, N.; Sobue, N.; Asano, I. 1972. Studies on piezoelectric effect of wood. IV. Effects of heat treatment on cellulose crystallites and piezoelectric effect of wood. Mokuzai Gakkaishi. 18(11): 535–542.

Hirai, N.; Yamaguchi, A. 1979. Studies on piezoelectric effect of wood. VI. Effect of moisture content on piezoelectric dispersion of wood. Mokuzai Gakkaishi. 25(1): 1–6.

Kellog, R.M. 1981. Physical properties of wood. In: Wangaard, F.F., ed. Wood: its structure and properties. Clark C. Heritage Memorial Series on Wood. University Park, PA: The Pennsylvania State University. 195–223. Vol. 1.

Knuffel, W. 1988. The piezoelectric effect in structural lumber. Part II. The influence of natural defects. Holzforschung. 42(4): 247–252.

Knuffel, W.; Pizzi, A. 1986. The piezoelectric effect in structural lumber. Holzforschung. 40(3): 157–162.

Kytmanov, A.V. 1967. Piezo-electric properties and shrinkage of compressed Larch wood. Drevesina, ee zascita i plastiki. 72–77. Moscow, USSR.

Lammer, H.J., inventor. 2006 (August 29). Flexible piezoelectric films. U.S. Patent 7,098,578 B2.

Lin, R.T. 1967. Review of the electrical properties of wood and cellulose. Forest Products Journal. 17(7): 54–66.

Maeda, H.; Tsuda, H.; Fukuda, E. 1977. Electrical and mechanical properties of bamboo and wood with various hydrations. Reports on Progress in Polymer Physics in Japan. 20: 739–742.

Nakai, T.; Igushi, N.; Ando, K. 1998. Piezoelectric behavior of wood under combined compression and vibration stress I: relation between piezoelectric voltage and microscopic deformation of Sitka spruce (*Picea sitchensis* Carr.). Journal of Wood Science. 44: 28–34.

Nakai, T.; Takemura, T. 1993. Piezoelectric behaviors of wood during compression tests. Mokuzai Gakkaishi. 39(3): 265–270.

Nakai, T.; Yamamoto, H.; Nakao, T.; Hamatake, M. 2005. Mechanical behavior of the crystalline region of wood and the piezoelectric response of wood in tension tests. Wood Science and Technology. 39: 163–168.

Pizzi, A.; Eaton, N. 1984. Correlation between molecular forces in the cellulose I crystal and the piezoelectric effect in wood. Holzforschung und Holzverwertung. 36(1): 12–14.

Sanders, J.F., inventor. 2001 (January 16). Composites under self compression. U.S. Patent 6,174,595 B1.

Shubnikov, A.V. 1946. Piezoelectric textures. Moskova, Russia: Izvestiya Akademii Nauk, Seriya Biologicheskaya [Proceedings of the Academy of Sciences, Biological Series]. 84 p. In Russian.

Smittakorn, W.; Heyliger, P.R. 2001. An adaptive wood composite: theory. Wood and Fiber Science. 33(4): 595–608.

Suzuki, Y.; Hirai, N. 1995. Piezoelectric relaxation of wood. II. Application of two-phase system model to piezoelectric relaxation in low temperature region. Mokuzai Gakkaishi. 42(3): 271–280.

Suzuki, Y.; Hirai, N.; Ikeda, M. 1992. Piezoelectric relaxation of wood. I. Effect of wood species and fine structure on piezoelectric relaxation. Mokuzai Gakkaishi. 38(1): 20–28.

Suzuki, Y.; Kataoka, Y.; Matsui, H. 2003. Electrical properties of composite cyanoethylated pullulan film. Journal of Wood Science. 49(1): 100–103.

Chapter 7

Nondestructive Testing in the Urban Forest

R. Bruce Allison, Adjunct Professor
University of Wisconsin–Madison, Madison, Wisconsin; and Allison Tree, LLC, Verona, Wisconsin

Xiping Wang, Research Forest Products Technologist
Forest Products Laboratory, Madison, Wisconsin

Trees within an urban community provide measurable aesthetic, social, ecological and economic benefits. When growing normally and stably, they contribute to making a city more livable and comfortable for its inhabitants. However, as large physical structures in close proximity to people and property, their failure can cause harm. The science of tree stability analysis uses both biological and engineering principles in determining a tree's structural soundness and predicting the probability of failure. Nondestructive testing methods of locating and quantifying wood decay and defect are used to measure the physical condition of trees within the urban forest to promote public safety. These methods are of special value to the urban forest managers and arborists responsible for the general safety of city residents, roadway transportation, and utility corridors. This chapter will discuss the commonly used methods of visual inspection, acoustic testing, and microdrill resistance with two case studies presented to illustrate how they are used in combination plus how to best interpret data collected in evaluating the nature and threat of discovered defects.

Tree Decay and Visual Inspection

Tree decay is an essential process that links tree growth to soil fertility, wildlife habitat, and many other critical functions in all forests. However, decay in roots, trunk, and limbs can be a major problem for tree managers. Concealed internal decay presents a special problem in managing urban trees for public safety. Knowledge and special tools to measure the presence of internal decay are needed by tree managers responsible for safety in parks and recreational areas, populated residential and commercial neighborhoods, and along utility and transportation corridors. Trees can reach great height, mass, and age. Wood decay and defect can cause structural failure damaging property, endangering lives, and affecting the efficiency of transportation and energy distribution. Urban forest managers need to understand how decay fungi interact with the tree and how and why visible external characteristics of the tree can reveal internal decay conditions.

Decay fungi enter standing trees through wounds or breaks in the bark. Wounds can result from a variety of incidents including storms, pruning, or root cutting. Once the decay fungus breaches the bark, it enters the sapwood and can eventually affect the heartwood.

A variety of fungi species affect woody plants and they can progress over time in succession, one species preparing the way for the invasion of another. They live in a tree's structure, and its reaction to the presence of the fungal parasite influences how the fungus advances within the tree. Decay fungi are parasites. Unable to produce their own carbohydrates for energy, they digest the carbohydrates within the tree's structure. The drawings in Figure 7.1, provided courtesy of the United States Forest Service, illustrate how decay fungi interact with trees (Shigo 1979).

Trees "wall off" or compartmentalize wounded areas to resist the spread of decay, confining it to the wood present at the time of wounding. The concept of compartmentalization was developed by Dr. Alex Shigo as part of his research for the U.S. Forest Service on the biology of tree decay (Shigo 1979, 1984). Following his retirement from the Forest Service in 1985, he continued to write and teach about tree biology until his death in 2006.

Compartmentalization produces chemical and anatomical boundaries that vary in effectiveness to resist the spread of decay. The ceiling and floor and the interior wall are usually less effective than the exterior wall formed by new growth of xylem tissue. Thus decay tends to move in columns and back to the interior. Understanding how decay advances within a tree allows the tree manager to visualize the shape of internal decay, estimate its point of origin, and predict the direction of movement.

The tree manager can use visual inspection of a tree for observing external indicators of internal decay and defect. Seams on the bark, for example, can indicate internal cracks and decay. Other external indicators of decay include open cavities. Fungal fruiting bodies are a sign of the presence of wood decay fungi. They present the opportunity to identify the species of fungus and thereby know its significance and probable course of advancement within the tree. Examples of useful wood decay identification books include *Wood Decay Fungi* by Christopher Luley (Luley 2005) and *Manual of Wood Decay in Trees* by Karlheinz Weber and Claus Mattheck (Weber and Mattheck 2003).

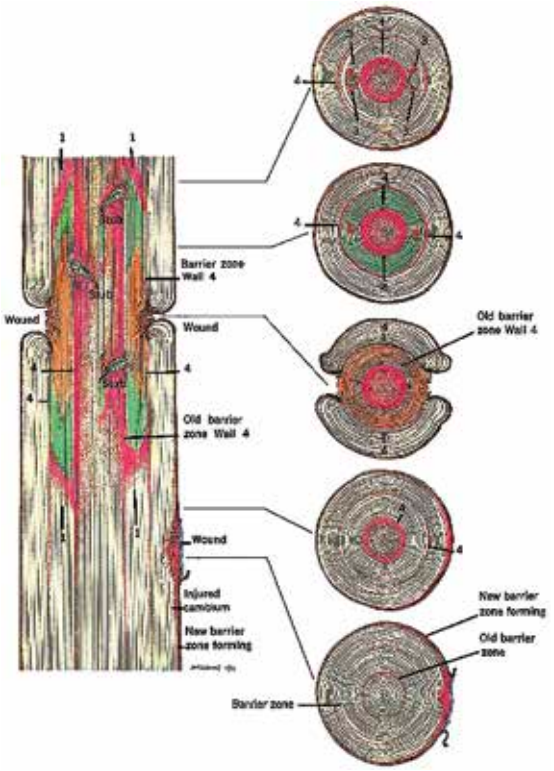

Figure 7.1—Wounds start the processes that could lead to discolored and decayed wood. The classical concept and the expanded concept both recognize wounds as the starting point for the processes. Trunk wounds can be caused by a variety of agents: insects, birds, small and large animals, wind, ice, snow, temperature extremes, chemicals, and people and some of their activities (Shigo 1979).

The visual inspection of a tree's "body language" is another way to estimate the presence of internal decay. For example a tree with an unusually expanded base sometimes called "bottle butt" could indicate the presence of extensive lower trunk decay. Trees are self-optimizing organisms highly reactive to the environmental stress around them. They are under constant mechanical stresses from holding their own weight, from leans or horizontal branching or dynamic loads from wind or ice. From Newtonian physics it is understood that a horizontal force against the tree will produce an equal and opposite resultant force tending to uproot the tree unless there is a reciprocal force to maintain stability. Wind loads in the crown are distributed down the trunk to the anchoring root system as mechanical stresses. The reciprocal force is the weight and friction of the soil against the root system resisting the shear force. Without it, tree trunks would be like the masts of sailing ships pushed along by wind forces.

Internal decay in branches or trunks reduces the area for those mechanical stresses to pass on the way to the root system. Living parts of trees can respond to those areas

Figure 7.2—Traditional tools for inspecting trees—Increment borer and sounding mallet.

of concentrated mechanical stresses by laying down additional wood. This process is called thigmomorphogenesis. It explains the bottle shape or bulges that are sometimes evident on trunks with internal decay. Evidence of this self-optimizing growth reaction to environmental mechanical stress is observed in cross sections of horizontal branches or leaning trunks that have produced wider annual rings on one side compensating for the extra gravitation loading. In angiosperms, the extra wood growth occurs on the tension side of the lean acting as a guy line holding back the trunk or limb. In gymnosperms, the extra wood growth occurs on the compression side acting as prop to hold up the trunk or limb. Examples of book references discussing this body language of trees and the visible anatomical indicators of decay are *The Body Language of Trees* by Claus Mattheck (1996) and *Evaluating Tree Defects* by Ed Hayes (2001).

In addition to these visual methods of internal decay detection, tree managers have used other traditional tools including increment borers and sounding mallets (Fig.7.2). Increment borers allow the visual examination of a core sample taken from the trunk using inexpensive, simple tools. But they have the disadvantage of leaving a significant wound at each location sampled. Small-diameter drill bits on a battery powered hand drill can also be used to "feel" for changes in resistance and look for wound-initiated discoloration in the shavings, but no core sample is produced and results are not graphically recorded.

Sounding mallets allow a trained ear to listen for the telltale drum sounds of internal cavities. They are limited in determining the extent or location and do not produce a record of the sound wave characteristics.

Electronic tools are available to vastly improve upon these traditional forestry methods. The increment borer and sounding mallet have evolved into sophisticated electronic tools of micro-drill resistance and acoustic measurements.

Table 7.1—Radial stress wave velocity and time-of-flight measured in healthy trees (Mattheck and Bethge 1993)

	Radial stress wave velocity		Time-of-flight per unit length	
Species	m/s	ft/s	μs/m	μs/ft
Hardwoods				
Ash	1162–1379	3810–4520	725–861	221–262
Birch	967–1150	3170–3770	870–1034	265–315
Black locust	934–1463	3060–4800	684–1071	208–326
Black poplar	869–1057	2850–3470	946–1151	299–351
Horse chestnut	837–1557	2860–5110	642–1145	196–349
Lime	940–1183	3080–3880	845–1064	258–324
Maple	1006–1600	3300–5250	625–994	191–303
Oak	1382–1610	4530–5280	621–724	189–221
Pine poplar	967–1144	3170–3750	874–1034	266–315
Plane	950–1033	3120–3390	968–1053	295–321
Red beech	1206–1412	3960–4630	708–829	216–253
Silver poplar	821–1108	2690–3640	903–1218	275–371
Sweet chestnut	1215–1375	3990–4510	727–823	222–251
Willow	912–1333	2990–4370	750–1096	229–334
Softwoods				
Douglas-fir	905–1323	2970–4340	756–1105	230–337
Fir	910–166	2990–3830	858–1099	261–335
Larch	1023–1338	3360–4390	747–978	228–298
Pine	1066–1146	3500–3760	873–938	266–286
Spruce	931–1085	3050–3560	922–1074	281–327

Acoustic Measuring Devices

Single-Path Stress Wave Timing

Simple stress wave measuring devices are used to record the time it takes for an impact-induced stress wave to travel through the wood sample. When used for tree inspection, this nondestructive testing procedure is often called single-path stress wave timing measurement. A stress wave is created with a strike to the tree. An accelerometer mounted at the strike point senses the impact and sends a start signal to the measuring device to start a timer. A second accelerometer attached to the opposite side of the tree senses the leading edge of the stress wave and sends a stop signal to the timer. The time between the start signal and stop signal is the time-of-flight (TOF) of the wave propagating through the tree trunk. The TOF data are usually measured in microseconds. Transmission time per unit length, such as microseconds per meter and velocity, such as meters per second, are calculated using the known distance between the sensors and the TOF.

The first instruments using acoustics to determine forest product quality were developed by Metriguard, Inc., of Pullman, Washington, in the early 1960s to evaluate particleboards (Pellerin and Ross 2002). In the 1990s, foresters began using longitudinal stress wave testing on both cut logs and standing timber for log selection and grading based on material strength. The first report of the use of stress wave testing to determine internal degradation of living trees was by Claus Mattheck and Klaus Bethge in 1993 (Mattheck and Bethge 1993).

Stress wave propagation in wood is related to the physical and mechanical properties of the wood. Stress waves travel faster in defect-free wood. Areas of cracks, cavities, or decay-induced low density will require longer times for the stress wave to arrive at the opposite timing sensor. By measuring TOF or wave transmission time through a tree stem in the radial direction, the internal condition of the tree can be determined.

The presence of deterioration from decay can greatly affect TOF in wood. TOF for decayed wood are much greater than that for non-decayed wood. For example, TOF for non-degraded Douglas-fir is approximately 800 μs/m (244 μs/ft), whereas severely degraded members exhibit values as high as 3,200 μs/m (975 μs/ft) or greater (Wang et al. 2004). A study conducted by Pellerin and others (1985) demonstrated that a 30% increase in stress wave TOF implies a 50% loss in strength. A 50% increase indicates severely decayed wood.

The speed of stress wave propagating perpendicular to grain is also affected by tree species. Mattheck and Bethge (1993) measured speed of sound in different species of healthy trees using a commercially available stress wave timing unit. The speed was determined by dividing the transit distance (tree diameter) by the TOF measured. Table 7.1 shows both radial stress wave velocity and TOF on a per length basis for 5 softwood species and 14 hardwood species.

Table 7.2—Reference stress wave velocity and time-of-flight in healthy trees (Divos and Szalai 2002)

	Radial stress wave velocity		Time-of-flight per unit length	
Species	m/s	ft/s	µs/m	µs/ft
Beech	1670	5479	599	183
Black fir	1480	4856	676	206
Larch	1490	4888	671	205
Linden	1690	5545	592	180
Maple	1690	5545	592	180
Oak	1620	5315	617	188
Poplar	1140	3740	877	267
Scotch fir	1470	4823	680	207
Silver fir	1360	4462	735	224
Spruce	1410	4626	709	216

Generally, stress waves travel faster in hardwood trees than in softwood trees. To account for species difference, Divos and Szalai (2002) provided some baseline reference velocities for different species for field tree inspection (Table 7.2). This reference velocity can be used to evaluate the actual measured wave velocity and assess the internal condition of the tree inspected.

Figure 7.3 shows the use of a stress wave timer. When measuring TOF across a tree trunk, an inspector should make sure that the start and stop sensor probes are aligned in a horizontal line across the diameter of the trunk. The spike of a sensor probe should penetrate the bark and reach the sapwood so that the probe is securely attached to the trunk. Use a small hammer that is provided along with the stress wave timing device to tap the start sensor probe and obtain several consistent TOF readings.

Figure 7.3—A Fakopp Microsecond Timer (Fakopp Bt., Agfalva, Hungary) was used to inspect a large red oak tree at the University of Wisconsin–Madison campus through a single-path stress wave timing measurement.

Acoustic Tomography

In recent years, tomography techniques that were developed for geophysical engineering and medical applications have been evaluated for their applicability in tree inspection. Investigations on urban trees showed great success using acoustic tomography to detect internal decay hidden from view within the trunks (Nicolotti et al. 2003, Gilbert and Smiley 2004, Wang and Allison 2008, Wang et al. 2009).

Acoustic tomography employs multiple sensors (usually 8 to 32) to measure stress wave transmission time at multiple directions. The distance between the sensors is measured with a caliper scale. An impact-induced stress wave is generated by striking each of the sensor recording points with the hammer. A computer records the time-of-flight of the stress wave to each of the other recording points. Knowing the distance and the TOF data, a velocity can be calculated by the computer. Computer projection software using stress wave data from these multi-path measurements creates an image of the distribution of relative acoustic wave velocity in the cross section.

Figure 7.4 shows the acoustic tomograms obtained from a black cherry tree at 50-, 100-, and 150-cm heights versus corresponding photographic images and 2D hardness maps of the cross sections (Wang et al. 2009). The tomogram in this example is displayed in four colors representing varying recorded velocities. Velocities from lower to higher values are displayed as blue, violet, green and brown. The acoustic shadows in the tomograms are in good agreement with the physical conditions revealed by visual examination and 2D hardness mapping of the cross-sections. This map of the acoustic characteristics of the sample cross section, with accurate interpretation, can determine the size and location of internal trunk decay and defect.

The acoustic tomogram is not a spatially precise map of the internal structure but only a representation of the wood's

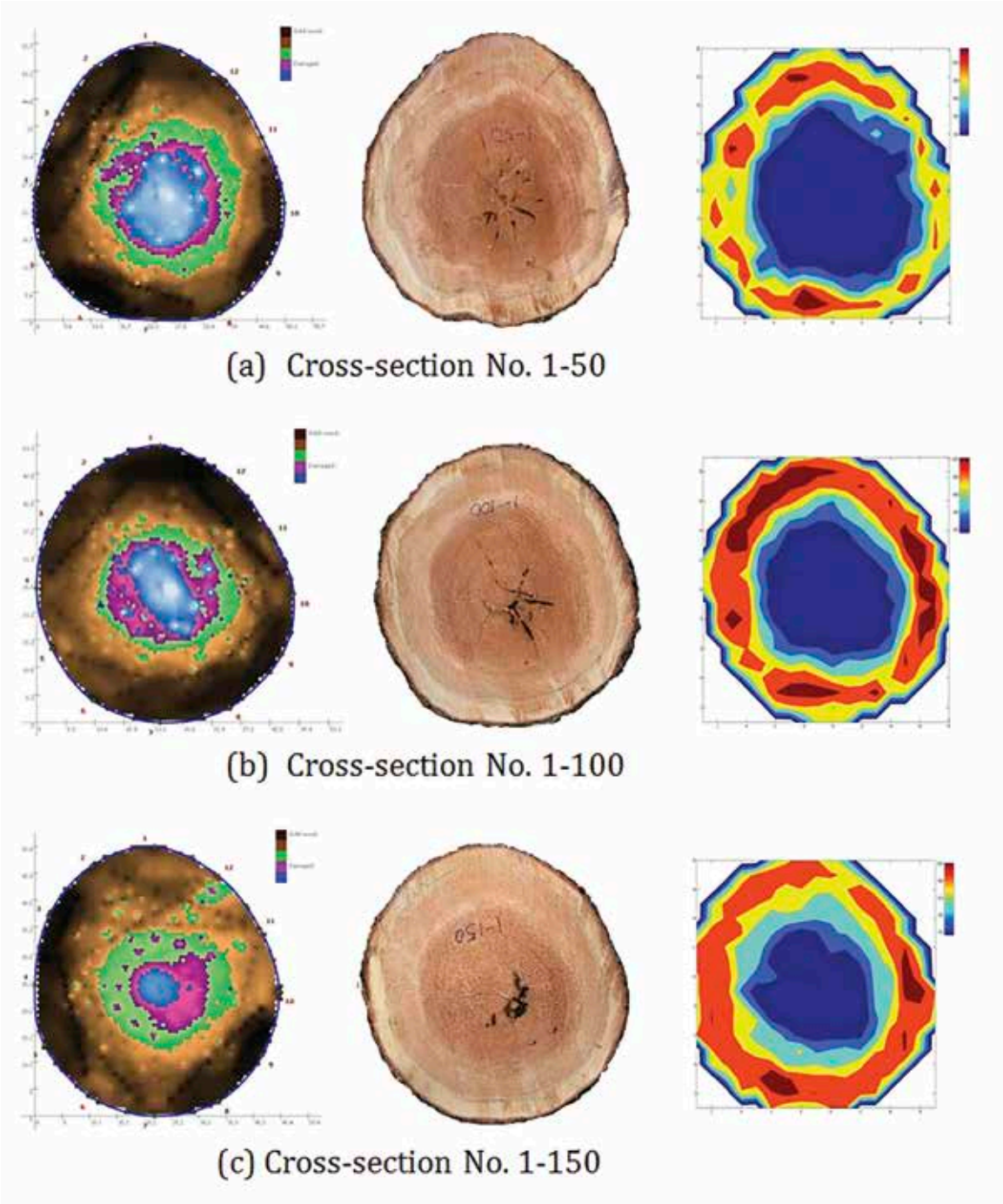

Figure 7.4—Acoustic tomograms of a black cherry tree compared with the photographic images and 2D hardness maps of the cross-sections at different elevations (Wang et al. 2009).

acoustic characteristics as determined by the perceived velocities of the stress waves moving between the sensors. The shape of a tomogram will vary depending upon the type of decay and defect within the trees. Areas of low velocity could be a result of a decay hollow, snake crack, or ring crack. When internal cracks are present in a tree trunk, acoustic tomography tends to overestimate the size of the defect. The acoustic shadows are usually in the form of wide band and its size is significantly greater than the true defect area as indicated in Figure 7.5.

Resistography

The Resistograph (RINNTECH, Heidelberg, Germany) is a portable electric drill with a long, thin metal drill bit. As the micro drill bit (1.5-mm diameter in shaft and 3-mm wide in tip) moves through the wood in a linear path, the penetration resistance along its path is measured and recorded. The denser the wood, the greater the resistance is. Hollows, cracks, and decayed wood with lower density are detected by the reduced resistance to the drill as it progresses through

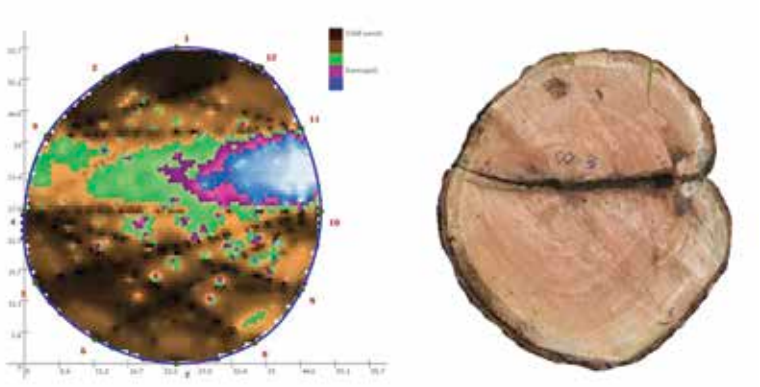

Figure 7.5—Acoustic tomogram and the cross-section image of a black cherry tree with internal crack (Wang et al. 2009).

the wood sample. The pattern of change in density measurements is recorded on scaled graph paper or in a digital representation display.

The Resistograph technique was developed in Germany in the 1980s as a portable tool for tree ring analysis. The first prototype of the resistance-based drilling machine was developed by Kamm and Voss in 1984 employing a spring-loaded recording mechanism (Rinn 2012). The resonance effects of the spring mechanism were later found to lead inaccurate readings and profiles. A study conducted at Hohenheim University (Stuttgart, Germany) and the Environmental Physics Institute Heidelberg University made a breakthrough in the resistance drilling concept and proved that electronic regulation and electronic recording of motor power consumption is able to achieve much more reliable and reproducible resistance profiles than the spring-loaded mechanism (Rinn 1988). Further experiments demonstrated that when the needle's tip was flat and twice the diameter of the shaft, the measured electrical power consumption (EPC) was proportional to the mechanical torque at the needle and it mainly depended on the local density at the point of contact of the drill bit (Rinn 1989, 1990). After thousands of tests, a shaft diameter of 1.5 mm and a 3-mm-wide tip was found to be a good compromise between minimizing damage and maximizing information in the profiles (Rinn 1989, 1990). With this breakthrough and new electronic improvements, the Resistograph tool can now simultaneously measure, display, and record the relative resistance profile through direct measurement of the EPC of a direct-current, needle-rotation motor while a drill bit is driven into the tree.

More research on urban tree decay detection has shown that Resistograph technique is effective in detecting and defining the extent of internal decay, including early stages of decay, if the drilling device is oriented so that its path goes through the decay zone (Wang et al. 2005). However, orienting the drill through the decay is difficult to guarantee. Considering the orientation limitation, Resistograph technique is best suited to confirm and determine the extent of decay in trees after suspect trees are identified by other inspection methods

Figure 7.6—Dr. R. Bruce Allison used rope and saddle techniques to climb an American elm to position him along the trunk crack for Resistograph testing. The goal of the testing was to determine by sampling if there was extensive heartwood decay associated with the crack that could compromise the holding strength of the remaining trunk wound.

such as visual assessment, stress wave timing, or acoustic tomography. Figure 7.6 shows the field use of the Resistograph tool for inspecting an American elm on Forest Products Laboratory property in Madison, Wisconsin.

Tree Decay Inspection Procedure

Based on previous studies and tree inspection practice, Wang and Allison (2008) have developed an effective tree decay inspection procedure that uses a combination of visual assessment, acoustic tools, and micro-drill. The steps of the procedure are the following:

1. Simple screening test using a combination of visual inspection and single-path acoustic wave testing
2. Multi-sensor acoustic tomography to identify the location and approximate magnitude of defects
3. Micro-drill resistance tool to confirm defects or differentiate between decayed wood and internal cracks

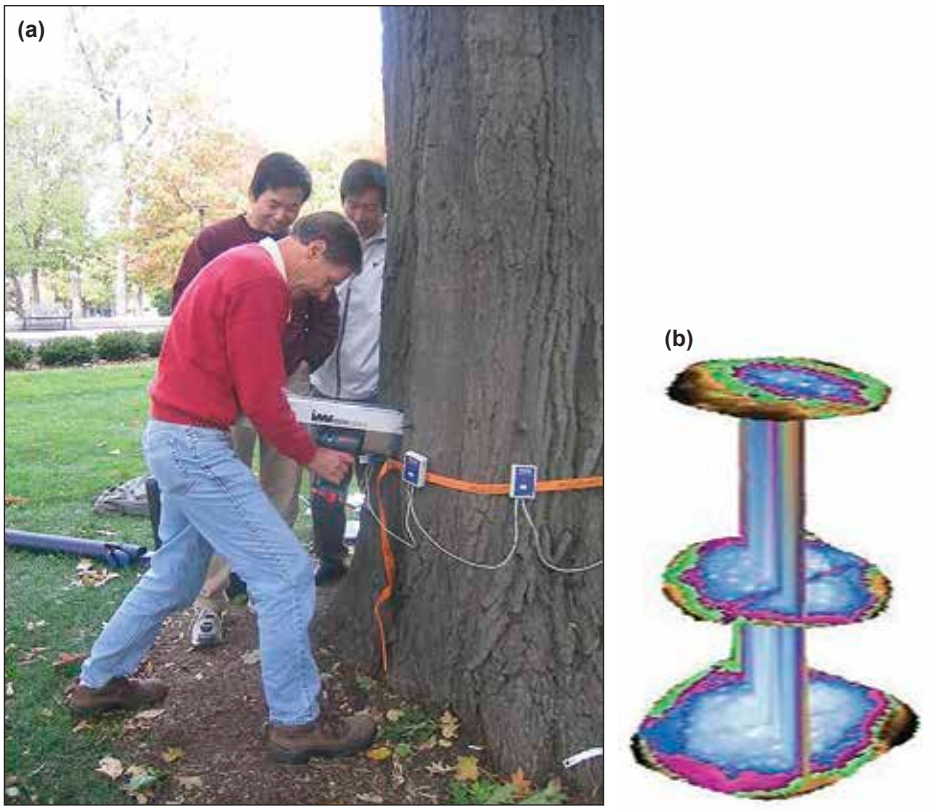

Figure 7.7—Case study in the Capitol Square, Madison, Wisconsin. (a) Decay detection in red oak trees using a combination of visual inspection, acoustic testing, and resistance microdrilling; (b) 3D acoustic tomogram generated by the computer software through combining three tomograms of three different elevations.

Two case studies, one in an urban park and the other in a forest camp ground, illustrate how this tree inspection procedure allows the tree manager to maximize the understanding of a tree's concealed, internal condition.

Case Study 1: Urban Park

A tree stability study was conducted on the 153 trees in the heavily used urban park surrounding the Capitol in Madison, Wisconsin (Allison 2005). The park managers were concerned about tree stability after some tree failures. The Forest Products Laboratory assisted in designing a nondestructive evaluation procedure for detecting internal decay. It started with a visual inspection of all directly and indirectly observable defects.

Next a simple, quick screening test using a single-path acoustic tool was conducted on all of the larger trees' lower trunks. The results were compared to the anticipated stress wave velocities in comparable tree species and were tabulated by Wang et al. (2004).

These tables offer a range of values only. There are no uniform reference standards. Stress wave velocities of solid wood can vary due to moisture levels and tree-growing conditions; therefore conducting a self-reference test on a part of the tree or comparable neighboring tree with known solid wood creates the preferred reference standard. In this study, if the sampled trunk cross section had a velocity reduction greater than 25% of the solid wood reference standard it was judged to have failed the screening test.

Multi-path acoustic tests were then conducted on those select trees with problems indicated by the visual and single-path acoustic tests (Fig. 7.7a). The multi-path acoustic tests generated tomograms requiring interpretation to identify the type, size and location of internal trunk defects. In the case of this 100-year old red oak (*Quercus rubra*) tests at cross section elevations of 10 cm, 100 cm, and 200 cm indicated decay and defect most severe at the root collar level. Tomography software is able to combine the three tomograms creating a 3D representation of the study area on the trunk (Fig. 7.7b). Resistograph test were then performed to verify the exact type and extent of the suspected defects and decay indicated on tomograms. The value of tomograms in those cases was that they identified the best location for the drilling, significantly reducing the number of drills required and enhancing the value of the data acquired. Resistograph testing indicated snake cracking and a large area of heartwood decay at the root collar area of the red oak.

Having carefully progressed using the procedure in gathering and interpreting the data, confidence was established to recommend the removal of this historic and very public tree. Measurements of the defect, knowledge of the way decay interacts with the wood, and understanding the physical requirements for mechanical tree stability led to the conclusion that this tree had a high probability of failure under loading. Tree risk assessment considered both the likelihood of tree failure and the severity of consequences to people, property, or disruption of activity (Dunster et al. 2013). In this frequently occupied public park, large tree failure could be catastrophic. A 300-page report was submitted to the park managers detailing the cases of internal decay and defect revealed using these combined nondestructive testing methods (Allison 2005). Select tree removal and pruning were conducted based on the report's conclusions. Just weeks before the last two trees were to be removed, a violent storm with unusually high velocity winds passed through the capitol park causing these two remaining trees to fail. Of the remaining 143 trees in the park, the only trees to fail were these two that had been identified as high risk using the procedure. Seldom does nature cooperate so fully in validating a procedure for testing tree stability.

Case Study 2: Forest Campground

Another example of the successful use of combined visual, acoustic, and micro-drill decay detection procedure occurred at a recreational ropes course located at the U.S. Forest Service's Camp Nesbit in Upper Michigan (Allison et al. 2008). The recreational course consists of steel cable and ropes attached to a cluster of twelve 60-ft-tall red pines (*Pinus resinosa*). Groups of school children regularly use the course, mounting the high suspended walkways and swinging from ropes. Undetected internal decay within any of the trees has the potential for disastrous consequences. A team of scientists from the U.S. Forest Service Forest Products Laboratory, Michigan Technological University, and the University of Minnesota Duluth were asked to nondestructively evaluate the trees for evidence of internal decay and instability.

First a visual inspection was conducted looking for cavities, cracks, seams, bulges, decay fruiting bodies, carpenter ants, or other evidence of decay activity. Then single-path stress wave tests were conducted on the lower trunks, and with the aid of an aerial lift, at select locations in the upper crown (Fig. 7.8). To establish a standard for stress wave velocities of solid wood in this particular stand, we conducted stress wave tests on red pines known to be without decay or defect. When velocities were at least 25% slower than this standard, the sampled tree failed the screening test.

At those locations where visual inspection and failed acoustic screening test indicated a problem, multi-path acoustic tests were conducted. Tomograms from those tests sites were interpreted to determine an estimate of the type, size, and location of internal decay and defects. Using the acoustic map of the sampled cross section to guide the entry point and direction of the micro-drill, additional crucial data were gathered while minimizing the number of drill holes.

Figure 7.8—Case study at the U.S. Forest Service Nesbit Lake Camp, Sidnaw, Michigan—Visual and nondestructive evaluation of red pines supporting a ropes course.

The use of the less time-consuming visual and single-path acoustic tool as screening tests reduced the use of the multi-sensor tomography test. And by using the tomography to guide the number and direction of the micro-drill, fewer drill holes were needed and more meaningful information was gathered. Single-path stress wave testing in two directions takes less than 5 min, each micro-drill test about the same. Multi-sensor tomograms with set up and measurements requires around 30 min per cross section tested.

Only one of the 12 tested trees was determined to have significant internal decay and was removed from the course. It is important to keep in mind that the mere presence of decay, even extensive decay, is just part of the story in determining whether a tree should be removed. Decay is a critical factor in tree stability because a loss of wood strength occurs as the percentage of decayed stem increases. Researchers have arrived at various formulas to evaluate the strength loss associated with wood decay (Table 7.3). Although useful to consider the possibility of failure, they should not be used as a threshold for tree removal without first considering the actual strength loading factors on the particular tree.

Table 7.3—Common methods to evaluate "strength loss" associated with wood decay (Harris et al. 2004)

Source	Formula[a]	Threshold for action	Comments
Coder 1989	$\left(d^4/D^4\right)\times 100$	20–44% caution >50% hazard	Based on engineering formula for bending stress in a cylinder. Thresholds based on experience.
Wagener 1963	$\left(d^3/D^3\right)\times 100$	33%	Adjusted formula to account for discontinuities in trunks. Applied only to conifers without aggravating defects.
Smiley and Fraedrich 1992	$\frac{d^3 + r\left(D^3 - d^3\right)}{D^3}\times 100$	33%	Modification of Wagener to account for cavity openings. Surveyed 54 fallen and 31 standing trees. Using 33% strength loss as a threshold for action, 50% of fallen and 13% of standing trees would have been removed.
Matteck, Gerhardt, and Breloer 1992	t/R	<0.30	Based on buckling failure in cylinders. Measured t/R for fallen and standing trees. Using a t/R of 0.3 as a threshold for action, 95% of the fallen trees and 35% of the standing trees would have been removed. Based on data, no conclusions can be made on threshold for trees >50 cm (20 in.) in diameter.

[a]Abbreviations: *d*—diameter of decayed wood; *D*—diameter of trunk; *r*—size of cavity opening/circumference of trunk; *t*—width of sound wood; *R*—radius of trunk.

These case studies illustrate that a combination of nondestructive tests, following a procedure of visual inspection then screening with quick single path stress wave tests, then progressing to more complex multi-path acoustic testing as needed with the use of a few directed micro-drill tests to assist in interpretation, offers tree managers an efficient method to measure hidden internal decay and defects in standing trees. Other less frequently used NDT techniques include ground penetrating radar (GPR) (Miller and Doolittle 1990; Nicolotti et al. 2003; Butnor et al. 2009), static pull testing (Peltola et al. 2000; Kane and Clouston 2008), electrical impedance (Gocke et al. 2008), and, on an experimental bases, portable x-ray CT scanning (Allison 2011).

Literature Cited

Allison, R.B. 2005. Capitol park tree structural stability study. Report submitted to Wisconsin Department of Administration Division of Building & Police. Allison Tree Care, Inc. Fitchburg, WI. 308 p.

Allison, R.B. 2011. Acoustic tomography and microdrill resistance density measurements compared to x-ray CT scan on white birch (*Betula papyrifera*). In: Proceedings of the 17th International Nondestructive Testing and Evaluation of Wood Symposium, September14–16, 2011. Sopron, Hungary: University of West Hungary, p. 191–197.

Allison, R.B.; Wang, X.; Ross, R.J. 2008. Visual and nondestructive evaluation of red pines supporting a ropes course in the USFS Nesbit Lake Camp, Sidnaw, Michigan. In: Proceedings of the 15th[t] International Symposium on Nondestructive Testing of Wood. September 10–12, 2007, Duluth, MN. Madison, WI: Forest Products Society. p. 43–48.

Butnor, J.R.; Pruyn, M.L.; Shaw, D.C.; Harmon, M.E; Mucciardi, A.N.; Ryan, M.G.. 2009. Detecting defects in conifers with ground penetrating radar: applications and challenges. Forest Pathology. 39: 309–322.

Divos, F.; Szalai, L. 2002. Tree evaluation by acoustic tomography. In: Proceedings of the 13th International Nondestructive Testing of Wood Symposium, August 19–21, 2002. Berkeley, CA. Madison, WI: Forest Products Society. p. 251–256.

Dunster, J.A.; Smiley, E.T.; Matheny, N.; Lilly, S. 2013. Tree risk assessment manual. Champaign, Illinois: International Society of Arboriculture.

Gilbert, E.A.; Smiley, E.T. 2004. Picus sonic tomography for the quantification of decay in white oak (*Quercus alba*) and hickory (*Carya* spp.). Journal of Arboriculture. 30: 277–280.

Gocke, L.; Rust, S.; Weihs U.; Gunther, T.; Rucker, C. 2008. Combining sonic and electrical impedance tomography for non-destructive testing of trees. In: Proceedings of the 15th International Symposium on Nondestructive Testing of Wood. September 10–12, 2007, Duluth, MN. Forest Products Society, Madison, Wisconsin. p. 31–42.

Hayes, E. 2001. Evaluating tree defects: a field guide. Safetrees. ISBN-10: 0971412804. 30 p.

Kane, B; Clouston, P. 2008. Tree pulling tests of large shade trees in the Genus Acer. Arboriculture and Urban Forestry. 34(2): 101–109.

Luley, C.J. 2005. Wood decay fungi: common to urban living trees in the Northeast and Central United States. Naples, NY: Urban Forestry, LLC. 58 p.

Mattheck C. 1996. Body language of trees: a handbook for failure analysis. Research for Amenity Trees. London: Stationery Office Books (TSO). ISBN-10: 0117530670. 260 p.

Mattheck, C.G.; Bethge, K.A. 1993. Detection of decay in trees with the Metriguard Stress Wave Timer. Journal of Arboriculture. 19(6): 374–378.

Miller, W.F.; Doolittle, J.A. 1990. The application of ground-penetrating radar to detection of internal defect in standing trees. In: Proceedings of the 7th International Nondestructive Testing of Wood Symposium, September 27–29, 1990. Pullman, Washington: Washington State University. p. 263–274.

Nicolotti, G.; Socco, L.V.; Martinis, R.; Godio, A.; Sambuelli, L. 2003. Application and comparison of three tomographic techniques for the detection of decay in trees. Journal of Arboriculture. 29: 66–78.

Pellerin, R.F.; Ross, R.J. eds. 2002. Nondestructive evaluation of wood. Madison, WI: Forest Products Society.

Pellerin, R.F.; DeGroot, R.C.; Esenther, G.R. 1985. Nondestructive stress wave measurements of decay and termite attack in experimental wood units. In: Proceedings, 5th International Symposium on Nondestructive Testing of Wood, September 9–11, 1985, Pullman, WA. Pullman, WA: Washington State University. p. 319–353.

Peltola, H.; Kellomaki, S.; Hassinen, A.; Granader, M. 2000. Mechanical stability of Scots pine, Norway spruce, and birch: An analysis of tree-pulling experiments in Finland. Forest Ecology and Management. 135:143–153.

Rinn, F. 1988. A new method for measuring tree-ring density parameters. Physics diploma thesis, Institute for Environmental Physics, Heidelberg University. 85 p.

Rinn, F. 1989. A new drilling method for wood inspection. Holz Zentralblatt. 34: 529–530.

Rinn, F. 1990. Device for material testing, especially wood, by drill resistance measurements. German Patent 4122494.

Rinn, F. 2012. Basics of typical resistance-drilling profiles. Western Arborist. Winter: 30–36.

Shigo, A.L. 1979. Tree decay: An expanded concept. United States Department of Agriculture Forest Service Information Bulletin Number 419. Washington, DC.

Shigo, A.L. 1984. Compartmentalization: A conceptual framework for understanding how trees grow and defend themselves. Annual Review of Phytopathology. 22 (1): 189–214.

Wang, X.; Divos, F.; Pilon, C.; Brashaw, B.K.; Ross, R.J.; Pellerin, R.F. 2004. Assessment of decay in standing timber using stress wave timing nondestructive evaluation tools–A guide for use and interpretation. Gen. Tech. Rep. FPL–GTR–147. Madison, WI: U.S. Department of Agriculture, Forest Service, Forest Products Laboratory. 12 p.

Wang, X.; Wiedenbeck, J.; Ross, R.J.; Forsman, J.W.; Erickson, J.R.; Pilon, C.; Brashaw, B.K. 2005. Nondestructive evaluation of incipient decay in hardwood logs. Gen. Tech. Rep. FPL–GTR–162. Madison, WI: U.S. Department of Agriculture, Forest Service, Forest Products Laboratory. 11 p.

Wang, X.; Allison, R.B. 2008. Decay detection in red oak trees using a combination of visual inspection, acoustic testing, and resistance microdrilling. Arboriculture & Urban Forestry. 34(1): 1–4.

Wang, X.; Wiedenbeck, J.; Liang, S. 2009. Acoustic tomography for decay detection in black cherry trees. Wood and Fiber Science. 41(2): 127–137.

Weber, K.; Mattheck C. 2003. Manual of wood decays in trees. Gloucestershire, UK: Arboricultural Association. 127 p.

Additional Source of Information

Harris, R.W.; Clark, J.R.; Matheny, N.P. 2004. Arboriculture: Integrated management of landscape trees, shrubs, and vines. Pearson Education, Inc., Upper Saddle River, New Jersey.

Chapter 8

Acoustic Assessment of Wood Quality in Trees and Logs

Xiping Wang, Research Forest Products Technologist
Forest Products Laboratory, Madison, Wisconsin

Peter Carter, Chief Executive Officer
Fibre-gen, Auckland, New Zealand

Assessing the quality of raw wood materials has become a crucial issue in the operational value chain as forestry and the wood processing industry are increasingly under economic pressure to maximize extracted value. A significant effort has been devoted toward developing robust nondestructive evaluation (NDE) technologies capable of predicting the intrinsic wood properties of individual trees, stems, and logs and assessing the value of stands and forests. Such technologies can help foresters make wise management decisions and grow higher quality wood and can lead to greater profitability for the forest industry.

Acoustic technologies have been well established as material evaluation tools in the past several decades, and their use has become widely accepted in the forest products industry for on-line quality control and products grading (Schad et al. 1995; Pellerin and Ross 2002; Ross et al. 2004). Recent research developments on acoustic sensing technology offer further opportunities for wood manufacturers and forest owners to evaluate raw wood materials (standing trees, stems, and logs) for general wood quality and intrinsic wood properties. This provides strategic information that can help make economic and environmental management decisions on treatments for individual trees and forest stands, improve thinning and harvesting operations, and efficiently allocate timber resources for optimal utilization. For example, the information could be used to sort and grade trees and logs according to their suitability for structural applications and for a range of fiber properties of interest to paper makers. Another example is to determine the relationships between environmental conditions, silvicultural treatments, and wood fiber properties so that the most effective treatment can be selected for desired fiber quality in future plantations.

Today, the precision of acoustic technology has been improved to the point where tree quality and intrinsic wood properties can be predicted and correlated to the performance of final products. With continuous advancements and refinements, this technology could assist in managing wood quality, assessing forest value, and improving timber quality of future plantations.

Background

Traditionally, the quality of trees, stems, and logs has been assessed through simple physical measurements (height/length, diameter, taper, and sweep) and human visual observation of surface characteristics (size and distribution of knots, wounds, and other defects). Assignment to one of several possible grades is based on simple, broad, allowable ranges for physical features. Although these grades may be sufficient where appearance is the primary consideration, the adequacy of visual grades for applications involving stiffness and strength is questionable because no measure of these properties is actually obtained. A concern over reliability and the broad conservative design values associated with visual grades for structural applications led to the development of machine strength rating (MSR) technology for lumber, which uses a pre-established relationship between stiffness and bending strength to define a set of strength-based lumber grades (FPS 1997; Galligan 2002). This provides a more refined and flexible approach than visual grading for identifying and sorting lumber into stress grades used in products such as structural framing, glued-laminated timber (glulam), and engineered trusses.

With the development and rapid growth of new engineered wood products such as laminated veneer lumber (LVL), I-beams, and I-joists, there has been a parallel growth in nondestructive testing for stiffness and strength of lumber and veneer used as components of these products. In addition, concerns with design values of structural lumber graded with visual methods are creating demand for stiffness verification of visually graded lumber. These trends have renewed interest of mills in nondestructive testing and evaluation methods. Mills seeking to capture a price premium by producing nondestructively tested lumber and veneer find that it is very expensive to process logs or purchase timber stands that have low yields of product with the stiffness and strength levels desired by their customers. Consequently, researchers have developed technology for applying acoustic methods to measure stiffness of logs and trees and improve sorting and matching with desired levels of lumber or

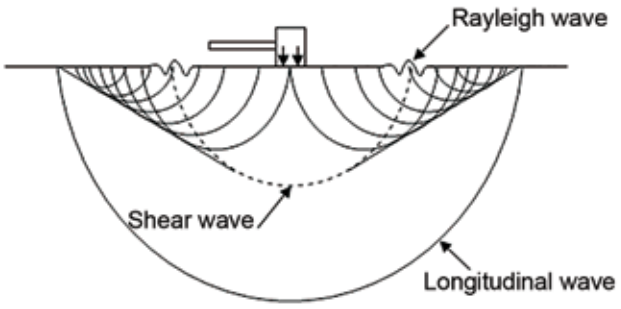

Figure 8.1—Types of stress waves in semi-infinite elastic material.

Figure 8.2—Longitudinal waves traveling in a long, slender material as compression and tension waves.

veneer stiffness (Aratake et al. 1992; Aratake and Arima 1994; Wang 1999; Harris and Andrews 1999; Huang 2000; Addis et al. 2000a,b; Wang et al. 2001, 2002; Harris et al. 2003; Andrews 2003). The research has led to the development and introduction of a series of acoustic tools that allow rapid assessment of wood resource quality at early stages of the operational value chain.

Fundamentals of Acoustic Wave Propagation in Wood

When stress is applied suddenly to the surface of wood, the disturbance that is generated travels through the wood as stress waves. In general, three types of waves are initiated by such an impact: (1) longitudinal wave (compressive or P-wave), (2) shear wave (S-wave), and (3) surface wave (Rayleigh wave) (Fig. 8.1). A longitudinal wave corresponds to the oscillation of particles along the direction of wave propagation such that particle velocity is parallel to wave velocity. In a shear wave, the motion of the particles conveying the wave is perpendicular to the direction of the propagation of the wave itself. A Rayleigh (surface) wave is usually restricted to the region adjacent to the surface; particles move both up and down and back and forth, tracing elliptical paths. Although most energy resulting from an impact is carried by shear and surface waves, the longitudinal wave travels the fastest and is the easiest to detect in field applications (Meyers 1994). Consequently, the longitudinal wave is by far the most commonly used wave for material property characterization.

One-Dimensional Wave Equation

A basic understanding of the relationship between wood properties and longitudinal wave velocity (hereafter referred to as wave velocity) can be acquired from fundamental wave theory. In a long, slender, isotropic material, strain and inertia in the transverse direction can be neglected and longitudinal waves propagate in a plane waveform (wave front) (Fig. 8.2). In this case, the wave velocity is assumed to be independent of Poisson's ratio and is given by the following equation (hereafter referred to as a one-dimensional wave equation):

$$C_0 = \sqrt{\frac{E}{\rho}} \tag{8.1}$$

where C_0 is longitudinal wave velocity, E is longitudinal modulus of elasticity, and ρ is mass density of material.

Three-Dimensional Wave Equation

In an infinite or unbounded isotropic elastic medium, a triaxial state of stress is present. The wave front of the longitudinal wave propagating through such a medium is no longer a plane. The wave propagation is governed by the following three-dimensional longitudinal wave equation (Meyers 1994):

$$C = \sqrt{\frac{1-\nu}{(1+\nu)(1-2\nu)}\frac{E}{\rho}} \tag{8.2}$$

where C is longitudinal wave velocity in unbounded medium and v is Poisson's ratio of the material. To differentiate from the longitudinal wave velocity in a slender rod, we will use the term "dilatational wave" for unbounded medium. The wave velocity is dependent on density and two elastic parameters, modulus of elasticity (MOE) and Poisson's ratio (v).

Wave Propagation in Logs and Standing Trees

The direct application of fundamental wave equations in wood, particularly in standing trees and logs, has been complicated by the fact that wood is neither homogeneous nor isotropic. Wood properties in trees and logs vary from pith to bark as wood transforms from juvenile wood to mature wood. Properties also change from butt to top within a tree and differ between trees. Genetics, soil conditions, and environmental factors all affect wood characteristics in both microscopic and macrostructure levels.

In spite of these natural variations, studies have shown that the one-dimensional wave equation is adequate to characterize the wave propagation behavior in logs that are in a long, slender form (Wang et al. 2004; Wang 2013). The modulus of elasticity of the logs predicted by this fundamental equation generally has a high accuracy. Consequently, log grading or sorting using acoustic wave technology has been very effective and widely adopted in the forest and wood processing industries.

For standing trees, the acoustic measurement approach is completely different from that in logs. Because there is no

access to an end surface (in contrast to a log) in a standing tree, acoustic waves have to be introduced from the side surface of the trunk, which results in a nonuniaxial stress state in the stem. The one-dimensional wave equation is therefore no longer valid for trees. If the dilatational wave is considered for acoustic measurement in standing trees, Poisson's ratio (v) of wood is needed to describe the relationship between wave velocity and modulus of elasticity, as shown in Eq. (8.2). Dilatational wave velocity is generally higher than C_0 (Eq. (8.1)) (Meyers 1994; Wang et al. 2007). As Poisson's ratio increases, the deviation of dilatational wave velocity from C_0 gets larger. For instance, the ratio of dilatational wave velocity to C_0 is 1.16 for $v = 0.30$. The velocity ratio becomes 1.46 as v increases to 0.40.

The Poisson's ratio of green wood is not explicitly known. Bodig and Goodman (1973) and other investigators obtained Poisson's ratios through plate or compression testing for dry wood. Poisson's ratio appears to change with species and material sources. However, statistical analysis by Bodig and Goodman (1973) indicated that Poisson's ratios do not seem to vary with density or other anatomical characteristics of wood in any recognizable fashion. Therefore, an average value of 0.37 (v_{LR}) has been suggested for both softwoods and hardwoods (Bodig and Goodman 1973; Bodig and Jayne 1982). This could translate into a dilatational wave velocity that is 1.33 times that of the one-dimensional longitudinal wave velocity, which is apparently in agreement with previous experimental results (Andrews 2003; Wang et al. 2001).

Acoustic Measurements in Trees and Logs

The use of longitudinal acoustic wave techniques for wood quality assessment is based on accurate measurement of propagation velocity of a stress wave generated by a mechanical impact. The success of any field application of this technique is directly related to understanding stress-wave behavior in wood materials and the physical and geometrical characteristics of wood itself. Wood, in the form of trees and logs, tends to have variable external and boundary conditions that create technical challenges for measuring acoustic velocities. This is particularly true in trees, where a stress wave has to be initiated from the surface of the trunk, and acoustic sensors need to be attached to the trunk through spikes (probes).

Trees—Time-of-Flight-Based Approach

A typical approach for measuring acoustic velocity in trees involves inserting two sensor probes (transmit probe and receiver probe) into the sapwood and introducing acoustic energy into the tree through a hammer impact on the transmit probe. The time-of-flight (TOF) is the time taken for the stress wave to travel from the transmit probe to the receiver probe. Acoustic velocity is subsequently calculated from the span between the two sensor probes and the TOF measure using

$$C_T = \frac{S}{\Delta t} \tag{8.3}$$

where C_T is tree acoustic velocity (m/s), S is distance between the two probes (sensors) (m), and Δt is TOF.

During field acoustic measurement, the probes are inserted into the tree trunk (probes are inserted through bark and cambium to extend into the sapwood) and aligned within a vertical plane on the same face (Fig. 8.3). The lower probe is placed about 40 to 60 cm above the ground. The span between the probes is determined from a practical standpoint, typically in the range 1.0–1.2 m; the probes need to be positioned at a comfortable height for the person who takes the measurements.

Logs—Resonance-Based Approach

Acoustic velocities in logs and long stems of known length are typically measured using a resonance-based approach. In log acoustic measurement, an acoustic sensor is mounted or held on one end of a log (Fig. 8.4). A stress wave is initiated by a mechanical impact on the same end, and the stress waveforms are subsequently recorded by an electronic unit. This acoustic approach is based on the observation of hundreds of acoustic pulses resonating longitudinally in a log and provides a weighted average acoustic velocity. Most resonance-based acoustic tools have a built-in fast Fourier transformation (FFT) program that can analyze and output the natural frequencies of the acoustic signals. Log acoustic velocity is then determined from

$$C_L = 2 f_0 L \tag{8.4}$$

where C_L is acoustic velocity of logs (m/s), f_0 is fundamental natural frequency of an acoustic wave signal (Hz), and L is log length (end-to-end) (m).

The resonance-based acoustic method is a well-established nondestructive evaluation (NDE) technique for measuring long, slender wood members such as logs, poles, and timber (Harris et al. 2003; Andrews 2003; Wang et al. 2004). The inherent accuracy and robustness of this method provide a significant advantage over TOF measurement in applications such as log measurement. In contrast to the TOF approach, the resonance method stimulates many, possibly hundreds, of acoustic pulse reverberations in a log, resulting in a very accurate and repeatable velocity measurement. Because of this accuracy, the acoustic velocity of logs obtained by the resonance-based measurement has served as a standard to validate the TOF measurement in standing trees (Wang et al. 2001; Andrews 2003; Carter et al. 2005).

Assessing Wood Quality of Logs

It is well recognized that the variation in wood and fiber properties is enormous within any pile of logs that has been

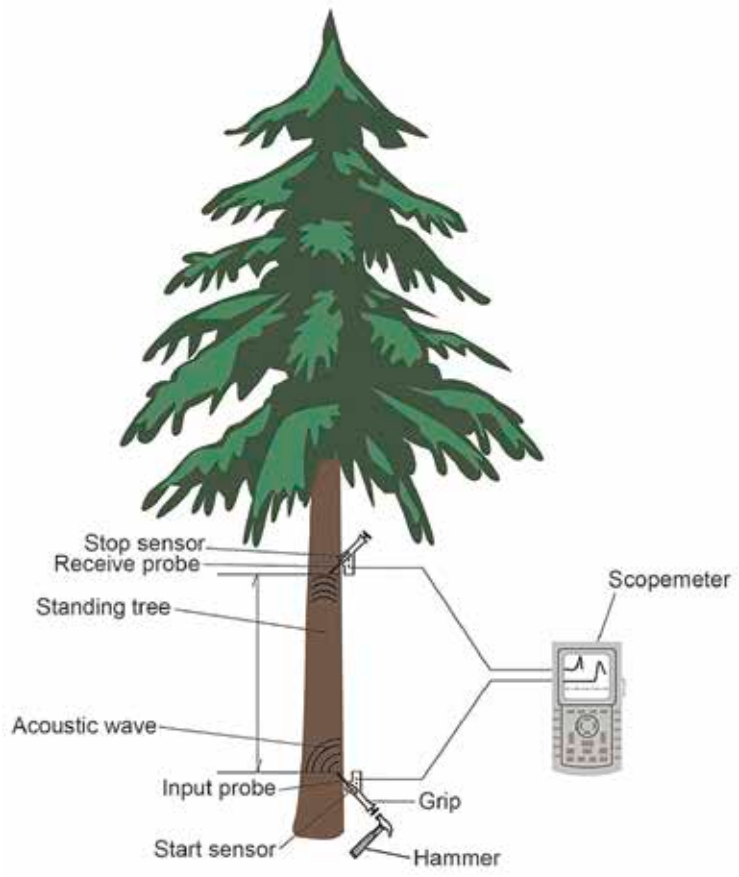

Figure 8.3—Acoustic measurement on standing trees.

Figure 8.4—Resonance acoustic measurement on a log.

visually sorted for similar grade. The same is true for logs from trees of the same age and from the same forest stand (Huang et al. 2003). Dyck (2002) reinforced this view by stating "All logs are different even if they are clonal and even if they come from the same tree." As an example, Figure 8.5 shows the acoustic velocity of a large sample of similar logs from two geographically distinct radiata pine forests in New Zealand, demonstrating the large variability in intrinsic wood properties of the logs (Andrews 2000). Clearly, there are major commercial benefits to be gained by assessing wood properties at the log level and optimizing the use of resource through appropriate log sorting and processing.

The ability to improve log sorting with resonance-based acoustic methods has been well recognized in the forest products industry (Walker and Nakada 1999; Harris et al. 2003; Huang et al. 2003; Carter and Lausberg 2003; Wang et al. 2002, 2004). This technology is based on the observation of hundreds of acoustic pulses resonating longitudinally in a log and provides an acoustic velocity dependent on the weighted average wood properties and moisture status of the log. Because the MOE of the log is simply equal to the density times the acoustic velocity squared, the technology is basically measuring fiber properties that influence macro properties such as stiffness, strength, and stability. The challenge is to interpret what the log is "saying" and translate this information into meaningful values (Dyck 2002).

Sorting Logs for Lumber Quality

Research has shown that log acoustic measures can be used to predict the strength and stiffness of structural lumber that would be produced from a log (Aratake et al. 1992; Aratake and Arima 1994; Ross et al. 1997; Iijima et al. 1997; Wang 1999; Wang and Ross 2000). In the early 1990s, scientists in Japan did some pioneering research exploring the possibility of using the natural frequency of longitudinal compression waves in a log to predict the strength and stiffness of the structural timbers (Aratake et al. 1992; Aratake and Arima 1994). They succeeded in identifying close relationships

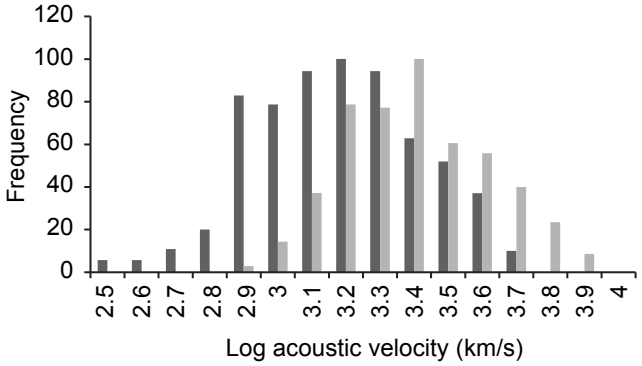

Figure 8.5—The acoustic velocity (km/s) of a large sample of similar logs from two geographically distinct radiata pine forests in New Zealand, demonstrating the large variability in the intrinsic wood properties of the logs (Andrews 2000).

between the fourth resonant frequency of the logs and MOE and modulus of rupture (MOR) of the scaffolding boards and square timbers cut from the log. Years later, a trial study in the United States also revealed a good correlation between acoustic-wave-predicted MOE and mean lumber MOE (Ross et al. 1997). This research opened the way for acoustic technology to be applied in mills for sorting logs and stems for structural quality.

To validate the usefulness of the resonance acoustic method for a practical log sorting process, Wang and Ross (2000) conducted a mill study and examined the effect of log acoustic sorting on lumber stiffness and lumber E-grades. After acoustically testing 107 red maple logs, they sorted the logs into four classes according to acoustic velocity. Figure 8.6 illustrates the average lumber MOE for each log class, with a significant differentiation and clear trend between the log acoustic classes. They further compared log acoustic classes to lumber E-grades and found a good relationship between them. Logs that have a high acoustic velocity contain higher proportions of high-grade lumber. A study in New Zealand revealed similar results when presorting untested logs of radiata pine into three acoustic classes (Addis et al. 1997). The logs with the highest acoustic velocity (the top 30%) produced timber that was 90% stiffer than that from the group with the lowest velocity (the bottom 30%).

In a practical log-sorting process, the industry can achieve benefits by developing a sorting strategy based on the log sources and desired end products. Currently, companies implementing acoustic sorting strategies measure only the velocity of acoustic waves and segregate logs into velocity groups using predetermined cut-off velocity values. Appropriate cut-off acoustic velocity values can be determined for either selecting the highest quality logs for superior structural applications or isolating the low grade logs for nonstructural uses.

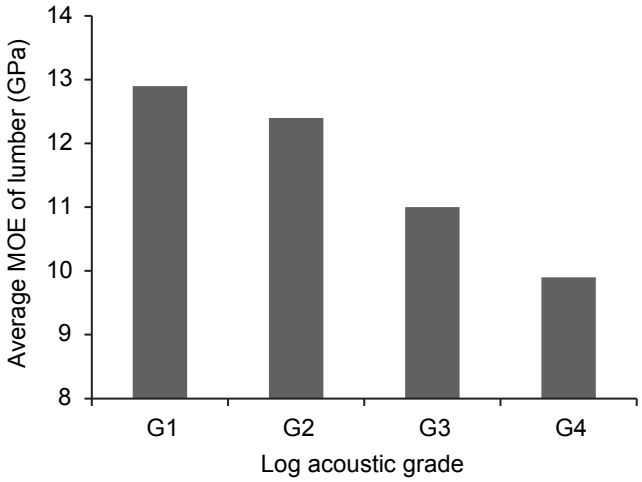

Figure 8.6—Relationship between log acoustic grade and average MOE of lumber (Wang and Ross 2000).

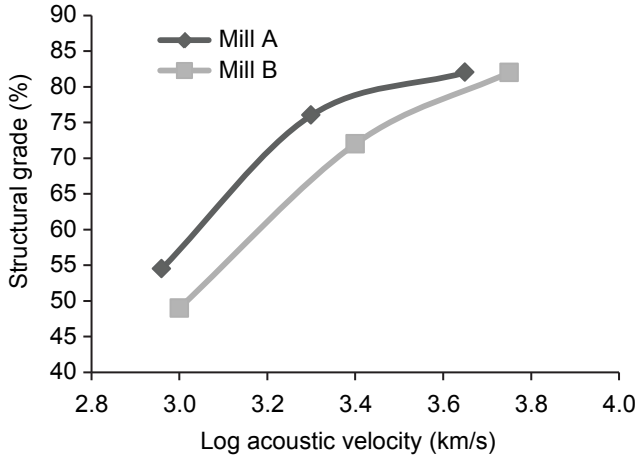

Figure 8.7—Relationship between log acoustic velocity and yield of structural grades of lumber for two New Zealand radiata pine sawmills (Carter et al. 2005).

Figure 8.7 demonstrates the increasing yield of structural grades of lumber with increasing acoustic velocity of logs processed, as measured at two New Zealand radiata pine sawmills. Assuming a price differential of NZ$200/m^3 (value estimated in 2004) between structural and nonstructural lumber, an increase in average log acoustic velocity of 0.1 km/s produces an increase in structural lumber yield of about 5%. This translates into a gain of about NZ$6/m^3 on log volume or about NZ$1.8 million for a mill processing 300,000 m^3 of logs per year.

Sorting Logs for Veneer Quality

Log acoustic measurement has also been successfully used to assess the quality of veneer obtained from logs. Figure 8.8 illustrates the relationship between acoustic velocity for Southern Pine log batches (10 percentile groups from log sample) and the average ultrasound propagation time (UPT)

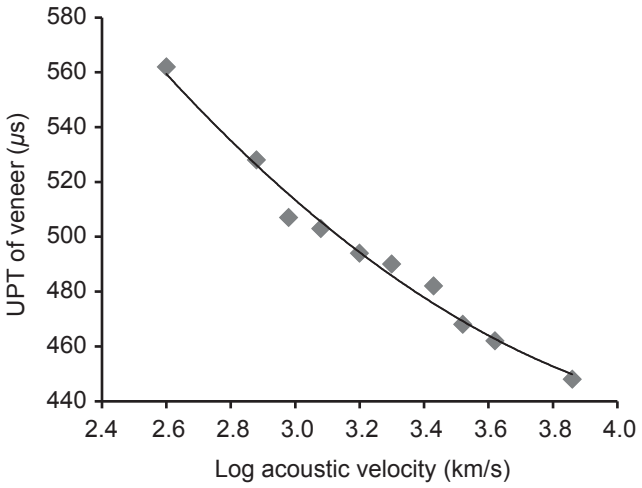

Figure 8.8—Relationship between acoustic velocity of Southern Pine log batches and the average ultrasound propagation time (UPT) of veneer from the logs (Carter et al. 2005).

of veneer peeled from the logs. UPT is the elapsed time for ultrasound to travel longitudinally within the veneer sheet between fixed roller wheel points on the Metriguard veneer tester.

Several trials have been run in New Zealand to quantify the effectiveness of acoustic sorting strategy and potential value gains from segregation of logs for veneer production (Carter and Lausberg 2003). Typical results show that for Central North Island logs segregated into three classes, the high stiffness logs resulted in production of 52% premium high stiffness veneer product, compared with unsegregated logs at 24%. These results clearly show that segregation using acoustics results in substantially higher proportions of higher stiffness veneer being produced. Equally, if a higher grade out turn is required for plywood veneer production, log segregation with acoustics will result in a value gain. An economic analysis of sorting veneer logs for LVL production in the United States resulted in a gain of about US$16/m^3 on log volume (about $80–$100 per thousand board feet Scribner log scale) (Carter et al. 2005).

Sorting Logs for Pulp and Paper Quality

One challenge that paper mills face is to quantify the quality of pulp logs going into the mill. Unlike saw logs that are used to produce structural lumber and veneer, quality specification for pulp logs deals with fiber characteristics, especially fiber length. Without appropriate sorting technologies to help "see through" individual logs for internal fiber quality, buyers or producers of pulp logs will not be able to know if logs meet the quality specifications for the product out turn. If unsorted, the below-specification logs must be processed along with the in-specification logs. This results in pulp and paper products of variable quality, depending on the proportion of below-specification logs entering the mill process at any time and the extent to which they depart from the specified quality (Albert et al. 2002).

Similar to sorting saw logs for improving structural uses, acoustic technology could be used in pulp and paper mills to segregate pulp wood for pulp and paper manufacture. Albert et al. (2002) tested the hypothesis that acoustic measures of pulp logs are linked to fiber characteristics and paper properties. In a trial with 250 radiata pine peeler cores, they sorted the cores into 18 classes using acoustic velocity. Subsequent chemical pulping and testing demonstrated that fiber length, wet strength, and various handsheet properties varied systematically. The acoustic velocity of the peeler cores was found to be strongly related to the length-weighted fiber length and the wet zero-span tensile strength of the fibers from the peeler cores. Two follow-up studies carried out in New Zealand were summarized by Clark et al (2003). In the first study, the velocity of sound was measured in each of 250 small-diameter radiata pine logs (120–420 mm large-end diameter), the logs were segregated into one of four groups based on velocity, the logs in each group were chipped, each chip sample was then chemically pulped, and the resultant pulps were evaluated. This study confirmed the relationship between a range of fiber properties and whole log acoustic velocity. The second study involved 5,000 radiata pine logs segregated into three acoustic velocity based groups and pulped through a commercial continuous digester. Resulting pulp characteristics are shown in Figures 8.9 to 8.11, and the conclusion was that acoustics offers a means of sorting pulp logs and this study demonstrates that commercially useful separations can be obtained.

Mechanical pulp properties were evaluated in another mill study with 2,247 radiata pine logs. Bradley et al. (2005) confirmed that acoustics could be used to segregate logs into groups that perform very differently in terms of pulp properties when refined to a given freeness or at a certain energy input. At a given target freeness, there was a 20% difference in energy requirement between the lowest and highest velocity logs for a given specific energy. They conclude that acoustic sorting and subsequent reblending has great potential to reduce fluctuations in pulp quality of the mill output.

Monitoring Moisture Changes in Log Stocks

A further application of acoustic methods has been identified for monitoring changes in moisture content of freshly harvested logs from as high as 150% down to an air-dry state of 30% to 40%. Moisture content (MC) is important for fuel wood supplies to determine at what stage a log should be chipped and burned, as well as for certain mechanical and semi-chemical pulping processes where MC is critical for effective processing. Traditional sampling methods are cumbersome and time consuming, and there is no convenient portable tool capable of measuring MC at these levels because standard electrical conductivity or impedance methods become inaccurate at MCs above fiber saturation

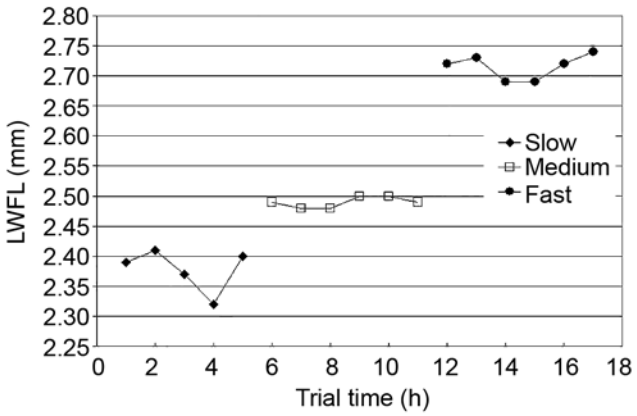

Figure 8.9—Chronological plot of pulp fiber length as each log group was processed (Clark et al. 2003).

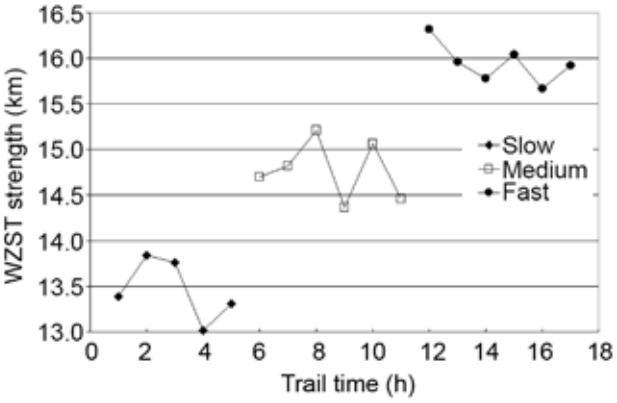

Figure 8.10—Chronological plot of pulp WZST strength as each log group was processed (Clark et al. 2003).

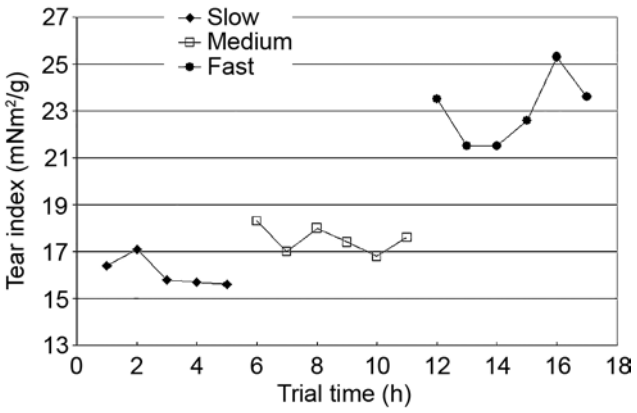

Figure 8.11—Chronological plot of pulp tear strength as each log group was processed (Clark et al. 2003).

point. Yet the defined relationship between acoustic velocity and green density enables the evaluation of changes in density caused by loss of moisture simply by monitoring the average increase in acoustic velocity that is observed as MC and associated green density decline with time.

Results are currently being evaluated (Foulon 2006) but look very encouraging for the emerging fuel wood sector in the United Kingdom where they need to measure and manage moisture content of log stockpiles because generating companies do not want to chip and burn wood above 40% to 55% MC (dry basis). The acoustic-based procedure has the following steps for monitoring the increase in velocity as green density declines:

- Establish a definitive MC start point using the traditional lab-based sampling method
- Mark a sample of logs within the log stack
- Measure acoustic velocities using a portable acoustic tool
- Remeasure acoustic velocities at any later date
- Compare average velocity increase, which defines loss of water such that reduction in green density is proportional to increase in velocity squared

Acoustic Verification of Log Supply for Visually Graded Lumber

The introduction of Verified Visual Grading (VVG) in New Zealand has been the response to variability in the design strength of visually graded lumber, typical of younger plantation-grown softwood resources around the world. Following an extensive consultation process, new standards and building regulations were introduced in New Zealand in 2006 with full compliance required by early 2007. According to the new standards, all visually graded lumber became subject to a sample proof test (1 in 1,000 pieces of lumber). A 30-sample rolling average must exceed the requirements for MOE and MOR, meeting both average and minimum standards. An implication of these new VVG standards is that the stiffness of log supply becomes even more critical to ensure that suitable logs are processed to meet end-of-line proof testing standards. Otherwise, structural lumber is cut and processed at significant cost, only to find that it does not meet end-of-line stiffness standards. Acoustic tools provide valuable guidance and decision support for the forest and wood processing sector to meet these new standards.

Assessing Wood Quality of Standing Trees

A logical and desirable extension from log acoustic assessment is to apply the technology to measure wood properties in standing trees, thereby providing timber sellers and purchasers with a means for improved harvest scheduling and timber marketing based on the potential yield of stress-graded products that can be obtained from trees within a stand.

The applicability of using acoustic waves to assess intrinsic wood properties of standing trees has been validated by many researchers around the world (Nanami et al. 1992a,b, 1993; Wang 1999; Ikeda and Kino 2000; Huang 2000; Wang

et al. 2001, 2005; Lindstrom et al. 2002). A typical approach for measuring acoustic velocity in standing trees involves inserting two sensor probes (transmit probe and receiver probe) into the sapwood and introducing acoustic energy into the tree through a hammer impact. Unlike the resonance method, which obtains the weighted average velocity by analyzing whole wave signals transmitted between the ends of a log, the standing tree acoustic tool measures TOF for a single pulse wave passing through the tree trunk from transmit probe to receiver probe.

Measuring Wood Properties of Standing Trees

Several trial studies aimed at proving the acoustic concept for measuring acoustic velocity and wood properties of standing trees have been conducted in the United States and New Zealand (Wang et al. 2005). A total of 352 trees were tested in 2003 and 2004. The species tested included Sitka spruce (*Picea sitchensis*), western hemlock (*Tsuga heterophylla*), jack pine (*Pinus banksiana*), ponderosa pine (*Pinus ponderosa*), and radiata pine (*Pinus radiata*). The trial data showed a good linear correlation between tree velocity and log velocity for each species tested. The relationship is characterized by the coefficient of determination (R^2) in the range of 0.71 and 0.93. However, further analysis revealed a skewed relationship between tree acoustic measurement and log acoustic measurement. Observed tree velocities were found significantly higher than log velocities. The results support the hypothesis that TOF measurement in standing trees is likely dominated by dilatational or quasi-dilatational waves rather than one-dimensional plane waves, as in the case of logs.

Because of the significant deviation in velocity and the skewed relationship between tree and log measurements, tree velocity measured by the TOF method needs to be interpreted differently when assessing wood properties of standing trees. To make appropriate adjustments on observed tree velocities, Wang et al. (2005) developed two models (multivariate regression model and dilatational wave model) for the species evaluated in those trials. As an example, Figure 8.12 shows the relationship between tree velocities adjusted through a multivariate regression model and log velocities. Their results indicated that both the multivariate regression model and dilatational wave model were effective in eliminating the deviation between tree and log velocity and reducing the variability in velocity prediction.

With simple velocity measurements, individual trees and stands can be evaluated and sorted for their structural quality and stumpage value. In a series of studies evaluating tree quality in terms of structural performance, Ikeda and Kino (2000) found highly significant correlations between tree velocity and MOE of logs and square sawn timbers. Through several mill trials, Huang (2000) demonstrated that trees with the potential to produce high and low stiffness lumber

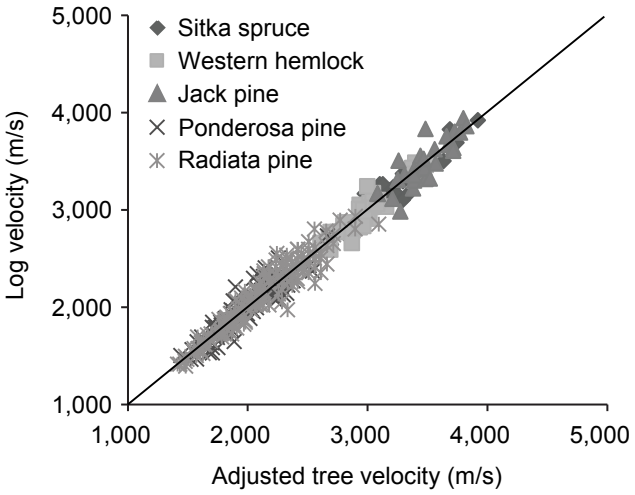

Figure 8.12—Tree acoustic velocity (adjusted) versus log acoustic velocity (Wang et al. 2007).

can be identified by tree acoustic velocity alone. The upper 15% and lower quartile of the population can be sorted by high and low velocity, respectively.

For standing trees, going from velocity measurement to wood property prediction is also a necessary step for many applications. Until recently, post-harvest NDE methods such as lumber E-rating, machine stress rating, and ultrasound veneer grading have been the standard procedures for evaluating wood stiffness and strength. The timber owner does not have a reliable way to assess the value of the final product prior to harvest. Recent wood quality research has shown that a range of wood and fiber properties can be predicted through a simple acoustic measurement in standing trees. Figures 8.13 and 8.14 show the relationships between tree acoustic velocity and MOE and microfibril angle (MFA) of core samples from trees measured by x-ray densitometry, diffractometry, and image analysis.

Assessing Silvicultural Treatment Effects

Quality and intrinsic wood properties of trees are generally affected by silvicultural practices, especially by stand density. Some silvicultural practices not only increase the biomass production of trees but also might improve the quality of the wood in trees. Nakamura (1996) used ultrasonically induced waves to assess Todo-fir and larch trees and observed significant differences in acoustic velocities and acoustic-determined MOE for trees in forest stands at different locations and trees of different ages.

Wang (1999) examined the effect of thinning treatments on both acoustic and static bending properties of young growth western hemlock and Sitka spruce trees obtained from seven sites in southeast Alaska. He found that trees with higher acoustic velocity and stiffness were mostly found in unthinned control stands and stands that received light thinning, whereas the lowest values were found in stands that received heavy and medium thinning. A typical trend of

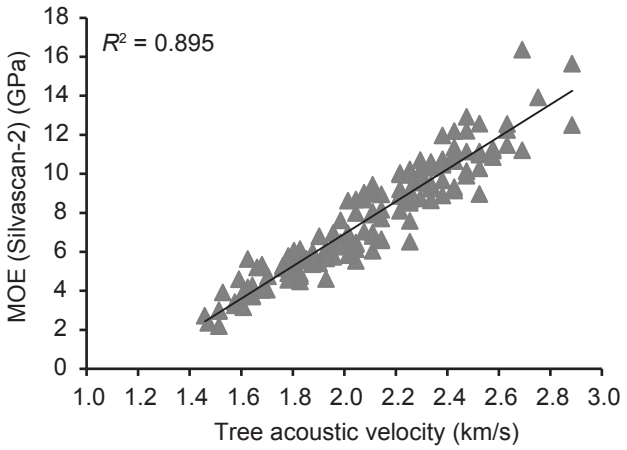

Figure 8.13—Relationship between tree acoustic velocity and modulus of elasticity (MOE) of the core samples measured by Silvascan-2 for radiata pine (Wang et al. 2007).

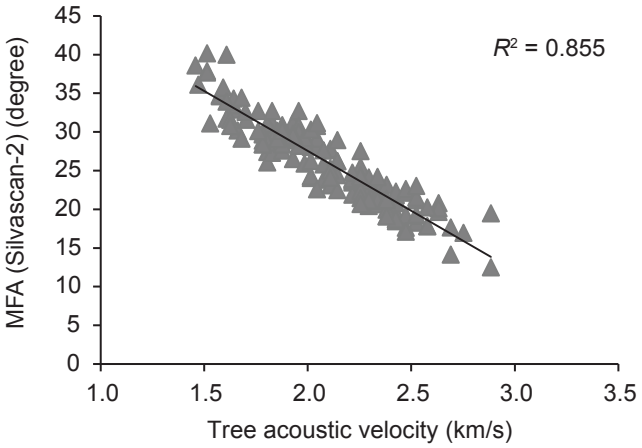

Figure 8.14—Relationship between tree acoustic velocity and microfibril angle (MFA) of the core samples measured by Silvascan-2 for radiata pine (Wang et al. 2007).

acoustic and static MOE as a function of thinning regimes is illustrated in Figure 8.15. These results were encouraging and indicated that TOF acoustic technology may be used in the future to monitor wood property changes in trees and stands and to determine how environmental conditions and silvicultural innovations affect wood and fiber properties so that the most effective treatment can be selected for future plantations for desired fiber quality.

Assessing Young Trees for Genetic Improvement

The future of the forest industry lies in fast-grown plantations. The economic imperative continuously seeks shorter rotations to meet the needs of a growing market. Young plantations will contain a higher percentage of juvenile wood, thus creating a lower quality and more variable wood resource for industry to process (Kennedy 1995).

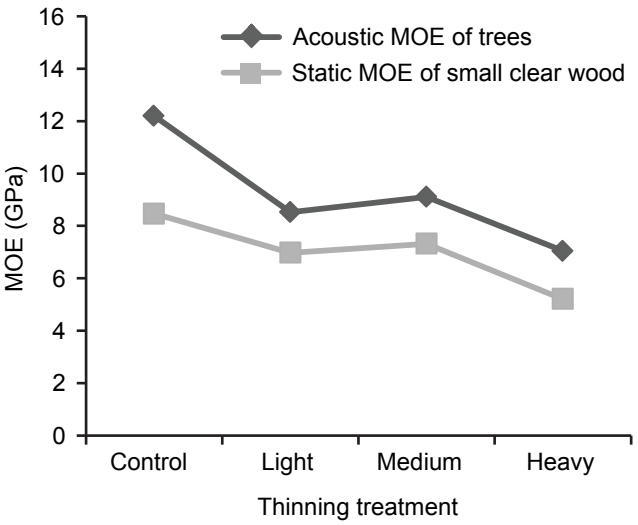

Figure 8.15—Modulus of elasticity (MOE) of young growth Sitka spruce in relation to thinning treatment (Wang et al. 2000).

Consequently, genetic improvement of juvenile wood properties is now receiving attention and getting higher priority in research. To help capture genetic opportunities, there is a need to determine wood quality at an early age (Lindstrom et al. 2002). The major challenge in operational tree improvement programs is to develop rapid and cost-effective assessment methods for selecting candidate trees with superior wood quality trait.

Wood stiffness is the most important property of structural lumber. The attractiveness of using MOE as a breeding criterion has been widely recognized in the forest industry (Addis et al. 2000a). In an investigation of sugi (C. japonica) clones from three different growth-rate groups, Hirakawa and Fujisawa (1995) found that juvenile wood in stiffer clones is much stiffer than mature wood of less stiff clones in all three growth categories. Similarly, Addis et al. (1998) reported that with radiata pine there is little difference in wood quality between juvenile wood of high stiffness trees and mature wood of low stiffness trees. Therefore the ability of selecting high stiffness trees opens the door to genetic improvement for future plantations.

With the ability to nondestructively assess wood properties of standing trees and raw log materials, acoustic methods have quickly been recognized as a useful tool in tree breeding programs (Walker and Nakada 1999; Huang et al. 2003). Lindstrom et al. (2002) investigated the possibility of selecting *Pinus radiata* clones with high MOE and found that acoustic measurement yielded results similar to traditional destructive and high-cost static bending methods. They conclude that acoustic tools could provide opportunities of mass screening for stiffness of fast-grown radiata pine clones at a very early age.

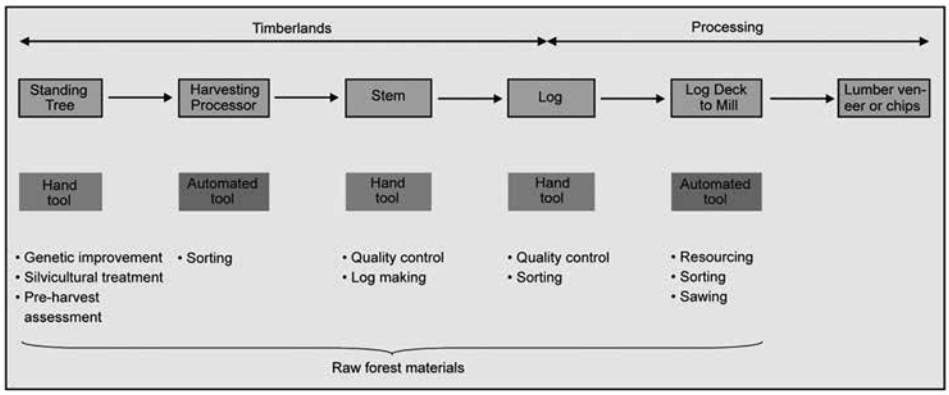

Figure 8.16—Schematic outlining potential application of acoustic technology through the operational value chain.

Evaluation of Plantation Resource for Wood Quality

In applying acoustic technology to a plantation resource, typically a number of stages will be considered. For example, a program to define wood quality for structural applications could have the goal of targeting extraction of greatest commercial value from the forest resource available, while recognizing the need to solve the problem of relatively low-stiffness wood in younger stands of much of the softwood plantation resource coming available in many countries.

Stages in a wood quality assessment program using acoustic hand tools for trial work and stand selection could include the following:

- Undertake a forest survey by mapping acoustic velocity at stand level across a range of topography, altitude, soils, ages, and silviculture (sample approximately 50 stands)
- Confirm the relationship between average standing tree velocity and average log velocity by felling 20 to 30 trees on each of 15 or more sites. Confirm velocity pattern up tree on a sub-sample of these
- Saw a sample of logs and confirm static MOE and MOR of lumber and grade out turn, relative to recorded log and standing tree velocity
- Correlate static MOE with predicted MOE from commercial testing devices (x-ray density, acoustic, mechanical bending)

By following this approach, the plantation resource can be characterized according to stiffness to enable management, planning, harvesting, and wood processing to be carried out in a way that optimizes stiffness-related value from the resource.

Operational Application of Acoustic Technology

As operational application of acoustic technology is considered, there is a recognized need for the technology to be applied at a number of stages in the operational value chain, from timberlands through to the processing site. Figure 8.16 illustrates potential application of acoustic technology through the forest-to-mill wood supply chain. Different tools have been developed to suit each specific application.

Standing tree assessment is relevant for tree breeding, preharvest assessment (PHA) for forest or stumpage valuation, and decision support at time of thinning, where trees cannot be cut. The harvesting processor application provides decision support for log-making as well as collation of data for subsequent forest management, harvest planning, and valuation. Felled stems can be tested to assist in optimization of value capture in log-making, while logs can be assessed for ranking of average wood quality (stiffness and related characteristics) or segregated for supply to different customers or processing options. Automated on-line log testing is relevant to valuation of log supplies, ranking of log supply sources, prediction of MSR yields for output planning, and providing a very efficient means for segregation of logs based on quality and suitability for different customers or processing options.

Automated On-Line Log Sorting/Grading

Although initial operational deployment of acoustic technology was undertaken using hand tools, automated log sorting or grading is now available, enabling log-by-log optimization of sawcut patterns to maximize the extracted value from a mixed quality log resource (IFI 2008; Carter 2011). Figure 8.17 shows the acoustic log grading operation in a sawmill where a Hitman LG640 automatic log grader is installed after the debarker where it measures logs just prior to sawing. The machine uses acoustic wave velocity to assess wood quality by swinging a hammer at the end of each log

Figure 8.17—Hitman LG640 automated log grader installed on the debarker out-feed. (Photo on the right shows the swinging hammer and microphone sensor.) (Photo courtesy of Fibre-gen Ltd.)

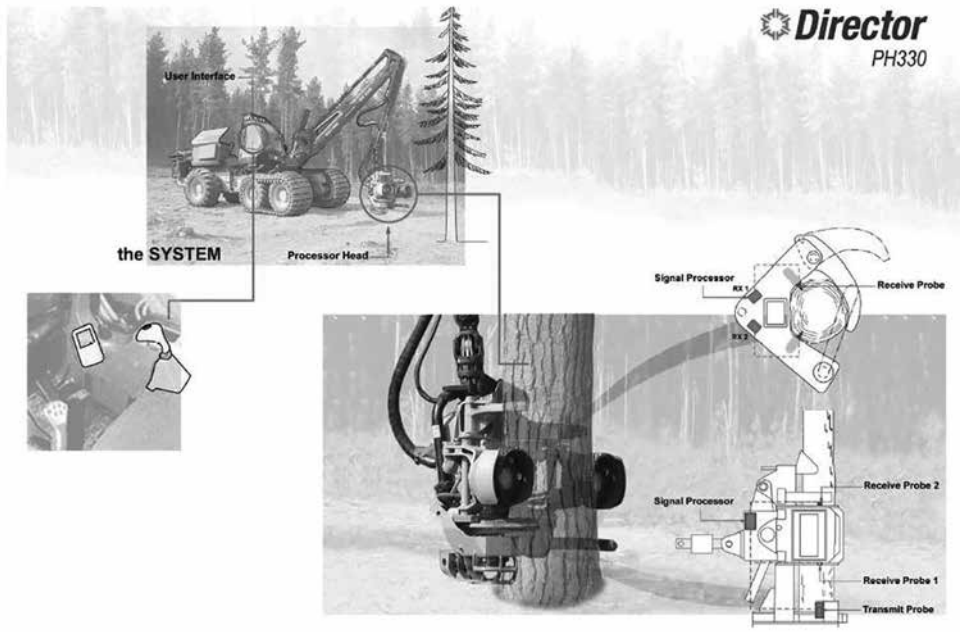

Figure 8.18—Schematics of a processor head integrated with an acoustic measurement system enabling tree quality evaluation during harvesting operation. (Drawing courtesy of Fibre-gen Ltd.)

going through the system and recording the acoustic signals using a microphone. By analyzing the resonant frequency of the longitudinal acoustic wave signals and calculating the acoustic velocity of the hit along the log, the machine is able to provide an immediate and accurate assessment of the stiffness of the wood and therefore its suitability for use as structural or nonstructural products. Logs are queued on the in-feed deck, and as each rolls into the machine infeed, its acoustic reading is displayed on the operator's control panel, which allows the operator to adjust the cut pattern to maximize the structural lumber grade out turn and profitability. The operational trial at Waimea Sawmillers in Nelson, New Zealand, has demonstrated at least a 3% gain in machine stress grading (MSG) recovery since installing the Hitman LG640 in-line acoustic grader.

Processor Head Acoustic Technology in Forest Harvest Operations

Recent research and development on acoustic technologies has brought the operational assessment of acoustic velocity as a measure of stiffness into timber harvesting and log making sectors of the forest and wood processing industry. Fibre-gen has developed a Hitman acoustic measurement system to be mounted in a processor head (Fig. 8.18). Previously reported field trials involved the integration of Hitman PH330 mechanized acoustic measurement devices into a Ponsse processor head in UK, two Waratah 626 processor heads in New Zealand, and one Waratah 624 processor head in Oregon, USA (Carter 2011). Further validation studies have been run in West Australia and Nelson, New Zealand.

The system measures the longitudinal TOF of a sound wave in the stem section held by the processor head, immediately following a cross-cut. With the acoustic velocity displayed in the cab, the operator can cut structural or nonstructural log product from the next section of stem and segregate the logs, based on a user-defined velocity threshold level. These trial studies have demonstrated the use of processor head acoustic technology in forest harvesting operations as a means to enable cutting to the correct log length and segregating logs for higher value structural markets. This avoids the need to test logs after they are cut to length and having to subsequently re-cut those logs that fail to meet the log buyer's acoustic speed specifications. Costs of sorting and re-cutting logs to a shorter length can significantly expend resources and generate waste, with the alternative of selling nonstructural logs at a discount in nonpreferred lengths.

Two alternative assessment strategies have been highlighted in recent performance validation projects: increase the average stiffness of a segregated log batch, or meet some specific minimum log velocity specifications defined by log resonance measurement (Carter et al. 2013). Processor head acoustic technology was able to identify lower stiffness sawlogs in the forest before any mill processing was undertaken. An example-based analysis of benefits and costs showed positive net benefits from the potential use of this technology to segregate structural logs from within stands otherwise considered nonstructural.

Processor head acoustic technology has now been demonstrated through a series of research, development, and validation projects over a period of 6 years and has been confirmed capable of delivering effective segregation to reliably meet a range of market and end user requirements.

Effect of Environmental Temperature on Field Acoustic Assessment of Trees and Logs

Depending on the geographic locations and the timing of forest operations, trees and logs can be acoustically tested and evaluated in different climates or different seasons. The wood temperature of trees and logs at the time of testing could range from above 30 °C to well below freezing. Previous studies on small wood samples and structural lumber suggest a direct effect of temperature on acoustic properties of wood. The observed effect of temperature on acoustic velocity in wood below fiber saturation point (FSP) is in agreement with generally accepted information on this subject, but conflicting results were reported for wood above FSP when wood temperature transitioned from above freezing to below freezing. There has been limited data showing the effect of temperature on acoustic velocity of wood measured on standing trees and logs. Little is known about the effect of seasonal temperature changes on acoustic evaluation of standing trees and freshly cut green logs. This information is important to field operations when the acoustic technology is used to assess the quality and values of logs, trees, and stands.

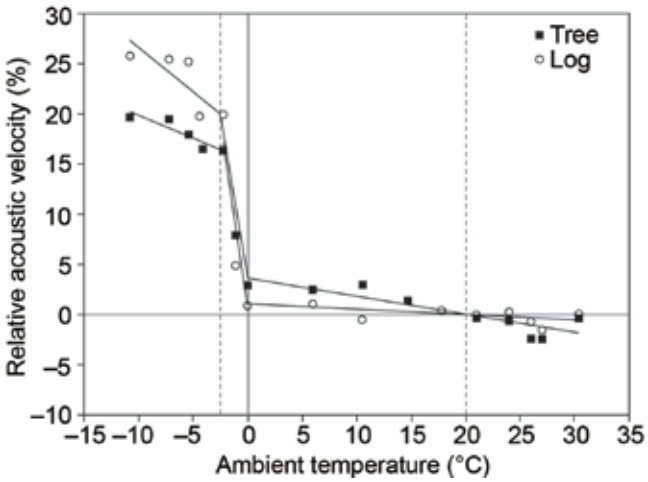

Figure 8.19—Effect of ambient temperature on change in acoustic velocity relative to 20 °C (Gao et al. 2013).

The laboratory study on red pine (*Pinus resinosa*) small clear specimens conducted by Gao et al. (2012) showed a significant change in acoustic properties of wood as wood temperature changed from –45 to 35 °C. A dramatic shift in acoustic velocity and energy loss was observed when the wood temperature changed to above or below the freezing point. Gao et al. (2013) further investigated the effects of environmental temperature on acoustic wave velocity of wood in standing trees and freshly cut logs over a duration of 12 consecutive months. Results indicated that ambient temperature had a significant effect on acoustic velocities of trees and logs in winter when temperatures were below freezing point. Acoustic velocities increased dramatically as the ambient temperature dropped below 0 °C, but then the change became less significant when the temperature decreased to below –2.5 °C. Above freezing point, acoustic velocities were found less sensitive to ambient temperature changes. Gao et al. (2013) further developed analytical models based on the change in acoustic velocity relative to a base temperature 20 °C. The relationships between the percentage of change in velocity (ΔV, %) and ambient temperature for red pine trees and logs are shown in Figure 8.19. Table 8.1 tabulates ΔV values for red pine trees and logs that were derived from the analytical models. Because acoustic velocity is more sensitive to temperature changes below freezing than above freezing, ΔV values are tabulated at a 1 °C increments from –11 to –2.5 °C and at 2 °C increments from 0 to 30 °C. From a practical standpoint, acoustic velocities of trees and logs measured well above freezing may not need a temperature adjustment, because the velocity changes observed were not large enough to have a practical significance.

From a practical standpoint, acoustic velocities of trees and logs measured at different climates or different seasons can

Table 8.1—Velocity change (Δ*V*) of red pine trees and logs in the range of –11 to 30 °C (Gao et al. 2013)

Ambient temperature (°C)	Tree Δ*V* (%)	Log Δ*V* (%)	Ambient temperature (°C)	Tree Δ*V* (%)	Log Δ*V* (%)
–11	21.0	27.5	6	2.5	0.8
–10	20.6	26.6	8	2.2	0.6
–9	20.1	25.7	10	1.8	0.5
–8	19.7	24.9	12	1.4	0.4
–7	19.2	24.0	14	1.1	0.3
–6	18.8	23.1	16	0.7	0.2
–5	18.3	22.2	18	0.4	0.1
–4	17.9	21.3	20	0.0	0.0
–3	17.4	20.4	22	–0.4	–0.1
–2.5	17.2	20.0	24	–0.7	–0.2
0	3.6	1.1	26	–1.1	–0.3
2	3.2	1.0	28	–1.4	–0.4
4	2.9	0.9	30	–1.8	–0.5

be adjusted to a standard temperature if measurements are conducted well above freezing temperatures or well below freezing temperatures. However, measurements conducted around freezing temperatures could cause complications in making temperature adjustments. Users should try to avoid conducting field acoustic testing when wood temperature is around the freezing point.

Literature Cited

Addis, T.; Buchanan, A.H.; Walker, J.C.F. 1997. Log segregation into stiffness classes. In: Ridoutt, B.G. (ed.), Managing variability in resource quality. FRI Bulletin No. 202, Forest Research Institute, Rotorua. p. 7–10.

Addis, T.; Buchanan, A.H.; Meder, R.; Newman, R.H.; Walker, J.C.F. 1998. Microfibril angle: determining wood stiffness in radiate pine. In: Butterfield, B.G. (ed.) Microfibril angle in wood. Christchurch: University of Canterbury. p. 323–336.

Addis, T.; Buchanan, A.H.; Walker, J.C.F. 2000a. Selecting trees for structural timber. Holz Roh-Werkstoff. 58(3): 162–167.

Addis, T.; Buchanan, A.H.; Walker, J.C.F. 2000b. Sorting of logs using acoustics. Wood Science and Technology. 34(2000):337–344.

Albert, D.J.; Clark, T.A.; Dickson, R.L.; Walker, J.C.F. 2002. Using acoustics to sort radiate pine pulp logs according to fibre characteristics and paper properties. International Forestry Review. 4(1): 12–19.

Andrews, M. 2000. Where are we with sonics? In: Proceedings, Capturing the benefits of forestry research: Putting ideas to work, Workshop 2000. October 18, 2000, Wood Technology Research Center, University of Canterbury. p. 57–61.

Andrews, M. 2003. Which acoustic speed? In: Proceedings, 13th International Symposium on Nondestructive Testing of Wood. August 19–21, 2002, University of California, Berkeley, California. p. 156–165.

Aratake, S.; Arima, T. 1994. Estimation of modulus of rupture (MOR) and modulus of elasticity (MOE) of lumber using higher natural frequency of log in pile of logs II—Possibility of application for Sugi square lumber with pith. Mokuzai Gakkaishi. 40(9): 1003–1007.

Aratake, S.; Arima, T.; Sakoda, T.; Nakamura, Y. 1992. Estimation of modulus of rupture (MOR) and modulus of elasticity (MOE) of lumber using higher natural frequency of log in pile of logs—Possibility of application for Sugi scaffolding board. Mokuzai Gakkaishi. 38(11): 995–1001.

Bradley, A.; Chauhan, S.; Walker, J.F.C.; Banham, P. 2005. Using acoustics in log segregation to optimize energy use in thermomechanical pulping. Appita Journal. 58(4): 306–311.

Bodig, J.; Goodman, J.R. 1973. Prediction of elastic parameters for wood. Wood Science 5(4): 249-264.

Bodig, J.; Jayne, B.A. 1982. Mechanics of wood and wood composites. New York, NY: Van Nostrand Reinhold Company, Inc.

Carter, P. 2011. Real-time measures of wood quality—transition from research to application. In: Proceedings, the 17th International Nondestructive Testing and Evaluation of Wood Symposium. September 14-16, 2011. Sopron, Hungary. Sopron, Hungary: University of West Hungary. p. 34–39.

Carter, P.; Lausberg, M. 2003. Application of Hitmam® acoustic technology—the Carter Holt Harvey experience. FIEA paper. 6 p.

Carter, P.; Briggs, D.; Ross, R.J.; Wang, X. 2005. Acoustic testing to enhance western forest values and meet customer wood quality needs. PNW–GTR–642. Productivity of Western Forests: A Forest Products Focus. Portland, Oregon: USDA Forest Service, Pacific Northwest Research Station. p. 121–129.

Carter, P.; Wang, X.; Ross, R.J. 2013. Field application of processor head acoustic technology in forest harvest operations. In: Proceedings, the 18th International Nondestructive Testing and Evaluation of Wood Symposium. General Technical Report FPL–GTR–226. Madison, WI: U.S. Department of Agriculture, Forest Service, Forest Products Laboratory. p. 7–14.

Clark, T.A.; Hartmann, J.; Lausberg, M.; Walker, J.C.F. 2003. Fibre characterization of pulp logs using acoustics. Proceedings, 56th Appita Annual Conference, Rotorua, New Zealand, March 18–20, 2002.

Dyck, B. 2002. Precision forestry—the path to increased profitability! In: Proceedings, 2nd International Precision Forestry Symposium. June 15–18, 2003. Seattle, Washington, USA. Seattle, Washington: University of Washington. p. 3–8.

FPS. 1997. Machine-graded lumber. Madison, WI: Forest Products Society. Wood Design Focus. 8(2): 1–24.

Foulon, N. 2006. Etudes de l'acoustique des bois en forêt, des billons et des bois sciés. Mémoire de fin d'études, Université Henri Poincaré, Nancy, France. 39 p.

Galligan, W.L. 2002. Chapter 7, Mechanical grading of lumber. In: Nondestructive Evaluation of Wood, R.F. Pellerin and R.J. Ross, Editors. Madison, WI: Forest Products Society. p. 93–128.

Gao, S.; Wang, X.; Wang, L.; Allison, R.B. 2012. Effect of temperature on acoustic evaluation of standing trees and logs: Part 1—Laboratory investigation. Wood and Fiber Science. 44(3): 286–297.

Gao, S.; Wang, X.; Wang, L.; Allison, R.B. 2013. Effect of temperature on acoustic evaluation of standing trees and logs: Part 2—Field investigation. Wood and Fiber Science. 45(1): 1–11.

Harris, P.; Andrews, M. 1999. Tools and acoustic techniques for measuring wood stiffness. 3rd Wood Quality Symposium: Emerging technologies for wood processing. Rotorua, Melbourne, Forest Ind Eng Assoc. 11 p.

Harris, P.; Petherick, R.; Andrews, M. 2003. Acoustic resonance tools. In: Proceedings, 13th International Symposium on Nondestructive Testing of Wood. August 19–21, 2002, University of California, Berkeley, California. p. 195–201.

Hirakawa, Y.; Fujisawa, Y. 1995. The relationships between microfibril angles of S2 layer and latewood tracheid lengths in elite sugi tree (*Cryptomeria japonica*) clones. Mokuzai Gakkaishi. 41(2): 123–131.

Huang, C.L. 2000. Predicting lumber stiffness of standing trees. Proceedings, 12th International Symposium on Nondestructive Testing of Wood, University of Western Hungary, Sopron, September 13–15, 2000. p. 173–179.

Huang, C.L.; Lindstrom, H.; Nakada, R.; Ralston, J. 2003. Cell wall structure and wood properties determined by acoustics—a selective review. Holz als Roh- und Werkstoff. 61(2003): 321–335.

IFI. 2008. Operation focus: making the grade. International Forest Industries, October 2008, p. 16–18.

Ikeda, K.; Kino, N. 2000. Quality evaluation of standing trees by a stress-wave propagation method and its application I. Seasonal changes of moisture contents of sugi standing trees and evaluation with stress-wave propagation velocity. Mokuzai Gakkaishi. 46(3): 181–188.

Iijima, Y.; Koizumi, A.; Okazaki, Y.; Sasaki, T.; Nakatani, H. 1997. Strength properties of sugi grown in Akita Prefecture III: Some relationships between logs and sawn lumber. Mokuzai Gakkaishi. 43(2): 159–164.

Kennedy, R.W. 1995. Coniferous wood quality in the future: Concerns and strategies. Wood Science and Technology. 29: 321–338.

Lindstrom, H.; Harris, P.; Nakada, R. 2002. Methods for measuring stiffness of young trees. Holz als Roh- und Werkstoff. 60(2002): 165–174.

Meyers, M.A. 1994. Dynamic behavior of materials. New York, NY: John Wiley & Sons. Inc.

Nakamura, N. 1996. Measurement of the properties of standing trees with ultrasonics and mapping of the properties. University Forest Research Rep. 96. Tokyo, Japan: Faculty of Agriculture, The University of Tokyo. p. 125–135.

Nanami, N.; Nakamura, N.; Arima, T.; Okuma, M. 1992a. Measuring the properties of standing trees with stress waves I. The method of measurement and the propagation path of the waves. Mokuzai Gakkaishi. 38(8):739–746.

Nanami, N.; Nakamura, N.; Arima, T.; Okuma, M. 1992b. Measuring the properties of standing trees with stress waves II. Application of the method to standing trees. Mokuzai Gakkaishi. 38(8): 747–752.

Nanami, N.; Nakamura, N.; Arima, T.; Okuma, M. 1993. Measuring the properties of standing trees with stress waves III. Evaluating the properties of standing trees for some forest stands. Mokuzai Gakkaishi. 39(8): 903–909.

Pellerin, R.; Ross, R.J. 2002. Nondestructive evaluation of wood. Madison, Wisconsin: Forest Products Society. 210 p.

Ross, R.J.; McDonald, K.A.; Green, D.W.; Schad, K.C. 1997. Relationship between log and lumber modulus of elasticity. Forest Products Journal. 47(2): 89–92.

Ross, R.J.; Erickson, J.R.; Brashaw, B.K.; Wang, X.; Verhey, S.R.; Forsman, J.W.; Pilon, C.L. 2004. Yield and ultrasonic modulus of elasticity of red maple veneer. Forest Products Journal. 54(12): 220–225.

Schad, K.C.; Kretschmann, D.E.; McDonald, K.A.; Ross, R.J.; Green, D.W. 1995. Stress wave techniques for determining quality of dimensional lumber from switch ties. Res. Note FPL–RN–0265. Madison, WI: U.S. Department of Agriculture, Forest Service, Forest Products Laboratory. 12 p.

Walker, J.C.F.; Nakada, R. 1999. Understanding corewood in some softwoods: a selective review on stiffness and acoustics. International Forestry Review. 1(4): 251–259.

Wang, X. 1999. Stress wave-based nondestructive evaluation (NDE) methods for wood quality of standing trees. Ph.D. dissertation. Houghton, Michigan: Michigan Technological University. 187 p.

Wang, X. 2013. Acoustic measurements on trees and logs: a review and analysis. Wood Science and Technology. 47: 965–975.

Wang, X.; Ross, R.J. 2000. Nondestructive evaluation for sorting red maple logs. In: Proceedings, The 28th Annual Hardwood Symposium, West Virgina Now—The Future for the Hardwood Industry?, Edited by Meyer D.A., May 11–13, 2000, Davis, West Virginia. p. 95–101.

Wang, X.; Ross, R.J.; McClellan, M.; Barbour, R.J.; Erickson, J.R.; Forsman, J.W.; McGinnis, G.D. 2001. Nondestructive evaluation of standing trees with a stress wave method. Wood and Fiber Science. 33(4): 522–533.

Wang, X.; Ross, R.J.; Mattson, J.A.; Erickson, J.R.; Forsman, J.W.; Geske, E.A.; Wehr, M.A. 2002. Nondestructive evaluation techniques for assessing modulus of elasticity and stiffness of small-diameter logs. Forest Products Journal. 52(2): 79–85.

Wang, X.; Ross, R.J.; Brashaw, B.K.; Punches, J.; Erickson, J.R.; Forsman, J.W.; Pellerin, R.F. 2004. Diameter effect on stress-wave evaluation of modulus of elasticity of small-diameter logs. Wood and Fiber Science. 36(3): 368–377.

Wang, X.; Ross, R.J.; Carter, P. 2005. Acoustic evaluation of standing trees—Recent research development. In: Proceedings, 14th International Symposium on Nondestructive Testing of Wood. Hannover, Germany, May 2–4, 2005. Shaker Verlag, Germany. p. 455–465.

Wang, X.; Ross, R.J.; Carter, P. 2007. Acoustic evaluation of wood quality in standing trees. Part 1. Acoustic wave behavior in standing trees. Wood and Fiber Science. 39 (1): 28–38.

Chapter 9

Laser Scanning of Logs and Lumber

R. Edward Thomas, Research Scientist
Northern Research Station, Princeton, West Virginia

The use of laser scanning technology has become an accepted and economical means of determining the size, shape, and features of logs and lumber. The key components of a laser-scanning system are a laser line generator and a camera. Figure 9.1 shows an industrial laser scanner unit manufactured by JoeScan (Vancouver, Washington) that can be used either with logs or lumber. On this particular scanner, the laser aperture is on the left and the camera is located to the right. Laser scanner design has several variations, as some have multiple laser beams and a single camera, whereas other scanners have two cameras and a single laser. Using two cameras avoids areas of missing data that occur when a protrusion on the surface prevents a camera from "seeing" the laser. Rather than project a single point, the scanners project a line onto the surface of the object being scanned. Figure 9.2 shows the laser line projected onto the surface of a log.

Figure 9.1—Typical industrial laser scan head used in log and lumber applications.

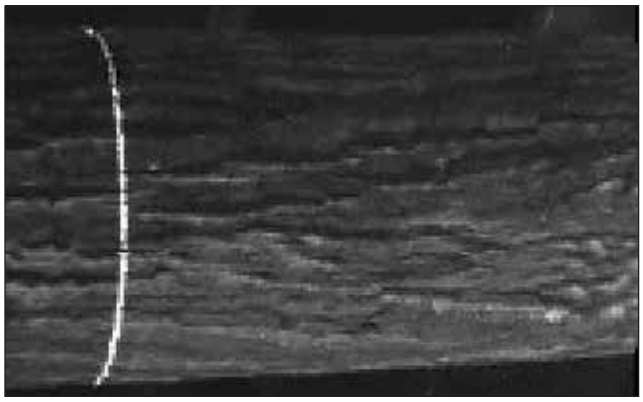

Figure 9.2—Laser scan line as projected onto a log during 3D scanning.

The camera and laser are separated by a measured distance and the camera is aimed toward the laser line at a specific angle. Using the camera angle, distance between camera and laser, and triangulation, the distance of points along the laser line projected on an object can be determined. In many instances, scanning systems are calibrated using an object with a known shape and size. Figure 9.3 shows the mechanics of projecting a point from the laser line onto the camera's image plane. Processing the location of points on the laser line onto the camera's image plane allows the shape and size of an object to be calculated.

Laser scanning systems must be able to discriminate between the laser line and the surface being scanned. Most scanners use lasers in the visible spectrum while others scan in the invisible (near infrared and ultraviolet) spectrum. Visible spectrum scanners must operate out of direct sunlight, exposure to which can prevent the scanner from finding the laser on the surface being scanned.

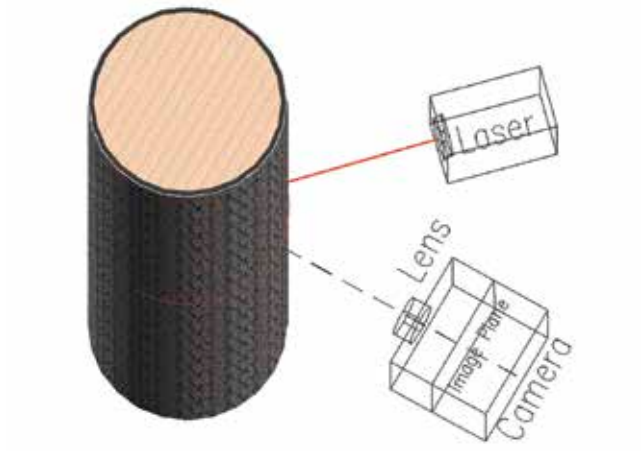

Figure 9.3—Diagram of scanning head showing laser, camera, and image plane.

Log Scanning

There are two typical methods of laser scanning logs. The first involves a stand-alone scanning system where the log passes through an array of three to four laser scanning heads arranged around the log (Figure 9.4a). Typically, the logs are on a chain and are passed through the scanner. In the second method, a series of laser scanning heads are mounted at the headrig of a sawmill (Figure 9.4b).

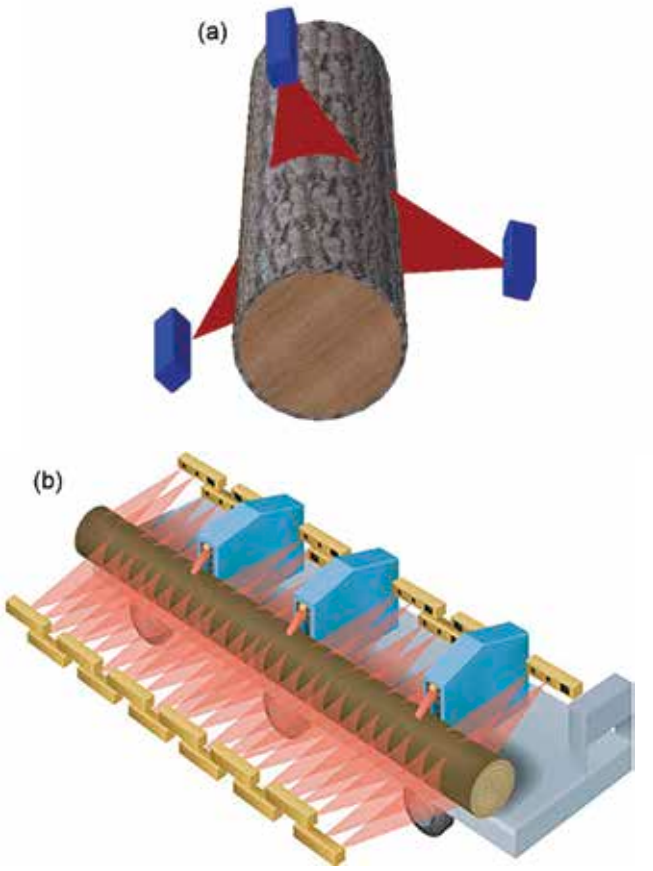

Figure 9.4—Typical configurations for laser scanning logs: (a) three headed scanner where log passes through the middle of scanning array; (b) array of laser scanning heads configured to scan front and back sides of logs on the headrig (image courtesy of JoeScan, Inc.).

Scanning at the headrig is more easily integrated into existing mills, as the first approach requires the addition of a separate log scanning station. However, the first approach can provide higher density scanning with fewer areas of missing data. The LogEye series of log scanners (Innovativ Vision, Linköping, Sweden) are one example of this type of scanner. Table 9.1 lists additional manufacturers of laser scanning equipment for logs and stems.

During laser scanning, a series of scan lines are projected around the circumference of the log along its length. The resolution of the scanning system is the distance between the scan lines. The shorter the distance between the scan lines, the higher the resolution. The resolution of a log laser scanning system is normally between 6 and 24 inches, although much higher resolutions are possible. The higher the resolution, the greater the detail captured about the log and the greater the amount of data that must be processed. Figure 9.5 shows a high-resolution scan of a hardwood log with a resolution of 0.0625 inches. This scan is from an experimental scanner developed by the Forest Service (Thomas et al. 2008). It is easy to discern defects in the image as well as the shape of the log.

Figure 9.5—High-resolution 3D scan of a hardwood log.

Laser scanning is normally done just before processing and is used to determine the diameter, shape (round, elliptical, fluted, etc.), length, sweep, and taper of logs. To efficiently convert logs into lumber, these aspects must be accurately measured. In hardwood sawmills, laser scanning is chiefly used to accurately position the log, given diameter, taper, and sweep measurements, such that the minimum opening face can be determined and sawn. The minimum opening face is the width of the first board cut from the face of a log (Malcolm 2000). If the width of the board is too narrow, then the grade and value of the board is decreased. If the width of the board is too wide, then too much wood was left in slab and is wasted. In addition, the most valuable wood in a hardwood log is normally in the jacket boards, the first boards sawn from the log. If the log has significant amounts of taper or sweep, the log can be positioned to minimize volume loss (Malcolm 2000).

The process of sawing hardwood lumber is significantly different from that of sawing softwoods. In hardwoods, the log is continually examined for the presence of defects during sawing, with the goal of producing lumber with a minimal number of defects. In softwoods, the presence of defects is much less of a concern and the sawing pattern can be optimally determined before sawing begins. A sawing pattern describes the steps involved in sawing the log and the sizes of boards that will be produced. Figure 9.6 shows the end view of a laser-scanned hardwood log with a proposed sawing pattern showing the fitting of boards within the log. With such a system, the volume yield of a log is known before sawing. More importantly, the grade yield and value of the lumber can be estimated and optimized before sawing.

With high-resolution laser scanning are additional processing applications. Given a high-resolution scan as shown in Figure 9.5, log volumes can be determined that are comparable in accuracy to those obtained using immersion tanks (Thomas and Bennett 2014). In addition, methods have been developed for automated detection of severe defects on hardwood log surfaces. (Thomas et al. 2008) Such data permits optimization of the sawing process to produce maximum value (Lin et al. 2011).

Laser Lumber Scanning

Laser scanning is commonly used in several aspects of lumber production and quality assessment in both hardwoods

Table 9.1—List of laser scanning equipment manufacturers

			Application		Scan type	
Company	Contact	URL	Logs	Lumber	Profile	Tracheid
ATB Blank GmbH Am Priel 2 D-89297 Roggenburg Germany	49.0.7300.9218.0 info@atb-technology.de	www.atb-technology.de	No	Yes	Yes	Yes
Automation & Electronics 4 Portside Drive PO Box 4044 Mount Maunganui New Zealand	64.7.574.6223 sales@automationelec.com	www.automationelec.com	Yes	Yes	Yes	No
COE USNR PO Box 310 Woodland, WA 98674 USA	1.800.289.8767 info@usnr.com	www.coemfg.com www.usnr.com	Yes	Yes	Yes	Yes
Comact 4000 40e Rue Ouest Saint-Georges, QC G5Y 8G4 Canada	1.418.228.8911	www.comact.com	Yes	Yes	Yes	No
Innovativ Vision AB Idögatan 10 SE-58278 Linköping Sweden	46.13.460.51.00 info@ivab.se	www.ivab.se	Yes	Yes	Yes	Yes
JoeScan 4510 NE 68th Dr., Ste. 124 Vancouver, WA 98661 USA	1.360.993.0069 sales@joescan.com	joescan.com	Yes	Yes	Yes	No
LIMAB UK Ltd Unit 3L Westpark 26 Wellington TA21 9AD England	44.0.1823.668633	limab.co.uk	Yes	Yes	Yes	No
LMI 1673 Cliveden Ave. Delta, BC V3M 6V5 Canada	1.604.636.1011	www.lmi3.com	Yes	Yes	Yes	No
Michael Weinig AG Weinigstraße 2/4 97941 Tauberbischofsheim Germany	49.0.9341.86.0 info@weinig.com	www.weinig.com	No	Yes	Yes	Yes
MicroTec GmbH Julius Durst Str. 98 I-39042 Brixen (BZ) Italy	39.0472.273.611 info@microtec.eu	www.microtec.eu	Yes	Yes	Yes	Yes
SOFTAC Systems Ltd. #220 - 19358 96th Ave. Surrey, BC V4N 4C1 Canada	1.604.888.9507 sales@softacsys.com	www.softacsystems.com	No	Yes	Yes	No

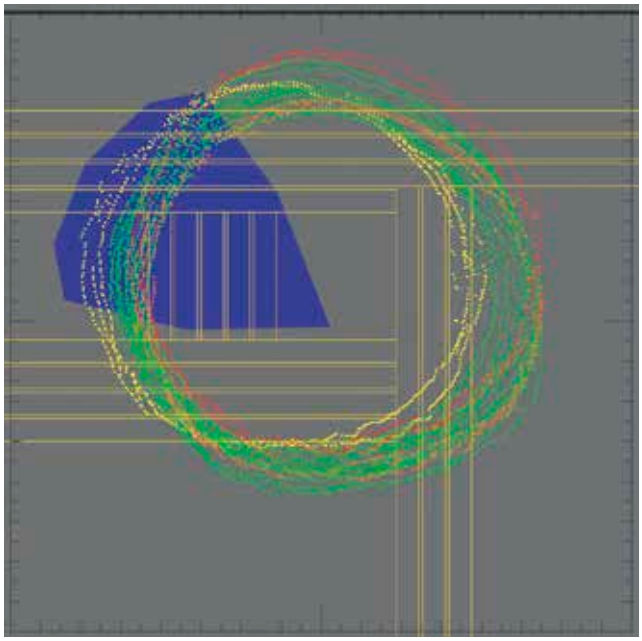

Figure 9.6—End view of laser scan imagery with proposed sawing pattern. Large blue area to left is potential internal knot defect.

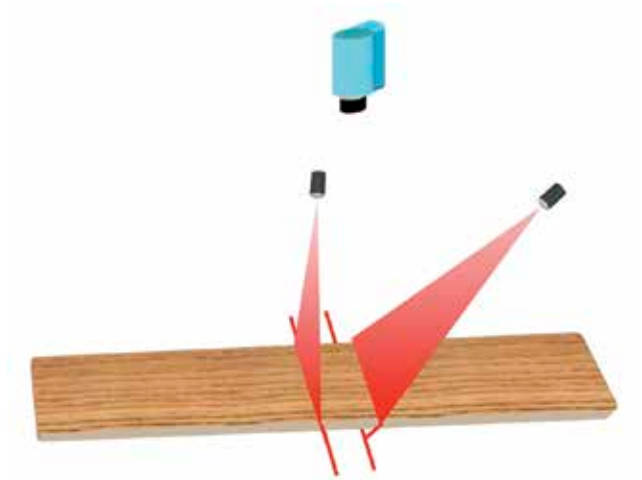

Figure 9.7—Diagram of laser scanner used in a lumber mill.

and softwoods. Figure 9.7 shows a typical configuration of a laser scanner in a lumber mill. This setup uses two lasers to capture two data types. The rightmost laser aimed at the board in shallow angle is for profile scanning. Profile scanning is used to detect void and wane on the edges of the board as well as splits, cracks, and holes. The laser perpendicular to the board is used to scan for the tracheid effect. This type of scanning is used to determine the angle of wood grain along the length of the board.

Profile Scanning

Profile scanning yields accurate measurements of the amount of wane, as well board width, and the distance between two edges with wane. This use is perhaps the largest application of laser scanning—the measurement and automated detection of wane and void on the edges of lumber. The amount of wane affects the grade and value of almost all hardwood and softwood boards and structural lumber (SPIB 2013; NELMA 2013; NHLA 2011). In addition, the accurate measurements of wane and board size can be used to automate the edging and trimming of lumber to produce maximum grade and value (Abbott et al. 2001). Several companies manufacturer laser scanners and systems for measuring lumber, determining wane, and optimizing edging and trimming of lumber (Table 9.1).

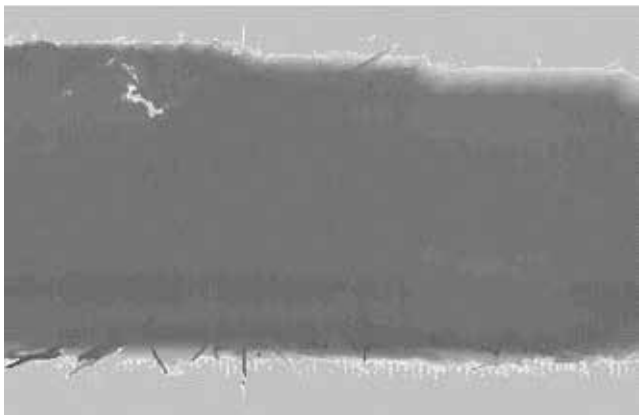

Figure 9.8—Sample laser profile image of a board.

Figure 9.8 shows a sample laser profile gray-level image. In the image, the normal, level surface of the board is shaded as dark gray. Slightly higher areas of the board are represented as darker shades of gray. Lower areas are shown as progressively lighter shades of gray. On the right hand side of the photo, along the upper edge, wane is represented in a narrow region along the edge where the dark gray of the normal board surface fades to almost white. In addition, taper can be seen along the upper edge of the image as the board outline narrows. A white jagged line inside the board above the wane area indicates a split, crack, or tear out in the board.

Tracheid Effect Scanning

When a laser beam strikes the surface of wood, the beam is propagated along the fibers of the wood, this beam propagation characteristic is commonly referred to as the tracheid effect. The angle of glow of the laser beam of the wood surface shows the angle of the wood grain. Thus, the angle of the wood around defects such as knots and pitch pockets can be detected and used as indicators for defects (Jolma and Mäkyen 2007). One of the first commercial systems to implement tracheid scanning was Cell-Scan (Barr-Mullin, Raleigh, North Carolina). This system was used to locate defects in hardwoods and softwoods for the production of furniture and mouldings. In addition, the tracheid effect can be used to detect sloped grain and as a result areas of potential weakness in the board (Olsson et al. 2013). Olsson

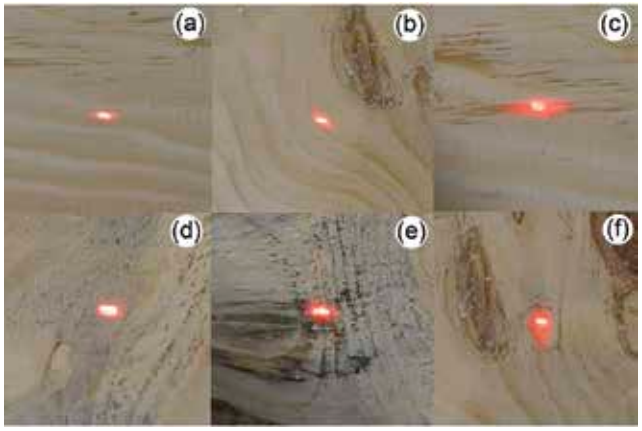

Figure 9.9—Photo demonstrating the tracheid effect of a laser for clear wood and different defect types on white pine (*Pinus strobus*): (a) clear wood; (b) clear wood with swirled grain; (c) pitch pocket; (d) sloped grain near a knot; (e) sloped grain with a pitch pocket; (f) small, resinous pin knot.

et al. (2013) used a WoodEye commercial lumber scanner (Innovativ Vision, Linköping, Sweden) to collect tracheid effect imagery then correlated it to the stiffness of the wood, allowing the use of tracheid imagery data as a strength predictor. Table 9.1 lists known manufacturers of tracheid scanning equipment.

Figure 9.9 shows a series of tracheid effect examples for various defect and grain types on a sample of white pine (*Pinus strobus*). In this series of pictures, the laser beam is slightly square and fixed in position to provide a consistent beam along the length of the board. What is important to notice is how the shape of the laser beam changes when areas of the board with different grain patterns are illuminated. Figures 9.9a and b show two examples of clear grain. However in 9.9b, the grain has a swirl and the edges of area illuminated by the laser are bent along the angle of the grain. Figure 9.9c shows an illuminated pitch pocket oriented along length of the wood grain. Figures 9.9d and 9.9e show sloped grain near knots. What is noteworthy is that the laser light is conducted almost completely into the board surface (note the decreased area or halo of light around the laser point) rather than along the surface as seen in Figures 9.9a and 9.9b. In addition, Figure 9.9e illuminates a pitch pocket, but the sloped grain characteristics conduct most light into the board, making this example significantly different than the example in Figure 9.9c. Finally, Figure 9.9f is a small resinous knot that is completely illuminated by the laser. In addition, the laser light is conducted along the length of the swirled grain toward the bottom of the image (Fig 9.9f).

Acknowledgments

Figures 9.7 and 9.8 are provided courtesy of Phillip Araman, U.S. Forest Service, Southern Research Station, Blacksburg, Virginia. Figure 9.4b is provided courtesy of JoeScan Inc., Vancouver, Washington.

Literature Cited

Abbott, A.L.; Schmoldt, D.L.; Araman, P.A.; Lee, S-M. 2001. Automatic scanning of rough hardwood lumber for edging and trimming. In: Proceedings of ScanTech International Conference, November 4–6, 2001, Seattle, WA. Wood Machining Institute, Berkeley, CA. p. 101–110.

Jolma, I. P.; Mäkyen, A.J. 2007. The detection of knots in wood materials using the tracheid effect. Proc. SPIE 7022. Advanced Laser Technologies 2007, 70220G.

Malcolm, F.B. 2000. A simplified procedure for developing grade lumber from hardwood logs. Res. Note FPL–RN–098. Madison, WI: U.S. Department of Agriculture, Forest Service, Forest Products Laboratory, 13 p.

Lin, W.; Wang, J.; Thomas, R.E. 2011. A three-dimensional optimal sawing system for small sawmills in central Appalachia. In: Proceedings of the 17th Central Hardwoods Forest Conference, April 5–7, 2010, Lexington, KY. Gen. Tech. Rep. P-78. Newtown Square, PA: U.S. Department of Agriculture, Forest Service, Northern Research Station. p. 67–75.

NELMA. 2013. Standard grading rules for Northeastern Lumber. Cumberland Center, ME: Northeastern Lumber Manufacturers Association.

NHLA. 2011. Rules for the measurement and inspection of hardwood and cypress. Memphis, TN: National Hardwood Lumber Association. 104 p.

Olsson, A.; Oscarsson, J.; Serrano, E.; Källsner, B.; Johansson, M.; Enquist, B. 2013. Prediction of timber bending strength and in-member cross-sectional stiffness variation on the basis of local wood fibre orientation. European Journal of Wood Products. 71: 319–333.

Thomas, R.; Edward, Thomas, L.; Shaffer, C. 2008. Defect detection on hardwood logs using high-resolution laser scan data. In: Proceedings of the 15th International Symposium on Nondestructive Testing of Wood, September 10–12, 2007, Duluth, MN. Natural Resources Research Institute, University of Minnesota, Duluth: 163–167.

Thomas, E.; Bennett, N. 2014. In: Groninger, John W.; Holzmueller, Eric J.; Nielsen, Clayton K.; Dey, Daniel C., eds. Proceedings, 19th Central Hardwood Forest Conference, March 10–12, 2014, Carbondale, IL. Gen. Tech. Rep. NRS–P–142. Newtown Square, PA: U.S. Department of Agriculture, Forest Service, Northern Research Station. p. 299–310.

SPIB. 2013. Standard grading rules for southern pine lumber. Pensacola, FL: Southern Pine Inspection Bureau.

Chapter 10

Ultrasonic Veneer Grading

Brian K. Brashaw, Program Manager
Forest Products Marketing Unit, USDA Forest Service, Madison, Wisconsin

The development and growth of the laminated veneer lumber (LVL) industry has been a direct result of the application of ultrasonic nondestructive evaluation (NDE) methods for assessing the properties of wood veneer. Individual veneer sheets are fed through opposing transducers that send and receive a wave. This wave travels longitudinally through the veneer. The time it takes for the wave to travel between the transducers is referred to as the propagation time and is used to calculate the velocity of the wave. With previously determined empirical relationships that relate wave velocity to wood stiffness and strength, each sheet of veneer is assigned to a strength category based on the velocity of the wave traveling through it. These relationships were derived from fundamental research studies in which samples of veneer were tested to determine the velocity at which a wave traveled through them and were then destructively tested to determine their strength and stiffness. Knowing the properties of each sheet of veneer enables manufacturers to design and produce engineered wood products that have properties with predictable performance characteristics.

Ultrasonic veneer grading is based on elementary one-dimensional stress wave theory, which states that the modulus of elasticity (MOE) of a material is a function of the velocity C of stress wave propagation and mass density ρ as defined by

$$\mathrm{MOE} = C^2 \rho$$

Metriguard, Inc. (Pullman, Washington), is the only commercial manufacturer of ultrasound veneer grading equipment. Their first commercial system was installed in 1977 at Trus Joist Corporation's first LVL plant in Eugene, Oregon (Pieters 1979). This system was capable of production speeds of 100 ft/min (30.5 m/min). Douglas-fir veneer was sorted into three grades based on veneer propagation time in the longitudinal grain direction. Figure 10.1 shows an original Metriguard Model 2600 commercial ultrasonic veneer grader.

Technical advances have coupled the velocity of the wave with the use of a radiofrequency probe to determine the specific gravity and moisture content of each veneer sheet (Logan 2000). Research resulted in the development of better relationships between the temperature of wood and wave velocity. These improvements resulted in the ability to sort veneer on the basis of calculated MOE based on the wave velocity and specific gravity (Logan 2000).

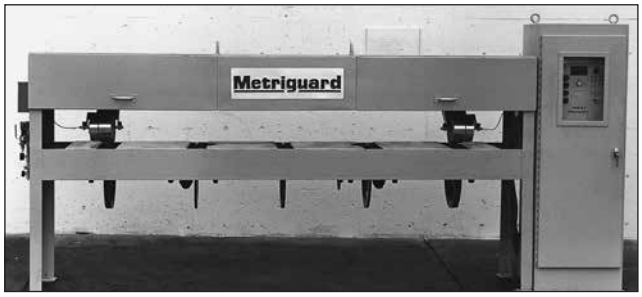

Figure 10.1—Metriguard 2600.

Figure 10.2—Metriguard 2800 DME.

Figure 10.2 shows the Metriguard Model 2800 DME capable of achieving production speeds of 300 to 425 ft/min (91.4 to 129.5 m/min). It is equipped with wood temperature compensation, radiofrequency measurement of specific gravity and moisture content, and sheet width and thickness detection capabilities.

Laminated Veneer Lumber Production

In 2000, approximately 150 ultrasonic veneer graders were in use around the world, resulting in a grading capacity of 15 million m^3 of veneer for LVL (Logan 2000). Today the number of ultrasonic veneer graders in-use totals nearly 200. Laminated veneer lumber is manufactured from C and D grade rotary-peeled veneer that is typically 0.17 to 0.10 in. (4.3 to 2.5 mm) thick. Species that are used for LVL include Douglas-fir, southern yellow pine, lodgepole pine, western

hemlock, western larch, aspen, black spruce, paper birch, and red pine. After drying, the veneer is graded through a commercial ultrasonic veneer grader into several grades. Adhesive is applied to the veneer, which is oriented in the longitudinal direction prior to pressing. Typically, LVL is manufactured in continuous length billets (1.25 to 3 in. thick, 52 in. wide (3.2 to 7.6 cm thick, 1.3 m wide)). The LVL is then sawn into sizes based on customer requirements. This LVL is used in many structural products including prefabricated wood I-joists, truss chords, headers, and beams.

Trus Joist Corporation (Boise, Idaho) was the initial entrant into the LVL industry in the early 1970s. They pioneered the manufacturing and grading technology that allowed for the exponential growth of LVL since 1992. The annual estimate for LVL production was approximately 9 million ft^3 (255,000 m^3) from six engineered wood products manufacturers in 1992 (Guss 1994). Laminated veneer lumber production increased to 51.9 million ft^3 (1.5 million m^3) in 1999 (APA 2000). Approximately 61% of the LVL production was used as flanges for wood I-joists in 1999, followed by 31% as headers and beams, and 8% for other applications (APA 2000). Although it would be difficult to estimate current production statistics, LVL production has increased considerably in recent years.

Technology Development

The concept for determining wave propagation time, stress wave velocity, and MOE for veneer was based on lumber studies that were completed at Washington State University (Pullman, Washington) (Galligan and Courteau 1965; Pellerin and Galligan 1973). The presence of stress waves in softwood lumber was detected using a probe that was sensitive to the piezoelectric charge in wood in response to strain caused by impact. The MOE for a sample set of 40 pieces of Douglas-fir lumber was determined through stress wave velocity and density and compared with the corresponding static MOE. A correlation coefficient of 0.95 was reported, which shows excellent potential for using the stress wave timing technique to grade lumber based on MOE.

An effort to apply this technology to veneer was initiated by Roy Pellerin of Washington State University (WSU) and Peter Koch of United States Department of Agriculture, Forest Service, Southern Forest Experiment Station (New Orleans, Louisiana). Rotary cut southern yellow pine veneer for this study was shipped to WSU for evaluation of MOE using a laboratory built experimental stress wave timer. Modulus of elasticity for each veneer sheet was determined from static tests conducted on samples obtained from each veneer sheet. There was a strong relationship between the static tensile MOE and ultrasound MOE as evidenced by a correlation coefficient of 0.92 (Koch 1967).

Based on this success, a faster stress wave grading apparatus was constructed by WSU and sent to the Southern

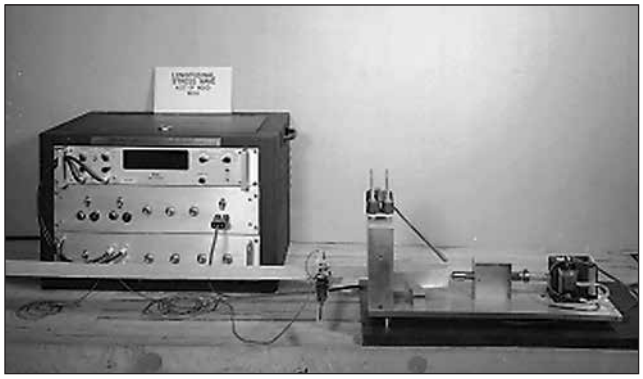

Figure 10.3—Washington State University stress wave timer.

Experiment Station for an extensive study of 10,350 southern yellow pine veneers that were to be manufactured into laminated beams. The goal was to determine the MOE of each veneer and use this information to place the stiffest veneer in the highly stressed tension and compression zones and to place the lowest stiffness near the neutral axis (Koch and Woodson 1968). Figure 10.3 shows the WSU stress wave timer used in that study. The stress wave was introduced through an anvil impact system and captured by a piezoelectric probe.

Each piece of southern yellow pine veneer was 0.17 in. thick by 2.75 in. wide and 100 in. long (4.3 mm thick by 7 cm wide and 2.5 m long). The stress wave velocity was determined across a 92-in. (2.6-m) span as an average of three consecutive time readings for each veneer. This was the basis for sorting the veneer into groups for manufacturing laminated beams. Every 50th veneer was also tested to determine the static tensile MOE for comparison against the ultrasound MOE. Figure 10.4 shows the regression of static MOE and ultrasound MOE for these veneers. The correlation coefficient was 0.94 for the 177 veneers evaluated.

The veneer was then strategically placed during beam layup with the stiffest veneers on the outside and those with the lowest stiffness near the neutral axis. The resulting beams had predictably high static MOE values with low standard deviations. These beams were essentially the first experimental LVL manufactured from stress wave graded veneer.

Subsequent laboratory studies (Hunt and others 1989; Jung 1979; Jung 1982) have been conducted to investigate the concept for use in evaluating veneer strands, in addition to examining the effect natural occurring defects have on wave behavior.

Metriguard, Inc., was founded in 1973 to commercialize the use of stress wave timing technology for lumber, wood composites, paper, and veneer. Metriguard's first system was the portable 239 stress wave timer, designed to measure the transit time of an impact-induced wave. The wave was introduced with a pendulum impactor to a clamp attached to the

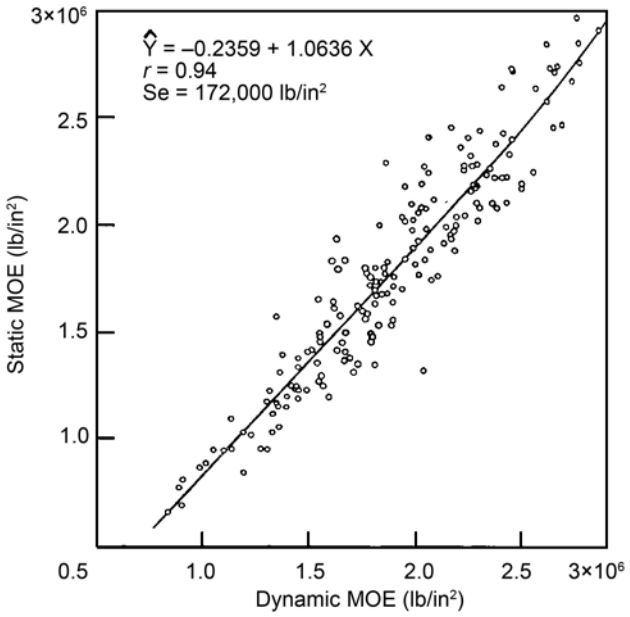

Figure 10.4—Regression of static and ultrasound MOE of southern yellow pine veneer (Koch and Woodson 1968).

sample. Piezoelectric transducers were placed at two points of the specimen and used to sense the passing of the wave. The time it takes for the wave to travel between the sensors was measured and displayed. This time was then used to compute wave propagation speed through the material.

Concurrently, Trus Joist was developing commercial LVL for use as a flange material for open web wood and steel trusses and wood I-joists. They began manufacturing LVL in 1972 but experienced wide variation in the mechanical properties of the LVL they manufactured. They found that there was no relationship between the visual grade mix of the Douglas-fir veneer and the strength properties of the LVL (Kunesh 1978).

Trus Joist approached Metriguard, Inc., about their portable stress wave timer to grade veneer. Robert Kunesh of Trus Joist Corporation and Roy Pellerin of WSU used a Metriguard Model 239 to grade 0.10-in.- (2.5-mm-) thick Douglas-fir C and D visual grade veneer. The veneer was sorted into several groups based on stress wave velocity. Laminated veneer lumber was then manufactured from these groups and tested to determine the relationships between the veneer stress wave velocity and bending and tension properties of the LVL billets. Correlation coefficients were 0.92 between ultrasound MOE and tension MOE and 0.91 between ultrasound MOE and static bending MOE. The use of stress wave NDE technology allowed Trus Joist to accurately assess veneer sheet quality and translate it into LVL with predictable properties with low variability (Kunesh 1978; Pieters 1979).

Based on the success of stress grading veneer, Metriguard focused development efforts on building an automated production line ultrasonic veneer grading system for Trus Joist. The Metriguard 2600 system used rolling ultrasonic transducers to input and receive stress waves that traveled along the longitudinal length of each veneer sheet. Approximately 60 ultrasonic pulses per second were sent into the material, resulting in 50 to 100 time measurements for each sheet of 27-in. wide veneer. These measurements were averaged for each sheet of veneer and used to sort the veneer into one of several grades based on transit time. Low transit time corresponded to high velocities, which is indicative of veneers with high stiffness as defined by fundamental one-dimensional wave theory.

The first commercial machine developed had a production speed of about 100 ft/min (30.5 m/min), which was limited by acoustic noise emissions produced by the veneer and by ultrasonic intensity of the sending transducer (Logan 1987; Logan 2000). Improvements in transducers and signal processing allowed production speeds to increase to 200 ft/min (61 m/min) by the early 1990s (Uskoski et al. 1993).

Metriguard continued to refine and develop ultrasonic veneer grading technology and equipment and introduced the Model 2650 DFX and 2800 DME in 2000. Digital signal processing coupled with continued noise reduction has increased the stress wave sampling rate by 60%, up to 200 ultrasonic pulses per minute. This resulted in increased production speeds of 300 to 425 ft/min (91.4 to 129.5 m/min) of veneer through the ultrasound veneer graders (Logan 2000). Newer/current models can operate up to 600 ft/min (e.g., 2655 and 2805). This system also includes temperature correction for stress wave propagation time and radio frequency measurement of specific gravity, moisture content, and veneer sheet width and thickness and computes the MOE of each sheet of veneer. As many veneer manufacturers evaluate hot veneer directly after the dryer outfeed, the temperature effect on stress wave velocity is important. The temperature correction factors are based on recent research completed at the Forest Products Laboratory and Metriguard (Green et al. 1999; Logan 2000). The ability to determine specific gravity allows for the determination and sorting by MOE instead of only by transit time and should allow for improved utilization of the resource (Logan 2000). Current equipment models provide ultrasonic propagation measurements along with specific gravity measurements and MOE determination and allow sorting veneer based on MOE. MOE sorting and corresponding LVL layup allow for very precise control of the MOE in the final LVL product (Moore 2002).

Ultrasonic Grading of Green Veneer

The initial application of ultrasonic methods to sort veneer for LVL manufacturer was restricted to dry veneer. By the time the veneer is sorted into stress grades, significant drying costs have been incurred. If a similar sorting procedure for green veneer could be developed, it would be

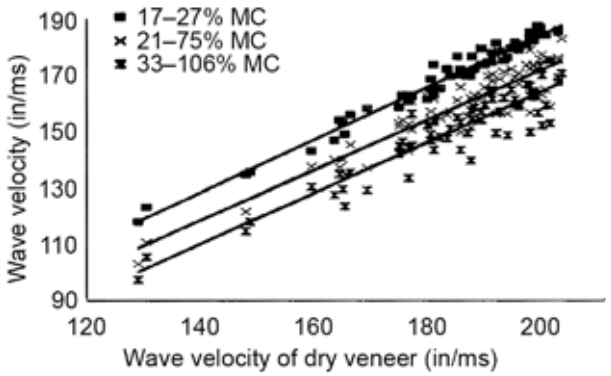

Figure 10.5—Stress wave velocities of southern yellow pine veneer at several moisture content (MC) ranges compared with stress wave velocity of dry veneer measured with a digital oscilloscope (1 in/ms = 25.4 m/s) (Brashaw et al. 1996).

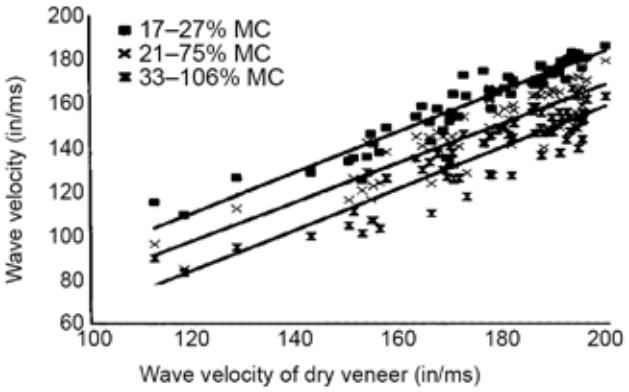

Figure 10.6—Stress wave velocities of southern yellow pine veneer at several moisture content (MC) ranges compared with stress wave velocity of dry veneer measured with a stress wave timer (1 in/ms = 25.4 m/s) (Brashaw et al. 1996).

possible to dry material with similar strength and stiffness together in customized drying schedules. These custom drying cycles, based on veneer strength and stiffness, could lead to increased efficiency, energy savings, and lower costs by reducing or eliminating veneer redrying.

Laboratory investigations of the use of ultrasonic methods for assessing the quality of green veneer have yielded promising results. Brashaw et al. (1996) evaluated the potential of using these methods to sort green southern yellow pine and Douglas-fir veneer into stress grades. Stress wave transit times were measured on a sample of veneer using both a digital oscilloscope and a commercial grading device. The stress wave transmission times were measured in both green (wet) and dry conditions. They found that wave velocities in green and dry veneers were strongly correlated. Figure 10.5 compares longitudinal wave velocities of southern yellow pine veneer at several moisture content ranges to the velocity of dry veneer measured with an oscilloscope. Figure 10.6 shows longitudinal wave velocities of southern yellow pine veneer at several moisture content ranges compared with the velocity of dry veneer as measured with a commercial stress wave timer. This research effort indicated that it is possible to sort green veneer prior to drying.

Radio frequency measurements for density and moisture content of the green veneer can be made with the Metriguard veneer grading equipment. The lack of physical sorting capability in green veneer lines is currently limiting implementation of these processes in manufacturing facilities.

Literature Cited

APA. 2000. Regional production and market outlook for structural panels and engineered wood products, 2000–2005. APA Economics Rep. E66. Tacoma, WA: American Plywood Association.

Brashaw, B.K.; Ross, R.J.; Pellerin, R.F. 1996. Stress wave nondestructive evaluation of green veneer. In: Proceedings, 10th international symposium on nondestructive testing of wood; 1996 August 26–28; Lausanne, Switzerland: 135–146.

Galligan, W.L.; Courteau, R.W. 1965. Measurement of the elasticity of lumber with longitudinal stress waves and the piezoelectric effect of wood. In: Proceedings, 2nd symposium on nondestructive testing of wood; 1965 April; Spokane, WA. Pullman, WA: Washington State University: 223–244.

Green, D.W.; Evans, J.W.; Logan, J.D.; Nelson, W.J. 1999. Adjusting modulus of elasticity of lumber for changes in temperature. Forest Products Journal. 49(10): 82–94.

Guss, L. 1994. Engineered wood products: a bright future or a myth. In: Proceedings, 28th international particleboard/composite materials symposium. 1994 April 12–14; Pullman, WA: Washington State University: 71–88.

Hunt, M.O.; Triche, M.H.; McCabe, G.P.; Hoover, W.L. 1989. Tensile properties of yellow poplar veneer strands. Forest Products Journal. 39(9).

Jung, J. 1979. Stress wave grading techniques on veneer sheets. General Technical Report FPL–GTR–27. Madison, WI: U.S. Department of Agriculture, Forest Service, Forest Products Laboratory. 10 p.

Jung, J. 1982. Properties of parallel-laminated veneer from stress-wave-tested veneers. Forest Products Journal. 32(7): 30–35.

Koch, P. 1967. Location of laminae by elastic modulus may permit manufacture of very strong beams from rotary-cut Southern pine veneers. Res. Pap. SO–30. New Orleans, LA: U.S. Department of Agriculture, Forest Service, Southern Forest Experiment Station.

Koch, P.; Woodson, G.E. 1968. Laminating butt-jointed, log-run southern yellow pine veneers into long beams of

uniform high strength. Forest Products Journal. 18(10): 45–51.

Kunesh, R.H. 1978. Using ultrasonic energy to grade veneer. In: Proceedings, 4th symposium on nondestructive testing of wood; 1978 August 28–30; Vancouver, WA. Pullman, WA: Washington State University: 275–278.

Logan, J. D. 1987. Continuous Ultrasonic Veneer Testing: Sorting Veneer for Structural Applications. Sawmill Clinic, Portland, OR.

Logan, J.D. 2000. Machine sorting of wood veneer for structural LVL applications. In: Proceedings, 34th international particleboard/composite materials symposium; 2000 April 4–6; Pullman, WA: Washington State University: 67–77.

Moore, H. W.; H. Bier. 2002. Predicting laminated veneer lumber properties from the sonic propagation time and density of dried veneer in the production environment. In: Proceedings of the 13th international symposium on nondestructive testing of wood, University of California, Berkeley, CA.: 89–96.

Pellerin, R.F.; Galligan, W.L. 1973. Nondestructive method of grading wood materials. Canadian Patent 918286.

Pieters, A.R. 1979. Ultrasonic energy: a new method for veneer grading. In: Proceedings, ASCE convention; 1979 April 2–6. Preprint #3534. Reston, VA: American Society of Civil Engineers.

Uskoski, D.A., Bechtel, F.K.; Gorman, T.M. 1993. Ultrasonic stress graded veneer. In: Proceedings, 1st international panel and engineered wood technology exposition; 1993 October 19–21; Atlanta, GA. San Francisco, CA: Miller Freeman.

Acknowledgment

Special thanks to Jim Allen, Vice President (retired), Metriguard, Inc., for providing an in-depth technical review and updated production statistics.

Chapter 11

Machine Grading of Lumber

William Galligan, Private Consultant
Keizer, Oregon

John Kerns, Manager
Wood Science and Engineering, Weyerhaeuser Company, Tacoma, Washington

Brian K. Brashaw, Program Manager
Forest Products Marketing Unit, USDA Forest Service, Madison, Wisconsin

Sorting lumber into classes suitable for an end-use is termed "grading." Grading is a nondestructive process, traditionally carried out by a visual evaluation of lumber characteristics known to affect strength and stiffness. Mechanical devices to enhance the grading process were introduced commercially to North America in 1963. These initial devices evaluated the stiffness of lumber on a piece-by-piece basis as part of a combined visual and mechanical process that evolved as machine stress rated (MSR) lumber. Starting with limited commercial ventures in 1963, the production of machine graded lumber exceeded 1 billion board feet by 1996 (Galligan and McDonald 2000).

As new mechanical devices, grades, and agency requirements developed, nomenclature for grades was created that was more specific to end uses and to agency requirements. Consequently, MSR and machine evaluated lumber (MEL) are the two types of machine graded lumber produced in North America under the auspices of the American Lumber Standard Committee (ALSC) (Galligan and McDonald 2000). The ALSC maintains the American Softwood Lumber Standard (Voluntary Product Standard PS 20, published by the National Institute for Standards and Technology) (NIST 2010) and in accordance with PS 20 administers an accreditation program for the grademarking of lumber produced under that system. (The American Lumber Standard (ALS) is an integral part of the lumber industry and provides the basis for acceptance of lumber and design values for lumber by the building codes throughout the United States. The ALSC is the guiding constituent committee; the ALS Board of Review is a certification and accreditation board.)

With regard to machine graded lumber, the Machine Graded Lumber Policy of the ALSC sets forth the procedures for grademarking of machine graded lumber conforming to the American Softwood Lumber Standard PS 20. The policy also includes requirements specific to the machine graded lumber process and to the approval of the machines (ALSC 2014). (The current lumber policy and list of machines is available at http://www.alsc.org/untreated_machinegraded_mod.htm.)

This chapter covers nondestructive evaluation (NDE) procedures that use mechanical devices as part of the grading process to assign allowable design properties to lumber. The mechanical device may measure physical or mechanical properties of a piece; the generic term "machine grading" will be used where specific technology is not cited. Grading systems in North America that incorporate mechanical devices most often include some visual evaluation. In-depth descriptions of the nondestructive tests used, specifically static bending, transverse vibration (vertical oscillation of a simply supported beam) and longitudinal stress wave (sometimes referred to as acoustic) are presented in Chapter 2, "Static Bending, Transverse Vibration, and Longitudinal Stress Wave Nondestructive Evaluation Methods."

This chapter traces the development of machine grading in North America with background research references. A discussion of some commercial processes is provided to indicate critical operating variables and interactions. This includes qualification and subsequent quality control of grades. Assessment and optimization of the grading system is included. The chapter closes with updates on recent developments including the development and use of acoustic based machine grading equipment.

Nondestructive Evaluation for Lumber Grading

Although mechanical grading made its commercial debut in North America in 1963, the nondestructive testing basis for the mechanical system had been explored at the research level for several years before. An example is the demonstration of the fundamental relationships published in 1962 and shown in Figure 11.1 (Senft et al. 1962). This figure suggests the usefulness of using modulus of elasticity (E) to predict modulus of rupture (MR, now commonly referred to as MOR). This, in fact, was the grading basis at that time under exploration for mechanical grading at Potlatch Corporation, Lewiston, Idaho, and the Western Pine Association, Portland, Oregon (McKean and Hoyle 1964). At that time, the relationship between density and strength shown

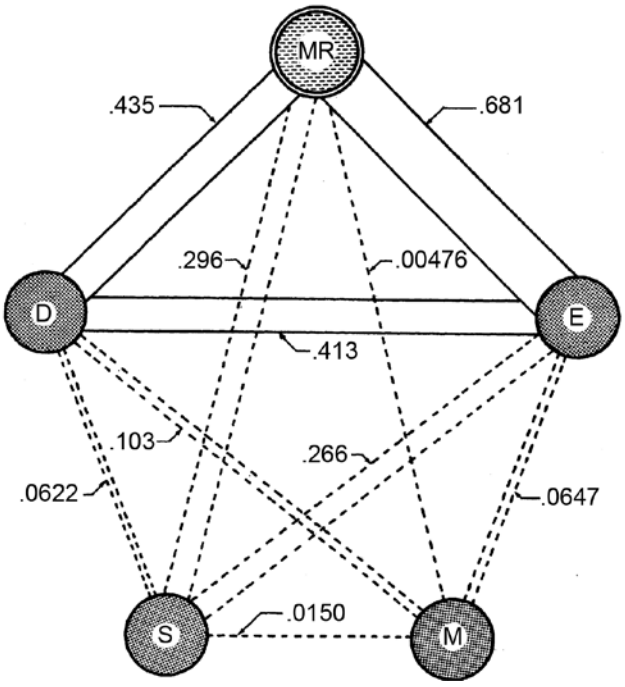

Figure 11.1—Diagram showing simple correlation between lumber variables. Based on studies at Purdue University. D, density; E, modulus of elasticity; M, moisture content; MR, modulus of rupture; S, slope of grain (Senft et al. 1962).

in Figure 11.1 was also being investigated using gamma ray and microwave through transmission; however, commercial development did not succeed until the early 1990s (Ziegler 1997).

Early development of machine lumber grading was marked by worldwide involvement and a commitment of Federal, State, and commercial funding. A 1968 compilation of research and development efforts estimated an accumulated 36 years of lumber-related research at seven Federal laboratories worldwide between 1961 and 1968, 28 years at U.S. universities, 15 years between Potlatch Corporation and the Western Pine Association (late 1950s and early 1960s), and 13 years among five machinery companies (Galligan and Moyer 1968). In recognition of this developing interest, the first symposium on nondestructive testing was held at the USDA Forest Products Laboratory (FPL) in 1963 (FPL 1964). It was followed in 1964 by a symposium that focused on "needs" for NDE, rather than on the technology (FPL 1965). In 1965, the first in a series of international symposia was sponsored by Washington State University (WSU), subsequently a joint effort by WSU and FPL (Galligan 1965). Although these symposia were not limited to lumber grading, development of machine grading technology was a principal component for the early symposia and has been reported on in subsequent symposia. A publication, *Fifty Years of Nondestructive Testing and Evaluation of Wood Research—International Nondestructive Testing and Evaluation of Wood Symposium Series*, was produced by the FPL (Ross and Wang 2012). The publication includes a brief history of the symposium series, summaries of each symposium, and searchable electronic copies of the proceedings from each symposium.

This chapter is limited to practices in the United States and Canada, with an emphasis on lumber grading machines approved by the ALSC Board of Review (ASLC 2014). Machine grading developments in other parts of the world have differing characteristics because of industry custom, governmental regulation, and commercial requirements. Early overviews of developments in other countries are found in Hoyle (1970). Galligan et al. (1986) published a list of early, important international research on machine lumber grading. Contemporary papers are found in the proceedings of the International Nondestructive Testing and Evaluation of Wood Symposium.

The advent of commercial NDE devices for lumber grading hinged on both technological and commercial feasibility. From the very beginning of NDE for lumber grading, these factors have been the subject of study and debate (Galligan 1965). The technology of machine lumber grading will be discussed first in this chapter, based on the two commercial machine-based predictors of strength, modulus of elasticity (MOE), and density.

Assignment of Design Properties

Machine grading methods provide measurements that have a predictive relationship to assigned properties. These grading systems sort lumber into categories to which allowable design properties can be assigned using standardized methodology. Regardless of the predictive mechanism (for example, density or MOE) and the extent of visual oversight, the output of the process is design properties that are not directly measured by the grading system. Grading systems, whether visual, mechanical, acoustic, or a combination, are based on predictive procedures.

Machine-Based MOE as the Predictive System

For the first 30 years of commercial practice, machine grading systems in the United States and Canada were based solely on stiffness measurement. Although the machines actually measured stiffness in some form, predictive relationships between properties were based on MOE, rather than stiffness, because adjusting for cross section allowed examination across sizes and directly addressed a fundamental wood property.

Predicting Modulus of Rupture

Early research emphasized MOR over MOE. Because the machines measured flatwise stiffness, flatwise MOE and MOR received attention. Figure 11.2 illustrates this early

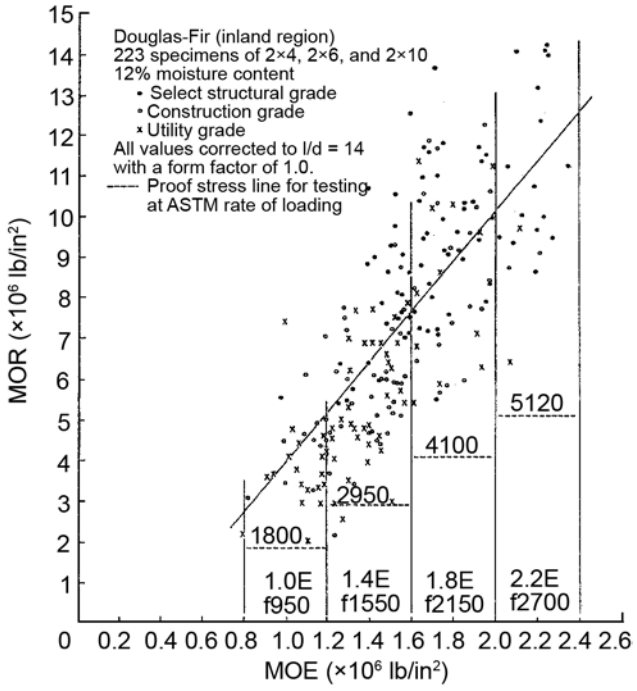

Figure 11.2—Relationship between flatwise modulus of rupture (MOR) and flatwise modulus of elasticity (MOE) for Douglas-fir lumber; both properties measured as plank (McKean and Hoyle 1964).

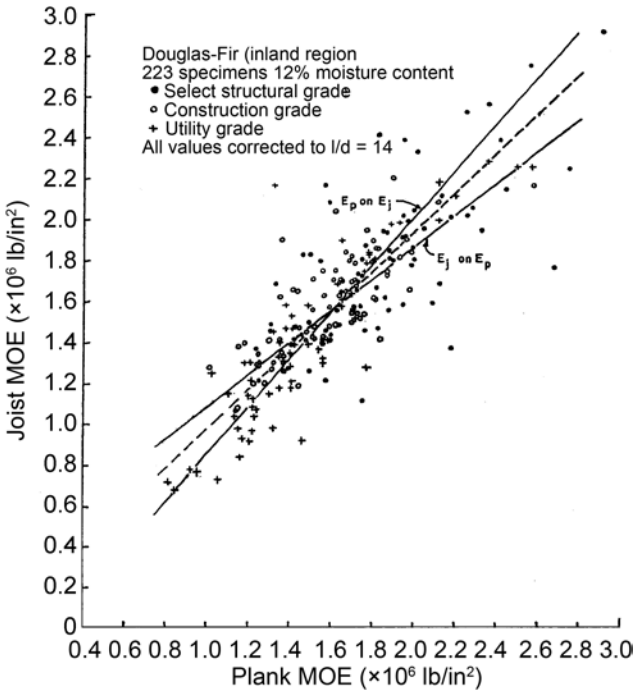

Figure 11.3—Relationship between edgewise and flatwise MOE (McKean and Hoyle 1964).

work (McKean and Hoyle 1964). Division of the flatwise MOE spectrum is based on potential flatwise MOR design values. Figure 11.3 shows the relationship between edgewise and flatwise MOE (McKean and Hoyle 1964). The variability between flatwise and edgewise MOE in Figure 11.3 is caused by the different effect of orientation of knots and other characteristics relative to that in the static test, the influence of shear in the different test modes, and the fact that different lengths of pieces were probably included within a piece of lumber tested flatwise (as a plank) or edgewise (as a joist) to obtain a proper MOE test. Adjustments were made for shear based on the "accepted" value for modulus of rigidity and a span/depth ratio of 14 in both orientations.

Interest in flatwise properties soon waned in favor of edgewise MOE and MOR because the latter were used more often in wood design. Consequently, even though the machine measurements were made in a flatwise orientation, research began to emphasize edgewise properties and industrial quality monitoring used the edgewise orientation. Johnson (1965) illustrated the different results and presentations possible because of the variety of test orientations (Fig. 11.4). In particular, Figure 11.4 shows the effect of selection of edgewise piece orientation ("worst" compared to "best" edge in tension) on the relationship between MOR and MOE. Flatwise MOE is the independent variable as a machine-related parameter, not the edgewise MOE "design value."

A summary of research on the relationship of MOE_{edge} to MOR_{edge} and other strength property relationships over a 20-year period was prepared by Hoyle in 1986 (Galligan et al. 1986). This compilation includes research in other parts of the world and distinguishes between reports with and without accompanying data.

Mechanical grading has focused primarily on the statistical relationship between MOE_{edge} and MOR_{edge}; however, this relationship is not statistically strong, often yielding R^2 values on the order of 0.6. The lack of statistical strength affects the efficiency of the grading system; nevertheless, it provides a practical level for grading. The relationship provides thresholds of stiffness below which unacceptable strength is unlikely to occur, as suggested for flat properties by McKean and Hoyle (1964) (Fig. 11.2). Figure 11.5 shows a superimposed 5% lower confidence level on MOR_{edge} for a small data set. From this plot, threshold MOE estimates can be established for machine operation. Figure 11.5 is from a publication by Galligan and McDonald (2000), which provides guidance for a producer wishing to study the feasibility of machine grading. This feasibility is measured as yield of machine grades against the yield of the traditional visual grading system.

Grading machines do not make the same measurements as those of the laboratory machines on which predictive research is carried out (see sections on MOE prediction).

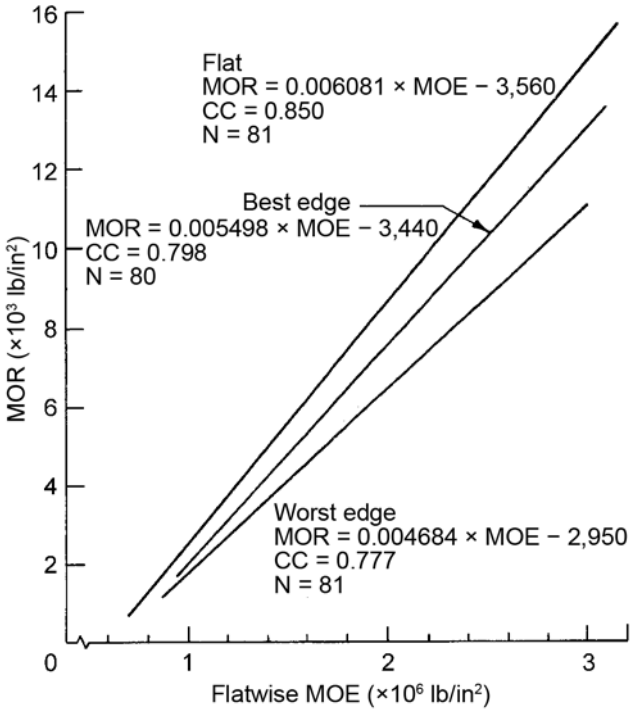

Figure 11.4—Influence of test orientation on relationship between MOR and MOE. MOR was measured flatwise. Edgewise "best" and "worst" edges were regressed on flatwise MOE (Johnson 1965).

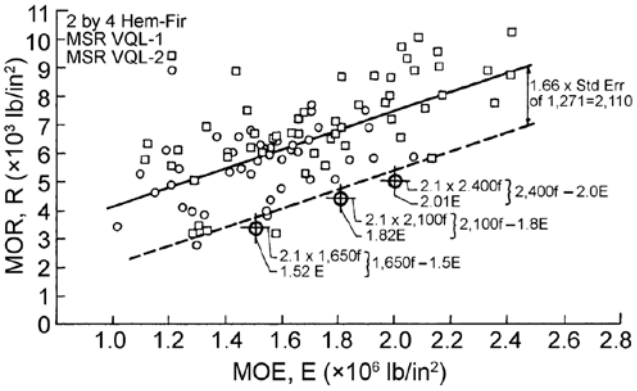

Figure 11.5—Estimation of MOE level required to maintain MOR_{edge} of a grade. Top line shows mean trend; bottom line is estimate of 5th percentile of MOR_{edge} distribution. VQL-1 and VQL-2 represent visual restrictions of 1/6 and 1/4 applied to edges of pieces (Galligan and McDonald 2000).

Some machine systems are based on measuring only the lowest stiffness in a piece, others seek the lowest stiffness but may also provide an average output, and others provide an average only. On the assumption that the lowest stiffness region of a piece is directly related to the strength of the piece, strength predictive models may show greater efficiency when the prediction is based on the lowest stiffness.

An example is provided by Corder (1965), who selected the minimum of nine static flatwise MOE measurements from each of 145 pieces and regressed this value against MOR_{edge}. This resulted in an improvement in the correlation of approximately 0.07 in R^2 (0.62 to 0.69) over using the average flat MOE in limited laboratory tests. Since this research, the capability of grading machines for identifying the lowest MOE value has improved and can be decidedly more sensitive than the Johnson laboratory measurements. Nevertheless, capabilities of industrial systems vary by machine and company practice. These installed systems are qualified through empirical testing of output, not by testing the predictive variables for their efficiency. Consequently, only careful yield studies of actual mill grade output can determine the relative actual efficiency of the stiffness measurement of a particular device in predicting MOR_{edge}.

The discussion of MOE versus MOR_{edge} is not complete without mention of visual restrictions. In practice in North America, most grading systems use visual grading restrictions or "overrides." The term override signifies the visual scrutiny of a piece after the grade category based on stiffness has been identified. If the visual characteristic is too large for the sort qualified by the stiffness, the piece is placed in a lower category— the grade sort suggested by stiffness alone is overridden. Visual overrides have two purposes: one is intended for improving appearance, and the second is designed to improve the efficiency of selection of strength properties. Both types of overrides can have an effect on sorting and consequently on assigned properties; however, strength-related criteria, such as restrictions on edge knot size, have the most effect on design values and must receive attention when considering the estimation of MOR_{edge}. In some operations, lumber is categorized by visual restriction prior to the stiffness test. This order may be chosen for operating efficiency but does not change the predictive function.

Although the term override continues to be used for historical reasons, this term tends to discount the contribution of the visual stress grading as part of the grading model. Modern machine grading usage in North America incorporates visual and mechanical criteria as part of qualification, grading, and quality control—these components act together to control performance and efficiency. Consequently, a preferred term for the visual stress-grading component is "criterion."

In response to a survey by the Federal Housing Administration of commercial machine-graded lumber in the first years of its existence, the industry adopted a sliding scale of restrictions on edge characteristics based on fraction of the cross section (Table 11.1) to increase efficiency of the grading system. This addition of another variable to the sorting criteria created a three-dimensional model, with some machine-estimated MOE_{flat} (from stiffness flat) and edge restrictions as two independent variables. The flexibility

Table 11.1—Traditional edge knot restrictions

Machine grade level	Edge knot restrictions
2100f and higher	1/6
1500f to 2050f	1/4
1200f to 1450f	1/3
900f to 1150f	1/2

and effectiveness of this three-dimensional model was later shown by FPL research (Ethington 1970). (Most written discussion focuses on the design property, MOE_{edge}, which is really not the predictor, itself predicted from a machine-measured flatwise stiffness.)

Commonly called "edge knot restrictions," the fraction of the cross section occupied by any strength-reducing characteristic, such as knots, distorted grain, or decay, is limited if the characteristic occurs at the edge of the piece. The allowable design value for bending strength is designated by the letter f and is expressed in pounds per square inch, as in 2100f. These restrictions began to appear in early grade rules (for example, WCLIB 1964, WWPA 1966). In recent years, some agencies address visual limitations in different ways; consequently, reference to the current rules of the appropriate agency is essential.

The variables of MOE and edge characteristics are not truly independent, because a characteristic such as a knot on the edge of lumber has a negative influence on stiffness. Nevertheless, the scheme of adding an edge restriction to an MOE limitation has formed the basis of all machine grading from approximately 1964 to the present. Consequently, the historical statement relating MOR to MOE in North American practice applies only if the third variable, edge restriction, is added. Furthermore, the actual machine stiffness measurement, varying by machine type, is not addressed. Empirical qualification systems and feedback quality monitoring insist on consistent, accurate estimation of design properties; however, they do not address efficiency.

Some rule-writing agencies have applied visual restrictions in different ways; the traditional limitations of Table 11.1 may not apply, and interpretation is often essential. It is important to refer to the most current version of agency grading rules. Of particular interest may be the enforcement of visual rules applying to those portions of the piece not measured by the grading machine. Some agencies have a long tradition of visual grading for knots and other strength-reducing characteristics, which is linked to the concept that the quality of the wood in the non-tested portions should approximate that in the areas that were subject to measurement. These rules stemmed from early resistance to machine grades by engineering and regulatory groups that were unaccustomed to the machine grade system. The addition of an "end-of-the-piece" rule that related quality to the test area enhanced the credibility of the system. Ancillary to these discussions, the industry found through observation in the early operating period that mill trimming practices could heavily bias the quality of the end of the piece. A particular concern was slope-of-grain in pieces cut from butt logs, but knots were also a serious concern. A visual rule to cover these issues is now commonly, but not uniformly, accepted. Specific visual criteria that may interact with machine measurement or grade yield may be required by customers in addition to the visual criteria of the grading rules. These customer-required criteria are in anticipation of further machining or fabrication, location of fasteners, or visual appearance.

In the balance of this chapter, bending strength will be referred to in terms of the allowable stress in bending (F_b), which is the 5th percentile MOR divided by 2.1; in machine grade labeling, this may be designated by the letter f after the allowable design strength value in bending.

Predicting Edgewise MOE

Edgewise MOE (MOE_{edge}) has wide application in design; consequently, it has received the greatest research emphasis and is included in the grade description for machine grades. MOE_{edge} can be estimated from flatwise measurements, as suggested in Figure 11.3; however, even though the machine is segregating in this flatwise mode, the relationship between flatwise and edgewise MOE is not often studied or emphasized in the industrial environment. The predictive relationship is strong; R^2 values of about 0.9 can be commonly experienced in laboratory tests. If the machine measurement output is an "average" MOE, this would emulate a laboratory flatwise average suggested by Corder (1965) as estimating MOE_{edge} with an R^2 of about 0.92; Corder's laboratory measurements based on minimum stiffness introduced a small amount of additional uncertainty, lowering the R^2 to about 0.88.

Many quality monitoring systems are based on direct measurement of MOE_{edge}, thus bypassing the information on the relationship between a standardized flatwise test and the machine-related flatwise measurement. This introduces "noise" from the edge versus flat relationship into the quality system if monitoring the efficiency of the actual machine flatwise function is an objective, such as part of grading machine quality control. If the mill quality monitoring system focuses only on adherence to the edgewise MOE specification and does not address machine function, this may be a moot point.

Predicting Flatwise MOE

The type of stiffness measurement made by a machine, the sampling on the piece, and the computation of the resulting data determine the results that will be obtained. Regardless of differences, however, flatwise stiffness remains the

fundamental measurement of many current North American machines. Consequently, if a producer wishes to qualify lumber for flatwise MOE (MOE_{flat}), the database from the actual machine measurement will probably relate more closely to this property than to any other. A discussion of MOE_{flat}, however, must address both measurement and assignment issues.

Even though MOE_{flat} is closely related to the flatwise stiffness measured in the grading machine, it was the late 1980s before a flatwise MOE was assigned as a design property for machine-graded lumber to be used in laminating (WCLIB 1989) and the 1990s when this flatwise MOE was assigned to MSR for use in 4 by 2 trusses, I-joists, and other applications (WCLIB 1997). In these applications, the flatwise MOE is defined by an American Society for Testing and Materials (ASTM) standard D 4761-13 test with a span/depth ratio of 100 using center-point loading (ASTM 2014).

As noted, commercial machines measure stiffness in different ways, such as different span/depth ratios, deflections, data collection, and computation. Consequently, the outputs produced by different machines—the signals produced after measurement and computation—will differ in relationship to a standardized ASTM static test. Machines that produce an "average" MOE by measuring stiffness of many samples along the length of a piece closely approximate the ASTM D 4761-13 MOE_{flat}. One example is

$$\text{ASTM D 4761 } MOE_{flat} = 1.22 \text{ (machine "average" MOE)} - 0.22 \quad (11.1)$$
$$R^2 = 0.99$$

based on 2 by 6 lumber ranging in MOE from 1.0 to 2.8×10^6 from two independent samples, one each from two different companies, both operating a machine that sampled frequently along the length and averaged the reading to produce an "average" MOE.

If the grading machine does not sample frequently along the length, takes only a small sample, or searches only for the lowest stiffness area of the piece, the relationship shown in Equation (11.1) will not apply. In many cases, a useful relationship may still result, but it will not be as robust as that shown in the equation. It is important to note that industrial machine-based measurements do not provide a database for comparability or standardization—all machine measurements depend upon calibration by standardized tests if the measurements are to be used on a comparative basis.

Because MOE_{edge} is assigned as an integral part of qualifying a machine grade, is there a relationship to a flatwise value to facilitate assigning an MOE_{flat} for design purposes? In early work, this relationship was found to be a function of grade and other factors. However, one principal element is the nature of the static test used to define the property because both MOE values are "apparent" values, that is, they are not corrected for shear and are influenced by the area of the piece being tested. The flatwise MOE is based on a test that is essentially shear free (span/depth of 100, center-point load); the edgewise test has a span/depth ratio of 21 with third-point loading. The result is a contribution (lowering) of the edgewise value as a result of shear.

However, edge characteristics such as knots may have a greater lowering effect on the apparent MOE_{edge} than do flat-face characteristics on the MOE_{flat} because of the predominance of critical edge characteristics in a test sample (resulting from mill sawing patterns). Consequently, studies conducted to relate MOE_{flat} and MOE_{edge} are influenced by mill practice as well as differences in the static tests employed.

In 1997, the West Coast Lumber Inspection Bureau (WCLIB) completed a survey of existing data on MOE_{edge} and MOE_{flat} and issued a report to the ALSC. The report concluded that trends in the data could be summarized to permit the design relationship $MOE_{flat} = MOE_{edge}$ + a "standardized increase," where MOE_{flat} is measured on a span/depth ratio of 100, center-point load, and MOE_{edge} is measured on a span/depth ratio of 21, third-point load. The approved increase was 100,000 lb/in^2 for MOE_{edge} values above 1.3×10^6 lb/in^2; a 50,000-lb/in^2 increase was selected for MOE_{edge} values of 1.3×10^6 lb/in^2 or less. This relationship was accepted and printed in grading rules in April 1997 (WCLIB 1997).

Establishing Fiber Stress in Tension Parallel to Grain

One of the earliest demonstrations of the basic relationship of tensile strength (F_t) to MOE was by Nemeth (1965). Before these tests of full-size lumber, the design value in tension was assumed equal to the assigned F_b. After these and a few other early observations, a ratio of 0.8 was assigned for F_t/F_b. Further changes were made in this relationship in 1969 as a result of accumulated research information. Table 11.2 chronicles these changes in the assignment process (Galligan et al. 1979).

In the early 1980s, the study of the relationship between tensile strength and MOE was rekindled with a series of proof-loading tests of more than 3,000 specimens of several species, sizes, and grades by the WCLIB (Galligan et al. 1993). This study illustrated that the ratio of F_t/F_b can be overstated and suggested verification of the assigned tensile value rather than use of the 1969 ratios as default values. As a result of this and subsequent work (Galligan and DeVisser 1998), the current practice is to use the 1969 ratios as a basic starting point. If qualification tests in tension justify use of a ratio different from that shown in Table 11.2, it must be supported by subsequent quality control. If the 1969 ratios are to be applied as a default, verification of assigned tensile values is required under ASTM D 6570-04(2010) (ASTM 2014e); if verification is not carried out, the default alternative is to use a ratio of tension/bending of 0.49, based on ASTM D 1990-14 (ASTM 2014a).

Table 11.2—Historical assignment of F_t/F_b ratio

Machine grade	Permissible edge characteristic	F_t/F_b ratio		
		Early 1960s	Mid-1960s	1969 to present
2400f–2.0E1	1/6	1	0.8	0.8
2100f–1.8E1	1/6	1	0.8	0.75
1500f–1.4E1	1/4	1	0.8	0.6
1200f–1.2E1	1/3	1	0.8	0.5

The grades shown in Table 11.2 are typical of those that dominated the selection of machine grades during the first approximately 15 years of production. In present practice, the values in the right column are subject to verification; some market grades may deviate from this schedule on the basis of test and quality control.

Galligan et al. (1993) illustrated the effect of piece width on F_b. The width effect was described by an exponent of 0.29 on width, the same factor used for visually graded lumber under ASTM D 1990-14. Because the machine grades examined were based on stiffness segregation, the tensile strength relationship for machine grades includes the average MOE of the test sample:

$$\text{Tensile strength TL} = 1869(\text{MOE}_{edge}/W^{0.29}) - 917 \qquad (11.2)$$

where TL is the 5% nonparametric tolerance limit (75% confidence) in pounds per square inch adjusted to a design value by a divisor of 2.1, W is the actual width of the piece (in.), and MOE_{edge} is the mean edgewise MOE of sample ($\times 10^6$ lb/in^2).

This relationship supports the current practice of requiring qualification of each width of a machine grade, regardless of the similarity of the sorting criteria.

Establishing Fiber Stress in Compression Parallel to Grain

Fiber stress in compression parallel to grain ($F_{c\parallel}$) was not studied extensively in the early work on MOE relationships. By 1964, however, the grading rules used a ratio of 0.8 for the relationship of $F_{c\parallel}F_b$ across all grades. In a 1968 review, Hoyle reported the positive correlations of $F_{c\parallel}$ on MOE in limited tests. The slope of the regressions was much lower than that reported for bending and for tensile strength on MOE (Hoyle 1968). The constant ratio of 0.8 for all grades was used until 1991, when it was replaced by the current relationship to correspond with similar changes for the visual grades:

$$F_{c\parallel} = (0.71F_b + 2061)/1.9 \qquad (11.3)$$

(for example, WCLIB 1991) where $F_{c\parallel}$ is allowable stress in compression parallel to grain (lb/in^2) and F_b is allowable stress in bending (lb/in^2). This formula follows the same format used for visual grades in ASTM D 1990-14 (ASTM 2014a). With use of this formula, $F_{c\parallel}$ is higher than previously for the lower grades and lower for grades above 2400f.

Assigning Specific Gravity, Fiber Stress in Shear, and Compression Perpendicular to Grain

From the earliest research until 1992, specific gravity, allowable stress in shear (F_v), and compression perpendicular to grain ($F_{c\perp}$) were assigned to machine grades by species with no differentiation by grade. These three properties are based on clearwood and are derived from ASTM D 2555-06(2011) (ASTM 2014b). The familiarity of these clearwood-based values and the lack of an accumulated database for machine grades made it expedient to use these properties in the same manner as in the visual grades. This practice did not make use of grade differentiation by MOE, and the higher machine grades suffered in end use by having specific gravity, F_v, and $F_{c\perp}$ properties that did not reflect the high level of F_b, F_t, and $F_{c\parallel}$ capability; that is, they were limited in certain design aspects by the value of the commercial species groups for these three properties. This practice has now changed. Each of these properties is discussed individually in the following text.

Specific Gravity—Until the late 1990s, specific gravity was not listed as an allowable property in the grading rules; however, it is used in critical applications, such as calculation of plating capacity (setting plate sizes for metal plate connected wood trusses). Specific gravity has also come to form the basis for other metal connectors such as nails and bolts (NDS 1991). Consequently, when the higher machine grades claimed increased capacity in allowable strength properties, use of the species specific gravity for all machine grades was a detriment to efficient use. This was particularly true for the higher grades of "lower" specific gravity species groups such as Hem–Fir. For example, the size of metal plates for trusses was selected on the species specific gravity of Hem–Fir, whereas the high machine grades of that species group could claim much higher strength properties than the specific gravity represented.

The variation of specific gravity by machine grade was reported in the late 1960s by Hoyle (1968). Even though the "relatively low" metal plate holding capacity assigned to the higher grades of "low" specific gravity species like true fir plagued the marketing of these grades for trusses, no action was taken to remedy this lack of alignment between strength properties and specific gravity until the 1980s. At that time, Frank Lumber Company (Mill City, Oregon) began the study of the effect of MOE segregation on the differentiation of specific gravity by grade, essentially building on the basic relationship between MOE and specific gravity shown by Senft et al. (1962) in Figure 11.1 and Hoyle (1968). Review of data on lumber specific gravity, collected over a period of several years, on several grades over four lumber widths verified that a useful trend of increasing specific gravity with MOE could be identified and maintained as a function

Table 11.3—Example of specific gravity assigned by MOE level to machine grades by WCLIB (1997)[a]

Species group	Grade modulus of elasticity ($\times 10^6$ lb/in^2)	Specific gravity
Douglas Fir	<2.0	0.50
	<2.0	0.51
	<2.1g	0.52
	<2.2	0.53
	<2.3	0.54
	<2.4	0.55
Hem–Fir	<1.6	0.43
	<1.6	0.44
	<1.7	0.45
	<1.8	0.46
	<1.9	0.47
	<2.0	0.48
	<2.1	0.49
	<2.2	0.50
	<2.3	0.51
	<2.4	0.52
Spruce–Pine–Fir South	All grades	0.36
Western Cedar	All grades	0.36
Western Woods	All grades	0.36

[a]Note the species effect. Some species groups have no standardized assignment by MOE level. Individual grade as assignments are possible with qualification by test and quality control.

of machine segregation. This relationship was clearly useful for both Douglas Fir and Hem–Fir and was independent of width.

By 1996, sufficient data had been collected by the Frank Lumber Company and the WCLIB to standardize the grade/specific gravity relationship for general machine grading rules for Douglas Fir and Hem–Fir. For the higher MOE grades, specific gravity values were specified, contingent upon the values being qualified by test and monitored as part of the WCLIB quality system (WCLIB 1997). Table 11.3 contains the values published by the WCLIB in 1997. Provisions of this type are agency dependent; for other species or geographical areas, the appropriate agency should be contacted.

Compression Perpendicular to Grain—Coincident with the study of the relationship of specific gravity to MOE, a study began of the other two "minor" properties, shear and compression perpendicular to grain. Initial emphasis was placed on compression perpendicular to grain ($F_{c\perp}$) because that property could limit bearing for higher strength grades when the species $F_{c\perp}$ value was used, particularly with Hem–Fir. Compression perpendicular to grain had been the subject of a series of publications in the 1970s when the design basis for the property changed from the proportional limit to the stress at 0.04-in. deformation. One result of these studies was the development of the relationship between deformation and specific gravity (Bendtsen and Galligan 1979). Consequently, in 1992, this information was used to develop a generalized relationship with specific gravity that could be applied to machine grades that were qualified and quality controlled for specific gravity:

$$F_{c\perp} = (2498.9\text{SPG}) - 537.7 \qquad (11.4)$$

(for example, WCLIB 1992) where SPG is specific gravity based on ovendry weight and volume at 12% moisture content and $F_{c\perp}$ is stress in pounds per square inch at 0.04-in. deformation. When stated on an ovendry volume and weight basis, the formula is

$$F_{c\perp} = (2252.4\text{SPG}) - 480 \qquad (11.5)$$

(for example, WWPA 1994). This relationship is used for many species groups (SPIB 1996; WCLIB 1997); however, reference to individual agency procedures should be made.

With this relationship, $F_{c\perp}$ can shift to higher values in step with other grade-related increases in other design values. The use of these increases is the prerogative of the manufacturer; if the specific gravity is not qualified and monitored or marketing does not claim the values for design, the default $F_{c\perp}$ value is the same as that for the visual grade, species, or species group.

Shear—The allowable design value for shear, F_v, is basically a clear wood property that has its roots in ASTM D 2555-06(2011) (ASTM 2014b). The data in this standard illustrates that this property is directly proportional to specific gravity. As the use of specific gravity for differentiating properties of MOE-based grades developed, increases in F_v by grade were also recognized to prevent limitations in use by the default species value. In 1992, this use was formalized in the WCLIB grading rules for western species:

$$F_v = 17.1 + (150.95\text{SPG}) \qquad (11.6)$$

(for example, WCLIB 1992), where SPG is specific gravity based on ovendry weight and volume at 12% moisture content and F_v is allowable shear stress in pounds per square inch. When stated on an ovendry volume and weight basis, the formula is

$$F_v = 20.6 + (136.08\text{SPG}) \qquad (11.7)$$

(for example, WWPA 1994). In July 1996, changes in the method of assigning shear values were made at the ASTM level for all structural lumber. These changes resulted in increased shear values and, for machine grades, a modified relationship for both western and southern species:

$$F_v = 40 + (266\text{SPG}) \qquad (11.8)$$

(for example, WCLIB 2000), where SPG is specific gravity based on ovendry weight and volume basis. These grade increases for F_v may be agency dependent with respect to both the assigned value and the criteria required by the agency.

F_v values that change by grade are optional for the manufacturer. Specific gravity must be qualified and monitored. If the manufacturer chooses not to use these values, the default value is that assigned to the species or species group.

Machine-Based Density as the Predictive System

As with stiffness-based machines, strength properties for density-based machines are determined through predictive relationships. In this case, density is used as the primary predictor for the strength properties. The strength of an individual piece of lumber ultimately depends on two properties: (1) the inherent clear wood strength given the individual species, density, and moisture content and (2) the strength-reducing defects contained within the piece, such as knots and grain distortions.

Conceptually, the predicted board strength can be represented as

Predicted strength = Clear wood strength × Effect of defects

The large differences in density between clear wood and strength-reducing defects (primarily knots) is used as the basis for identifying the size and location (effect) of these defects (Hansen and Schajer 1988; Schajer 2001).

Predicting Strength

Density profile data are obtained at regular intervals along the length and across the width of each individual board. The strength prediction procedure identifies and quantifies two significant features from these measured profiles: the mean clear wood strength and the localized increases in density resulting from knots. Knots are easily distinguished because their density values are about double that of the surrounding wood (Fig. 11.6).

The impact of a knot on clear wood strength is estimated from its size as determined by the size of the peaks in the density profile. The relationship between the size of the density peaks and board strength is established empirically through experimentation. With multiple scans across the width of the board, it becomes possible to estimate not only the relative size of the knot but also its location. Location of the knot relative to the edge of the piece is also important because it allows the application of different weighting factors depending on the location of the particular defect.

Because of the resolution of the density profile measurements, this technique allows estimates of the impact for each defect corresponding to localized areas separated by fractions of an inch. In addition, the measurements come from the interior of the wood and are not limited by what can be seen or interpreted from the surface. The empirically derived prediction algorithms for MOR (bending strength) will typically have R^2 values of 0.70 to 0.75, with standard error estimates of 1,300 to 1,400 lb/in^2. As with bending, the predicted tensile strength of the board is taken as the lowest value for all sections within the scanned density profile. However, unlike the loading for static bending tests, the applied loading for tensile testing is uniform throughout the piece and failures are more apt to occur at the predicted location during testing. The prediction algorithms for ultimate tensile strength (UTS) will typically have R^2 values of 0.75 to 0.80 with standard error estimates of 900 to 1,100 lb/in^2, which are somewhat better than the bending predictions. The predictive algorithms for all properties are considered proprietary information and have not been publicly disclosed.

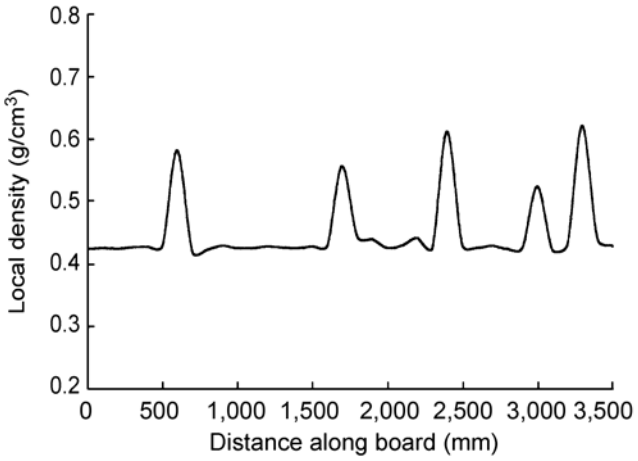

Figure 11.6—Density profile scan as measured along length of board.

Predicting Modulus of Elasticity

As previously discussed, MOE_{flat} is closely related to the measurements made by stiffness-based grading machines. This is not the case with density-based machines. The MOE determination is predicted on the basis of the density measurements. The predictive algorithm uses the average density of the piece and the localized grain deviation around the main defect. The MOE is also dependent on the microfibril angle within the cell wall. Juvenile wood and compression wood have high microfibril angles compared to normal and mature wood, which have low microfibril angles. The high microfibril angle reduces the MOE of the material, independent of density, and therefore introduces more variability into the MOE predictions. The R^2 values for the MOE predictive algorithms range from 0.65 to 0.75, with standard error estimates of 120,000 to 150,000 lb/in^2.

Establishing Compression Parallel to Grain

Although it is theoretically possible to develop predictive algorithms for compression parallel to grain ($F_{c\parallel}$), this has not yet taken place on a commercial installation. Grading of lumber with density-based machines currently uses the same formula as that for visual grades in ASTM D 1990-14 (ASTM 2014a), which is identical to that used for lumber graded with stiffness-based machines as previously discussed.

Assigning Specific Gravity, Fiber Stress in Shear, and Compression Perpendicular to Grain

Because density-based machines produce the same lumber grades as do stiffness-based machines, the assigned values

for shear and compression perpendicular-to-grain are the same regardless of which type of machine is used. The assigned values are species and grade dependent. However, because density-based machines measure density, they have the capability to more easily produce grades with nonstandard specific gravity values. Some mechanically graded lumber standards do allow the assignment of alternative specific gravity values, provided additional quality control procedures are implemented. This typically involves specific gravity testing on the same samples that are selected for bending or tension quality control testing. Density-based equipment currently in operation has density as one of the grade selection parameters, which may or may not be utilized in the grade selection process. Use of density depends on the objectives of the individual manufacturer.

Development of Stiffness-Based Grading Machines

Early Development

Two grading machines were responsible for the early acceptance of mechanical grading in the United States and Canada, the Continuous Lumber Tester (CLT) and Stress-O-Matic (SOM). The Potlatch Corporation of Lewiston, Idaho, conducted research and development for the CLT; the Western Pine Association of Portland, Oregon, developed the concepts behind the SOM. Commercial models of both machines were finalized by machinery firms. Although output from both the CLT and SOM was based on stiffness measurement, the operating concepts were different. Lumber passing through the CLT was bent flatwise, first in one direction and then the other. The lumber followed a prescribed radius; signal output was based on resistance to the curvature as measured with two electronic load cells, one for each bend orientation. The loading could be visualized as fixed ends and a centerpoint load measurement. Many samples (load signals) were taken along the length of the piece. The computer then processed the signals to produce a signal proportional to the "average" stiffness along the piece and a value corresponding to the lowest stiffness detected along the cross section. Signal output could be calibrated to correspond to a static test value, keeping in mind that the machine measurement system was not exactly duplicated by any standardized test. The stiffness of the ends of the piece was not measured because gripping the ends reduced the test length. The CLT was developed for dimension lumber of approximately 1.5 in. thick up to 12 in. wide; only moderate adjustment for thickness could be accommodated. These early machines were adjustable in speed; common operation was approximately 700 to 1,000 ft/min.

The SOM also bent lumber in the flatwise orientation; however, it loaded in only one direction with a third-point load on a total span of 48 in. This was principally a mechanical rather than electrical device. It imposed a load on the piece as it traversed the machine. If the piece deflected beyond a set limit, the load was reduced. The load reduction proceeded until the deflection limit was not reached. That last load level determined the stiffness sort for the piece, essentially estimating the lowest stiffness of the piece. The choice of load levels set the number of grade sorts. A speed of about 600 ft/min was maximum. This placed the machine in smaller mills or off-line with production speed planers. The SOM was designed for lumber not exceeding approximately 2.5 in. thick.

Capabilities of early U.S. and foreign grading machines were summarized by Galligan et al. (1977). In addition to the CLT and SOM, one machine that has been in relatively constant use in North America since the 1960s is the E-Computer. The E-Computer is a transverse vibration system that measures stiffness from the fundamental frequency of the flatwise vibration of a piece of lumber supported at the ends. One advantage of this system is the diversity of piece thicknesses that can be accommodated. The E-Computer is often thought of as only a research or survey tool. However, it has been in commercial use for sorting structural stock for cooling towers. In addition, for several years, the E-Computer has been the production line grading machine for several producers, grading dimension (nominal 2-in.) lumber destined for trusses or laminated beam construction. This system has low piece throughput, measured in pieces per minute, depending on the material handling requirements of the installation. In fact, the use of transverse vibration is the only NDE technique guided through a consensus standard, ASTM 6874-12, Standard test methods for nondestructive evaluation of wood-based flexural members using transverse vibration (ASTM 2014f).

Subsequent Developments

Advances in all segments of mechanical and electronic technology have greatly benefited mechanical grading. Early electronic "1960s quirks" disappeared with the advent of solid-state systems. Feedback to the operator and clarity of instruction have kept pace. Serious temperature effects that were poorly understood and not controlled in early operation are now better understood and controlled where possible. All machines now rely on computer control and output. Most modern machines focus on dimension lumber; however, they have different throughput capabilities. As a consequence, some machines continue to focus on high-speed planer mill operation, even exceeding 2,000 ft/min, whereas others are optimized for lower planer speeds or off-line applications such as grading laminating stock. Lumber producers that focus on large markets, such as lumber for metal-plate-connected trusses, often select a high-capacity machine to match planer capability. Machines of more limited capacity are well suited for operations that may focus on a limited number of grades and/or sizes.

In addition to machines that bend lumber to measure stiffness, machines use dynamic measurements, one transverse vibration and the other longitudinal or "stress wave"

propagation. These developments are based on scientific concepts first explored and proven in the 1960s at Washington State University (WSU). During the 1960–1970s time period, WSU conducted many field trials to demonstrate and evaluate early prototypes of both stress wave and transverse vibration machines. Collaborators included the Western Canadian Laboratory in Vancouver, BC, Canada; BC Hydro, Vancouver, BC, Canada; Western Pine Association, Portland, Oregon; West Coast Lumber Inspection Bureau (WCLIB) and the Western Wood Products Association, Portland, Oregon; Oregon State University, Corvallis, Oregon; Metriguard, Inc., Pullman, Washington; and the USDA Forest Products Laboratory (Madison, Wisconsin). Wood products tested included structural lumber, proprietary structural members, laminating lumber, and laminated beams. The WSU–Metriguard–FPL collaboration resulted in a prototype longitudinal stress-wave-based lumber grading machine using microprocessors to control the testing and analysis (Logan and Kreager 1975). These field trials provided basic experience with commercial wood products, established the viability of the testing concepts, and helped spur similar work in other laboratories and machinery companies in the United States, Canada, and many other countries.

Development of Density-Based Grading Machines

Early development of a commercial density-based grading system was conducted in the mid- to late 1980s. Weyerhaeuser filed a patent in 1988 for a method to estimate the strength or stiffness of a piece of wood by measuring its longitudinal density profile. This patent was issued in July 1990. Initial development by Weyerhaeuser involved the use of gamma ray absorption to measure density and generate density profiles. As development progressed, the use of a radiation source was discontinued in favor of using X-rays, which were found to be more suitable for commercial installations (Schajer 2001). The X-rays are similar to those used for baggage inspection in airports, allowing the machines to be classified as "Cabinet X-Ray Machines." In 1992, Weyerhaeuser licensed their density-based technology to CAE–Newnes, a commercial equipment manufacturer in Salmon Arm, British Columbia. The first commercial prototype was installed the following year in a lumber mill in southeastern United States.

CAE–Newnes and Weyerhaeuser continued to participate in a cooperative development project, and the first commercial X-ray lumber gauge (XLG) was built and installed in 1993. One advantage of this concept was the capability to scan the entire board from end to end. This capability eliminated the need to apply additional visual restrictions to the ends of the pieces as is common with stiffness-based machines. With its noncontact methodology, the XLG is capable of processing pieces as short as 4 ft and can operate with line speeds of greater than 2,000 ft/min. Its footprint of 8 by 8 ft generally allows easy inline installation or retrofit directly behind existing planers. The XLG is designed to process 2-by-3 to 2-by-12 dimension lumber. Both the ALS Committee and the Canadian Lumber Standards Accreditation Board accept the XLG as an approved mechanical grading machine.

Approved ALSC Machine Grading

A mill planning to produce machine-graded lumber under the ALS using bending, transverse vibration, longitudinal stress wave (acoustic), or density technologies must utilize an approved grading machine. These machines are approved under the ALSC through the application to and supervision of a sponsoring certified grading agency. The criterion for approval is that the machine demonstrates the ability to segregate lumber in accordance with the measurement system employed, such as stiffness or density measurement. The evidence provided shall include determination of measurement accuracy, including appropriate statistical analysis, relative to an accepted consensus standard. Information listing the manufacturer's recommended operational limits is required including information on machine measurement repeatability, variability, and recommended limits for the machine environment such as temperature, operational speed, and humidity, as well as lumber conditions such as temperature, moisture content, and warp.

Demonstration of the relationship between the measurements made by the machine system and design properties is not an integral part of ALSC approval of the machine. Requirements for this latter step are part of the machine qualification conducted on lumber of the candidate grades from the producing mill after installation and are specified by the operations manual of the ALS-approved agency. This qualification step not only includes the ability of the machine to make the claimed measurements but also incorporates agency-required visual criteria and specific tests, the influence of grade choices on sampling and test results, and mill operating variables such as sawing patterns and lumber dryness.

Detailed specifications for machine approval, agency accreditation, qualification procedures for a mill or facility by an agency, agency requirements for mill quality control, residual production, and ALSC monitoring of agencies is provided in the ALSC machine graded lumber policy (ALSC 2014). Approved lumber grading machines operating on the basis of stiffness and density measurement by ALSC are listed in the Appendix to this chapter. Although not included in this chapter, ALSC Board of Review identifies operation limitations for this equipment. Current information and limitations can be accessed at the ASLC webpage (www.alsc.org).

Application of Stiffness-Based Machine Grading

Machine Measurement

The intent of a machine grading system based on the measurement of stiffness is to sort using flatwise MOE. In

actuality, each machine makes a mechanical measurement that relates to stiffness response. In some machines, this will be the load to accomplish a target deflection; in others, it may be a deflection measurement under prescribed load. However, because the machine must grip or support the specimen in some fashion, the response is conditional upon the mechanical arrangement and processing of the signal. This can be compared to running a static test with the ends of the specimen firmly gripped in one case; in another case, to using "free–free" support at the ends; and in yet another case, to using intermediate supports so that the test section may be less than the length of the piece. Each static test arrangement in this example will yield a different apparent stiffness. In the same manner, the direct machine output is determined by the physical support, gripping, and measurement system.

In the early period of machine development, output could be quite simple, the average or the low point was based on a rudimentary measurement. Some early machines output only a voltage. It was the responsibility of the mill to calibrate this output to a grade level of MOE. Other machines produced only a "go–no go" response. Now, machines employ more sophisticated algorithms that can process the signal to account for multiple measurements and other variables.

Regardless of the type of machine, the objective is to determine a grade sort based on the machine measurement. However, because this is a machine-based stiffness measurement, not MOE, the machine output must be converted (calibrated) to relate to a recognized standard static measurement. Some modern machines output a reading in MOE, having done conversion in the machine algorithm for standard piece size and, perhaps, containing adjustments for the support and handling system of the machine. It is important to remember, however, that unless the machine also measures the size of each piece coincident with stiffness, the machine output is based on size assumptions. Consequently, the more accurately the lumber is machined, the more accurately the machine output will report apparent MOE.

Static MOE measurements are the basis for grade, not dynamic machine output. Supervisory agency procedures will specify the standard test to be used. This may be an edgewise or a flatwise test (or both), depending upon the target grade or grades. Without exception, these static tests will have specimen support and measurement systems that differ from the dynamic machine system. These differences produce different apparent stiffness values between the machine and the static test because of differing contributions of shear, differing specimen "samples," and computational choices.

The nature of the "sampling" influence needs to be understood, particularly by the quality control technician. Compared to a machine system, the static test may be able to sample more (flatwise test) or less (edgewise test) of the piece, depending on the machine configuration. Some machines take periodic readings and average the result; usually the static test selects one location to center the apparatus. If the output is based on only the lowest stiffness, the machine output may be either simple or complex (algorithm based). With a corresponding static test, it is often very difficult to identify the same location. Consequently, differences between the machine output and the static test cannot achieve agreement for all pieces even with the most careful calibration.

Influence of Lumber Characteristics

Individual pieces of lumber vary in size, moisture content, and MOE. All these characteristics vary both within and between pieces, even if the lumber is well manufactured.

Size

Within-piece variability in dimensions will be "inferred" as differences in MOE by stiffness-based machines when, in fact, the effect is one of changing moment of inertia, I, where $I = bh^3/12$, with b the width and h the thickness for machines making a flatwise measurement. Differences in thickness (h) thus have a cubic effect on apparent MOE, whereas width (b) differences have less influence. As an example, assume the finished thickness target is 1.500 in. If the planer is set in error at 1.450 in. (keeping in mind that the machine is still calibrated for 1.500), the lumber will have 90% of the flatwise stiffness it would have shown if it were correctly sized. Pieces that should have graded at 2.0E6 when correctly sized will grade instead as 1.8E6. If the mill problem is skip or another variation in thickness along the length of the piece, each area that is "thin" will contribute a low stiffness reading to the machine computer that searches for the lowest area (low point) or integrates readings to obtain a mean value.

The influence of variation in piece width is less than that of thickness, as shown by the formula for moment of inertia described in the previous text. Some machines have been set to grade rough or uneven-edged material through a calibration that conservatively compensates for width variation.

These significant influences of size control have forced machine grading mills to hold tight tolerances in planing. The best thickness control is maintained if planing and grading are done in tandem, that is, "in line." If machine grading is done "off line" sometime after planing, moisture gradient adjustment and moisture pickup or loss will affect the dimension at time of grading and thus the accuracy of the MOE prediction.

Moisture Content

The influence of within-piece variability in moisture content can be serious but subtle because often the lumber is not scanned and marked by moisture distribution. The change in apparent MOE with moisture content (MC) is essentially linear in the MC region of S–Dry or MC–15 lumber. An

increase of 1% in MC can result in a 1.7% decrease in MOE. A "wet spot" that is 10% higher than the average MC of a piece will indicate an MOE in that area 17% lower than would be the case if the piece were uniform in moisture (assuming a uniform real MOE).

In some species, "wet-spot" issues may not be as important as the general issue of variation in MC within a lot of lumber. If the goal is S-dry lumber, often the assumption is a mean of 15% and a maximum of 19%. This often implies a range in MC within the lot of about 12% to 19%. To illustrate the significance of this moisture range on machine grading using stiffness, consider the following two examples. In both examples, it is assumed that planing takes place at the time of grading so that the sizes are uniform.

1. If all pieces in a sample had the same MOE of 1.8E6 at a MC of 15%, but actually ranged in MC within the sample from 12% to 19%, the grading machine would evaluate the stiffness of the 19% MC pieces as if they were 1.7E6 and the 12% MC pieces as 1.9E6.
2. Assume a grading system intends to sort out (exclude from the grade) all pieces in the sample that are below 1.8E6 (on a 15% MC basis) as perceived by the machine. Assume the same sample distribution of moisture as in example 1. Pieces that are 19% MC when graded would have to be 1.9E6 at 15% MC to have the stiffness at 19% to pass the sort "cut-off" of 1.8E6.

These moisture-induced variations in MOE are real in the sense that they reflect real differences in stiffness. These effects are found in lumber graded by any system; however, for stiffness-based grading systems, moisture-induced variation in MOE introduces some of the variation in grading machine quality control. Therefore, the effect of moisture influences mills to improve and control drying through better drying technology and better judgment in selecting schedules, electronic controls, and in-mill operating priorities. Yield loss and loss of control of the grading process are the primary issues when mill control is lost or is imprecise.

MOE Variation

Modulus of elasticity is an intrinsic wood property; that is, it is controlled by the fiber orientations and growth patterns in the wood. If the lumber is sized accurately and the moisture content is well controlled, variation in stiffness sensed by the grading machine is caused by variation in MOE within the piece. Regardless of the method of stiffness sensing used by the machine, there is a linear relationship between the actual MOE and the machine-sensed stiffness. Variation in MOE along a piece occurs naturally and is the result of factors such as local slope of grain around a knot or knot hole, spiral grain variation along the length, slope of grain changes caused by distortion in the bole of the tree, growth patterns such as pith-associated wood (juvenile wood), and local incidence of abnormal wood such as compression wood. All these sources of variation can contribute to the measurement of the apparent piece stiffness and in fact are positive factors, because the response of stiffness-based machines to local slope of grain, for example, is an asset. Nevertheless, relating machine output to a static quality control test is sometimes difficult unless the laboratory measurement can accurately replicate both the location and level of stiffness of localized, low (or high) stiffness areas sensed by the machine.

Quality control tests to emulate the machine measurement of low stiffness have often used the Pelster tester, a static testing system developed originally to replicate the loading system of the Stress-O-Matic (Galligan and McDonald 2000). This system has been adopted by ASTM in Standard D 4761-13 (ASTM 2014d). Although the Pelster design may not match other grading machines as well as it does the Stress-O-Matic, this design has been shown to be useful for quality control with other machines since the relatively short span (48 in.) permits searching for variation in stiffness along a piece. Being able to sense the low area with a static test can be particularly critical in quality control where the lowest area of stiffness is a criterion for a grade boundary.

The sensitivity of the machine grading system, including the accuracy of the calculation method, to the average stiffness of the piece and/or the lowest stiffness is critical to the operating efficiency of the machine. This will be reflected in the sort criteria selected and verified by qualification and quality control. Some machines output both an average and a "lowest" signal, which can be used to set grade boundaries. The selection and balance between these selections depends on the grades selected, the number and interaction of the grades, the dependency of the strength test results to lowest stiffness criteria, and the dependency of the grade MOE to the "averaging" and/or "lowest" stiffness output. Because these decisions inherently interact with grade qualification, supervisory grading agency involvement is often critical in setting limits. Prequalification tests in concert with the agency are useful.

Relating Machine Measurement to Specifications and Quality Monitoring

Grading machines vary both from one another and from standard static tests in the manner of loading, sensing response, and analyzing the response. Further, machines produce a result that is used to estimate, not duplicate, the design properties, as previously shown. To further illustrate the "estimation" issue, consider the edgewise properties used most commonly for design.

Design specifications for wood structural design primarily focus on edgewise stiffness and strength properties, whereas grading machines that use bending measurements develop a "flatwise" value. Static laboratory tests used for quality monitoring commonly use flatwise tests but usually cannot completely emulate the grading machine. Further,

most bending machines use measurement and analysis procedures based on "sampling" as the lumber passes through the machine. The machine design determines the sample "size" (length of measurement), frequency of sampling, and the subsequent analysis that presents the machine output. Portions of the piece may not be stressed or included in the analysis. Stress-wave-based machines develop a unique longitudinal value; transverse vibration machines a different and unique value. Both of the latter may include essentially the entire length; however, all portions of the length do not have equal influence on the output (Murphy 2000).

Considering differences between machine measurement and output, design specifications, and mill quality monitoring, it is usually advised to focus separately on mill and specification needs. Specification tests may necessarily be arbitrary with respect to test method and orientation and placement of the piece in testing. Specification adherence will be controlled by supervisory agency requirements. For example, if testing an 18-ft 2 by 8 for adherence to agency requirement, the test span would be 152 in., approximately 70% of the piece length. Because one-third point loading is used, the full bending moment will be applied to only 51 in. (or 24%) of the piece. For agency qualification, the location of the test apparatus may be stipulated by a standard. If the piece is tested for both stiffness (MOE) and strength (MOR), both results are dependent upon a relationship to grading machine measurements that are not measured in the qualification or quality adherence tests. Thus, as noted above, successful adherence depends upon supervisory agency procedures for quality measurement and monitoring and upon consistent mill quality assurance procedures.

Mill quality assurance procedures, however, may be considerably different from the agency monitoring requirements. Because the intention is machine performance monitoring, rather than only adherence to the standard, the question is what laboratory tests can best emulate actual machine measurement. This includes selection of the location on the piece to collect the sample data and how to analyze the data.

One approach is to realize that the relationship between the specification MOE and the machine measurement, although very useful, is empirical and may be only loosely related to process control. For example, regardless of whether the grade being generated is an ALS joist grade (edgewise properties) or a laminating (lam) stock grade (flatwise properties), a bending-type grading machine based on "lowest" stiffness measures all pieces in the same empirical way. A grading machine that integrates short-span, flatwise values for an "average" value presents the piece output differently, and perhaps more closely to the lam grade MOE, but also only with an empirical relationship to the ALS joist grade MOE.

Static testing against the specification using edgewise tests, or even some flatwise tests, may be of limited value for process control if the machine makes no measurements in that configuration. On the other hand, the "lowest" stiffness area flatwise may be a useful predictor of bending edgewise or tensile strength. Is the short-span flatwise measurement by the machine accurate? This requires an effort to emulate the machine measurement with an appropriate short-span static test. Is the product a lam stock grade where the principal interest is in a long span flatwise MOE? How well do the machine measurement and algorithm predict the long-span flat value? For this, a full-length flatwise test (or at least a long "sample" of the length) is required to assess machine performance.

Where possible, it is desirable to use standard test methods for process control as well as for tests against the specifications. This enhances communication and prevents variation between and within tests. One example is the use of the Pelster test referenced in ASTM D 4761-13 for short-span MOE measurement. This may not be the optimum test to emulate all machine measurement systems; however, its status as a "standard" test permits comparative testing. Nevertheless, to the mill operating personnel focusing on process control, tests specifically developed to emulate machine function may be most effective. The ultimate goal is to have a quality system that meets the specification requirements of the supervisory agency while providing meaningful measures of machine function for operating personnel. Regardless of machine function, the mill quality assurance challenge is assessing the function of the machine on the line. The better this machine function is understood, the better the quality monitoring challenge is understood, and the better yield and adherence to performance can be achieved. Although some of these issues will be incorporated in mill qualification and subsequent quality control interaction with the supervisory agency, the mill will bear the primary responsibility for identifying and controlling the interactions between wood quality, machine function, and grade yield.

Application of Density-Based Machine Grading

Machine and Test Measurement

Predicting the bending strength of a board is generally much more difficult than predicting the strength at a single location on the board because the applied load during testing is dependent on the particular load arrangement used. The arrangement typically used to conduct bending tests on machine-graded lumber has uniform load only in the central span of the bending test (Fig. 11.7).

The entire test span, which is normally 21 times the depth of the piece, could be only slightly more than 30% of the total length of a 20-ft 2 by 4 board, with about 10% of the piece undergoing maximum stress. As total length of the test piece becomes shorter, a higher percentage of its overall length falls within the area of maximum stress. Further

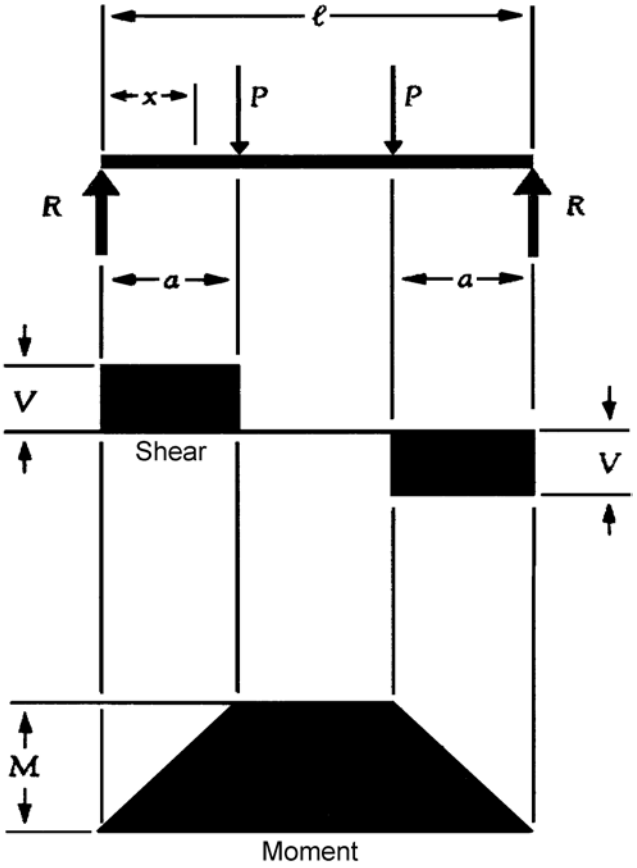

Figure 11.7—Symmetric placement of two equal concentrated loads (*P*).

complicating the bending prediction is the test protocol for machine-graded lumber, which typically allows the board to be oriented randomly (with regard to edge orientation). This will place the maximum strength-reducing defect on the tension edge for some tests and the compression edge for others. Normally an attempt is made to locate the maximum defect within the area of maximum moment, but this is not always possible because of its location within the piece; for example, the maximum defect might be too close to the end. Judgment must also be made as to which defect will actually be the most strength-reducing. These are some factors and challenges that must be considered when developing predictive algorithms for bending strength based on density measurements.

Influence of Lumber Characteristics

Size

Because predictive algorithms of density-based grading machines are based on an assumed constant "net" lumber dimension, actual variations from the assumed values induce variation in the results from the predictive formulas. Maintaining good size control at the planer will minimize size effects that might otherwise occur within and between pieces and will provide more accuracy in the strength and stiffness predictions.

Moisture Content

Moisture content is another variable that must be considered when predicting MOE using density-based equipment. The predictive algorithms are based on an assumed moisture content, generally 12%. Because water absorbs radiation just as wood does, higher MC material will appear to be denser and therefore stronger and stiffer. The error induced for strength prediction is relatively minor because the impact of the knots in the algorithms is much more influential. However, the error could be as high as 3% to 4% in the MOE predictions. Integrating an in-line moisture meter with a density-based machine has improved MOE prediction because it allows density to be calculated based on the actual MC of the piece rather than an assumed MC.

Although the addition of a moisture meter permits some improvement in MOE prediction, additional technology is currently under development to incorporate other MOE measuring technologies into density-based machines. When fully developed and integrated, it is likely that the MOE measuring capability of density-based machines will be on par with that of stiffness-based machines, with R^2 values expected in the 0.85 to 0.95 range.

Sampling

Density data are generated by passing X-rays through the lumber and measuring the amount absorbed by the wood. X-ray detectors located on the opposite side from the X-ray source measure the intensity of the X-rays after passing though the wood. The resulting intensity is dependent on source strength, local density of the wood material, length of the radiation path, and a material-dependent constant. Current X-ray detectors are about 1 in^2 in area. If intensity measurements are taken at approximately 1/2-in. intervals along the length of the piece, then a longitudinal density profile can be determined, as shown in Figure 11.6. The same procedure takes place across the width. Wider lumber requires the addition of multiple X-ray sources and detectors. Not only can the width and shape of the X-ray beam be adjusted, but the increment of the density measurements can be varied as well. The predictive algorithms have the ability to be fine tuned by either decreasing or increasing the density measurements to account for how much area is included in each predictive segment along the length of the piece. Finer resolution detectors (0.1 in^2) will be used in newer version of the XLG machine.

Commercial Machine-Graded Lumber

Truss Lumber

From the beginning of commercial machine grading in 1963 until about 1968, machine grade emphasis was on

development of grades for the growing metal-plate-connected roof truss market. The incentive for this emphasis came from the visual grading system of that era that set allowable design values significantly lower for "secondary" species such as white fir than for "primary" species such as Douglas Fir. Consequently, there was economic incentive to machine grade species such as white fir and Hem–Fir to develop grades that could compete with Douglas Fir in the roof truss application. The target grade of the time was 1500f. This grade could not be produced in a significant quantity by visual means from secondary species, but machine grade yields were economically attractive for white fir from the inland empire and Hem–Fir from coastal Oregon and Washington.

As the metal-plate-connected wood truss industry began to grow and the lumber for that use began to approach a commodity, an important but specialized outlet for the higher grades of machine-graded lumber was developed by Trus Joist Corporation. The use of Trus Joist's proprietary metal web industrial truss grew rapidly in the 1960s and 1970s. It required machine-graded lumber flanges of the higher grades such as 2100f and 2400f—grades higher than normally required in the metal-plate-connected wood truss industry, which was dominated by a relatively short-span house truss at that time. Trus Joist consumed a high percentage of the higher grades produced by the major western machine grading operations, thus providing an essential yield/economic balance for those mills: mid-level grades to the metal-plate-connected wood house truss market and high grades to the proprietary metal-web/wood flange industrial truss.

By the mid-1970s, continued development of the proprietary industrial truss market began to outstrip the supply of high grades from the few western producers. No machine grade production was available in Canada or in the southern United States in this early period. Trus Joist's needs resulted in the development of Canadian production; the company produced some machine grades in Georgia to support the developing market. Projections of ever-increasing needs for high-quality stock for the flanges of both the proprietary trusses and the newly developing I-joists contributed to the development of laminated veneer lumber by Trus Joist and, subsequently, less dependence on machine grades. Some high machine grades are still used on the flanges of metal-web industrial trusses. However, since the 1980s, the metal-plate-connected wood truss industry has developed longer span and industrial truss systems; at present, the full spectrum of machine grades, low to high, is consumed in that industry.

During the late 1970s, the major emphasis on efficient use of "secondary" species began to shift; interest increased in Canadian Spruce–Pine–Fir (SPF), Southern Pine, and Douglas Fir. The dominance of the 1500f grade, both visual and machine grades, had changed to a machine grade target of 1650f by the mid-1970s as a result of visual grade adjustments. Inquiries about the potential of machine grading spurred the issuance of a guide for lumber companies interested in estimating the potential benefits of machine grading (Galligan et al. 1977; superseded by Galligan and McDonald 2000).

The period 1980 to 2000 was one of continual refinement of the machine grade market. Acceptance of machine grades by the metal-plate-connected wood truss industry and by code and regulatory bodies is now unquestioned. Modern design procedures and associated design and analysis software for roof trusses permit evaluation of any potential grade and species. Machine grades in the range of 1500f to above 1800f are regarded as commodity items. Lower grades (for example, 1450f) can be used for some trusses; "high" grades (2100f and above) are used in higher performance trusses.

Producers have concentrated on optimizing yield, with a focus on allowable properties. What was once a small, orderly set of machine grades—such as 1500f, 1800f, 2100f—has now changed to include intermediate grades, such as 1950f. In fact, the Southern Pine Inspection Bureau (SPIB 2014) lists 28 MSR classifications ranging from a low of 1.4E–750f to a high of 2.4E–3000f.

The advent of qualification of grades in both tension and bending and an understanding of the width effect on strength led to grades with different combinations of strength properties. For example, where 2.0E–2400f with a tensile value of 1925t was accepted previously, combinations based on performance tests yielded grades such as 2.2E–2750f–1925t in 2 by 4 lumber, with a comparable grade of 2.3E in 2 by 6 lumber. The need for marketing uniformity sometimes added to this scenario by insisting on one property claim across lumber width, even though properties were different by width and controlled for quality on that basis. The advent of the machine evaluated lumber (MEL) grading system in the 1990s added another set of nomenclature and grade choices. The choice of grading system and subsequent uniformity across widths (affecting yield and efficiency in use) as opposed to individuality by width (affecting communication and design) is a commercial decision; however, these choices illustrate the evolution of the industry during the past 40 years.

Perhaps the most recent changes in the marketing of machine grading are applications beyond roof systems. In the 1960s, efforts to promote the use of machine stress rated (MSR) lumber in floor systems were not successful. Recent research suggests potential for this application where credit can be given in the design for the reduced variability in the machine grades, compared with the visual grades, that are accepted as the standard floor component (Suddarth et al. 1998). Lower grades of MSR, such as 1350f and 1450f, have shown feasibility as wall framing members (DeVisser et al. 1993; Galligan et al. 1994). In combination with

traditional roof and specialty truss markets, floor and wall applications offer a broader market base for MSR. This broadening of the use of machine grades has the ultimate potential of simplifying the grading operation within a mill (now a combination of many grading "systems" operating simultaneously) as well as marketing (now a combination of grades from a variety of grading "systems").

Laminating Lumber

In the late 1960s, one research objective was to explore the use of machine grades for glued laminated beams. In a cooperative project between Timber Structures, Inc. (Portland, Oregon), Oregon State University (OSU), and machine grade suppliers of the West Coast Lumber Inspection Bureau (WCLIB) and the Western Wood Products Association (WWPA), beams were constructed of MSR lumber and tested at OSU in 1968 and 1970 (Johnson 1969, 1971). Subsequent studies within the laminating industry led to the exploration of E-rated grades in the late 1970s. E-rated grades were standardized by AITC in the 1980s and recognized under AITC/AITC A190.1-2012. The current title of the standard is ANSI A190.1-2012, "American National Standard for Wood Products—Structural Glued Laminated Timbers" (ANSI 2012). (WCLIB acquired the AITC glulam design, grading, and certification programs in 2013 (WCLIB 2015). APA–The Engineered Wood Association replaced AITC as the Secretariat for ANSI standards ANSI/AITC A190.1, and AITC 117. ANSI/AITC A190.1-2012 was renamed ANSI A190.1-2012, retaining the same title. AITC 117-2010 was renamed ANSI 117-2010, retaining the title, "Standard Specification for Structural Glued Laminated Timber of Softwood Species.")

E-rated grades are selected by stiffness criteria based on "long-span" MOE (100/1 span/depth ratio, flatwise orientation) and by MC and visual criteria that ensure laminating quality for gluing and appearance (AITC 1988). There are no strength requirements for E-rated grades. For E-rated grades to be used in laminating, their knot characteristics and wood strength characteristics are considered in a manner similar to that used for visual grades in the referenced ASTM standard D 3737-12 (ASTM 2014c).

E-rated grades are compatible with MSR grading. The two systems can exist simultaneously in a grading operation if the criteria of both systems are maintained. The fact that an E-rated grade, which is not qualified for strength, is produced using the same machine as that for MSR production has created a legacy of confusion among both lumber producers and laminators who have not focused on the different requirements; that is, a history of calling an E-rated grade "MSR" because the lumber went through a machine has not enhanced the understanding of grading essentials.

In the 1980s, the WCLIB introduced tension testing (qualification) of MSR grades. This provided another avenue for machine grade use in laminating by meeting the requirements of lumber for the critical tension zone of the glued laminated beam. The traditional lumber for the tension zone, denoted by the nomenclature 302-24, 302-22, and 302-20, has to fulfill severe visual grading requirements to meet ASTM D 3737-13 (AITC 1988; ASTM 2014c). The performance requirements of these grades are tensile strength and MOE. Consequently, if an MSR grade is qualified in tension and meets the MOE requirements, grades "equivalent" to the 302 series can be developed. In addition to their MSR nomenclature, these MSR grades are labeled C14-24, C14-22, and C14-20 to show the correspondence to the 302 series. These labels are required to be ALSC-qualified and quality-controlled MSR grades where the qualification is in tension (AITC 1988). Because use of these grades is now common, the yield of tension zone material has benefited significantly.

Grade Labels

Machine grades are required to have a label that displays the grade and the species, MC category, mill of origin, identity as a machine grade, and supervisory agency (Figs. 11.8–11.10). Agencies may develop a unique format to display the required information. If the grade has been qualified for more than one category, for example as MSR and E-rated, this may be indicated by additional notation. Additional qualification of an MSR or MEL grade for a tension laminating grade such as C14-24 may not appear on the stamp; the qualification may be handled by correspondence. Stamps are permitted to carry other information essential to proper interpretation in end use. Mills must work closely with the supervisory agency for conformance to requirements. This is particularly important when two agencies are involved, for example, an ALSC grading agency that is supervising qualification of a laminating grade by test and subsequent quality control and an ANSI A190.1 agency that is concerned with proper interpretation and application of the grade in laminating.

Prediction of Production Potential

One challenge to potential producers of machine grades is prediction of production yield. The investment of production personnel and equipment alone justifies a thorough study; however, experience demonstrates that incorporation of machine grading affects the entire mill operation and consumes significant effort in marketing and sales.

In most instances, machine grading production will be added to an existing visual grading operation. In fact, usually more than one visual grading system is in place (for example, visual stress grading and visual appearance grading). The spectrum of visual grades and their respective yields are the source for the projected machine grades; yet, this will change the status quo in the visual grading to which the mill is accustomed. Consequently, an assessment of machine grade potential starts with a clear picture of the current visual grading systems—variability in species, grades, and

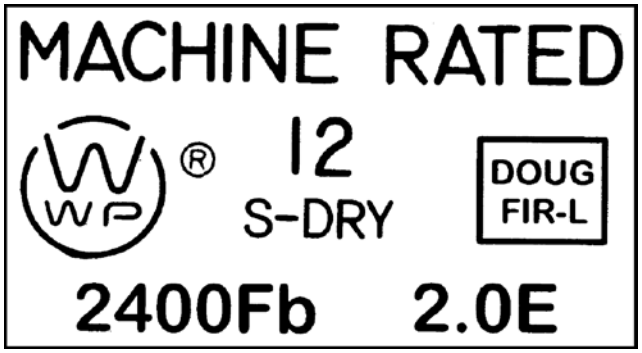

Figure 11.8—Facsimile of MSR grade stamp. Essential components include notations for grade, moisture content, species, MSR, mill, and agency. Other information may be incorporated as well.

Figure 11.9—Facsimile of MEL grade stamp.

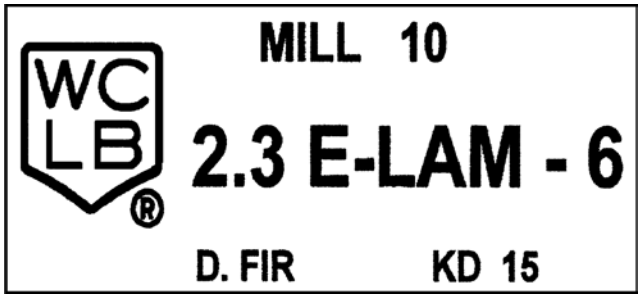

Figure 11.10—Facsimile of grade stamp for an E-rated grade.

yields, and interactions with mill operating variables (such as log sourcing, dry kiln operation, species selection, and market swings). The second step is market oriented: What machine grades does the mill wish to sell? The assessment of machine grade potential must have targets. Of course, these targets may be modified as knowledge is accumulated; however, the initial targets should be based on market analysis.

Once these two elements, understanding of the status quo and the selection of market targets, are completed, the assessment of production potential moves to mill studies using the grading criteria of the target grades, analyzing the yield by grade, and projecting the combined yields, including that of the visual grades. The process is described with examples and discussion in the FPL General Technical Report FPL–GTR–7, *Machine Grading of Lumber—Practical Concerns for Lumber Producers* (Galligan et al. 1977; Galligan and McDonald 2000). Originally published in 1977, FPL–GTR–7 was revised in 2000 to incorporate recent practice. The original histograms and data presentation were preserved; however, modern users of the projection method have often converted the process to a spreadsheet format for analysis. In FPL–GTR–7, grading based on bending stiffness is used to illustrate estimating grade yield. The same general approach can be used for other grading systems with appropriate changes in testing procedures.

A word of caution concerning mill yield projections is appropriate. Mill studies of this type invariably identify operating variables that the mill may wish to modify, regardless of the yield study output. These mill observations result from the focus on process by those best suited to identify the variables—mill operators and supervisors. Consequently, assumptions basic to the study, including log breakdown, edging and trimming practices, drying efficiency, and planing and grading, may be changed as a result of the attention given the assessment. These potential changes can affect machine grade projections and should be considered in completing the analysis.

Installation and Operation of Grading Machines

Machines for grading lumber vary widely in size, capacity, and installation. Some machines are suited for very high-speed production (potentially in excess of 2,000 ft/min velocity through the machine); others are more suited for lower capacity operations. The installations can vary widely as well. In the past, some machines were well suited for "off line" production and consequently required dedicated lumber infeed and outfeed equipment. Today, many machines closely couple to the planer where the feed is linear, whereas others, require lumber moving transverse to the grading unit. These factors influence capital cost, maintenance, and efficient material flow. Lumber handling for older systems are discussed in FPL–GTR–7 (Galligan and McDonald 2000). This publication provides actual mill flow patterns to aid estimating equipment needs and discusses environmental concerns of mill operation. Temperature, vibration, dust, and noise are all important considerations for measurement equipment. Because these concerns change as technology progresses, it is important to work closely with equipment manufacturers.

The operation of a grading machine has always required an investment in technician and/or quality control personnel beyond previous staffing. Without this added personnel, agency quality control requirements and maintenance of

the machine and its auxiliary devices are difficult to accomplish. As machines have become more sophisticated, electronic technician skills have become more important. Mills concerned about optimization of yield and process variables have found it desirable to have support personnel that understand wood properties, can participate technically with the supervisory grading agency, and communicate well within the mill operating structure, particularly in support of marketing. The lack of emphasis on these factors in the early days of machine grading contributed to many commercial failures.

Optimization of Machine Grading

Processing Interactions

The actual machine grading operation is one of the final processing steps in a mill. As a result, lumber that reaches the grading machine is the result of all previous processing steps. Because machine grading measures some physical or mechanical properties and also incorporates visually detected characteristics, the process is more sensitive to some processing steps than is visual grading. As noted previously, these include the effect of drying on stiffness measurement and the quality of surfacing on machine response. However, this sensitivity to processing extends well "upstream" to initial log selection, log breakdown, and all subsequent operations that affect the variable or variables measured by the machine system.

Log Selection and Primary Breakdown

The influence of log selection and initial breakdown is based on wood quality. This, in turn, is affected by the age of the tree and by the location of the log in the stem, as well as other variables. A number of log features can produce less desirable lumber. Machine grading will sense these features—a desirable result from a grading perspective. However, negative effects on grade yield may be countered somewhat by such practices as the proper selection of the log and the method of log bucking.

All trees contain juvenile wood; the proportion of this wood varies by the age of the wood and by log location in the stem. Juvenile wood is lower in stiffness and strength than is mature wood and directly affects the yield of machine grades. Butt logs often contain severe swell, which results in growth ring and fiber distortion in the lumber cut from this region. Severe taper and sweep can result in lumber with severe slope of grain, which is detected by some grading systems. Logs from leaning trees may contain compression wood (softwood species) or tension wood (hardwood species); both are termed abnormal wood and will reduce lumber yield of higher machine grades. The incidence of abnormal wood and its characteristics varies with species. In summary, the most fundamental wood characteristics observed in machine grade yield studies originate in and are controlled in large measure by tree and log selection.

Sawmill Processing

When the tree-length log is bucked into processing log lengths, the lumber quality scenario narrows in focus. Log length decisions interact with market desires for lumber length. Market desires for length vary by grade: for example, longer lengths for higher grades (longer span end uses) and shorter lengths for lower grades (wall and floor elements). However, grade can also interact—long length wood consisting of juvenile wood will not make a high grade. This is further confounded by the radial gradient of quality of the stem, generally low to high, pith to bark. Because the geometry of cutting rectangles from circles dictates that wide widths must be cut close to the pith, the grade influence of radial wood quality gradients interacts with lumber width. These variables all affect yield of machine grading systems that are sensitive to wood quality in the stem. This, in turn, affects market targets for the mill.

Mill edging and trimming operations are critical to any lumber grading system. They are particularly important to machine grading because grading machines will respond adversely to physical or mechanical characteristics in the lumber, such as slope of grain, that may have been avoided with better processing. Conversely, the machine system can respond positively to good wood such as higher density/higher stiffness wood next to acceptable wane from the outer part of the stem. If the machine grade target is E-rated laminating (lam) stock, edging for lam stock takes special attention and can be linked to discernable wood quality features. Good edging practices are rewarded.

It should also be noted that machines configured to capture stiffness or density measurements along the length of the board have the potential to optimize value by length and grade.

Drying and Planing

The importance of proper drying was discussed previously in this chapter. However, drying for structural applications often receives too little attention. Structural wood should not be produced with severe drying-related stress gradients that will encourage subsequent distortion. Wood that is dried at too high a temperature loses strength; lumber that is dried below approximately 8% to 10% MC has lost strength. Lumber that retains severe wet spots can reduce grade yield. Because machine-graded lumber is qualified by strength tests as well as by MOE, mill yield is affected by the processing decisions made prior to grading. MOE and density grading systems and subsequent quality control will not identify weak wood created by poor drying practices. Efficiency in drying is often measured by hours in the kiln or by British thermal unit (Btu) per charge. In a mill that produces structural material, especially by machine grading technology, drying efficiency includes consideration of grade yield and structural performance in qualifying tests and quality monitoring.

Lumber size and surface quality interact with drying practices as well as many "upstream" mill processing procedures. Surfacing quality is important to any system that must contact the lumber—as in stiffness-based machines that employ rolls and contact sensors. Holding tight planing tolerances is feasible with modern planers; this enhances yield coupled with good mill sizing and dry kiln practices. However, sizing tolerances are strict for machine-graded lumber destined for laminating. Good planing opens this market potential.

Grading Interactions

In most traditional visual grading mills, more than one grading system operates concurrently with little apparent confusion or conflict. The most prominent example is visual stress grades (such as #1 & Btr, #2, Standard) and appearance grades (C & Btr, for example) being graded on a chain at the same time. Because this is traditional and all decisions are visual, decisions of precedence are often merely based on price or value. With the introduction of machine grading, which involves nonvisual variables, decisions of precedence become somewhat more complicated and some rules are applied.

Concurrent Grading Systems

In most mills, the machine grading system operates concurrently with one or more other systems. In other words, all systems present options to the final grading decision. All systems compete for yield; price differentials exist for each piece of lumber. Three competing systems are common: ALS visual stress, ALS visual appearance, and ALS machine grade. Five systems are readily found: ALS visual stress, ALS visual appearance, ALS machine grade, ANSI E-rated, and foreign visual. Some mills will add further systems for proprietary grades.

Grading systems with different selection criteria will conflict when operating concurrently. Resolution of the conflict depends on either value-added comparison or arbitrary rules. Traditionally, clear lumber will have greater value than one of the higher machine stress grades. Consequently, even though a given piece of lumber could meet both the high stress requirement by a measured criterion (such as density) and the clear criteria by visual assessment, the higher valued clear piece would be selected. Likewise, some lumber will meet both visual stress grade and machine stress grade criteria. Although there may be a yield difference depending on the resource and grading criteria, the machine grade will often have a higher allowable design value for roughly the same visual criterion, which will translate to a higher market value. This is also where the arbitrary rule that governs precedence between visual and machine stress grade rules is applied.

The ALSC rule states that the highest visual stress grade that may be produced simultaneously with machine grades must be lower in bending stress value than that of the lowest machine grade being produced. This recognizes the comparative grading efficiency of the machine system and eliminates the risk of selecting visually stress-graded lumber from lots of lumber that had been rejected at that stress level by the quality-controlled machine stress system.

It is important that a producer consider grading system options prior to beginning machine grade qualification tests. Will pulling grades simultaneously affect qualification levels? Will competing grades be added in the near future and thus should be included now in sampling? Even if there were no effects on qualification levels, will noncurrent but anticipated grades affect yield significantly in the future? For example, there are no ALSC restrictions on nonstress grade selection concurrent with machine grades. Yet, if a nonstress grade removes a significant quantity of good wood from the resource, the mill may have trouble holding the necessary quality control levels or, more simply, the yield of the machine grade may reach an uneconomic level.

Laminating grades of L1, L2, and L3 are ALSC and ANSI nonstress grades commonly graded on the same chain as are visual and machine stress grades. Similarly, ALS and ANSI E-rated grades can be graded at the same time as stress grades. Mill-specific experience may show that this simultaneous grading does not cause conflict in qualification levels because of different selection criteria. However, in other mill scenarios, simultaneous grading may exert a measurable effect, and this almost always causes yield conflict. It is strongly advised that mills, in concert with their supervisory grading agency, examine potential grading scenarios and address them appropriately in qualification and subsequent quality monitoring.

Virtually all grades that are simultaneously on the grading chain interact in the overall yield. If one grade is changed (for example, criteria adjusted or grade removed), one or more other grades will be affected, either in performance, appearance, yield, or some combination of these. Understanding concurrent grading is critical to mill practice.

Optimizing Grades

Customer requirements change, grading technology improves, knowledge increases, and mill resources change. All these factors are dynamic—all have occurred during the maturation of machine grading. To respond, new levels of MOE and F_b have been developed. Traditional MOE/F_b/F_t relationships have been challenged by test and are now more flexible. The variety of machine grades, grading machines, and grading systems has increased. ASTM D 6570-04(2010) (ASTM 2014e) provides new guidance, a framework within which all allowable properties of machine grades can be examined, and the most appropriate method of assignment used.

There will always be a creative tension between marketing (the concomitant desire for maximum flexibility to adjust to the customer and stability), grading technology (which appears to yield an infinite variety of options, though limited

in actual practice by the nature of wood and knowledge), and mill operation (given finite resources and short-term goals). The mutual objective is to optimize the resource for yield to the mill and value to the customer. Close communication with supervisory agencies and customers is needed to make grade optimization effective.

In-Plant Assessment

Visualizing relative grade yield and possible grade potential with respect to actual strength performance of mill grades is often difficult in the mill environment, where the primary emphasis is on meeting (and not overstating) grade strength criteria. But how "rich" are the grades? What is the strength profile of each grade with respect to the adjacent grades in the grading matrix? Is there a potential for improved yield or for different grade combinations?

The evaluation of mill machine grades can be visualized as a matrix in which samples of each grade are proof-loaded to the design level of the highest grade. The performance of each grade is measured against both expected performance related to its design level, the percentage of pieces failing to meet requirements, and the percentage of pieces that would qualify for a higher strength grade if they could be identified in the grading system. If the grading system were perfect, exactly 5% of each grade would fall below the target value for the grade and each grade would be tightly grouped by strength into a unique group (that is, no overlap in strength between grades). The fact that both of these concepts are basically unobtainable in the practical world of mill grading was introduced by Miller (1964). Consequently, the matrix test of mill grades gives a real-world assessment of grades being produced. This look at machine grades actually in production is a useful tool to reassess both mill efficiency and market targets at intervals during production.

A more detailed presentation of the basics of grade matrix evaluation was published in Galligan (1985). A practical matrix example for a mill with four machine grades, including an explanatory diagram, appears in Galligan and McDonald (2000).

Recent Advances and Developments in Nondestructive Science and Commercial Applications

Nondestructive Science

Commercial machine measurements vary in load application and measurement. Also, static measurements conducted as a part of quality assurance programs differ from on-line machines. Consequently, the relationship between machine output and static calibration varies. Complexities in these relationships force empirical approaches and can thwart thorough analysis.

Several noteworthy scientific contributions regarding machine grading during the past 10 years begin to address these issues. Bechtel (2007) performed an in-depth analysis, based on fundamental engineering mechanics, of the effect nonuniform mechanical properties have on the measurement of stiffness, as currently practiced. Murphy (2000) developed a numerical solution for vibrating tapered beams. The method used approximation by portioning the beam into constant property short lengths. While directed towards solving a tapered beam problem, it accounts for mass density and moment of inertia changes along the length of the beam. Given that most pieces of structural lumber have considerable variation in properties along their length as a consequence of naturally occurring defects, the works of Bechtel and Murphy point out the inherent limitations of measurement systems currently used and lay the foundation for the next generation of analysis techniques used in commercial equipment.

Commercial Applications

During the past decade, significant growth in the use of mechanical grading concepts for structural lumber has occurred worldwide. Research and development efforts on the use of these concepts for grading lumber from a wide variety of species has taken place, the results of which are being implemented in Asia, Australia and New Zealand, Europe, North America, and South America. Many excellent scientific papers presenting results from these efforts are included in proceedings of the International Nondestructive Testing and Evaluation of Wood Symposia (Ross and Wang 2012).

In addition to widespread growth of mechanical grading of lumber utilizing bending type nondestructive testing technologies, there has been recent growth in the development and use of acoustic/stress-wave-based lumber grading systems. Several machine manufacturers, including Brookhuis Micro Electronics, Calibre Equipment Limited, Dynalese AB, Falcon Engineering, and Metriguard, Inc., now supply acoustic/stress-wave-based grading machines approved under ALS for grading structural lumber.

Integration of nondestructive technologies within a mill has been an important objective for maximum efficiency for many years. Advances in lumber size measurement and control in saw centers, intelligent scanning for trimming decisions, advanced drying monitoring and control, and effective moisture monitoring have made significant impacts and they are partners with good grading practices. It is now possible to add log scanning for anticipating lumber quality levels—in effect, moving nondestructive testing upstream in the mill to further enhance the overall mill grading quality processes. In-depth presentation of the science and application of nondestructive evaluation of logs is covered in detail in Chapters 8 ("Acoustic Assessment of Wood Quality in Trees and Logs") and 9 ("Laser Scanning of Logs and Lumber"). The science and technology

has advanced significantly and has resulted in development of commercially available tree and log grading systems.

Future Developments

Forecasting future developments is a perilous task and not fruitful in the context of this chapter. Rather, the appropriate emphasis is on deficiencies in current systems, that is, issues that can be objectives for the future. These issues can be grouped loosely in three categories: grading efficiency, integrated systems, and design reward. These categories are not intended to be all inclusive and are offered to spur creative future work.

Grading Efficiency

Although there are differences in the efficiency with which strength properties are estimated by existing strength predictors, efficiency, as measured by R^2, seldom exceeds 0.65. This means that approximately 40% of the variability in strength is not related to the property being measured for estimation purposes. This level of efficiency has been sufficient to sustain a machine grading industry only because it is more efficient than the visual grading system it supplements. This is not a strong endorsement. Increases in strength property estimation with practical mill measurements are seriously needed. An ancillary concern is that attention be given to the concomitant properties (such as MOE and shear) that are essential for design.

Integrated Systems

Many machine grading systems in North America make multiple mechanical or physical measurements. These systems include visual appraisal as well as the mechanical or physical measurement made by a device. Some of this visual appraisal is integrated into the process for predicting properties, for example, the size of the permitted edge characteristic. Another aspect of visual appraisal is cosmetic—no less important than the prediction of mechanical properties but not directly integrated into this process. In addition, size and MC are not only components of the grade description but also variables that affect mechanical property prediction. With few exceptions, all these grading-related variables are controlled independently in the production mill, yet most are not independent of each other. The previous statement on grading efficiency is further confounded by this simplistic treatment of a covariate process. Comprehensive integrated systems at the practical level are needed for mill operation.

Design Reward

From a mill perspective, the increased efficiency of a machine grading system compared with that of its visual counterpart is measured as yield—more yield of a given grade level or yield of grades not identifiable with the visual grading system. For about 40 years, this yield reward has been sufficient to satisfy the machine grading community. However, if the resource is being differentiated more efficiently, should this be reflected in design efficiency? Currently, there is design credit for machine-graded material in a limited number of applications such as compression chords of trusses, wall framing, and column design. However, it is utilized widely only in truss design. Except in the cases mentioned, the piece-by-piece machine grading and associated quality control are not rewarded in the marketplace by formal design recognition. Restricting all the reward for an expensive mill grading process to mill yield limits encouragement for improving the system. Design recognition of the quality-controlled, lot-based performance of machine-graded products should be an important goal. Proposed more than 40 years ago, this goal of comprehensive design recognition of the lot by lot efficiency of nondestructive testing of lumber by machine has yet to be achieved (Galligan and Snodgrass 1970).

Acknowledgment

We thank Don Devisser, Executive Vice President, West Coast Lumber Inspection Bureau, for his valuable comments.

Literature Cited

AITC. 1988. Manufacturing standard specifications for structural glued laminated timber of softwood species. AITC 117–88. (See latest edition.) Englewood, CO: American Institute for Timber Construction.

ALSC. 2014. Machine graded lumber policy. Germantown, MD: American Lumber Standards Committee. http://www.alsc.org/greenbook%20collection/UntreatedProgram_MachineGradedPolicy.PDF

ALSC. 2015. Grading machines approved by the board of review. Germantown, MD: American Lumber Standards Committee. http://www.alsc.org/greenbook%20collection/Grading_Machines.PDF

ANSI. 2012. American national standard for wood products—structural glued laminated timber. ANSI A190.1–2012. Tacoma, WA: American National Standards Institute/APA.

ASTM. American Society for Testing and Materials, West Conshohocken, PA. (See latest editions for current provisions.)

2014a. ASTM D 1990–14. Standard practice for establishing allowable properties for visually-graded dimension lumber from in-grade tests of full-size specimens.

2014b. ASTM D 2555–06(2011). Standard test methods for establishing clear wood strength-values.

2014c. ASTM D 3737–12. Standard practice for establishing stresses for structural glued laminated timber (glulam).

2014d. ASTM D 4761–13. Standard test methods for

mechanical properties of lumber and wood-base structural material.

2014e. ASTM D 6570–04(2010). Standard practice for assigning allowable properties for mechanically graded lumber.

2014f. ASTM D 6874–12(2014). Standard test methods for nondestructive evaluation of wood-based flexural members using transverse vibration.

Bechtel, F.K. 2007. Estimating local compliance in a beam from bending measurements. Part 1. Computing "span function". Wood and Fiber Science 39(2):250-259.

Bendtsen, B.A.; Galligan, W.L. 1979. Mean and tolerance limit stresses and stress modeling for compression perpendicular to grain in hardwood and softwood species. Res. Pap. FPL–RP–337. Madison, WI: U.S. Department of Agriculture, Forest Service, Forest Products Laboratory.

Corder, S.E. 1965. Localized deflection related to the bending strength of lumber. In: Proceedings, 2nd nondestructive testing of wood symposium; 1965 April; Spokane, WA. Pullman, WA: Washington State University: 461–472.

DeVisser, D.A.; Galligan, W.L.; Suddarth, S.K. 1993. Comparing machine stress-rated and visually graded lumber used in walls. Madison, WI: Forest Products Society. Wood Design Focus 4(3).

Ethington, R.L. 1970. Some stress-grading criteria and methods of grade selection for dimension lumber. Res. Pap. FPL–RP–148. Madison, WI: U.S. Department of Agriculture, Forest Service, Forest Products Laboratory.

FPL. 1964. Proceedings of the symposium on nondestructive testing of wood. Res. Note FPL–RN–040. Madison, WI: U.S. Department of Agriculture, Forest Service, Forest Products Laboratory.

FPL. 1965. Proceedings of the symposium on the needs for nondestructive testing in the forest products industries. Res. Note FPL–RN–080. Madison, WI: U.S. Department of Agriculture, Forest Service, Forest Products Laboratory.

Galligan, W.L., ed. 1965. Proceedings of the 2nd symposium on the nondestructive testing of wood; 1965 April; Spokane, WA. Pullman, WA: Washington State University.

Galligan, W.L. 1985. Reflections on model-based QC for MSR lumber. In: Proceedings, 5th symposium on nondestructive testing of wood; 1985 September 9–11; Pullman, WA: Washington State University: 613–644.

Galligan, W.L.; DeVisser, D.A. 1998. Evaluating the ratio of allowable tensile strength to allowable bending strength for MSR grades. Presented at annual meeting of Forest Products Society; 1998 June; Merida, Yucatan, Mexico.

Galligan, W.L.; McDonald, K.A. 2000. Machine grading of lumber: Practical concerns for lumber producers. Gen. Tech. Rep. 7 (Rev.). Madison, WI: U.S. Department of Agriculture, Forest Service, Forest Products Laboratory.

Galligan, W.L.; Moyer, L. 1968. A status report: Nondestructive testing of lumber. In: Proceedings, symposium "Focus 70"; 1968 September; Vancouver, B.C., Canada: Council of Forest Industries.

Galligan, W.L.; Snodgrass, D.V. 1970. Machine stress-rated lumber: challenge to design. In: Proceedings, American Society of Civil Engineering. Journal of Structural Division (ST12)96: (Pap. 7772): 2639–2651.

Galligan, W.L.; Snodgrass, D.V.; Crow, G.W. 1977. Machine stress rating: Practical concerns for lumber producers. Gen. Tech. Rep. FPL–GTR–7. Madison, WI: U.S. Department of Agriculture, Forest Service, Forest Products Laboratory.

Galligan, W.L.; Gerhards, C.C.; Ethington, R.L. 1979. Evolution of tensile design stresses for lumber. Gen. Tech. Rep. FPL–GTR–28. Madison, WI: U.S. Department of Agriculture, Forest Service, Forest Products Laboratory.

Galligan, W.L.; Hoyle, R.J. Jr.; Pellerin, R.F. [et al.]. 1986. Characterizing the properties of 2-inch softwood dimension lumber with regressions and probability distributions: Project completion rep. Madison, WI: U.S. Department of Agriculture, Forest Service, Forest Products Laboratory.

Galligan, W.L.; Shelley, B.E.; Pellerin, R.F. 1993. The influence of testing and size-variables on the tensile strength of machine stress-rated lumber. Forest Products Journal. 43(4): 70–74.

Galligan, W.L.; Suddarth, S.K.; DeVisser, D.A. 1994. The MSR alternative. Alexandria, VA: Construction Specifier.

Hansen, J.M.; Schajer, G.S. 1988. Density-based wood strength prediction. Weyerhaeuser Proprietary Res. Rep. 1988.

Hoyle, R.J. Jr. 1968. Background to machine stress grading. Forest Products Journal. 18(4): 87–97.

Hoyle, R.J. Jr. 1970. Experiences with MSR grading in other countries. In: Hoyle, R.J., ed. Machine stress-rated lumber. Proceedings, 3rd short course. Pullman, WA: Washington State University.

Johnson, J.W. 1965. Relationships among moduli of elasticity and rupture: seasoned and unseasoned coast-type Douglas Fir and seasoned Western Hemlock. In: Proceedings, 2nd symposium on nondestructive testing of wood; 1965 April; Spokane, WA: Pullman, WA: Washington State University: 419–459.

Johnson, J.W. 1969. Flexural tests of large glued-laminated beams made of nondestructively tested lumber. Rep. T–26. Corvallis, OR: Oregon State University, Forest Research Laboratory.

Johnson, J.W. 1971. Design and tests of large glued-laminated beams made of nondestructively tested lumber. Report T–27. Corvallis, OR: Oregon State University, Forest Research Laboratory.

Logan, J.D.; Kreager, P.S. 1975. Using a microprocessor: a real-life application. Part 1—hardware. Computer Design, September, 1975. p. 69–77.

McKean, H.B.; Hoyle, R.J. Jr. 1964. Stress-grading method for dimension lumber. Special Tech. Pub. 353. Philadelphia, PA: American Society for Testing and Materials.

Miller, D.G. 1964. Effect of tolerance on selection efficiency of nondestructive strength tests of wood. Forest Products Journal. 14(4): 179–183.

Murphy, J.F. 2000. Transverse vibration of a simply supported frustrum of a right circular cone. JTEVA 28(5): 425-419.

NIST. 2010. Voluntary product standard PS 20-10. Gaithersburg, MD: National Institute of Standards and Technology. 50 p.

NDS. 1991. National Design Specification. (Formerly published by the National Forest Products Association) (See latest edition.) Washington, DC: American Forest and Paper Association.

Nemeth, L.J. 1965. Correlation between tensile strength and modulus of elasticity for dimension lumber. In: Proceedings, 2nd symposium on nondestructive testing of wood; 1965 April; Spokane, WA. Pullman, WA: Washington State University: 391–416.

Ross, R.J.; Wang, X. 2012. Nondestructive testing and evaluation of wood—50 years of research: international nondestructive testing and evaluation of wood symposium series. General Technical Report FPL–GTR–213. Madison, WI: U.S. Department of Agriculture, Forest Service, Forest Products Laboratory. 6,702 p.

Schajer, G.S. 2001. Lumber strength grading using X-ray scanning. Forest Products Journal. 51(1): 43–50.

Senft, J.S.; Suddarth, S.K.; Angleton, H.D. 1962. A new approach to stress grading of lumber. Forest Products Journal. 12(4): 183–186.

SPIB. 1996. Standard grading rules for Southern Pine lumber. Pensacola, FL: Southern Pine Inspection Bureau.

SPIB. 2014. Machine stress rated lumber design values. Pensacola, FL: Southern Pine Inspection Bureau. http://www.spib.org/pdfs/design-values-msr-mel-2014.pdf

Suddarth, S.K.; Galligan, W.L.; DeVisser, D.A. 1998. Achieving equivalence in floor deflection performance with differing lumber grading systems. Forest Products Journal. 48(6): 61–65.

WCLIB. West Coast Lumber Inspection Bureau, Portland, Oregon.

1964. Standard grading and dressing rules, Rules 15, September 1, 1964.

1989. Standard grading rules for West Coast lumber, Rules 16, 1989.

1991. Standard grading rules for West Coast lumber, Rules 17, September 1, 1991.

1992. Standard grading rules for West Coast lumber, Rules 17, 1992.

1997. Standard grading rules for West Coast lumber, Rules 17, Supplement VIII(B), April 24, 1997.

2000. Standard grading rules for West Coast lumber, Rules 17, 2000.

2015. Don Devisser. Personal communication.

WWPA. Western Wood Products Association, Portland, OR.

1966. Mechanical stress rating rules, Supplement 1, 1965 Standard grading rules, January 1, 1966.

1994. Western lumber grading rules 95, October 1, 1994.

Ziegler, G. 1997. Machine grading processes for softwood lumber. Madison, WI: Forest Products Society. Wood Design Focus. 8(2): 7–14.

Appendix—ALSC-Approved Machine Manufacturers Known to be in Commercial Production at Time of Publication (ALSC 2015)

For detailed information on approved models, refer to ALSC (www.alsc.org).

Manufacturer	Method
Brookhuis Micro Electronics Institutenweg 15 7521 PH Enschede Enschede, Netherlands www.brookhuis.com	Stress wave/acoustic
Calibre Equipment Limited PO Box 2783 Wellington, New Zealand calibre-equipment.com	Stress wave/acoustic
Conception R.P., Inc. 405 Galilee Ave, Quebec, QC, Canada, G1P 4M6 www.conceptionrp.com	Bending
CRiQ, Centre de recherche industrielle du Québec 333 rue Franquet QC, G1P4C7, Canada www.criq.qc.ca	Bending
Dimter GmbH Maschineenfabric Illertissen, Germany www.weinig.com	Density Stress wave/acoustic
Dynalyse AB Brodalsvägen 7, SE-43338 Partille, Sweden www.dynalyse.se	Stress wave/acoustic
Falcon Engineering USA 4475 Mission Blvd #234 San Diego, CA 92109 www.falconengineeringusa.com	Stress wave/acoustic
Lucidyne Technologies, Inc. 155 SW Madison Ave. Corvallis, OR 97333 www.lucidyne.com	Density
Measuring and Process Control Ltd. Unit 2 Tabrums Industrial Estate, Tabrums Lane Battlesbridge, Essex, SS11 7QX UK www.mpcuk.co.uk	Bending
Metriguard, Inc. 2465 NE Hopkins Ct, PO Box 399 Pullman WA 99163 USA www.metriguard.com	Bending Transverse vibration Stress wave/acoustic
Microtec Via Julius-Durst Str. 98 39042 Bressanone/Brixen (BZ), Italy www.microtec.eu/en	Stress wave/acoustic Density
USNR 1981 Schurman Way Woodland, WA USA 98674 www.usnr.com (approved under Newnes Machine Ltd. Company)	Density
Weyerhaeuser PO Box 9777 CH 2C27 Federal Way, WA 98063	Density

Chapter 12

Inspection of Timber Structures Using Stress Wave Timing Nondestructive Evaluation Tools

Robert J. Ross, Supervisory Research General Engineer
Forest Products Laboratory, Madison, Wisconsin

Roy F. Pellerin, Professor Emeritus
Washington State University, Pullman, Washington

The purpose of this chapter is to provide guidelines on the application and use of the stress wave timing inspection method in locating and defining areas of decay in timber structures. Practical procedures for field testing, workable forms for gathering evaluation data, and guidelines for interpreting data are provided. This information was derived from research that quantified the ability of stress wave timers to detect decay in wood, from laboratory and field studies of deteriorated timber bridges, and most importantly from the experience of timber bridge inspectors familiar with the use of commercially available devices. A table that lists current manufacturers of these devices is included. Properties of wood and important aspects of wood deterioration are also reviewed to provide those who are unfamiliar with wood the basic information necessary to detect decay.

This chapter was originally published in 2014 as chapter 3 of the *Wood and Timber Condition Assessment Manual, Second Edition*, a Forest Products Laboratory General Technical Report:

> White, Robert H.; Ross, Robert J. (Eds.). 2014. Wood and timber condition assessment manual: second edition. General Technical Report FPL–GTR–234. Madison, WI: U.S. Department of Agriculture, Forest Service, Forest Products Laboratory. 93 p.

Principles of Stress Wave Nondestructive Testing for Condition Assessment

As an introduction, a schematic of the stress wave concept for detecting decay within a rectangular wood member is shown in Figure 12.1. First, a stress wave is induced by striking the specimen with an impact device (such as the hammer shown in the illustration) that is instrumented with an accelerometer that emits a start signal to a timer. A second accelerometer, which is held in contact with the other side of the specimen, senses the leading edge of the propagating stress wave and sends a stop signal to the timer. The elapsed time for the stress wave to propagate between the accelerometers is displayed on the timer.

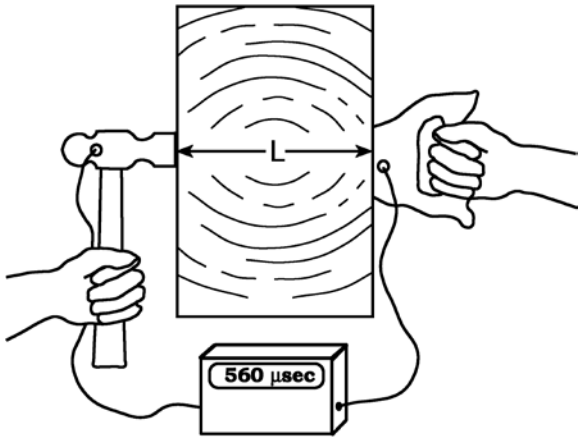

Figure 12.1—Stress wave timer.

The velocity at which a stress wave travels in a member is dependent upon the properties of the member only. The term ultrasonic and sonic refer only to the frequency of excitation used to impart a wave into the member. Ultrasound frequencies begin at 20 kHz; sonic frequencies are between 20 Hz and 20 kHz. All commercially available timing units, if calibrated and operated according to the manufacturer's recommendations, yield comparable results.

The use of stress wave velocity to detect wood decay in timber bridges and other structures is limited only by access to the structural members under consideration. It is especially useful on thick timbers or glued-laminated (glulam) timbers ≥89 mm (≥3.5 in.) where hammer sounding is not effective. Access to both sides of the member is required.

Because wood is an organic substance, material properties and strength vary in accordance with the direction wood is hammered compared with the cell structure orientation. Hammering the end grain of a beam or post will cause a primarily longitudinal shock wave along the length of the

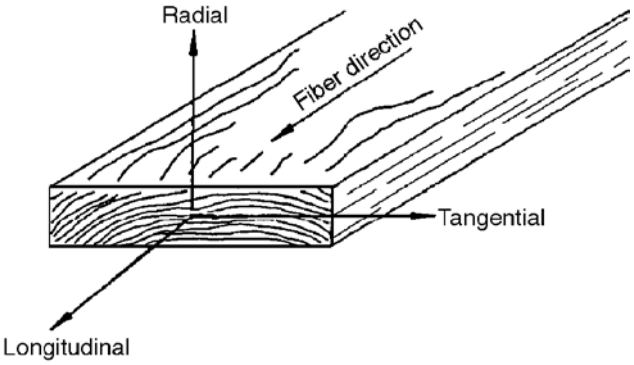

Figure 12.2—Three principal axes of wood with respect to grain direction and growth rings.

cell structure in the timber. Hammering the side or top of the beam will cause a wave across or transverse to the wood cells. Cells are arranged in rings around the center of the tree.

The velocity at which a stress wave propagates in wood is a function of the angle at which the fibers of wood are aligned (which is also a determinant of other physical and mechanical properties). For most structural members, fibers of the wood align more or less with the longitudinal axis of the member (Fig. 12.2).

Stress wave transmission times on a per length basis for various wood species are summarized in Table 12.1. Stress wave transmission times are shortest along the grain (parallel to the fiber) and longest across the grain (perpendicular to fiber). For Douglas-fir and Southern Pine, stress wave transmission times parallel to the fiber are approximately 200 μs/m (60 μs/ft). Stress wave transmission times perpendicular to the fiber range from 850 to 1,000 μs/m (259 to 305 μs/ft).

Effect of Ring Orientation

Researchers have determined that the longest transverse-to-grain transmission times are found at a 45° orientation to the annual rings. The shortest is about 30% faster in a path that is radial (Fig. 12.3). Table 12.2 and Figure 12.4 show stress wave transmission time for wood of good quality at 12% moisture content. These values can vary ±10% for species variation. These times are based on an assumed stress wave transmission time of 668 μs/m radially, 800 μs/m tangentially, and 995 μs/m at 45° to grain.

Effect of Decay

The presence of decay greatly affects stress wave transmission time in wood. Table 12.3 summarizes stress wave transmission values obtained from field investigations of various wood members subjected to degradation from decay. Stress wave transmission times perpendicular to the grain are drastically increased when the member is degraded. Transmission times for nondegraded Douglas-fir are approximately 800 μs/m (244 μs/ft), whereas severely degraded members exhibit values as high as 3,200 μs/m (975 μs/ft) or greater.

Table 12.1—Summary of research on stress wave transmission times for various species of nondegraded wood

Reference	Species	Moisture content (% OD)[a]	Stress wave transmission time (μs/m (μs/ft))	
			Parallel to grain	Perpendicular to grain
Smulski 1991	Sugar maple	12	256 to 194 (78 to 59)	—
	Yellow birch	11	230 to 180 (70 to 55)	—
	White ash	12	252 to 197 (77 to 60)	—
	Red oak	11	262 to 200 (80 to 61)	—
Armstrong et al. 1991	Birch	4 to 6	213 to 174 (65 to 53)	715 to 676 (218 to 206)
	Yellow-poplar	4 to 6	194 to 174 (59 to 53)	715 to 676 (218 to 206)
	Black cherry	4 to 6	207 to 184 (63 to 56)	689 to 620 (210 to 189)
	Red oak	4 to 6	226 to 177 (69 to 54)	646 to 571 (197 to 174)
Elvery and Nwokoye 1970	Several	11	203 to 167 (62 to 51)	—
Jung 1979	Red oak	12	302 to 226 (92 to 69)	—
Ihlseng 1878, 1879	Several	—	272 to 190 (83 to 58)	—
Gerhards 1978	Sitka spruce	10	170 (52)	—
	Southern pine	9	197 (60)	—
Gerhards 1980	Douglas-fir	10	203 (62)	—
Gerhards 1982	Southern pine	10	197 to 194 (60 to 59)	—
Rutherford 1987	Douglas-fir	12	—	1,092 to 623 (333 to 190)
Ross 1982	Douglas-fir	11	—	850 to 597 (259 to 182)
Hoyle and Pellerin 1978	Douglas-fir	—	—	1,073 (327)
Pellerin et al. 1985	Southern pine	9	200 to 170 (61 to 52)	—
Soltis et al. 1992	Live oak	12	—	613 to 1,594 (187 to 486)
Ross et al. 1994	Northern red and white oak	green	—	795 (242)

[a]OD, ovendry.

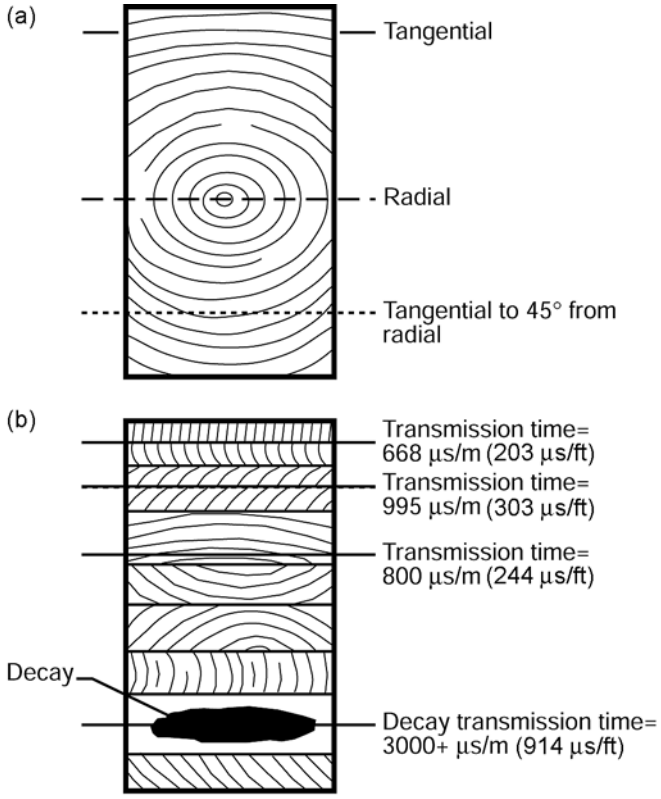

Figure 12.3—Transverse stress wave paths and transmission times: (a) timber, (b) glulam beam.

Table 12.2—Typical stress wave transmission times for nondecayed Douglas-fir at 12% moisture content

Path length (mm (in.))	Stress wave transmission time (µs)		
	Radial	Tangential	45° to grain
64 (2.5)	43	51	64
89 (3.5)	60	71	88
140 (5.5)	94	112	139
184 (7.25)	123	147	183
235 (9.25)	157	188	234
292 (11.5)	195	234	290
342 (13.5)	229	274	340
394 (15.5)	264	315	392
444 (17.5)	297	355	442
495 (19.5)	331	396	492

A 30% increase in stress wave transmission times implies a 50% loss in strength. A 50% increase indicates severely decayed wood (Fig. 12.5). Transverse travel paths are best for finding decay. Parallel-to-grain travel paths can bypass regions of decay.

Weight loss is not a good indicator of decay because considerable strength loss can occur without significant weight loss. As Figure 12.5 illustrates, significant loss of strength occurs before noticeable weight loss.

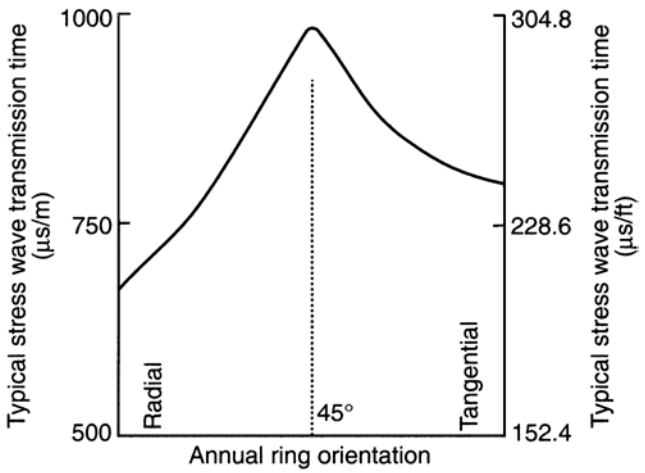

Figure 12.4—Transverse stress wave transmission time compared with annual ring orientation.

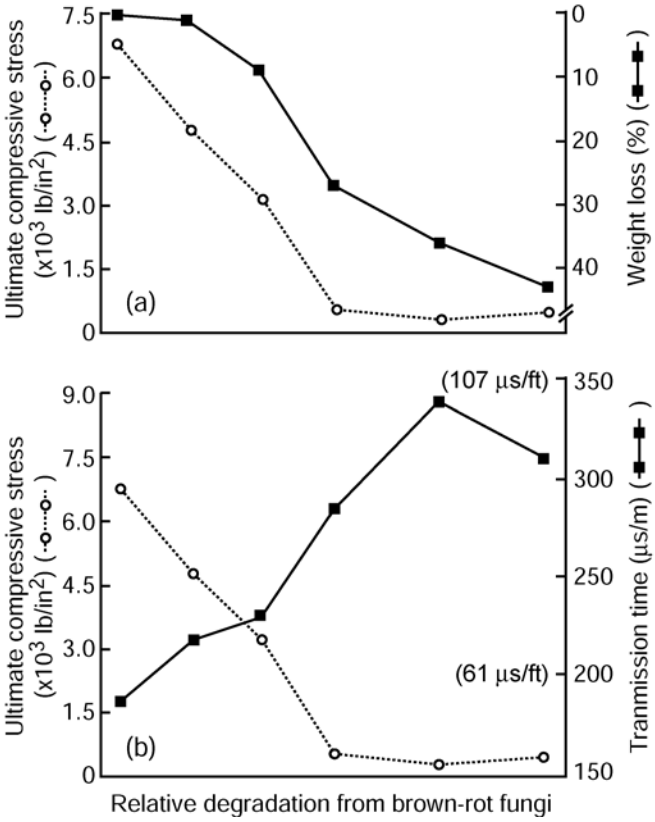

Figure 12.5—Relationship between stress wave transmission time and fungal degradation (Pellerin et al. 1985) (1 lb/in^2 = 6.9 kPa).

Effect of Moisture Content

Considerable research has shown the effect of moisture in wood on stress wave transmission time. Several studies have revealed that stress wave transmission times perpendicular to the grain of wood follow the relationship shown in Figure 12.6. At moisture contents less than approximately

Table 12.3—Summary of research on use of stress waves for detecting decay in timber structures

Reference	Structure	Wood product	Test	Analysis
Volny 1992	Bridge	Douglas-fir glulam, creosote pressure treated	Stress wave transmission time perpendicular to grain, across laminations at 0.3-m (0.98-ft) intervals	Sound wood: 1,279 μs/m (390 μs/ft) Moderate decay: 1,827 μs/m (557 μs/ft) Severe decay: 2,430 μs/m (741 μs/ft)
Ross 1982	Football stadium	Solid-sawn Douglas-fir, creosote pressure treated	Stress wave transmission time perpendicular to grain, near connections	Sound wood: 853 μs/m (260 μs/ft) Incipient decay: –Center of members: 1,276 μs/m (389 μs/ft) –38-mm-thick solid wood shell: 2,129 μs/m (649 μs/ft) Severe decay: >3,280 μs/m (1,000 μs/ft)
Hoyle and Pellerin 1978	School gymnasium	Douglas-fir glulam arches	Velocity of stress wave transmission time perpendicular to grain, near end supports	Sound wood: 1,073 μs/m (327 μs/ft) Decayed wood: 1,574 μs/m (480 μs/ft)

30%, transmission time decreases with decreasing moisture content. Corrections for various moisture content values are summarized in Table 12.4.

At moisture content values greater than approximately 30%, little or no change in transmission time occurs. Consequently, there is no need to adjust the measured values for wood that is tested in a wet condition.

Effect of Preservative Treatment

Treatment with waterborne salts has almost no effect on stress wave transmission time. Treatment with oilborne preservatives increases transmission time to about 40% greater than that of untreated wood. Round poles are usually penetrated to about 37 to 61 mm (1.5 to 2.5 in.). Table 12.5 was calculated to show expected travel time for round poles treated with oilborne preservatives. Although these data illustrate the effect oilborne treatments have on transmission time, these values should not be used to estimate level of penetration.

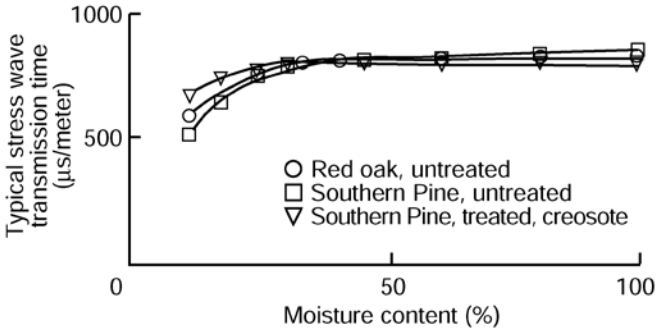

Figure 12.6—Transverse stress wave transmission times in Southern Pine and red oak piling.

Interpretation of Stress Wave Velocity Readings

The guidelines in this chapter are useful in interpreting readings that are less than those for sound wood. Voids and checks will not transmit stress waves. Knots will act as parallel-to-grain wood but are usually oriented perpendicular to the long axis of timber.

Based on the direction and length of the stress wave path in the wood, moisture content of the wood, and whether or not preservative treatment is present, the velocity and travel time for sound wood can be determined. For the transverse direction, the annual ring orientation and the existence of seasoning checks should be recorded.

Table 12.4—Stress wave transmission time adjustment factors for temperature at various moisture contents for Douglas-fir

Moisture content (%)	Adjustment factors			
	–18 °C (0 °F)	3 °C (38 °F)	27 °C (80 °F)	49 °C (120 °F)
1.8	0.94	0.95	0.97	0.98
3.9	0.95	0.96	0.98	0.99
7.2	0.93	0.98	1.00	1.01
12.8	0.97	0.99	1.00	1.01
16.5	0.99	1.01	1.03	1.05
23.7	1.05	1.07	1.09	1.14
27.2	1.07	1.10	1.12	1.17

Table 12.5—Stress wave transmission times for round poles treated with oil-borne preservatives

Pole diameter (mm)	Stress wave transmission time (μs) for various levels of penetration		
	37 mm	61 mm	Full penetration
294	222	240	300
343	254	271	350
392	286	305	400
441	321	338	450
490	350	370	500
539	386	403	550
588	422	436	600

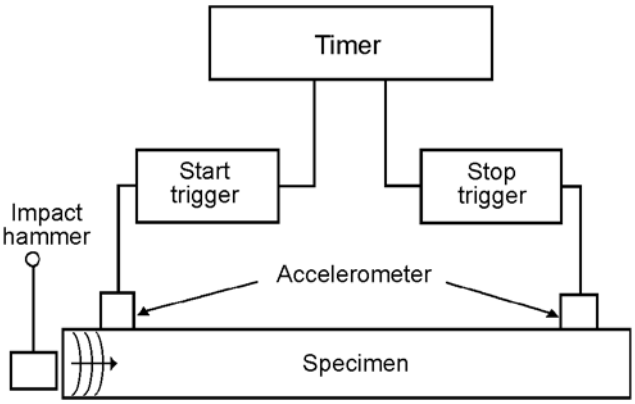

Figure 12.7—Technique used to measure impact-induced stress wave transmission times in various wood products.

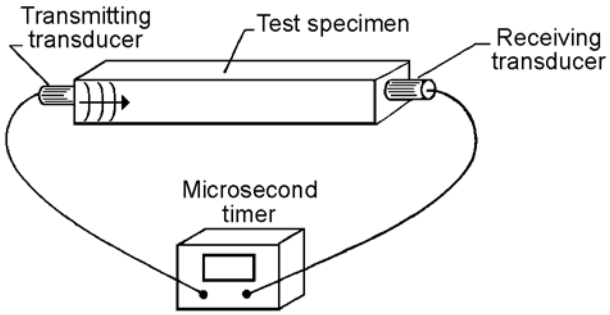

Figure 12.8—Ultrasonic measurement system used to measure stress wave transmission times in various wood products.

Measurement of Stress Wave Transmission Time

General Measurement

Several techniques can be used to measure stress wave transmission time in wood. The most common technique uses simple time-of-flight-type measurement systems. Two commercially available systems that use this technique are illustrated in Figures 12.7 and 12.8. Note that for ultrasonic measurement systems, a couplant may be used between the transducers and the specimen.

With these systems, a mechanical or ultrasonic impact is used to impart a wave into the member. Piezoelectric sensors are placed at two points on the member and used to detect passing of the wave. The time required for the wave to travel between sensors is then measured.

Commercially Available Equipment

Several equipment development firms are producing portable equipment based on this concept. Table 12.6 presents contact information for obtaining information on these devices.

Field Considerations and Use of Stress Wave Methods

Stress Wave Transmission Time

Figure 12.9 outlines the general procedures used with stress wave nondestructive evaluation methods for field work. Before venturing into the field, it is useful to estimate stress wave transmission time for the size of the members to be inspected. Preceding sections provided information on various factors that affect transmission time in wood. This information can be summarized, as a starting point, by simply using a baseline transmission time of 1,300 μs/m (400 μs/ft). Transmission time, on a per length basis, less than this would indicate sound material. Conversely, transmission time greater than this value would indicate potentially degraded material. Using this value, you can estimate the transmission time for a member by knowing its thickness (path length) and the following formula:

$$T_{baseline}(\mu s) = 1{,}300 \times \text{WTD}$$

where $T_{baseline}$ is baseline transmission time (μs) and WTD is wave transmission distance (path length) (m).

[Inch–pound formula: $T_{baseline}$ (μs) = 400 × WTD, where WTD is wave transmission distance (path length) (ft)]

By knowing this number for various thicknesses, field work can proceed rapidly.

Field Data Form

An example of a typical field data acquisition form is shown in Figure 12.10. Key items to include on the form are structure name, location, number, inspector, and date of inspection.

Field Measurements

Field use should be conducted in accordance with instructions provided by equipment manufacturers. In the field, extra batteries, cables, and sensors are helpful. Testing should be conducted in areas of the member that are highly susceptible to degrading, especially in the vicinity of connections and bearing points.

The baseline values provided serve as a starting point in the inspection. It is important to conduct the test at several

Table 12.6—Commercially available stress wave timing equipment

Manufacturer	Product	Website	Location
Agricef	USLab	www.agricef.com.br	
CBS-CBT	Sylvatest-Duo	www.cbs-cbt.com	Saint-Sulpice, Switzerland
Fakopp Enterprise	Various models	www.fakopp.com	Agfalva, Hungary
IML GmbH	IML Micro Hammer	www.imlusa.com	Moultonborough, New Hampshire, USA
Metriguard, Inc.	Models 239A Stress Wave Timer	www.metriguard.com	Pullman, Washington, USA
James Instruments, Inc.	V-Meter MK IV	www.ndtjames.com	Chicago, Illinois, USA
Olson Instruments, Inc.	Various models	www.olsoninstruments.com	Wheat Ridge, Colorado, USA

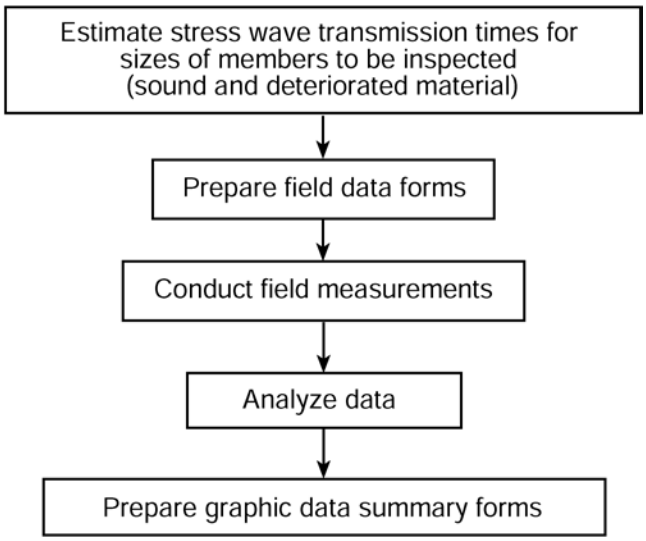

Figure 12.9—General procedures used to prepare and use stress wave timing methods for field work.

points at various distances away from the suspect area. In a sound member, little deviation is observed in transmission times. If a significant difference in values is observed, the member should be considered suspect.

Data Analysis and Summary Form

When data have been gathered, it is useful to present them in an easy-to-read manner. Figure 12.11 illustrates several data summaries. From these, the presence and extent of degradation can readily be seen. The top drawing illustrates the side view of a timber, with stress wave travel times noted and decay mapped. The middle and bottom illustrations show a timber cross section with internal defects and stress wave times noted.

Literature Cited

Armstrong, J.P.; Patterson, D.W.; Sneckenberger, J.E. 1991. Comparison of three equations for predicting stress wave velocity as a function of grain angle. Wood and Fiber Science. 23(1): 32–43.

Elvery, R.H.; Nwokoye, D.N. 1970. Strength assessment of timber for glued laminated beams. In: Proceedings, Paper II, Nondestructive testing of concrete and timber, organized by the Institution of Civil Engineering and the British Commission for Nondestructive Testing; 1969 June 11–12. London, BC: Institute of Civil Engineering: 105–110.

Gerhards, C.C. 1978. Effect of earlywood and latewood on stress-wave measurements parallel to the grain. Wood Science. 11(2): 69–72.

Gerhards, C.C. 1980. Effect of cross grain on stress waves in lumber. Res. Pap. FPL–RP–368. Madison, WI: U.S. Department of Agriculture, Forest Service, Forest Products Laboratory.

Gerhards , C.C. 1982. Effect of knots on stress waves in lumber. Res. Pap. FPL–RP–384. Madison, WI: U.S. Department of Agriculture, Forest Service, Forest Products Laboratory.

Hoyle, R.J.; Pellerin, R.F. 1978. Stress wave inspection of a wood structure. In: Proceedings, 4th symposium on nondestructive testing of wood; 1978 August 28–30; Vancouver, WA. Pullman, WA: Washington State University: 33–45.

Ihlseng, M.C. 1878. The modulus of elasticity in some American woods, as determined by vibration. Van Nostrand's Engineering Magazine. Vol. XIX: 8–9.

Ihlseng, M.C. 1879. On a mode of measuring the velocity of sound in wood. American Journal of Science. 3d Series. 17I(98): 125–133.

Jung, J. 1979. Stress wave grading techniques on veneer sheets. Gen. Tech. Rep. FPL–GTR–27. Madison, WI: U.S. Department of Agriculture, Forest Service, ForestProducts Laboratory.

Pellerin, R.F.; De Groot, R.C.; Esenther, G.R. 1985. Nondestructive stress wave measurements of decay and termite attack in experimental wood units. In: Proceedings, 5th symposium on nondestructive testing of wood; 1985 September 9–11; Pullman, WA. Pullman, WA: Washington State University: 319–353.

Page _____ of _____

Data Log—Stress Wave Transmission Times

Structure _____

Location _____ Date _____

_____ Equipment _____

_____ _____

_____ _____

Inspector _____

Member	Location	WTD	Equipment reading (µs)	Transmission time (µs/m) (µs/ft)	Condition	Grain orientation

Figure 12.10—Typical field data acquisition form.

Ross, R.J. 1982. Quality assessment of the wooden beams and columns of Bay C of the east end of Washington State University's football stadium. Unpublished research. Pullman, WA: Washington State University.

Ross, R.J.; Ward, J.C.; TenWolde, A. 1994. Stress wave nondestructive evaluation of wetwood. Forest Products Journal. 44(7/8): 79–83.

Rutherford, P.S. 1987. Nondestructive stress wave measurement of incipient decay in Douglas Fir. Pullman, WA: Washington State University. M.S. thesis.

Smulski, S.J. 1991. Relationship of stress wave and static bending determined properties of four northeastern hardwoods. Wood and Fiber Science. 23(1): 44–57.

Soltis, L; Baker. A.; Ferge, L.; [et al.]. 1992. USS Constitution—inspection and evaluation procedures for live and white oak members. Report submitted to U.S.Navy, Maintenance and Repair, USS Constitution, Boston Naval Shipyard, Charlestown, MA.

Volny, N.J. 1992. Timber bridge inspection case studies in use of stress wave velocity equipment. In: Proceedings, 8th symposium on nondestructive testing of wood; 1991 September 23–25; Vancouver, WA. Pullman, WA: Washington State University.

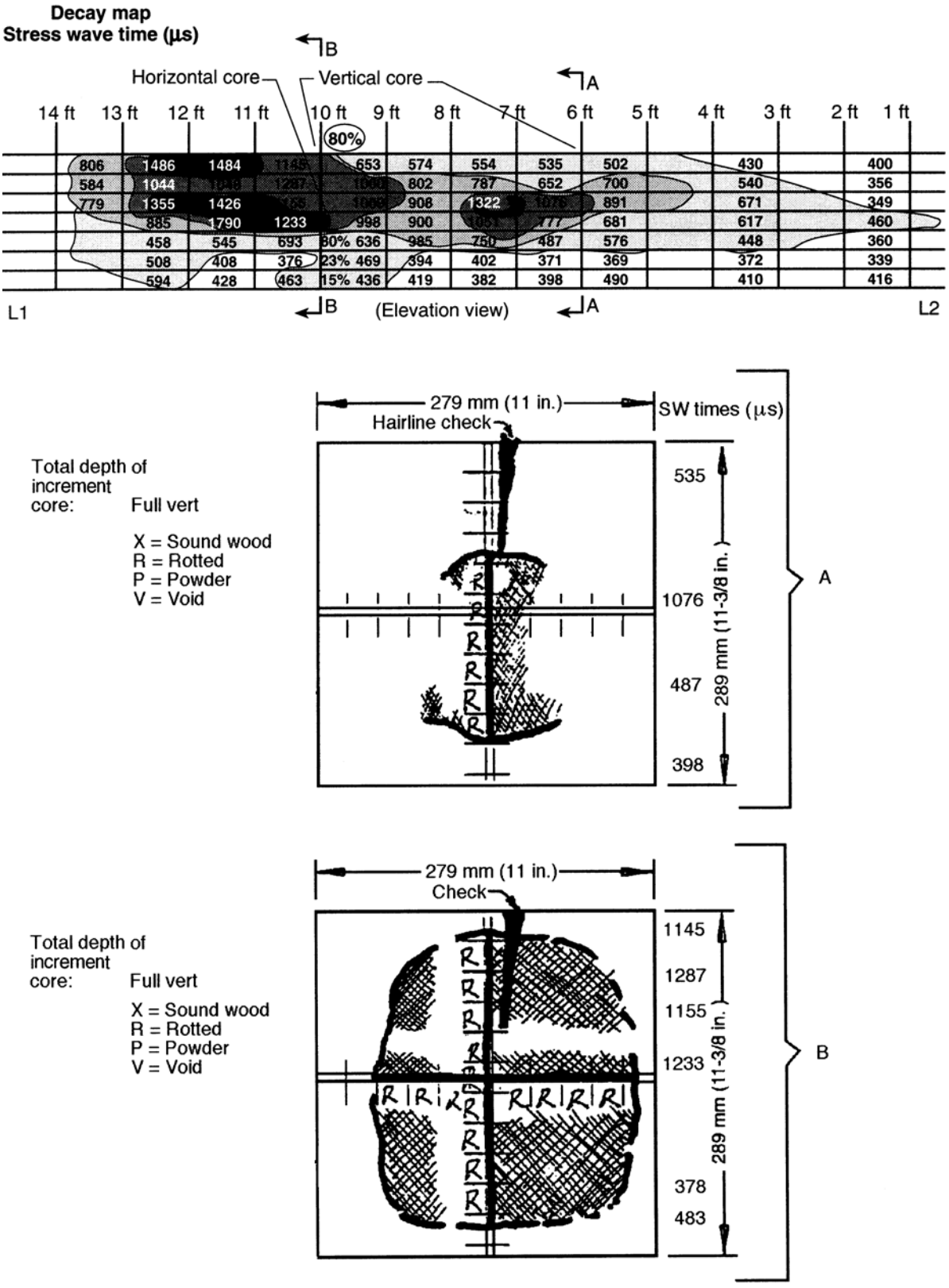

Figure 12.11—Examples of stress wave data summary (top) and illustrations of the cross-section conditions.

Chapter 13

Use of Laser Scanning Technology to Obtain As-Built Records of Historic Covered Bridges

Robert J. Ross, Supervisory Research General Engineer
Forest Products Laboratory, Madison, Wisconsin

Brian K. Brashaw, Program Manager
Forest Products Marketing Unit, USDA Forest Service, Madison, Wisconsin

Samuel J. Anderson, Engineer
Natural Resources Research Institute, University of Minnesota Duluth, Minnesota

Covered bridges are part of the fabric of American history, and several hundred historic covered bridges still exist today. Although much effort is expended to preserve these structures, the high cost of restoration, neglect, vandalism, and arson often take their toll. Many are lost forever. One of the more famous bridges from *The Bridges of Madison County* movie fame was burned in 2003, and Hurricane Irene destroyed a number of New England bridges in 2011. Because we cannot completely prevent these types of incidents from occurring, the National Park Service's Historic American Engineering Record (HAER) has efforts under way to document historic structures. Their Level I documentation is defined in the Secretary of the Interior's Standards and Guidelines for Architectural and Engineering Documentation. It consists of measured and interpretive drawings, large-format photographs, and written historical reports. To assist in this effort, newer technologies need to be explored that can provide as-built records at a fast rate and with greater accuracy.

The demonstration study summarized in this chapter was conducted to examine the technical feasibility of using laser scanning technologies for obtaining as-built records for historic covered timber bridges. A secondary objective was to identify other applications of this technology, notably for other transportation structures.

This chapter was originally published in 2012 as a Forest Products Laboratory Research Paper:

Ross, Robert J.; Brashaw, Brian K.; Anderson, Samuel J. 2012. Use of laser scanning technology to obtain as-built records of historic covered bridges. Research Paper FPL–RP–669. Madison, WI: U.S. Department of Agriculture, Forest Service, Forest Products Laboratory. 18 p.

Literature Review

Three-dimensional (3D) laser scanners are instruments that record precise and accurate surface data of objects in a nondestructive manner. These instruments use an infrared beam of light to calculate and record the distance to an object, typically as data points with spatial coordinates. These data are then analyzed using various types of computer software to generate a detailed image of coordinates and dimensions. Three-dimensional laser scanners have successfully been used to digitize objects of various sizes ranging from small diagnostic artifacts to large, complex sites of monumental architecture (FARO Technologies 2011a, b).

A wide number of companies manufacture various types of 3D laser scanners. Generally, these units use light detection and ranging technology (LiDAR), where laser pulses determine the distance to an object or surface. The distance to an object is determined by using time-of-flight between transmission of a pulse and detection of the reflected signal. A point cloud of data is then collected and can be converted into the true shape of the object.

The units used in this project, a FARO LS 880 model and a Photon 120 model (FARO Technologies, Lake Mary, Florida), used similar technology to acquire the scan points. A laser beam is emitted from a rotating mirror out toward the area being scanned. The laser beam is then reflected back to the scanner by objects in its path. The distance to the objects defining an area is calculated, as well as their relative vertical and horizontal angles (FARO Technologies 2011a, b).

Several bridge projects were noted in the literature review. The Pennsylvania Department of Transportation (PennDOT) completed an initial study in 1999. In this study, the goals were to evaluate the technology for creating as-built drawings. A comparison of traditional and 3D scanning estimated an overall time savings of 100+ person-hours through the

Table 13.1—Background information on the historic covered timber bridges used in this study

State	City	Bridge	Year built	Span (ft)	Placement on National Register of Historic Places	Design
Wisconsin	Cedarburg	Red	1876	120	March 14, 1973	Lattice through truss
Iowa	Winterset	Roseman	1883	106	September 1, 1976	Lattice through truss
Iowa	St. Charles	Imes	1870	81	February 9, 1979	Lattice through truss
Iowa	Winterset	Hogback	1884	106	August 28, 1976	Lattice through truss
Iowa	Winterset	Cutler–Donahoe	1871	79	October 8, 1976	Lattice through truss
Minnesota	Zumbrota	Zumbrota	1869	120	February 20, 1975	Lattice through truss

use of 3D scanning (Foltz 2000). Based on this assessment, PennDOT purchased two laser scanners in 2000. A second assessment was completed by Jaselskis and others in 2003, showing that laser scanning could be used cost effectively for preliminary surveys to develop triangular network (TIN) meshes of roadway surfaces and to measure bridge beam camber more safely and quickly compared with conventional approaches. Other applications noted in this publication showed potential applications for laser scanning to include developing as-built drawings of historical structures such as the bridges of Madison County.

Methods

Selection of Bridges

The bridges for scanning and assessment used in this study are located in Wisconsin, Iowa, and Minnesota. Key background information (Table 13.1), detailed descriptions, and photographs are summarized in the following paragraphs. Contact was made with the appropriate government or administrative staff for each bridge, and permission was also secured to obtain scans. Note that four of the bridges scanned included the historic Madison County, Iowa, bridges.

Cedarburg, Wisconsin, Covered Bridge

The last remaining historic covered bridge in Wisconsin, the "Red Bridge," was built in 1876. It is located just outside the city of Cedarburg, Wisconsin, in Ozaukee County (Figs. 13.1, 13.2). According to Ozaukee County records (2011),

> Built in 1876, the original span measured 120' long and 12' wide. Its construction was of a certain type of pine found near Baraboo, Wisconsin. All of the timber and planks were cut and squared in a mill near that city. The lumber was then hauled to the proposed site on Cedar Creek where all pieces were fitted and set in place. The type of construction is known as lattice truss with interlacing 3 × 10 inch planks all held together by 2 inch hardwood pins and floored with three inch planking. In 1927, a center abutment was placed to carry the heavier traffic of automobiles and trucks. (Ozaukee County 2011)

Madison County, Iowa Covered Bridges

The bridges in Madison County, Iowa, are world famous, and they are excellent examples of the construction of covered bridges in the 1870–1880s. As noted in 2011 on the Madison County, Iowa, website,

> Our historic, world-famous covered bridges were popularized by Robert James Waller's novel, *The Bridges of Madison County*, and the feature film starring Meryl Streep and Clint Eastwood. Five of the original covered bridges remain, all listed on the National Register of Historic Places. The bridges were covered by order of the County Board of Supervisors to help preserve the large flooring timbers that were more expensive to replace than the lumber covering the sides and the roof. Most of the construction was done by farmers to pay their poll taxes. The bridges were usually named for the nearest resident. (Chamber of Commerce 2011)

Four bridges were selected for laser scanning in Madison County: the Roseman, Imes, Hogback, and Cutler–Donahoe Bridges. Photographs of these bridges are shown in Figures 13.3–13.6.

Zumbrota Bridge

Minnesota's only remaining truly historic covered bridge is located in the City of Zumbrota. Listed on the National Historic Register, it was originally constructed in 1869 and relocated in 1932, 1979, and finally in 1997. It currently spans the Zumbro River in the 65-acre Covered Bridge Park. Considered a lattice through truss design, it is now a pedestrian-only bridge that spans 120 ft. A special documentary of the bridge and its importance to the history of Zumbrota can be found at http://www.youtube.com/watch?v=EVFd1YwcHww&feature=related. As a measure of its importance to Zumbrota, an annual covered bridge festival occurs every June. A photograph of the bridge is shown in Figure 13.7.

On September 23–25, 2010, the Zumbro River flooded, creating a dangerous situation for the Zumbrota Covered Bridge. As Figure 13.8 illustrates, floodwaters rose to nearly the same elevation as the bottom of the bridge.

Three-Dimensional Laser Scanning and Data Processing

The laser scanning was completed by Sightline, LLC (Milwaukee, Wisconsin), a private firm that specializes in the use of laser scanning technologies with structures. Approximately 20–30 scans were completed for each bridge from a variety of angles using a FARO LS 880 laser scanner. Figure 13.9 shows a FARO laser scanner being used to inspect an historic covered bridge.

The scanning process consisted of scans that were completed by Sightline, and data processing was completed by the University of Minnesota Duluth's Natural Resources Research Institute (UMD NRRI). The following steps were completed and an estimate of the time duration was provided for each step:

1. Paper "targets" are placed in numerous locations on the bridge for use in linking up to 30 individual laser scans together. Time duration: 2 person-hours.
2. A FARO LS 880 3D laser scanner was used to conduct the scan. The scanner is placed at several vantage points inside and outside the bridge, so that all visible surfaces of the bridge can be documented. Individual scans are completed in approximately 15–20 min. When a single scan is completed, it is saved to a computer as an .ls file. It is highly recommended that a computer with significant computing power and high levels of RAM memory be used to process the millions of data points created during the scanning process. Time duration: 10 person-hours.
3. After all visible portions of the bridge have been scanned, the software files are linked using FARO Scene software. This software allows an individual to identify the targets placed prior to the scanning process and use them to link or attach one scan to another. It is also possible to filter, using various techniques or software, extraneous images (for instance, a vehicle traveling across the bridge or background vegetation). The process of linking two individual scans is repeated several times until all scans have been compiled into one large scan depicting the entire bridge. Time duration: 9 person-hours.
4. Once a bridge has been completely assembled using all of the individual scans, it can be exported as a point cloud, depicting all visible aspects and actual dimensions of the bridge. This cloud of data was then exported into AutoCAD software (Autodesk, Inc., San Rafael, California) using an add-in provided by Kubit USA (Houston, Texas). This add-in allows a user to import point cloud files in addition to the ones inherently recognized by AutoCAD 2011 and has additional modeling tools for working directly with point cloud data in AutoCAD. Once a point cloud has been exported into AutoCAD, it can be divided into multiple cross sections. This is done so that specific components of the bridge can be seen more clearly. From this point, two-dimensional (2D) and 3D models of the bridge can be generated. Time duration: 40+ person-hours.

Results

Laser Scanning

A number of types of images can be presented from processing point cloud data. These images include a point cloud image resulting from only one scan, a point cloud image created from multiple scans, a parametric picture created from a point cloud scan, a point cloud image imbedded in AutoCAD, and 2D/3D AutoCAD images. These images can be created using FARO Scene software or AutoCAD 2011 with a Kubit USA add-in.

As to the project activities, the majority of the scan processing for the Cedarburg, Wisconsin, bridge was completed by Sightline, LLC. The processing of the scan data for the Madison County, Iowa, bridges and the Zumbrota, Minnesota, bridge was completed by the UMD NRRI. The project team decided that based on the processing time estimates, detailed in-point cloud and 3D AutoCAD, data would be provided for the Cedarburg, Imes, and Zumbrota Bridges, with only point cloud data for the Hogback, Cutler–Donahoe, and Roseman Bridges. All the digital points could be further processed to develop detailed dimensional information, as the point cloud images are considered accurate data. The point cloud images could also be further processed using Kubit USA add-ins for AutoCAD 2011. Each bridge scan and AutoCAD image is shown in the following sections.

Cedarburg, Wisconsin, Covered Bridge

Figures 13.10–13.17 show various images created from 3D laser scanning conducted during the project for the Cedarburg Bridge. This includes point cloud images and AutoCAD drawings created from the point cloud images. The Imes Bridge is the only Madison County Bridge where the point cloud data was used to create AutoCAD drawings. Our project team has all of the point cloud data that could be used in the future to create AutoCAD drawings for the other Madison County bridges (Hogback, Cutler–Donahoe, and Roseman) scanned during the project.

Imes Bridge, Madison County, Iowa

For the Imes Bridge, the data show the accurate dimensions and shape of the bridge at the time of scanning. No corrections were made to straighten any bridge members, such as would be done to create new construction drawings. Figures 13.18–13.23 show that the bridge is no longer perfectly plane, but that it has twisted and moved over time.

Roseman Covered Bridge, Madison County, Iowa

Figures 13.24–13.25 shows various planar views and point cloud images created from 3D laser scanning conducted during the project for the Roseman Bridge, located in Madison County, Iowa. These point images are fully dimensioned computer files that can be used to determine dimensions, skew of the bridge, deflection, and other characteristics as needed, without importing into AutoCAD or other software platforms.

Hogback Covered Bridge, Madison County, Iowa

Figure 13.26 shows various point cloud images created from 3D laser scanning conducted during the project for the Hogback Bridge located in Madison County, Iowa. These point images are fully dimensioned computer files that can be used to determine dimensions, skew of the bridge, deflection, and other characteristics as needed, without importing into AutoCAD or other software platforms.

Cutler–Donahoe Covered Bridge, Madison County, Iowa

Figures 13.27 and 13.28 show various point cloud images created from 3D laser scanning conducted during the project for the Cutler–Donahoe Bridge, located in Madison County, Iowa. These point images are fully dimensioned computer files that can be used to determine dimensions, skew of the bridge, deflection, and other characteristics as needed, without importing into AutoCAD or other software platforms.

Zumbrota Covered Bridge, Zumbrota, Minnesota

Additional project funds were received from the Minnesota Local Road Research Board's Operational Research Program (OPERA) to conduct 3D laser scanning of the most significant historic covered bridge in Minnesota, located in Zumbrota. The bridge, built in 1869 (and relocated several times), is now located in a city park and spans the Zumbro River. Figures 13.29–13.36 show various scalar images and point cloud images created from 3D laser scanning conducted during the project. These figures show each different type of possible image that can be created using FARO Scene software or AutoCAD 2011 with a Kubit USA add-in. These images include a point cloud image resulting from only one scan, a scalar image created from a point cloud scan, a point cloud image created from multiple scans, a point cloud image imbedded in AutoCAD, and 2D/3D AutoCAD images. All of the scan data, images, and figures were provided to the City of Zumbrota for any further processing as appropriate.

In contrast to the Imes Bridge, significant efforts were made to straighten the dimensions of the bridge in AutoCAD in an effort to create a drawing that could be used to construct a new bridge. This was a significant undertaking, and added nearly 40 h of processing time to data processing. This process creates a drawing that would be more consistent with the original construction of the bridge, not its current shape and condition (Brashaw 2010).

Rapid Prototype Development

Following processing and development of the 3D scanning images, a digital 3D CAD file was used to generate a 1/100th 3D scale replica of the bridge at the Northern Lights Technology Center of UMD NRRI. In processing the data, we found that it would only be possible to produce an accurate external version of the bridge. We could not create a true replica of the inside of the bridge because a 1/100th scale of a 6-in.-wide beam would only have a thickness of 0.06 in. This is below the thickness that can be created using rapid prototyping, and these thin members would not have strength because many of the beams and members are only connected at the ends. The 3D image that was used by the Vanguard unit to create the 1/100th model shown in Figure 13.37 from Vanguard Si2 selective laser sintering (SLS) equipment (3D Systems, Valencia, California) was used to create the scale replica of the bridge (Fig. 13.38). Because the scan data were corrected to achieve straight members, this model would be consistent with the true nature of the bridge at construction, not its condition in 2010.

Comparison of Laser Scanning Equipment Results with Field Measurements

One of the objectives of this project was to assess the accuracy of laser scanning to determine accurate dimensions of the bridges. The FARO laser scanner used for the project was rated at an accuracy of 1/4 in. at a distance of 150 ft. However, the typical distance of the laser scanner in this project ranged from 50–100 ft, improving the accuracy over the rated number. For this phase of the project, only the Madison County, Iowa, bridges were measured to verify the accuracy. To conduct this task, digital photos of each bridge were taken as soon as the project team arrived. These photos were then printed on a portable printer and used to record the accurate dimensions measured with traditional tape measures (1/16-in. accuracy).

Each bridge was then scanned using the laser scanner at up to 20+ locations. The raw scan data were processed into point cloud data. The locations measured using traditional measuring equipment on the photographs were then located in the digital files and the digital dimensions noted. Based on these data, a comparison between the actual and digital measurements was taken. The comparison data are reported for each of the four Madison County bridges in the following sections. Fourteen to sixteen locations were samples for each bridge with a very small error noted. This mean error of the 14–16 measurements ranged from 0.04–0.08 in. (1.01–2.02 mm), within the rated accuracy of 1/4 in. at 150 ft.

Imes Covered Bridge, Madison County, Iowa

Figure 13.39 shows the locations on the bridges where the actual measurements were collected using traditional tape measures to a resolution of 1/16 in. Once the point cloud was developed from the multiple laser scans of a bridge,

Table 13.2—Comparison of measurement data from traditional tape measures and point cloud measurements for the Imes Covered Bridge, Madison County, Iowa

	Method for measurement				
	Tape measurement (in., to nearest 1/16 in.)	Point cloud		Difference between tape and point cloud	
Member number		3 points (in.)	Mean (in.)	(in.)	(mm)
1	2.88	2.68 2.76 2.74	2.73	0.15	3.77
2	2.88	2.84 2.84 2.64	2.77	0.10	2.58
3	11.25	11.40 11.20 11.04	11.21	0.04	0.93
4	5.50	5.24 5.40 5.64	5.43	0.07	1.86
5	11.50	11.32 11.20 11.38	11.30	0.20	5.08
6	11.50	11.40 11.48 11.56	11.48	0.02	0.51
7	11.75	11.72 11.84 11.62	11.73	0.02	0.59
8	11.63	11.52 11.52 11.60	11.55	0.08	1.99
9	11.75	11.76 11.80 11.80	11.79	0.04	0.93
10	12.13	12.24 12.04 11.80	12.03	0.10	2.50
11	1.75	1.76 1.68 1.64	1.69	0.06	1.44
12	11.88	11.84 11.72 11.80	11.79	0.09	2.24
13	11.63	11.84 11.44 11.52	11.60	0.03	0.64
14	11.75	11.88 11.72 11.80	11.80	0.05	1.27
15	12.00	11.96 12.08 11.80	11.95	0.05	1.35
16	1.88	1.80 1.80 1.88	1.83	0.05	1.23
Average difference				0.07	1.83

Table 13.3—Comparison of measurement data from traditional tape measures and point cloud measurements for the Hogback Covered Bridge, Madison County, Iowa

	Method for measurement				
	Tape measurement (in., to nearest 1/16 in.)	Point cloud		Difference between tape and point cloud	
Member number		3 points (in.)	Mean (in.)	(in.)	(mm)
1	8.00	7.96 8.04 8.08	8.03	0.03	0.68
2	11.75	11.84 11.76 11.56	11.72	0.03	0.76
3	12.00	12.16 12.04 12.00	12.07	0.07	1.69
4	15.75	15.96 15.68 15.68	15.77	0.02	0.59
5	11.38	11.20 11.28 11.52	11.33	0.04	1.06
6	11.88	11.96 11.80 11.68	11.81	0.06	1.57
7	11.63	11.60 11.48 11.68	11.59	0.04	0.97
8	14.88	14.96 14.88 14.80	14.88	0.01	0.13
9	11.38	11.20 11.40 11.24	11.28	0.09	2.41
10	15.88	16.00 15.76 15.88	15.88	0.01	0.13
11	11.50	11.40 11.48 11.64	11.51	0.01	0.17
12	11.75	11.64 11.80 11.64	11.69	0.06	1.44
13	12.00	11.84 11.84 12.00	11.89	0.11	2.71
14	12.00	11.72 11.84 12.04	11.87	0.13	3.39
Average difference				0.05	1.26

Table 13.4—Comparison of measurement data from traditional tape measures and point cloud measurements for the Roseman Covered Bridge, Madison County, Iowa

	Method for measurement				
	Tape measurement	Point cloud		Difference between tape and point cloud	
Member number	(in., to nearest 1/16 in.)	3 points (in.)	Mean (in.)	(in.)	(mm)
1	11.63	11.76 11.50 11.60	11.62	0.01	0.13
2	11.88	12.00 11.92 11.80	11.91	0.03	0.80
3	11.88	11.96 11.72 11.84	11.84	0.04	0.89
4	11.75	11.64 11.72 11.76	11.71	0.04	1.10
5	11.88	11.76 11.84 11.76	11.79	0.09	2.24
6	15.75	15.52 15.60 15.96	15.69	0.06	1.44
7	11.63	11.72 11.50 11.60	11.61	0.02	0.47
8	5.88	5.92 6.00 5.60	5.84	0.04	0.89
9	11.50	11.52 11.48 11.40	11.47	0.03	0.85
10	11.50	11.48 11.56 11.44	11.49	0.01	0.17
11	11.63	11.76 11.72 11.64	11.71	0.08	2.07
12	11.50	11.60 11.52 11.60	11.57	0.07	1.86
13	16.00	15.96 15.96 16.00	15.97	0.03	0.68
14	11.63	11.64 11.60 11.56	11.60	0.02	0.64
15	11.63	11.56 11.68 11.60	11.61	0.01	0.30
16	7.63	7.48 7.56 7.64	7.56	0.07	1.65
Average difference				0.04	1.01

the data were extracted from the digital file and simply compared for accuracy. Table 13.2 shows the results of this comparison, showing that laser scanning is a very accurate means of determining dimensions for use in creating as-built documentation.

Hogback Covered Bridge, Madison County, Iowa

Figure 13.40 shows the locations on the bridges where the actual measurements were collected using traditional tape measures to a resolution of 1/16 in. Once the point cloud was developed from the multiple laser scans of a bridge, data were extracted from the digital file and simply compared for accuracy. Table 13.3 shows the results of this comparison, showing that the laser scanning is a very accurate means of determining dimensions for use in creating as-built documentation.

Roseman Covered Bridge, Madison County, Iowa

Figure 13.41 shows the locations on the bridges where the actual measurements were collected using traditional tape measures to a resolution of 1/16 in. Once the point cloud was developed from the multiple laser scans of a bridge, the data were extracted from the digital file and simply compared for accuracy. Table 13.4 shows the results of this comparison, showing that laser scanning is a very accurate means of determining dimensions for use in creating as-built documentation.

Cutler–Donahoe Covered Bridge, Madison County, Iowa

Figure 13.42 shows the locations on the bridges where the actual measurements were collected using traditional tape measures to a resolution of 1/16 in. Once the point cloud was developed from the multiple laser scans of a bridge, data were extracted from the digital file and simply compared for accuracy. Table 13.5 shows the results of this comparison, showing that laser scanning is a very accurate means of determining dimensions for use in creating as-built documentation.

Summary and Conclusions

This project successfully demonstrated the potential for using 3D laser scanning to accurately develop as-built documentation of historic covered timber bridges as a means to develop historical documentation. The following conclusions can be made from the project.

- Three dimensional laser scanning can be used to rapidly scan historic covered bridge structures. A number of technologies and commercial vendors are available. A commercial FARO scanner was used in this project and operated by using a phase shift technology rather than time of flight. This means that instead of a single pulse being reflected and the time of flight measured, constant waves of varying length are projected. Upon contact with an object, they are reflected back to the scanner.

Table 13.5—Comparison of measurement data from traditional tape measures and point cloud measurements for the Cutler–Donahoe Covered Bridge, Madison County, Iowa

	Method for measurement				
	Tape measurement (in., to nearest 1/16 in.)	Point cloud		Difference between tape and point cloud	
Member number		3 points (in.)	Mean (in.)	(in.)	(mm)
1	11.63	11.60 11.64 11.40	11.55	0.08	1.99
2	11.63	11.72 11.48 11.52	11.57	0.05	1.31
3	11.75	11.60 11.76 11.76	11.71	0.04	1.10
4	11.50	11.48 11.72 11.68	11.63	0.13	3.22
5	1.75	1.76 1.64 1.80	1.73	0.02	0.42
6	5.88	5.80 5.72 5.68	5.73	0.14	3.60
7	3.75	3.68 3.80 3.80	3.76	0.01	0.25
8	12.00	11.96 11.84 11.88	11.89	0.11	2.71
9	11.50	11.56 11.56 11.80	11.64	0.14	3.56
10	12.00	12.16 12.04 11.96	12.05	0.05	1.35
11	1.63	1.64 1.72 1.56	1.64	0.01	0.38
12	12.00	11.92 11.88 11.68	11.83	0.17	4.40
13	5.75	5.68 5.72 5.72	5.71	0.04	1.10
14	3.88	3.60 3.88 3.72	3.73	0.14	3.60
Average difference				0.08	2.07

The distance from the scanner to the object is accurately measured by measuring the phase shifts in the waves of infrared light.

- Post-processing of scan data requires experience and skill to cost-effectively create as-built documentation. The staff at Sightline, LLC, was very efficient in linking the 3D scans, importing them into AutoCAD and creating detailed 2D and 3D CAD drawings. Our project student engineer faced a steep learning curve but developed an excellent skillset in processing the files during the project. For experienced staff, this technology can reduce the time associated with creating as-built documentation.
- A 3D scanner can be used to create a range of outputs that include point cloud scans, parametric images, and 2D and 3D AutoCAD drawings. For historic covered bridges, this information can be used for a variety of purposes including as-built documentation and structural assessment, while also providing detail on the land topography adjacent to the bridge.
- One of the objectives of the project was to assess the accuracy of laser scanning to determine accurate dimensions of the bridges. Each bridge was then scanned using the laser scanner at up to 20+ locations. Raw scan data were processed into point cloud data. The locations measured using traditional measuring equipment on the photographs were then located in the digital files and the digital dimensions noted. Based on these data, a comparison between the actual and digital measurements was taken. The comparison data are reported for each of the four Madison County bridges in the following sections. Fourteen to sixteen locations were samples for each bridge with a very small error noted. This mean error of the 14–16 measurements ranged from 0.04–0.08 in. (1.01–2.02 mm), within the rated scanner accuracy of 1/4 in. at 150 ft.

Literature Cited

Brashaw, B.K. 2010. Use of laser scanning technology to obtain as-built records of the Zumbrota covered bridge. NRRI Tech. Rep. NRRI/TR-2011/04. Duluth, MN: University of Minnesota.

Chamber of Commerce. 2011. Madison County, Iowa—the bridges of Madison County [Website]. Winterset, IA: Madison County Chamber of Commerce. http://madisoncounty.com/index.php?page=the-bridges. Accessed October 6, 2011.

FARO Technologies. 2011a. FARO laser scanner training [Print presentation]. Lake Mary, FL.

FARO Technologies. 2011b. Measuring arms, laser tracker, laser scanner. In: FARO laser scanner focus 3D—applications. Lake Mary, FL. http://www.faro.com/focus/applications.

Foltz, L. 2000. 3D laser scanner provides benefits for PennDOT bridge and rockface surveys. Professional Surveyor magazine. (May). http://www.profsurv.com/magazine/article.aspx?i=590.

Jaselskis, E.; Cackler, E.; Andrle, S.; Gao, Z. 2003. Pilot study on improving the efficiency of transportation project using laser scanning. Final Rep. CTRE Project 02-109. Ames, IA: Iowa State University, Center for Transportation Research and Education.

Ozaukee County. 2011. History of the covered bridge. Port Washington, WI: Ozaukee County public records. http://www.co.ozaukee.wi.us/history/bridge.html. (October 6, 2011).

Figure 13.1—Photograph of the Cedarburg Covered Bridge (Cedarburg, Wisconsin), circa 1934. From the Library of Congress.

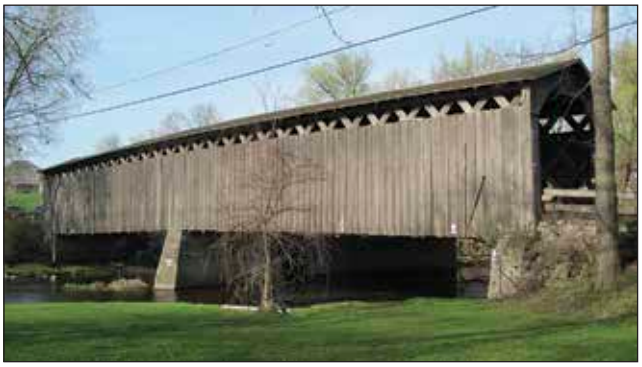

Figure 13.2—Recent (2010) photograph of the Cedarburg Covered Bridge.

Figure 13.3—Roseman Bridge, Madison County, Iowa (2010).

Figure 13.4—Imes Bridge, Madison County, Iowa (2010).

Figure 13.5—Hogback Bridge, Madison County, Iowa (2010).

Figure 13.6—Cutler–Donahoe Bridge, Madison County, Iowa (2010).

Figure 13.7—Zumbrota Bridge, Zumbrota, Minnesota (2011).

Figure 13.8—Zumbrota Bridge on September 23, 2010, during flooding on the Zumbro River. (a. Photo courtesy of kstp.com, b. Photo courtesy of fox9.com.).

Figure 13.9—A FARO laser scanner used to scan a historic covered bridge.

Figure 13.10—Point cloud image of the Cedarburg Bridge (SightLine, LLC).

Figure 13.11—3D AutoCAD image of the Cedarburg Bridge embedded in point cloud data (SightLine, LLC).

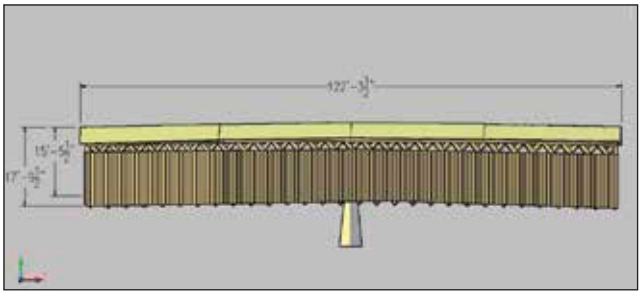

Figure 13.12—Dimensioned 2D AutoCAD® image of the Cedarburg Bridge (SightLine, LLC).

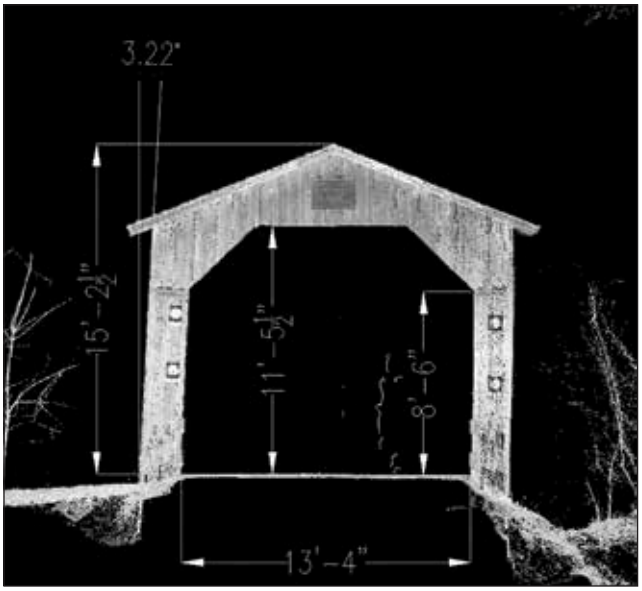

Figure 13.13—Dimensioned point cloud image of bridge entry on Cedarburg Bridge (SightLine, LLC).

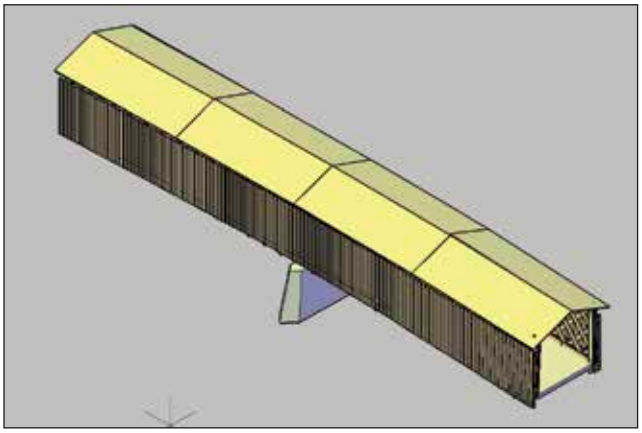

Figure 13.14—CAD image of the Cedarburg Bridge (SightLine, LLC).

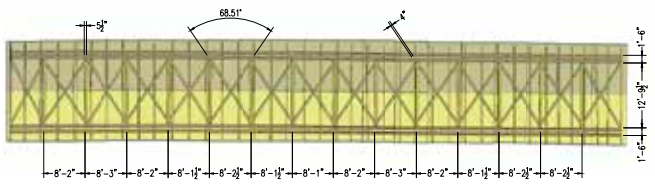

Figure 13.15—CAD dimensions of ceiling structure of the Cedarburg Bridge (UMD NRRI).

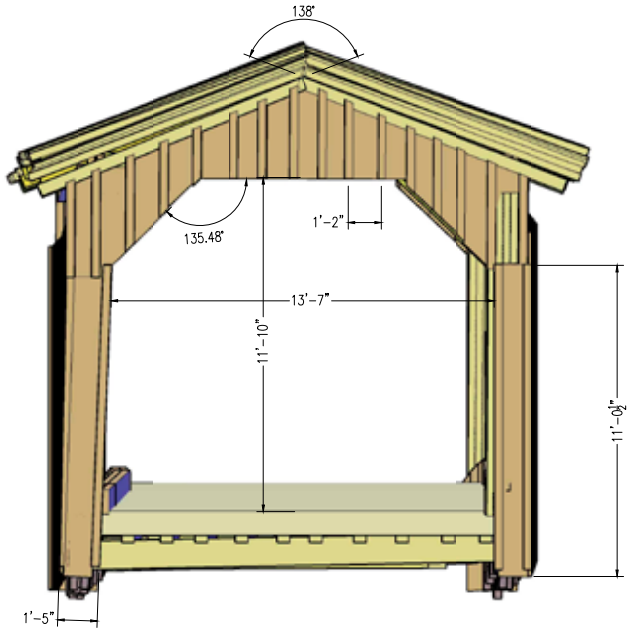

Figure 13.16—CAD drawing and dimensions of front entrance of the Cedarburg Bridge (UMD NRRI).

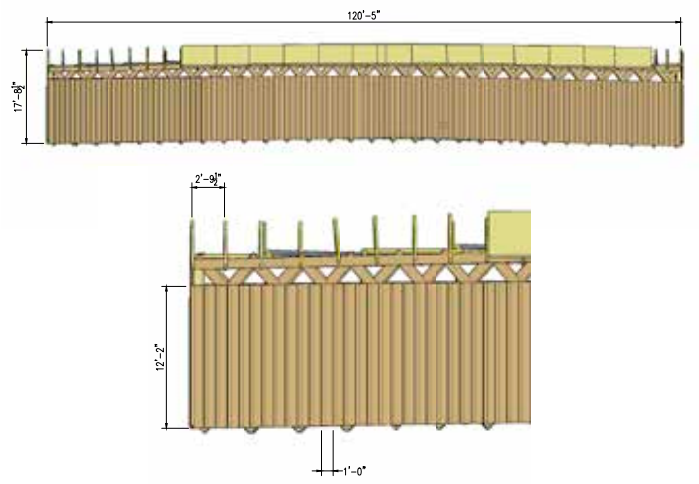

Figure 13.17—CAD drawing and dimensions of side wall and trusses of the Cedarburg Bridge (UMD NRRI).

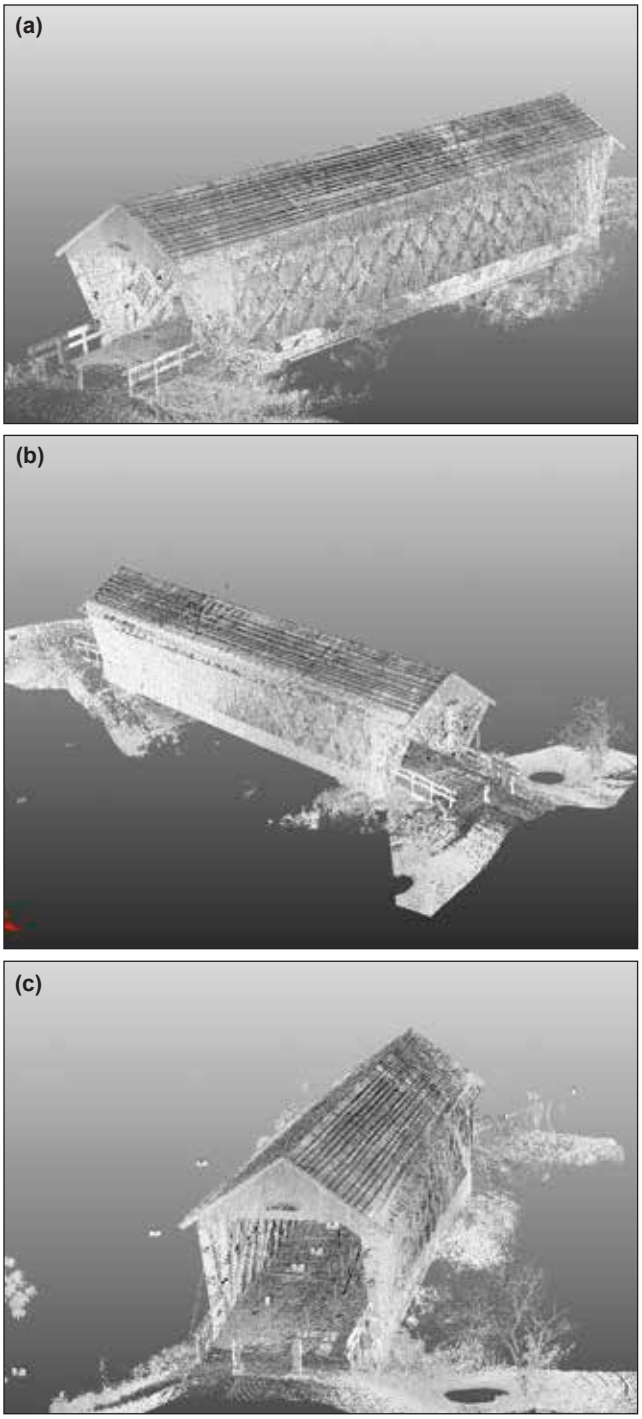

Figure 13.18—Point cloud images of the Imes Bridge (UMD NRRI).

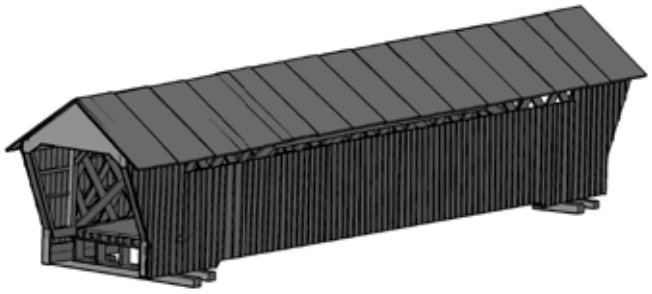

Figure 13.19—Isometric 3D AutoCAD image of the Imes Bridge (NRRI).

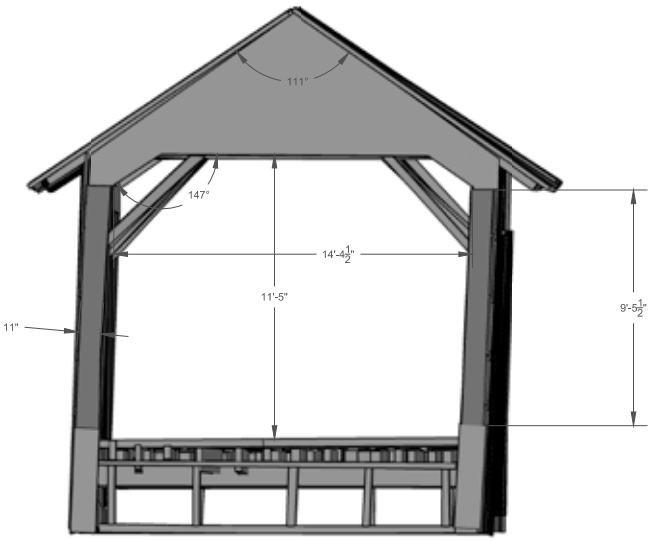

Figure 13.20—Dimensioned 3D AutoCAD image of the Imes Bridge showing the existing rotation and out-of-plane nature of the bridge (NRRI).

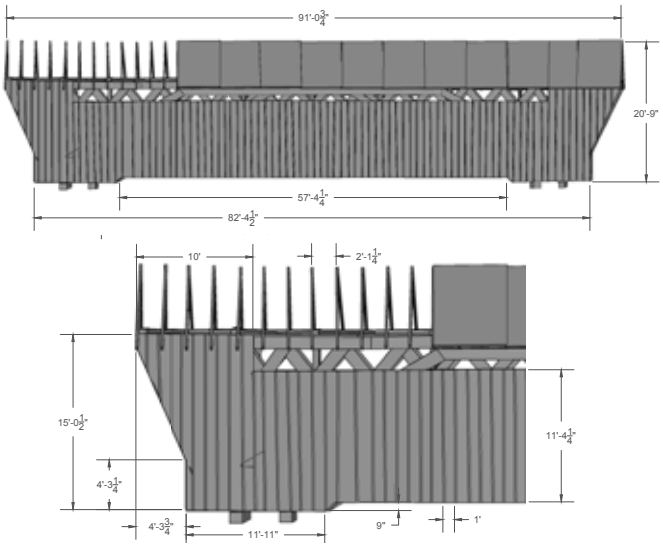

Figure 13.21—Dimensioned 3D AutoCAD side view image of the Imes Bridge (NRRI).

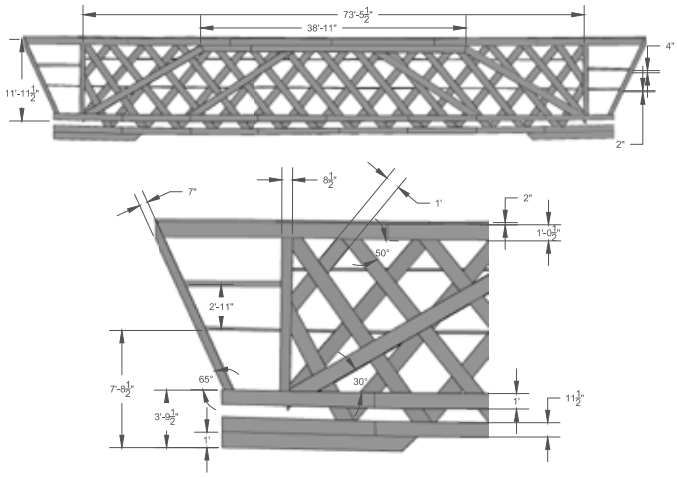

Figure 13.22—Dimensioned 3D AutoCAD internal side wall image of the Imes Bridge (NRRI).

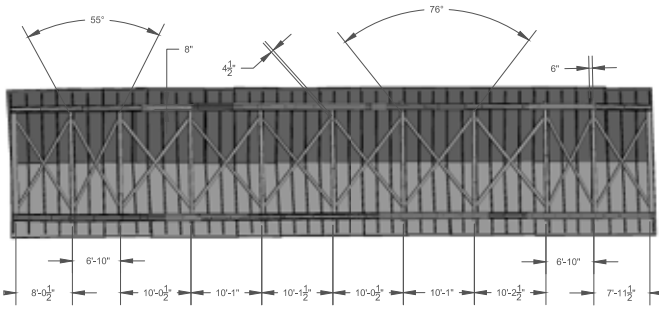

Figure 13.23—Dimensioned 3D AutoCAD ceiling image of the Imes Bridge (NRRI).

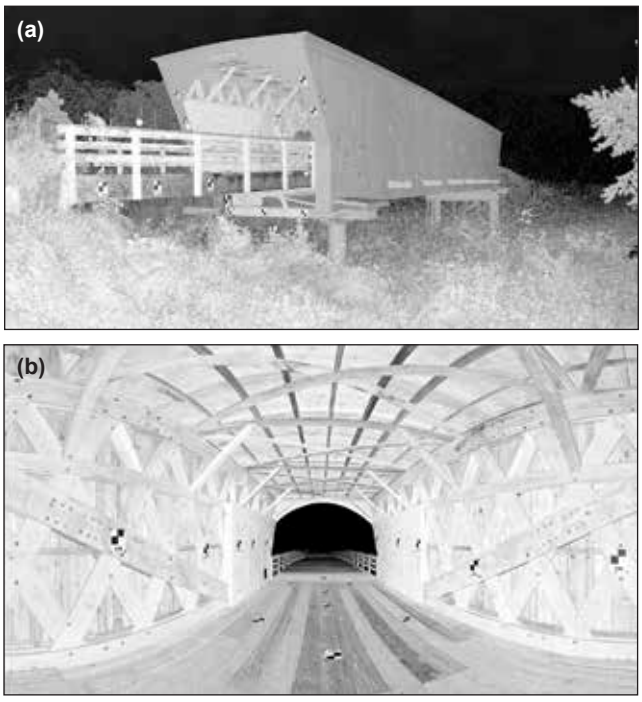

Figure 13.24—Planar views of a single laser scan of the Roseman Bridge (NRRI).

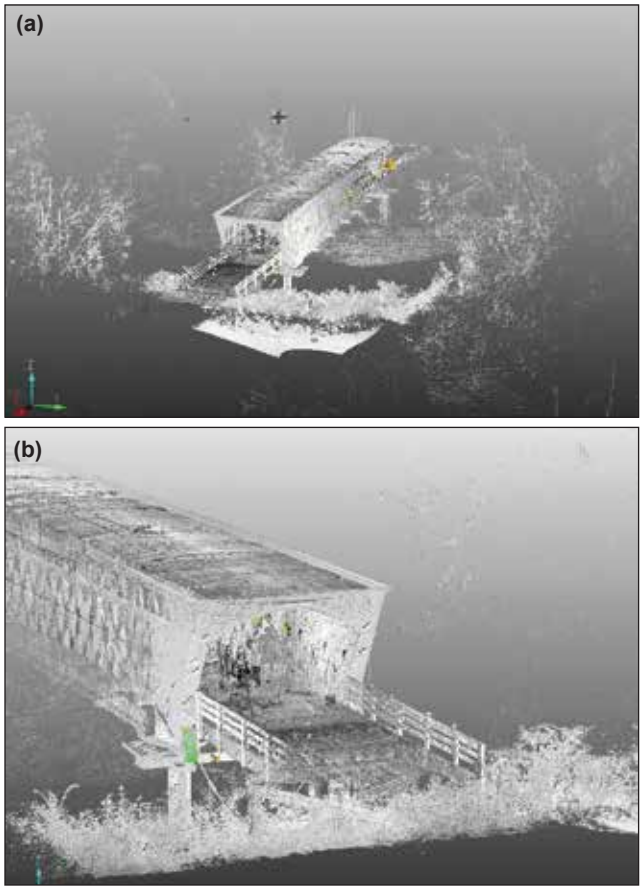

Figure 13.25—Point cloud images of the Roseman Bridge (NRRI).

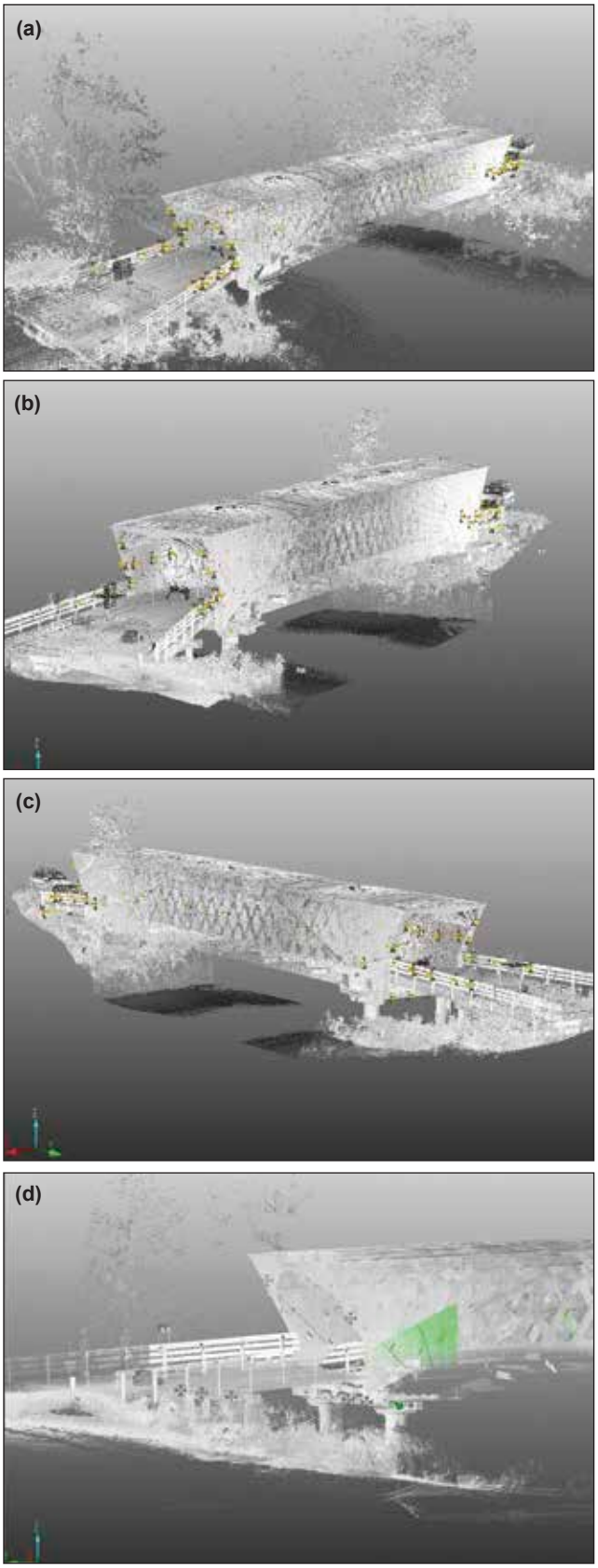

Figure 13.26—Point cloud image of the Hogback Bridge (NRRI).

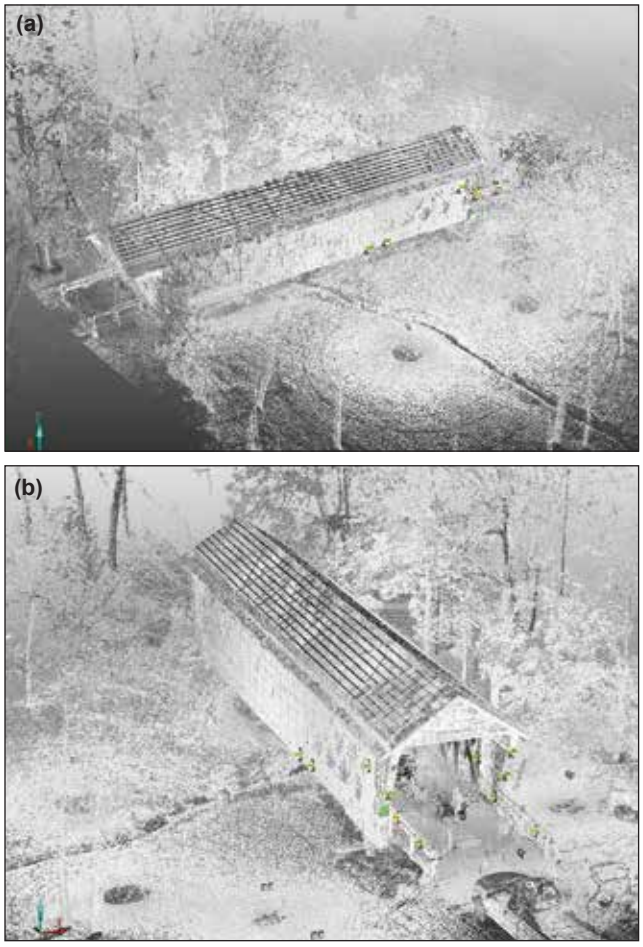

Figure 13.27—Point cloud images of the Cutler–Donahoe Bridge (NRRI).

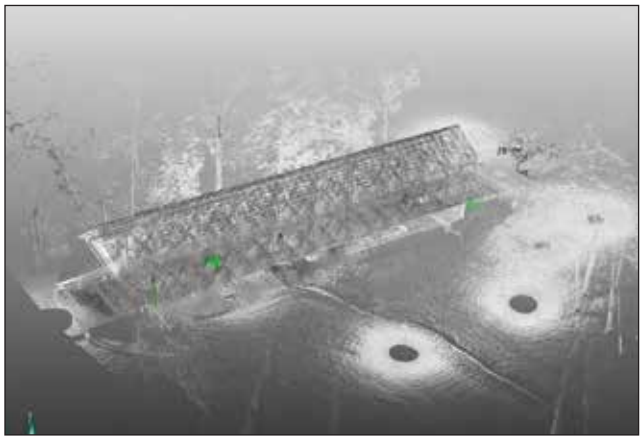

Figure 13.28—Point cloud image (enhanced with clear view software setting) of the Cutler–Donahoe Bridge (UMD NRRI).

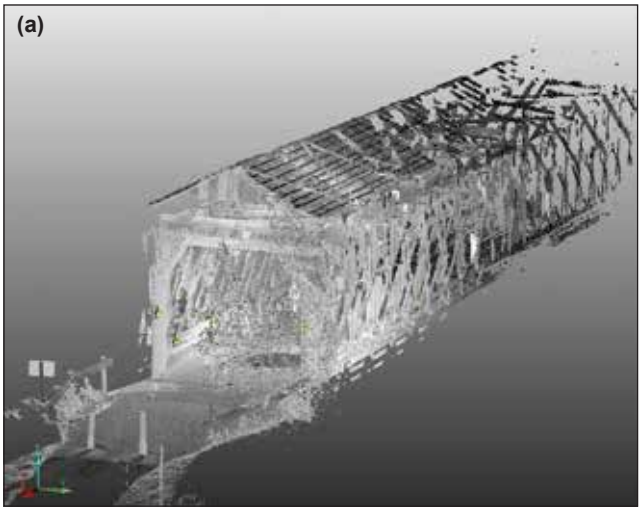

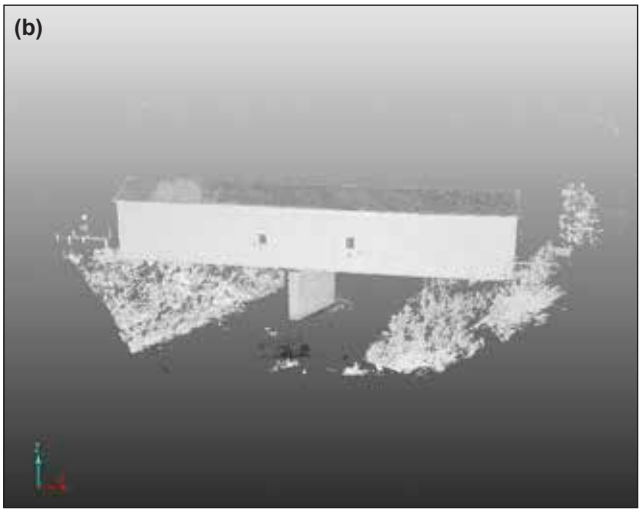

Figure 29—First scalar image of the outside of the Zumbrota Bridge Point Cloud.

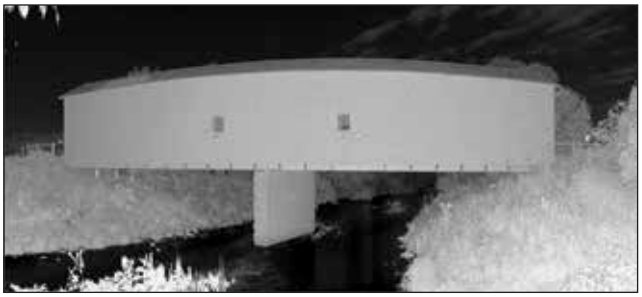

Figure 13.30—Scalar image of the outside of the Zumbrota Bridge created from a single exterior scan processed with Faro Scene software.

Figure 13.31—Scalar image of the inside of the Zumbrota Bridge created from a single interior scan processed with Faro Scene software.

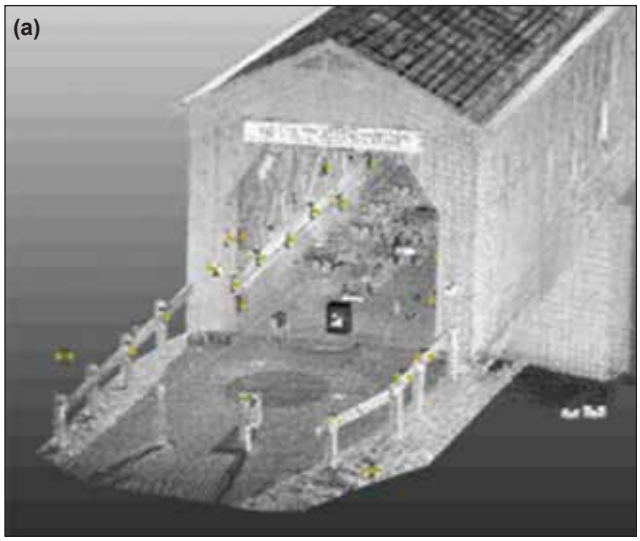

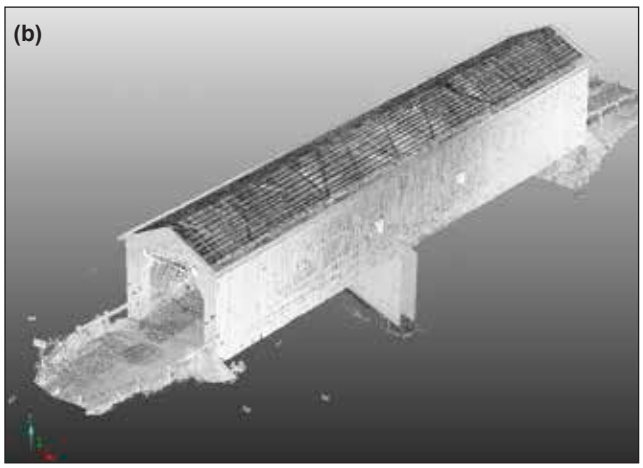

Figure 13.32—Point cloud images of the Zumbrota Bridge created from multiple scans and linked together with Faro Scene software.

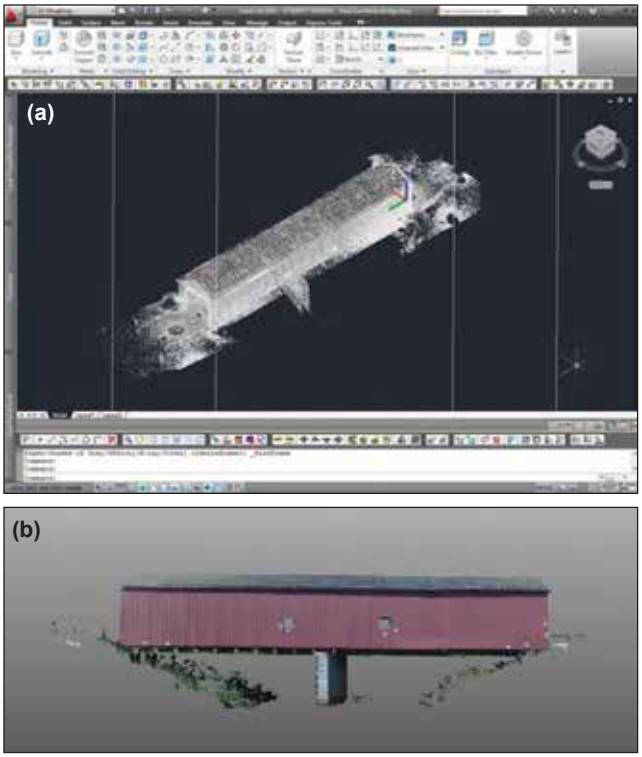

Figure 13.33—Point cloud images of the Zumbrota Bridge created from multiple scans and linked together with Faro Scene software, imbedded into AutoCAD with a Kubit USA add-in.

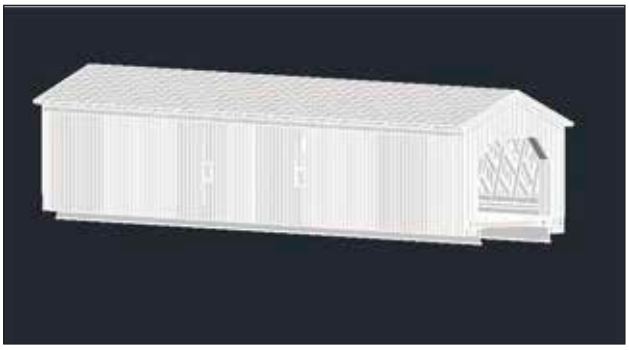

Figure 13.34—An AutoCAD 3D image of the Zumbrota Bridge created from scanning data.

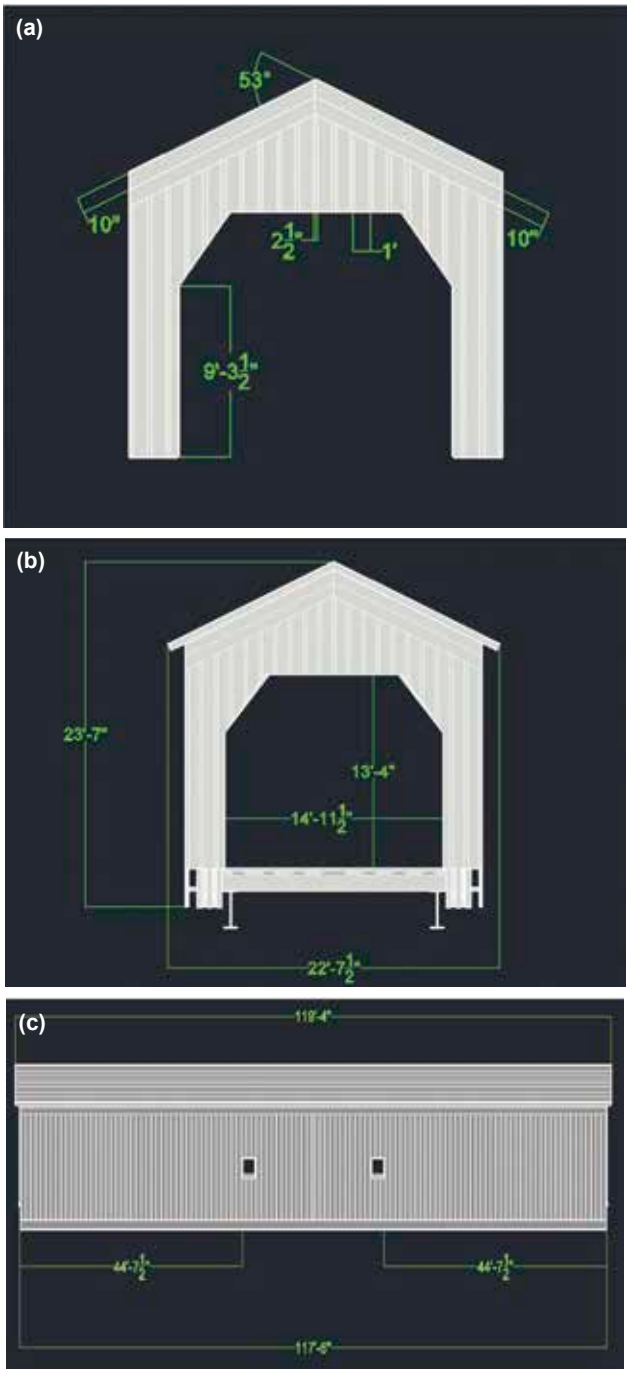

Figure 13.35—AutoCAD 2D images of the Zumbrota Bridge created from scanning data.

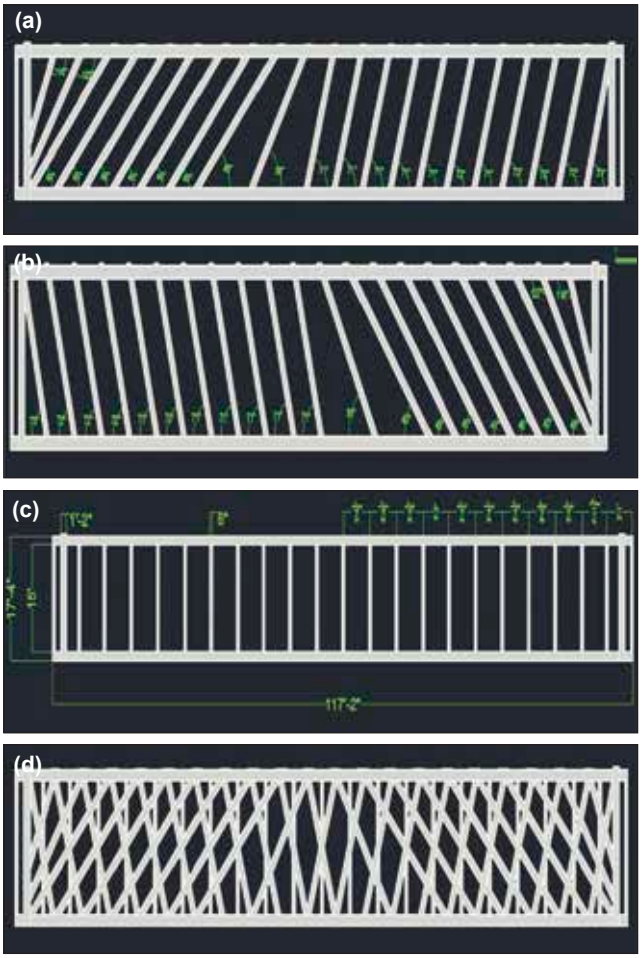

Figure 13.36—Three AutoCAD 2D images (top 3) of wall components used to create a composite of the Zumbrota bridge wall.

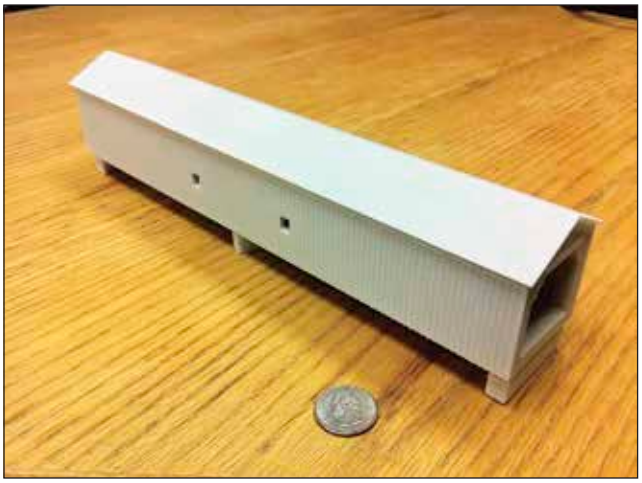

Figure 13.37—A 1/100th model of the Zumbrota Bridge created using selective laser sintering rapid prototyping equipment.

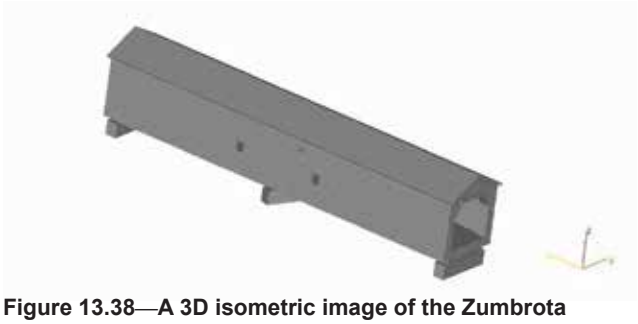

Figure 13.38—A 3D isometric image of the Zumbrota Bridge used to produce a 1/100th model using selective laser sintering rapid prototyping equipment.

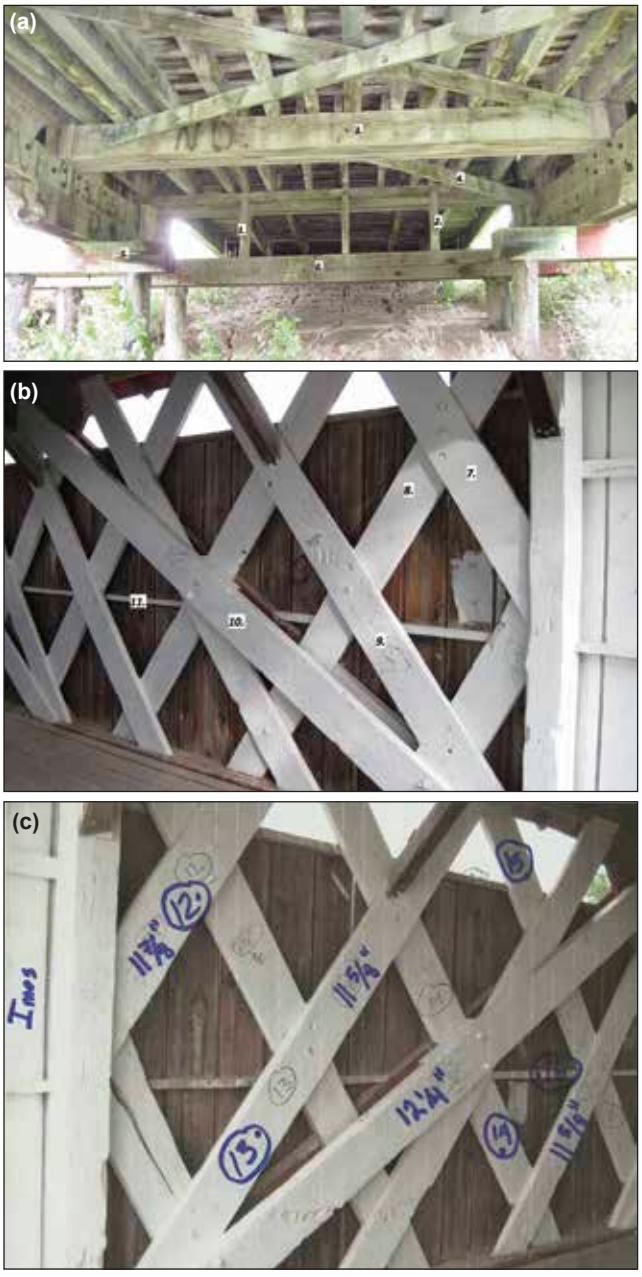

Figure 13.39—Locations on the Imes Bridge where comparison measurements were taken using traditional tape measures and extracted from the digital point clouds created from the laser scanning process.

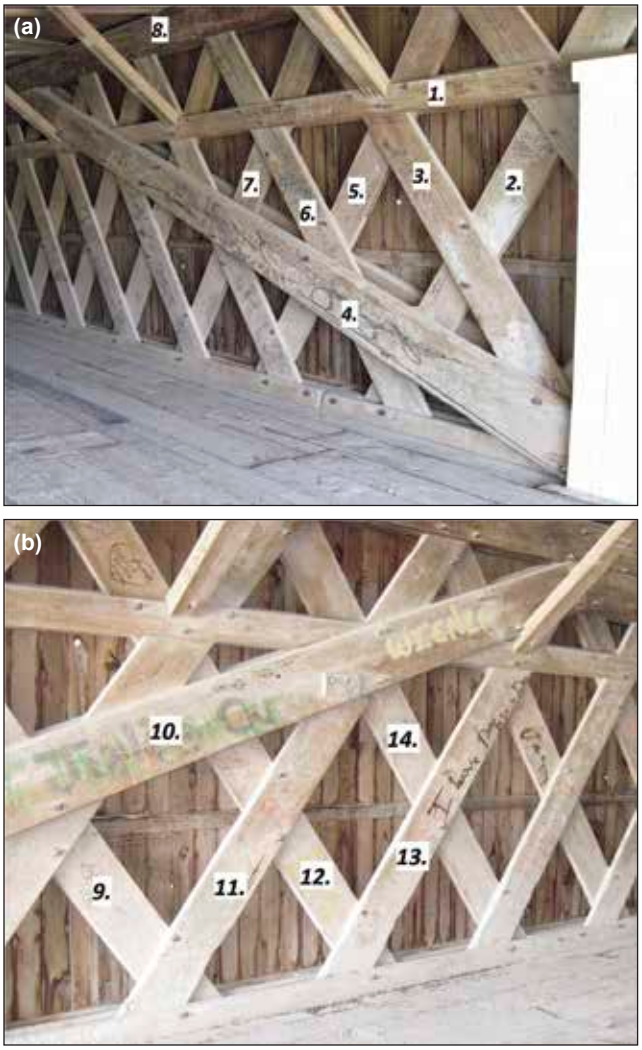

Figure 13.40—Locations on the Hogback Bridge where comparison measurements were taken using traditional tape measures and extracted from the digital point clouds created from the laser scanning process.

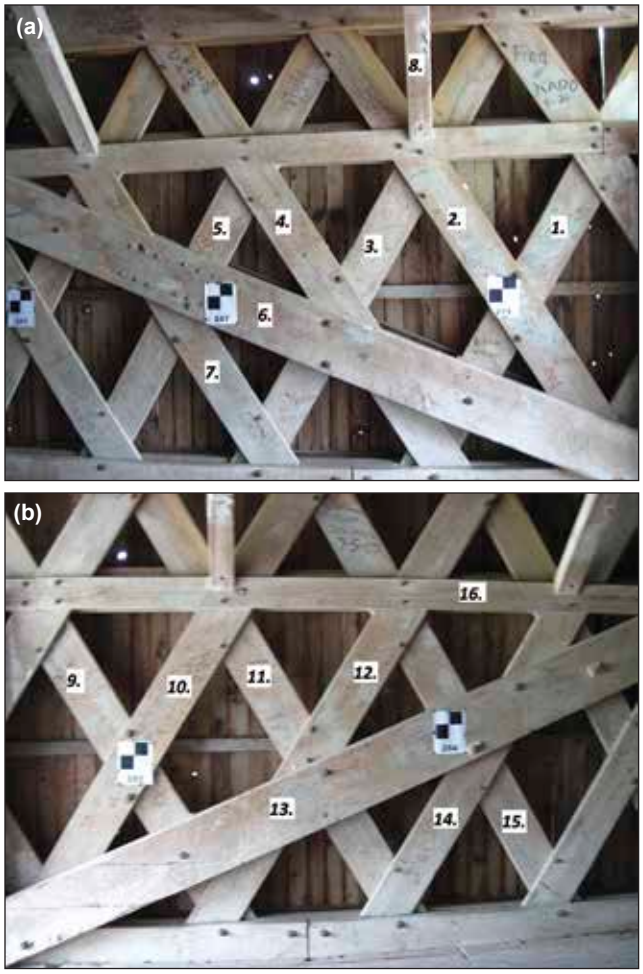

Figure 13.41—Locations on the Roseman Bridge where comparison measurements were taken using traditional tape measures and extracted from the digital point clouds created from the laser scanning process.

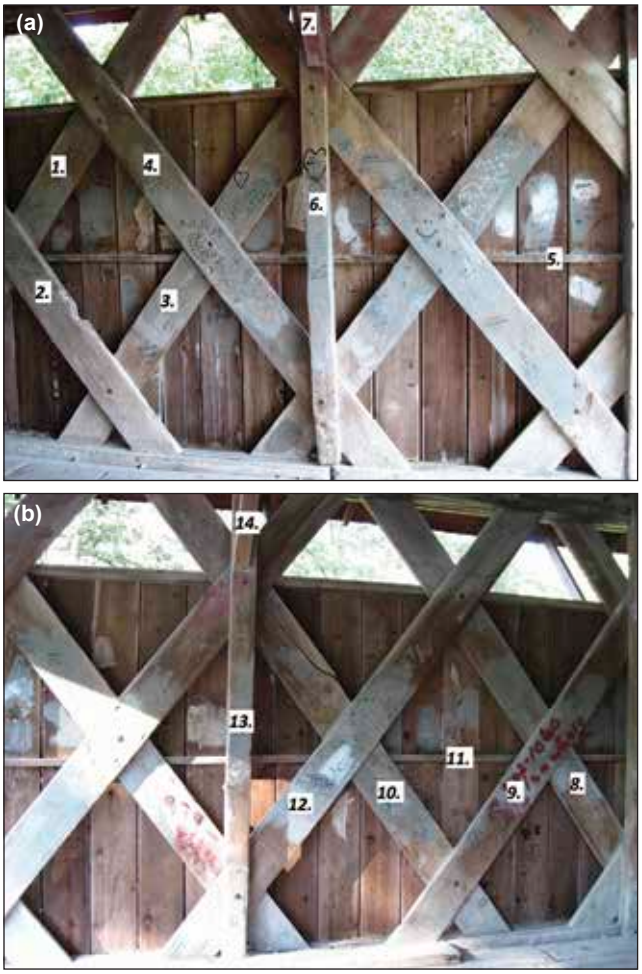

Figure 13.42—Locations on the Cutler–Donahoe Bridge where comparison measurements were taken using traditional tape measures and extracted from the digital point clouds created from the laser scanning process.

Appendix

Proceedings of the International Nondestructive Testing and Evaluation of Wood Symposium Series

The International Nondestructive Testing and Evaluation of Wood Symposium Series was initiated by Washington State University (WSU) and the USDA Forest Products Laboratory (FPL). The first symposium was held at FPL in fall 1963, with proceedings produced and distributed in 1964. At that meeting, nearly 100 scientists, engineers, and industry leaders discussed the possibilities of a wide range of scientific means for testing wood nondestructively. The goals of this series of symposia were (1) to provide a technical and scientific forum for researchers to present and exchange results from their latest research endeavors and (2) to bring researchers and industry together in an attempt to bridge the gap between the results of the researchers' efforts and use of those results by the wood industry.

Eighteen symposia have been held to date at sites in China, Germany, Hungary, Switzerland, and the United States. Early symposia focused on basic nondestructive evaluation (NDE) principles and efforts on lumber assessment procedures. The third symposium was devoted entirely to the machine stress rating lumber grading process. Symposia have attracted researchers and industry representatives from throughout the world. Recently, papers have been presented on new NDT techniques including those that focus on tomography, near-infrared scanning, and innovative combinations of stress wave, laser, and ultrasound techniques. A significant number of papers have been presented on assessment of trees and logs, with most work on lumber focusing on use of well-established techniques for evaluating species in Asia, Europe, and South America. More than 800 technical presentations have been delivered during these symposia, and proceedings containing corresponding papers were produced and published.

In 2012, all printed proceedings from the first 17 symposia were assembled, digitized, and published in searchable digital format (Ross and Wang 2012). Proceedings of the 18th symposium were published in searchable digital format and made available at the symposium (Ross and Wang 2013). The hundreds of papers making up these two publications offer an unprecedented wealth of information on nondestructive testing and evaluation of wood.

Literature Cited

Ross, R.J.; Wang, X. 2012. Nondestructive testing and evaluation of wood—50 years of research: International Nondestructive Testing and Evaluation of Wood Symposium series. General Technical Report FPL–GTR–213. Madison, WI: U.S. Department of Agriculture, Forest Service, Forest Products Laboratory. 6,702 p. (http://www.fpl.fs.fed.us/documnts/fplgtr/fpl_gtr213.pdf)

Ross, R.J.; Wang, X., eds. 2013. Proceedings: 18th International Nondestructive Testing and Evaluation of Wood Symposium. General Technical Report FPL–GTR–226. Madison, WI: U.S. Department of Agriculture, Forest Service, Forest Products Laboratory. 808 p. (http://www.fpl.fs.fed.us/documnts/fplgtr/fpl_gtr226.pdf)